Author:
Avsejs, Luke Andrei

Title:
The organic geochemistry and compound specific radiocarbon dating of peat and other sedimentary materials.

THE ORGANIC GEOCHEMISTRY AND COMPOUND SPECIFIC RADIOCARBON DATING OF PEAT AND OTHER SEDIMENTARY MATERIALS

Luke Andrei Avsejs

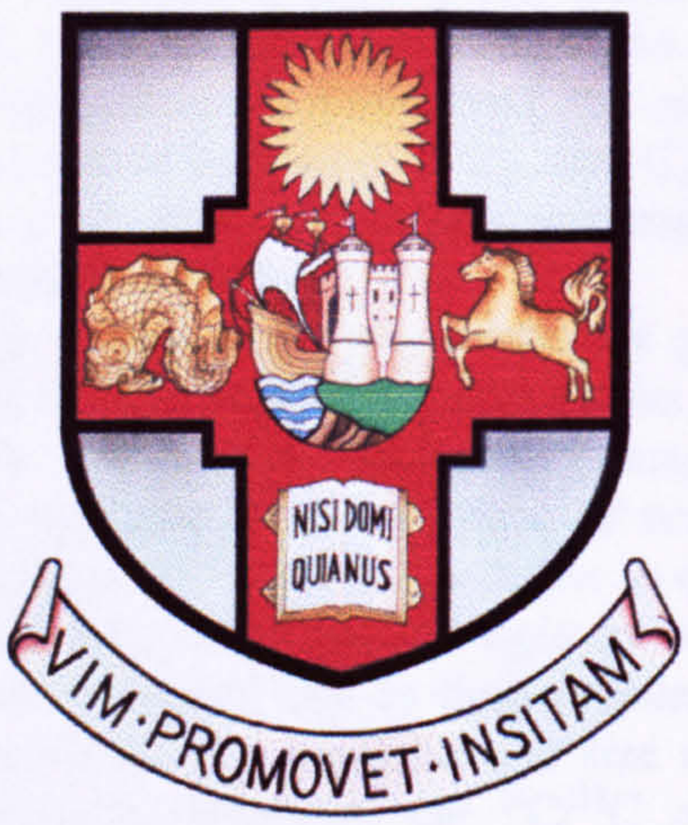

A dissertation submitted to the University of Bristol in accordance with the requirements of the degree of Doctor of Philosophy in the Faculty of Science, School of Chemistry.

February 2001

Word Count *ca.* 53,000

ABSTRACT

Previous studies relating past environments to lipid stratigraphy in peat bogs have had limited success and have involved the correlation of pollen, macrofossil and lipid records. However, these approaches provided only limited agreement and did not include specific biomarker compounds for the peat inputs. The present study investigated the composition of Bolton Fell Moss (BFM) peat on a molecular scale at different depths and tried to identify their origins with respect to plant material present in the peat.

This study examined the lipid composition of selected horizons throughout peat cores from BFM using capillary gas chromatography (GC) and mass spectrometry (MS). Samples (1 cm) from a 5 m (9 cm diameter) core were taken and 4 cm^3 sub-samples removed for macrofossil analysis. The biomarker composition of peat samples from major excursions in the macrofossil record were examined and related to the peat components. The C_{25} to C_{31} *n*-alkane ratio was found to be a good indicator of the *Sphagnum* input to the peat, a ratio of 0.2-0.5 indicating a high *Sphagnum* contribution. The diagenetic products of sterols and ββ hopanes and hopanols were found to increase with increasing depth and novel sterol diagenetic products were observed. These compounds were found to have the androstane skeleton and are thought to result from microbial oxidation of the sterols.

Lipids were characterised from peat deposited during the earliest phase of bog development where macrofossil data was absent due to extensive humification. These lipids were used to identify the different stages during the development of the bog and this was compared to an established model of bog formation.

Macrofossil analysis revealed that at approximately 435 cm depth the plant communities living on the surface of the bog changed from predominantly sedge to *Sphagnum* species, indicating a significant shift from a dry to a wet climate. Changes in lipid composition from thirty 1 cm samples from 419-448 cm were studied and related to the plant components present. Although diagenetic changes were not observed, the species switch was reflected in the *n*-alkanes and *n*-alkanols. Increased abundances of C_{23} and C_{25} *n*-alkanes related to increased abundances of Sphagnum remains and a high predominance of odd numbered *n*-alkanol homologues was found to indicate Ericaceous inputs.

The radiocarbon dating of peat to fix timescales for proxy-climate records has many complications. The radiocarbon content of bulk organic carbon in peat is assumed to reflect the age of the horizon from which it was taken. However, a major uncertainty in these organic carbon-based measurements is the unknown proportion of reworked carbon within the peat. Even with purified bulk sub-fractions it is still not possible to directly equate these ages with a specific source. Only on a molecular level can ^{14}C ages be related to individual compounds whose structures indicate an unmistakable link to lipid precursors of known biological origin and which are resistant to reworking. The small sample size requirement of accelerator mass spectrometry has allowed the measurement of the $^{14}C/^{12}C$ ratio of components of various sedimentary materials and has overcome some of the problems associated with conventional radiocarbon dating of sediments, where the $^{14}C/^{12}C$ ratio of the whole sample, less carbonate, is measured.

Ten bulk peat samples at 3 cm intervals over the 419-448 cm profile were radiocarbon dated together with selected compounds isolated from the peat by preparative gas chromatography (PCGC). Comparison of the dates of the compounds with those of the bulk peat revealed that the lipids were younger than the surrounding matrix and this was attributed to the lipids having a plant source which fixed CO_2 directly from the atmosphere whereas other peat components may be affected by old reworked carbon sources. β-Sitosterol and 3-stigmastanol were isolated from the ten 1 cm intervals and radiocarbon dated. However, they were found to be highly enriched in ^{14}C. Further experiments revealed that the PCGC system was susceptible to cause fractionation of isotopes due to a time delay between the FID and the traps, which can significantly alter the radiocarbon content of trapped lipids. However, this could be corrected for by adjusting the trapping windows.

PUBLICATIONS AS A RESULT OF THIS STUDY.

Avsejs, L. A., Nott, C. J., Maxwell, J. R., and Evershed, R. P. (1998). Hydroxy and ketonic androstanes: a new class of sterol diagenetic product in peat. *Organic Geochemistry* **28,** 749-753.

Nott, C. J., Xie, S., Avsejs, L. A., Maddy, D., Chambers, F. M., and Evershed, R. P. (2000). *n*-Alkane distributions in ombrotrophic mires as indicators of vegetation change related to climatic variation. *Organic Geochemistry* **31,** 231-235.

ACKNOWLEDGEMENTS

Firstly I wish to thank my advisors, Prof Richard Evershed and Prof James Maxwell and other past and present members of the OGU, including, Pim, Anke, Gareth, Cheggs, Andy T, Ant, Matt F, Matt L, Helen T, Hazel, Ian, Rob, Simon, Alex, The Guv, Mohammed, Andy G, Jim C, Susie, Helen B, Mark C, Paul C, Sophie, Gordon, Vicky, Zoë, Matt H, Xie, Ruth, Dave and Sue. Also Kath for discussions and Stotty for invaluable PGCG advice.

I would especially like to thank Chris Nott, a better person to do a PhD alongside would be hard to find.

Christopher Ramsey and the staff at the Radiocarbon Accelerator Unit, Research Laboratory for Archaeology and the History of Art, for AMS analyses and helpful discussion.

I would also like to thank Dmitri Maquoy, Paul Hughs, Nick Cross, Darrel Maddy, Frank Chambers for their help in obtaining samples, macrofossil analysis and everything palaeoclimatically related.

My past flatmates, especially Jim, Wood and Flower are also thanked for nights out, nights in and one or two beers.

My thanks go to my Parents who have supported me all the way through.

And to Sam.

AUTHOR'S DECLARATION

I declare that the work in this thesis dissertation was carried out in accordance with the Regulations of the University of Bristol. The work is original except where indicated by the special reference in the text and no part of the dissertation has been submitted for any other degree.

Any views expressed in the dissertation are those of the author and in no way represent those of the University of Bristol.

The dissertation has not been presented to any other University for examination either in the United Kingdom or overseas.

SIGNED: 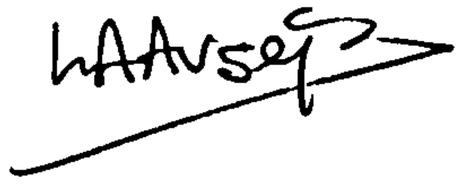 DATE: 5/7/01

CONTENTS

LIST OF TABLES

LIST OF FIGURES

ABBREVIATIONS

ADD	Androsta-1,4-diene-3,17-dione
AMS	Accelerator Mass Spectrometry
b/c	Branched and Cyclic
BFM	Bolton Fell Moss
BP	Before Present
BSTFA	*N,O*-bis(trimethylsilyl)trifluoroacetamide
CIE	Chromatographic Isotope Effect
CPI	Carbon Preference Index
DCA	Detrended Correspondence Analysis
DCM	Dichloromethane
FAME	Fatty Acid Methyl Ester
FID	Flame Ionisation Detector
GC	Gas Chromatography
GC/MS	Gas Chromatography/Mass Spectrometry
HBI	Highly Branched Isoprenoid
irm-GC/MS	Isotope Ratio Monitoring-Gas Chromatography/Mass Spectrometry
PCGC	Preparative Capillary Gas Chromatography
TLE	Total Lipid Extract
TMS	Trimethylsilyl
TMY	Theoretical Maximum Yield
TOC	Total Organic Carbon
UOM	Unidentified Organic Matter
vPDB	Vienna Pee Dee Belemnite
WLM	Walton Moss

1. INTRODUCTION

1.1 Peat Bogs

Peatlands cover about 3% of the Earth's land surface, mostly in Canada and Russia, and contain about 180 GT of organic carbon (Kivinen and Pakarinen, 1981). Peatlands play an important role in the biosphere. They interact with fundamental life-support processes, involving biogeochemical cycling, food-chain support, hydrological dynamics and water quality, and provide habitats for many characteristic (and some highly adapted) plant and animal species.

Peat is a heterogeneous mixture of more or less decomposed plant (humus) material that has accumulated in a water-saturated environment and in the absence of oxygen. Its structure ranges from more or less decomposed plant remains to a fine amorphic, colloidal mass. Most peat-forming systems consist of two layers:

Acrotelm - everything above the lowest level reached by the water table in a dry summer. This is a 10-50 cm deep aerobic layer where the rate of decay is relatively fast.

Catotelm - permanently waterlogged peat. This is a thicker, usually anaerobic layer with a much slower rate of decay (Ingram, 1978).

The accumulation of peat depends on the uptake of carbon being greater than the loss of carbon through decomposition. Photosynthesis at the top of the acrotelm fixes carbon and as the peat grows about 10-20% of the material formed at the top of the acrotelm passes into the catotelm with the acrotelm remaining the same thickness (Clymo, 1984). The warmer the climate, the quicker the plant material will decompose. The rate of accumulating plant material is greatest in the areas where the temperature is high enough for plant growth but too low for the vigorous microbial activity that breaks down plant material. Such conditions are found more frequently in the northern hemisphere.

Peatlands or mires are the wetland ecosystems that are characterised by the accumulation of organic matter, which is produced and deposited at a greater rate than it is decomposed, leading to the formation of peat. There are three types of peatland:

Fens - bogs which form from vegetation which is fed from the ground waters rich in nutrients. They are very often an early stage in the formation of raised bogs which grow on top of the fen.

Blanket bogs - shallow bogs which form a blanket-like layer over the surface of the underlying mineral soil, where rainfall levels are relatively high.

Raised bogs - or ombrotrophic bogs have a dome-shaped surface and receive nutrients only in the form of precipitation or wind-borne dust. Ombrotrophic conditions represent the extreme situation at the lower end of nutrient availability, and ombrotrophic sites usually have a thick peat layer (Godwin, 1981).

1.2 Bog Development

The last glaciation period, or ice age, ended about 13,000 years ago. The ice fields had melted and retreated northwards, and left behind glacial deposits (i.e. eskers, moraines, drumlins) which resulted in a very irregular topography. The undulating landscape had many deep hollows or basins which filled with water due to the poor drainage characteristics of the basin soils. Lakes were formed and between the lake basins were many gravel ridges (i.e. of esker and moraine origin) which impeded drainage. As the climate gradually became warmer, a range of vegetation types grew in these lakes: reeds grew along the margins, water lilies in shallow bays and floating pondweeds on the deeper waters. When these plants died they only partially decayed and their remains accumulated at the bottom of the lakes. Over time the plant residues built up and the lake became shallower and gradually infilled. When fen peatlands formed and their depth increased to the level where the surface vegetation could no longer be influenced by mineral rich ground waters or surface waters, the type of vegetation changed to plant species, such as *Sphagnum* mosses, which grew and tolerated the low nutrient conditions present in rainwaters. The raised bog peats formed when the *Sphagnum* mosses partially decayed and accumulated in annual cycles over hundreds or thousands of years in the anaerobic waterlogged environment (Foss, 1987).

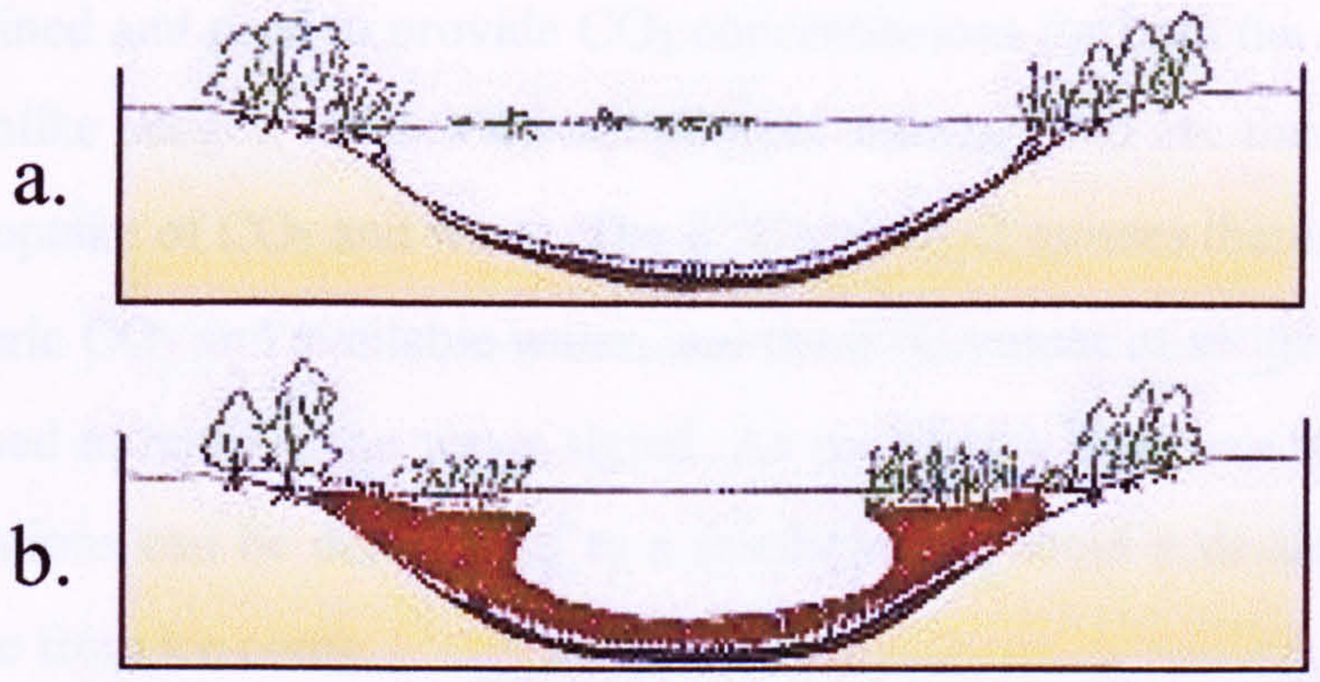

Figure 1.1 Stages in the formation of a raised peat bog. (a) Lake, (b) infilling of lake, (c) fen and (d) raised peat bog.

The exceptional preservation qualities of peat bogs make them unique in retaining plant fossils. The records that these fossils produce contain valuable information about past climates. Changes in the surface wetness of a bog through differences in precipitation and evaporation can influence which species of plants thrive there. Therefore, the plant fossil records that are retained in the peat can be used as a proxy for climate (Barber, 1985). Where sedge species such as *Eriophorum vaginatum* thrive under drier conditions and *Sphagnum* moss species such as *S. cuspidatum* prefer wetter climates. As most currently 'living' bogs have accumulated during the Holocene, the records that they contain are especially relevant to understanding and predicting the present climate. Research into peat bogs containing records of past climates has existed since the 19th century. However, it is only relatively recently that multiproxy investigations of these unique environments have been made (Barber, 1993). Use of other techniques in peat studies to establish past climates, such as monitoring $^{13}C/^{12}C$ ($\delta^{13}C$) ratios to determine past atmospheric CO_2 concentrations has been made (White *et al.*, 1994). The $\delta^{13}C$ values of peat macrofossil components (sedge and moss species)

can be determined and used to provide CO_2 concentrations for both the atmosphere and peat water. Unlike sedges, mosses do not possess stomata, and are therefore unable to regulate their uptake of CO_2 and water. The $\delta^{13}C$ values of mosses therefore depends on both atmospheric CO_2 and available water, and the $\delta^{13}C$ values of sedges from the same peat can be used to remove the water signal. As peat has a high accumulation rate the CO_2 concentrations can be determined to a resolution of about a decade, much higher than is possible from ice cores.

The degree to which peat decomposition has occurred can also be used as a proxy-record for climate, as the decomposition is related to the water content of the peat at the time of deposition, i.e. the drier the peat, the greater the decay (Blackford and Chambers, 1993). This method for the determination of past climates, estimates the degree of decomposition and humification using: visual examination and classification, measurement of physical properties, measurement of chemical properties, and the chemical extraction of soluble material. Visual examination is used to place the peatified remains into one of ten humification classes. This ranges from yellow-light brown peat with undamaged *Sphagnum* leaves (H1) to blackish-brown peat consisting of totally destroyed organic matter (H10). Physical properties such as water holding capacity are assessed where the greater the degree of humification of the peat, the less water is absorbed as pore space between particles is reduced. Relatively rapid and simple techniques such as the determination of the calorific content of peat are employed to assess the chemical properties of peat. However, these properties have been found to be species specific and can only be assessed in peat with unchanging inputs. The soluble material within the peat can also be assessed. NaOH extracts are used to determine the humic acid content of peat. The humic acid abundance has been found to increase with increasing peat humification.

Peat has also been investigated in order to understand the formation of coal deposits and its potential as a fuel itself. One investigation included research into lipid composition of peats with differing heat values so as to try to determine why some types of peat produce higher grade fuels (Ketola *et al.*, 1987). More recently, studies have employed coal petrographical techniques to characterise different peat samples and compared these results to their environment of deposition (Dehmer, 1995). However, as peat has such remarkable preservation properties it is surprising how little this extraordinary material has been studied.

1.3 Organic Geochemistry of Peat

Under aerobic conditions a large proportion of organic material (protein, lipids and simple carbohydrates) decomposes very quickly, either completely so as to be removed from the material, or in part to leave molecular fossils. Under anaerobic conditions, such as those found in the formation of peat, the decomposition of organic compounds is impeded. Most decomposition is due to the enzymatic processes associated with aerobic microorganisms, which are depleted in peat as there is limited access to oxygen. A peat bog contains approximately 90% water, whereas most microbial decomposition occurs within the aerobic, non-waterlogged peat (acrotelm). When conditions occur that cause the bog to become drier, there is a sharp increase in the abundance of microorganisms, which results in acceleration of the decomposition of the peat. The record of decomposition that is left behind in the peat can be an indicator of the past climate during the development of the peat (Blackford and Chambers, 1991). During the formation of peat, organic matter classified under the general term 'humic substances' is formed. These humic substances are composed of: (1) humic acids, (2) fulvic acids, (3) humins. These compounds are classified by their solubility in various solvents. Humic acids are soluble in alkali. Fulvic acids remain in solution after precipitation of the humic acids with acid. Humins are the organic residues that remain in the peat after extraction of humic acids (Oden, 1919).

Another class of organic compounds found in peat are lipids. These are compounds that are soluble in organic solvents and insoluble in water. Previous studies involving the analysis of peat have revealed that dry peat contains about 5-20% lipidic matter (Ketola *et al.*, 1987). However, the lipids present in peat can vary widely depending on such factors as peat forming plant communities, bacterial and fungal populations and the level of preservation. Early studies of peat revealed the first confirmation of steroidal compounds in sedimentary materials, where β-sitosterol and β-sitostanol were identified (McLean *et al.*, 1958). The reduction of double bonds in these sterols to yield stanols (Fig. 1.2), has also been reported in peat and is believed to occur through sterone intermediates (Ives and O'Neil, 1958).

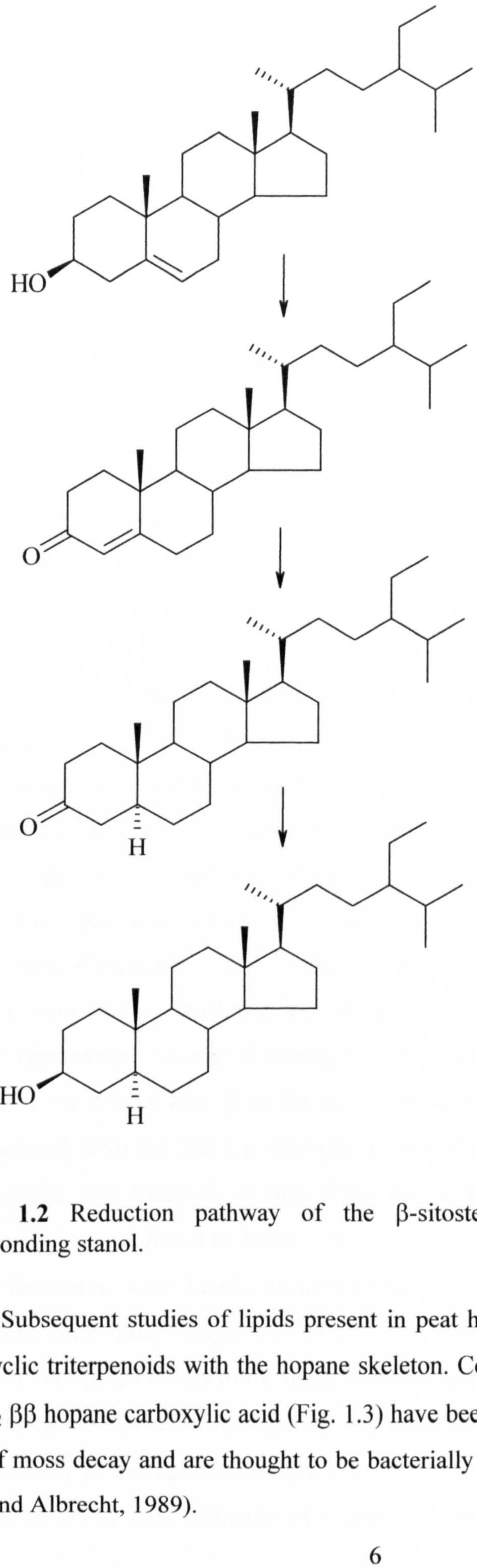

Figure 1.2 Reduction pathway of the β-sitosterol double bond yielding the corresponding stanol.

Subsequent studies of lipids present in peat have included the identification of pentacyclic triterpenoids with the hopane skeleton. Compounds such as C_{31} αβ hopane and C_{32} ββ hopane carboxylic acid (Fig. 1.3) have been associated with the very earliest stage of moss decay and are thought to be bacterially derived (Quirk *et al.*, 1984; Ries-Kautt and Albrecht, 1989).

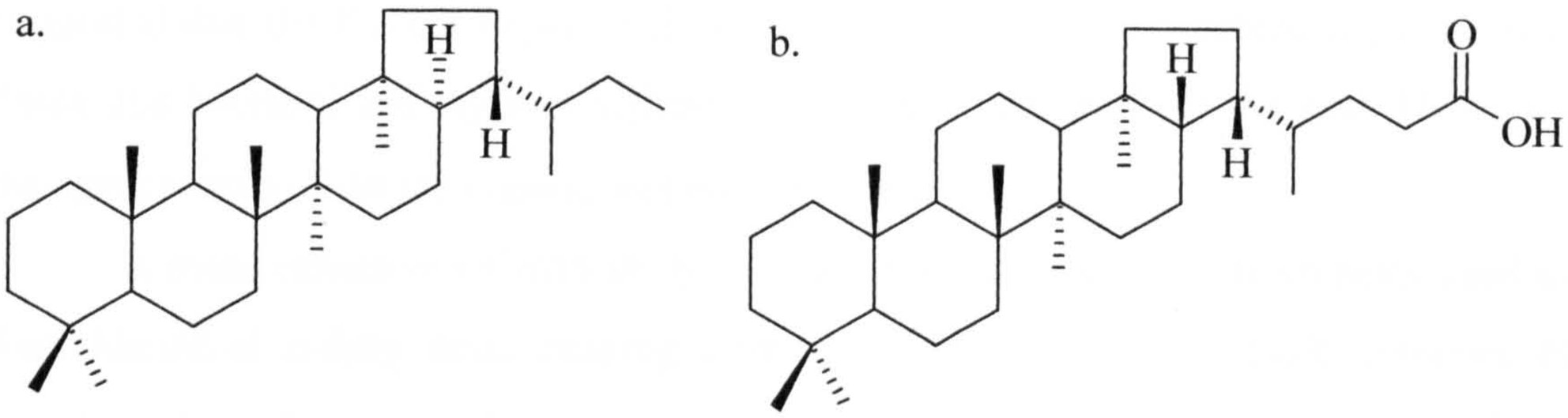

Figure 1.3 Major hopane components identified in peat (a) C_{31} αβ hopane and (b) C_{32} ββ hopane carboxylic acid.

One study compared extended hopanoid alkanes found in different peat environments (*Sphagnum* raised bog, *Scirpus/Phragmites* reedswamp/fen peat and a peat deposit from a small eutrophic lake where the surface had been polluted by an oil-derived source) in an attempt to elucidate the origin of these compounds which are found ubiquitously in sediments (Quirk *et al.*, 1984). Soxhlet extracts of the peat samples were separated into neutral and acid fractions and analysed by gas chromatography (GC) and GC/mass spectrometry (GC/MS). It was revealed that in the *Sphagnum* and reedswamp/fen peat the C_{31} αβ hopane (Fig. 1.3a) was by far the major branched and cyclic (b/c) component in all the samples studied and in peat from the eutrophic lake both the αβ and ββ C_{31} hopanes dominated the b/c alkanes. The αβ hopane was found to be present as two epimers (22*R* or 22*S*) in some samples studied and the ratio of these was used to assess the possible sources of the hopanoid alkanes. Previous work had revealed that a predominance of the 22*S* epimer indicated a oil-derived contaminant source (Ensminger, 1977) and quantification of the different epimers in the surface peat from the eutrophic lake revealed that the peat had indeed been polluted, with the 22*S* C_{31} αβ hopane epimer predominating. The b/c alkanes of plant species and bacterial isolates from the raised bog peat were identified and compared with those found in the peat. *Sphagnum* moss contained very low quantities of hopane derivatives with the C_{31} αβ hopane epimers occurring as a ~1:1 mixture, i.e. of oil-derived contaminant origin. All of the other species of plants that were examined contained very little or none of the hopanes found in the peat. However, the hopanes that were found in these plant species (*Eriophorum* and *Cladonia*) were present predominantly as the 22*R*-isomer. The C_{31} αβ hopanes found in bacterial isolates were assigned an oil-derived contaminant source and the contamination was presumed to

have occurred during the large-scale culturing of the isolate. In conclusion the authors suggested that the C_{31} αβ hopane (22*R*) was formed at the very earliest stage of moss decay and bacterial activity was highest in the uppermost levels of the peat. However, the exact source of the αβ hopane was not identified.

A more extensive GC/MS study of total lipid extracts (TLE) from peats used as fuel, identified *n*-fatty acids ranging from C_{12} to C_{30} as major lipidic components together with ω-hydroxy acids ranging from C_{12} to C_{28} and sterols of which β-sitosterol was the most abundant (Ketola *et al.*, 1987). Four Finnish milled peats which consisted of *Carex*/lignous species, *Sphagnum*/*Carex*, *Sphagnum*/*Eriophorum* and *Carex*/*Sphagnum* remains, respectively, were Soxhlet extracted and the lipidic components identified. The *Carex*/lignous species peat was found to contain the highest amount of lipid extract (180 mg g^{-1} dry peat) and the *Carex*/*Sphagnum* peat the lowest (49 mg g^{-1} dry peat). The high lipid content of the *Carex*/lignous species peat was attributed to its high degree of humification and this peat also had a higher heat value (27.1 MJ kg^{-1}) than the other peats (20.2-22.7 MJ kg^{-1}). The lipid distributions of the higher heat value peat also showed differences to the other peat samples studied. The former was found to contain a higher amount of shorter chain compounds (<C_{21}, *n*-fatty acids, ω-hydroxy acids, dicarboxylic acids, *n*-alkanols and *n*-alkanes), with approximately four times the content (16.51 mg g^{-1} dry peat) of the other samples. Also the ω-hydroxy acids from this peat constituted the main group of the acidic compounds whereas in the other peats the *n*-fatty acids dominated. In conclusion, although differences in the lipid components from the different peat types were seen, a direct correlation between peat extracts and its heating capabilities could not be established.

A further investigation of specific sub-fractions of peat lipids identified long-chain acyclic methyl ketones as lipidic components (Lehtonen and Ketola, 1990). The ketone sub-fractions from *Sphagnum* and *Carex* peats of various degrees of humification were studied and *n*-alkan-2-one distributions established. These compounds were found to range from C_{17} to C_{35} with a high odd-over-even carbon predominance (carbon preference index (CPI) = 6.6-15.0) and the shorter-chain homologues (C_{17}-C_{23}) were found to be in increasing abundance with increasing humification of the peat. Of these compounds, heptadecan-2-one and henicosan-2-one were found to be the most abundant methyl ketones in *Sphagnum* and *Carex* peats, respectively. It was suggested that the methyl ketones could have come from mosses and grasses, whose remains make up the peat. However, they could also have been formed

by the oxidation of *n*-alkanes and/or bacterial β-oxidation and decarboxylation of *n*-fatty acids.

In addition to the above compounds, triterpenoids containing the lupane skeleton, e.g. betulinic acid (3β-hydroxylup-20(29)-en-28-oic acid), lupeol (lup-20(29)-en-3β-ol) and betulin (lup-20(29)-ene-3β,28-diol) have also been identified in lipid fractions of peat as well as other triterpenoids such as friedelan-3β-ol (Lehtonen and Ketola, 1993). The authors explored the diagenetic changes to peat lipids in 4 different peat types, *Sphagnum*, *Carex*, *Bryales* and *Carex/Bryales*. Soxhlet extractable material was further separated into hydrocarbon, ketone, alcohol, sterol and acidic fractions, the lipid monomer components of which were identified by GC and GC/MS. The hydrocarbon fraction was found to be almost exclusively composed of a homologous series of *n*-alkanes which had a high odd-over-even carbon preference (CPI = 3.0-10.2) over the C_{16}-C_{36} range. The average CPI values were found to decrease in the range *Sphagnum* > *Carex* > *Carex/Bryales* > *Bryales* peat. Also the longer chain homologues (C_{29}, C_{31} and C_{33}) were found to increase in relative abundance with increasing humification in the *Sphagnum* peat, with these homologues accounting for 13% of the total *n*-alkanes in the least humified peat and 61% in the most. A similar trend was also seen in the other peat samples. However, the increase was not so pronounced. The alcohol fraction was found to be composed of a homologous series of *n*-alkanols (≥ 94% of the fraction) which ranged from C_{12} to C_{34} and one isoprenoid alcohol, phytol (3,7,11,15-tetramethylhexadec-2-en-1-ol). The *n*-alkanols had a high even-over-odd predominance (CPI = 5.4-13.1) and the C_{26} compound was the major homologue in nearly all of the peat samples with the exception of the *Bryales* peat which was dominated by the C_{28} homologue. Contrary to the *n*-alkanes, the *n*-alkanol chain lengths became shorter with increasing humification in the *Carex* and *Carex/Bryales* peat. However, no specific humification effects were found in the *n*-alkanol distributions of *Sphagnum* and *Bryales* peats. The sterol fraction was found to consist of 4 major components i.e. β-sitosterol, stigmasterol, campesterol and 3-stigmastanol, which together comprised over 90% of the fraction in most of the peat samples. Comparisons with the sterol fractions of various *Sphagna* revealed that the stanols present in the peat were most likely to be products of microbial hydrogenation of the corresponding sterols. The acidic lipid fraction comprised *n*-alkanoic acids and ω-hydroxy acids. The *n*-alkanoic acids were present in all the samples ranging from C_{13} to C_{34} as bimodal distributions centred at C_{16} or C_{18} and C_{24} or C_{26}. These showed a high even-over-odd

predominance (CPI = 5.4-18.9) and the contribution of longer chain homologues ($\geq C_{22}$) was found to increase with increased humification. The ω-hydroxy acids ranged from C_{12} to C_{28} and were almost completely comprised of even-carbon acids and the C_{24}, C_{26} and C_{28} homologues comprised the predominant part of the fraction in all the peat types. Also present was the unsaturated 18ω-hydroxyoctadec-9-enoic acid. Similarly to the *n*-alkanoic acids the longer chain hydroxy acids ($\geq C_{22}$) increased in relative abundance with increased humification. Overall the peat lipid components were attributed to moss and higher plant source as indicated by the high CPI values of the lipid groups, and the decrease in CPI values of *n*-alkanes with increased humification was ascribed a microbial effect.

Lipid based studies of peat from other types of deposit other than raised bogs have been conducted and this has involved the comparison of organic extracts of peats from tropical, subtropical, temperate and cool temperate climates (Dehmer, 1995). Aliphatic and aromatic hydrocarbon fractions were studied and the author identified odd numbered *n*-alkanes as the major components of the aliphatic fraction. These ranged from C_{14} to C_{40} in tropical mesotrophic peats and C_{21} to C_{35} in subtropical mesotrophic peat. Although the *n*-alkane distributions were fully investigated, the author only suggested that the odd numbered *n*-alkanes C_{25}, C_{27} and C_{29} were indicative of higher plant waxes and that the *n*-alkanes with chain lengths less than C_{23} may be due to bacterial activity. Several hopanoid compounds were identified in the aliphatic fraction. However, these were found to comprise less than 20% of the fraction in most cases. 17α,21β(H)-22*R*-homohopane was again found to be the main hopane present and the author reaffirms that the appearance of hopanoids in peats is likely to be related to microbial activity. The author also identified non-hopanoid aromatic triterpenoids in peat samples from subtropical climates of which 1,2,9-and 2,2,9-trimethyl-1,2,3,4-tetrahydropicene (Fig. 1.4) were the major components. These compounds were identified by their GC retention times and published mass spectra. Their formation is thought to occur through bacterially mediated aromatisation of α-and β-amyrin, as their unsaturated analogues were seen in ombrotrophic peats from cool temperate climates. However, these compounds were found to be absent in poorly humified peats.

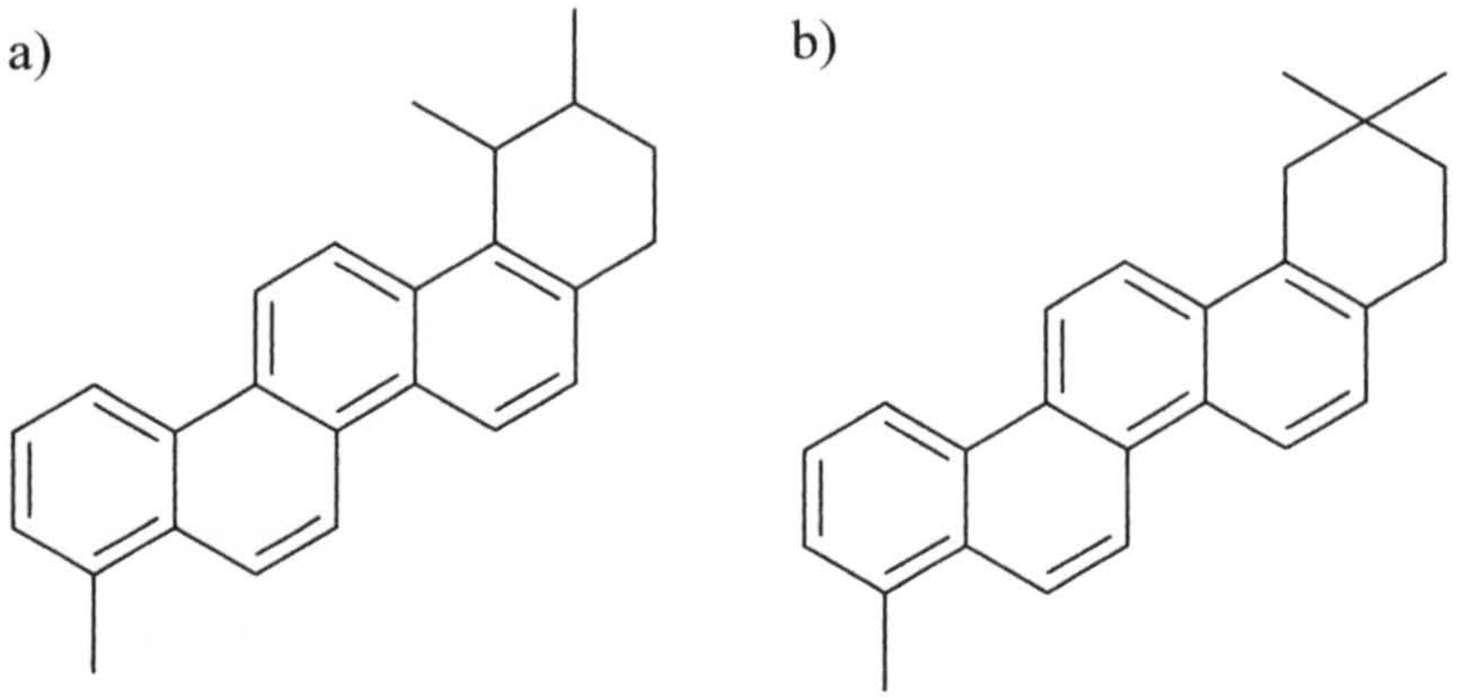

Figure 1.4 Aromatic hydrocarbons, (a) 1,2,9-trimethyl-1,2,3,4-tetrahydropicene and (b) 2,2,9-trimethyl-1,2,3,4-tetrahydropicene present in subtropical mesotrophic peat.

The comparison of pollen and lipid records of changing plant input during the accumulation of a peat bed has also been studied (Farrimond and Flanagan, 1996). In this study the *n*-alkane, *n*-alcohol, sterol and hopanoid contents of 18 samples from a 93 cm thick continuous section of peat were determined and the lipid distributions were correlated with pollen assemblages. As with other studies of peat, the *n*-alkanes were found to have a high odd-over-even carbon number predominance (CPI = 4.7-14) and ranged from C_{17} to C_{35}. Although the *n*-alkane distributions were found to vary significantly among samples, the lack of contributing plant lipid data prevented the identification of plant components from the lipid profiles. However, a multivariate statistical approach was applied to the data set in order to identify the major sources of variation. It was found that the relative abundances of C_{31}-C_{33} and C_{27}-C_{29} *n*-alkanes contributed to the bulk of the variation. Using these as the principal components, it was discovered that a large change in lipid stratigraphy occurred in the upper part of the peat profile, where increased levels of the C_{31}-C_{33} *n*-alkanes prevailed. However, this was found not to relate to the pollen record where tree pollen was concerned and a better correlation was seen with the identified *Sphagnum* spores and the abundances of the C_{27}-C_{29} *n*-alkanes. Similarly, where *n*-alcohol distributions were found to vary pollen data recorded no significant change in plant input. Overall, it was found that although lipid and pollen data show comparable trends in plant input, they did not correlate well in detail and this was attributed to the lipids being derived from autochthonous plant debris and pollen, transported in from surrounding areas.

The $\delta^{13}C$ values of moss and sedge macrofossils from peats have previously been used to reconstruct records of atmospheric CO_2 concentration (a proxy record for

climate) during the Holocene (White *et al.*, 1994). However, this requires that the deposit be well-preserved and contains both sedges and mosses. A recent investigation has taken a compound specific $\delta^{13}C$ approach to try to determine climatic changes over the last 2000 years (Ficken *et al.*, 1998). The study compared the $\delta^{13}C$ values of *n*-alkanes with lipid and macrofossil stratigraphy, to provide information about atmospheric CO_2 concentration and the changing plant inputs to a peat bog. The lipid distributions of peat (54 cm profile) and 12 identified plant species that had been growing on the bog, were determined and compared to establish the origin of the peat lipids. The *n*-alkanes present in the peat samples ranged from C_{19} to C_{33} with the C_{31} homologue as the dominant component in all samples. However, the *n*-alkanes from plants including *Sphagnum* and *Carex* species were found to have C_{25}, C_{27}, C_{29} or C_{31} as the major homologues. The authors found that even in the topmost layer of peat, where plant debris should be least decomposed and macrofossil data well documented, discrepancies occurred between the lipid distributions and the biological inputs. This was especially apparent with *n*-alcohol distributions, where a higher even-over-odd carbon number predominance was observed in peat samples (CPI = 10.0-18.3) than in all but two of the plant species (*Sphagnum capillifolium*, CPI 10.7 and *Carex bigelowii*, CPI 20.3). The $\delta^{13}C$ values for C_{29} and C_{31} *n*-alkanes were established down the 54 cm peat core and compared with values for previously estimated atmospheric CO_2. It was discovered that apart from the $\delta^{13}C$ values of *n*-alkanes in the top 6 cm there was very little variation down the core and the depletion of ^{13}C seen in the topmost samples (average $\delta^{13}C$ for C_{29+31}, -31.5 to -30.7‰) was attributed to burning of fossil fuels lowering the atmospheric ^{13}C content. ^{13}C values of *n*-alkanes from deeper peat samples (average $\delta^{13}C$ for C_{29+31}, -30.1 to -29.7‰) however, did not show a variation that could be used as an assessment for changes in palaeoclimate. Overall, the authors came to the conclusion that it is possible that the macrofossil record betrays the record of plant input, favouring plant species more resistant to decay than others. This was illustrated by the lack of lichen macrofossil data because lichens were present on the surface of the peat deposit. Analysis of the *n*-alkanes from lichens showed C_{29} and C_{31} homologues to be prevalent and as it was suggested that as these lipids were found in high abundance in the peat samples, that a greater proportion of lichens contributed to the peat than suggested by macrofossil analysis.

1.4 Dating Methods

Research on peat bogs to determine past environments and associated climates has a long history, including pollen, macrofossil and humification studies. Accurate dating is of fundamental importance to such palaeoclimatic studies. Without reliable estimates on the age of events in the past it is impossible to investigate if they occurred synchronously or if certain events lead or lag others; neither is it possible to assess accurately the rate at which past environmental changes occurred. Strenuous efforts have therefore been made to date all proxy materials, to avoid sample contamination, and to ensure that the stratigraphic context of the sample is well understood. It is equally important that the assumptions and limitations of the dating procedure used are understood so that a realistic interpretation of the date obtained can be made. It is just as important to know the margins of error associated with a date as to know the date itself (Bradley, 1996).

Absolute dating methods fall into four basic categories: (a) radioisotopic methods, which are based on the rate of atomic disintegration in a sample or its surrounding environment; (b) palaeomagnetic methods, which rely on past reversals of the Earth's magnetic field and their effects on a sample; (c) organic and inorganic chemical methods, which are based on time-dependent chemical changes in the sample, or chemical characteristics of a sample, and (d) biological methods, which are based on the growth of an organism to date the substrate on which it is found. However, when dating peat deposits only radioisotopic methods such as radiocarbon and ^{210}Pb dating or chemical and biological methods such as amino acid dating and dendrochronology are useful in producing reliable dates.

1.4.1 Radio-isotopic methods

Generally, each element has one or more stable isotopes which account for the bulk of its occurrence on Earth. Unstable atoms undergo spontaneous radioactive decay by the loss of nuclear particles (α or β particles) and, as a result, they may transmute into a new element. Furthermore, the decay rate is invariable so that a given quantity of the radioactive isotope will decay to its daughter product in a known interval of time; this is the basis of radio-isotopic dating methods. Providing that the radio-isotope

"clock" is started close to the stratigraphically relevant date, measurement of the isotope concentration today will indicate the amount of time which has elapsed since the sample was emplaced. The amount of time which it takes for a radioactive material to decay to half its original amount is termed its half-life.

For a radioactive isotope to be directly useful for dating it must possess several attributes: (a) the isotope itself, or its daughter products, must occur in measurable quantities and be capable of being distinguished from other isotopes, or its rate of decay must be measurable; (b) its half-life must be of a length appropriate to the period being dated; (c) the initial concentration level of the isotope must be known, and (d) there must be some connection between the event being dated and the start of the radioactive decay process (the "clock", Bradley, 1996).

Radiocarbon dating - Radiocarbon (^{14}C) is produced in the upper atmosphere by neutron bombardment of atmospheric nitrogen atoms:

$$^{14}_{7}N + ^{1}_{0}n \rightarrow ^{14}_{6}C + ^{1}_{1}H$$

The neutrons have a maximum concentration at around 15 km and are produced by cosmic radiation entering the upper atmosphere. Although cosmic rays are influenced by the Earth's magnetic field and tend to become concentrated near the geomagnetic poles (thus causing a similar distribution of neutrons and hence ^{14}C), rapid diffusion of ^{14}C atoms in the lower atmosphere obliterates any influence of this geographical variation in production. ^{14}C atoms are rapidly oxidised to $^{14}CO_2$, which diffuses downwards and mixes with the rest of atmospheric carbon dioxide and hence enters into pathways of the biosphere.

During the course of geological time, an equilibrium has been achieved between the rate of new ^{14}C production in the upper atmosphere and the rate of decay of ^{14}C in the global carbon reservoir. This means that the 7.5 kg of new ^{14}C estimated to be produced each year in the upper atmosphere is approximately equal to the weight of ^{14}C lost throughout the world by the radioactive decay of ^{14}C to nitrogen, with the release of a β particle (an electron):

$$^{14}_{6}C \rightarrow ^{14}_{7}N + \beta + \text{neutrino}$$

The total mass of global ^{14}C thus remains constant. This assumption of an essentially steady concentration of radiocarbon during the period useful for dating is fundamental to the method, although small fluctuations in the production of ^{14}C have to be considered.

Plants and animals assimilate a certain amount of ^{14}C into their tissues through photosynthesis and respiration; the ^{14}C content of these tissues is in equilibrium with that of the atmosphere because there is a constant exchange of new CO_2 as old cells die and are replaced. However, as soon as an organism dies, this exchange and replacement of ^{14}C from the atmosphere ceases. From that moment on the ^{14}C content of the organism declines as the ^{14}C decays to nitrogen, and the ^{14}C content is therefore purely a function of time (Fig. 1.5).

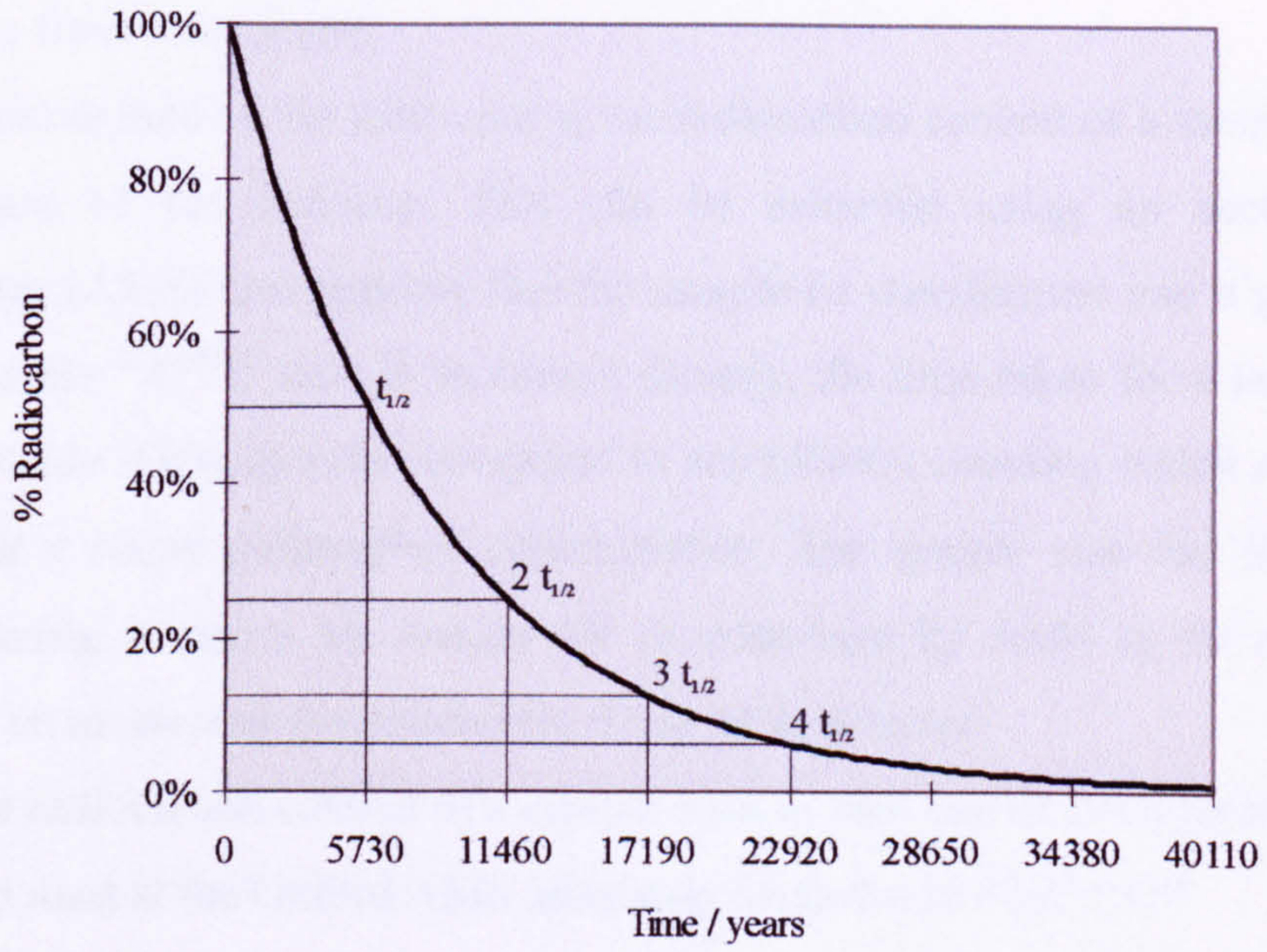

Figure 1.5 Radiocarbon decay curve

One method for the determination of the ^{14}C content of a sample is to measure the rate of β-particle emission. This can be done in one of two ways, either by proportional gas counters or liquid scintillation techniques. In the former method, carbon is converted into a gas (methane, carbon dioxide, or acetylene) which is then put into a "proportional counter" capable of detecting β particles. In liquid scintillation procedures, the carbon is converted into benzene or some other organic liquid and

placed in an instrument which detects scintillations (flashes of light) in the liquid, produced by β-particle emissions (Fig. 1.6).

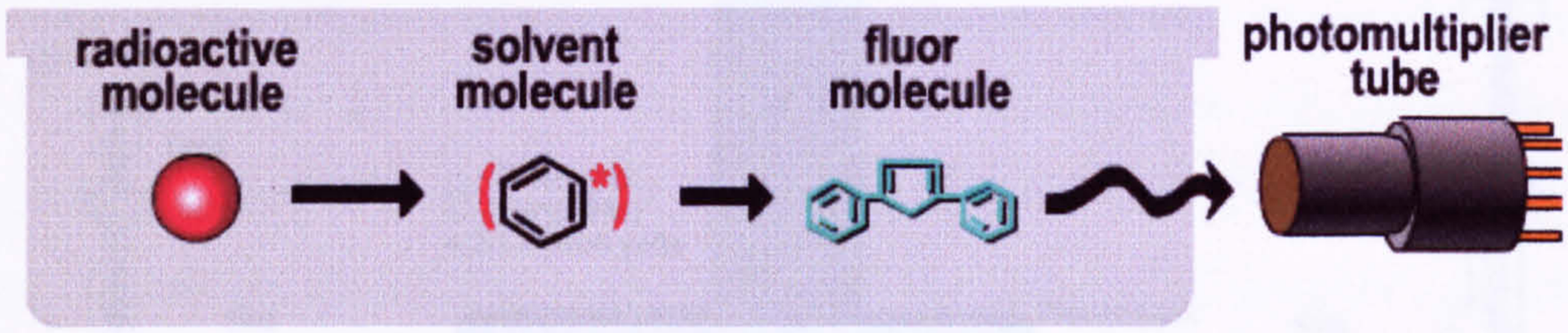

Figure 1.6 Schematic of liquid scintillation counting.

In both cases, stringent measures are necessary to shield the sample counters from extraneous radioactivity in the instrument components, laboratory materials, and surrounding environment, including the occasional cosmic ray penetrating the Earth's atmosphere from outer space.

Another method for determining the radiocarbon content of a sample is by direct measurement of the isotopes. This can be achieved using an accelerator mass spectrometer (AMS) and requires that the sample be transformed into a graphite target or CO_2. As the $^{14}C/^{12}C$ ratio is measured directly, the time taken for a measurement is reduced to only a few minutes, compared to scintillation counting which can take hours or days for a single radiocarbon determination. The sample size that is required for accurate dating is also a lot smaller for measurement by AMS as the method is not dependent on measuring the radioactive decay of an artefact.

The radiocarbon content of a sample such as peat can be determined using AMS. The system used at the Oxford AMS laboratory is shown in Figure 1.7.

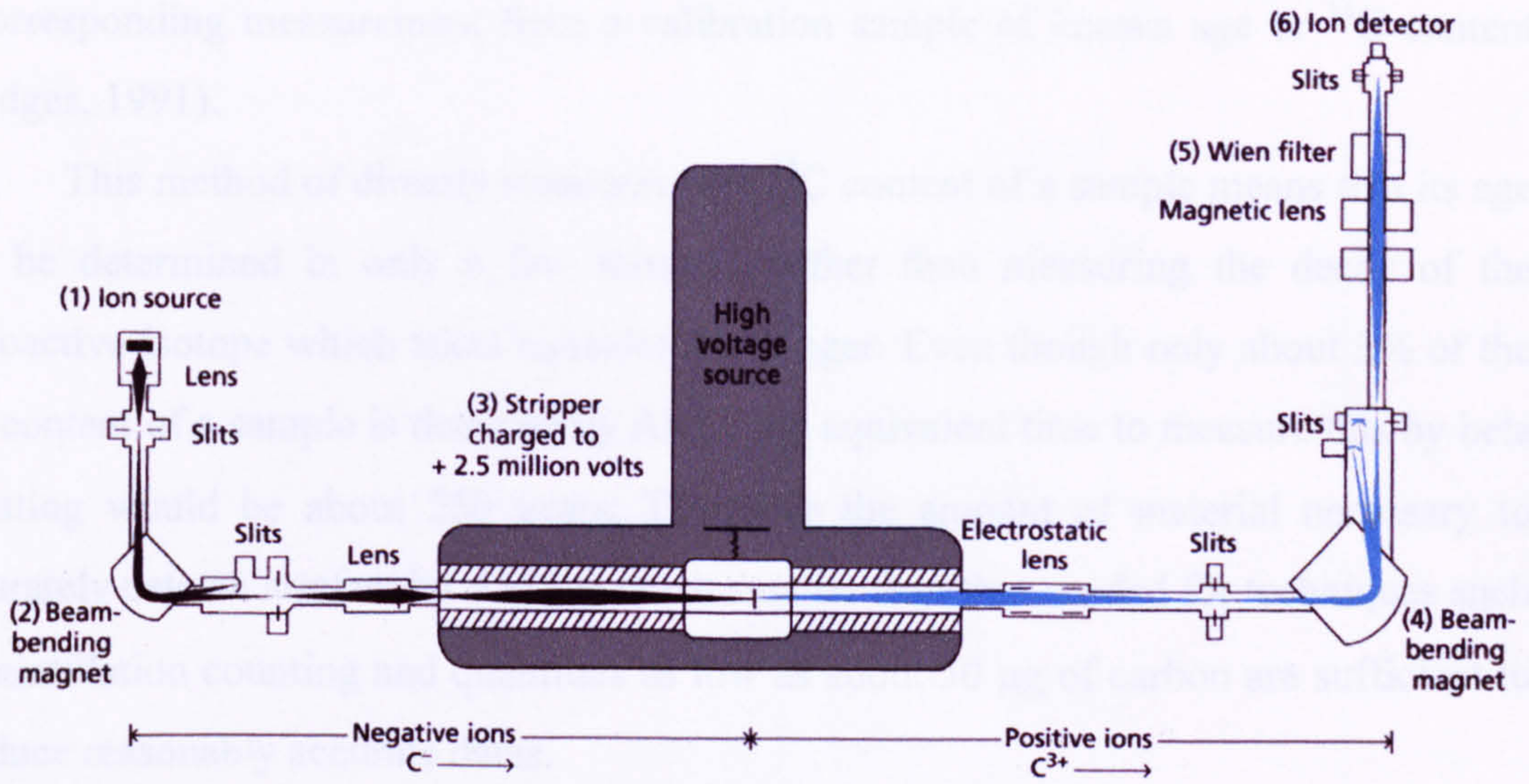

Figure 1.7 The accelerator mass spectrometer at the Oxford AMS laboratory. Negative ions in black, positive ions in blue.

The carbon sample is introduced into the ion source (1) after being converted into either a graphite target or CO_2, where it is bombarded with caesium ions. This produces both positive and negative ions. The negative ions are accelerated out of the ion source by a positive field towards a beam-bending magnet (2). As ^{14}N does not form negative ions that live long enough to pass through the accelerator they are eliminated (Bennett *et al.*, 1977). Here ions of mass 14 are selected from the ion beam and travel towards the stripper (this will include $^{12}CH_2^-$ and $^{13}CH^-$ as well as $^{14}C^-$ ions).

The stripper (3) is charged to +2.5 million volts. The negative ions are accelerated to high energies by the powerful electric field and enter the stripper. Here, the ions collide with gas molecules to form multiple-charged positive ions. These ions are then accelerated away from the stripper to a second magnet (4), where, $^{14}C^{3+}$ are selected (any remaining $^{12}C^{3+}$ or $^{13}C^{3+}$ ions are removed). However, other ions with a similar momentum and charge to the $^{14}C^{3+}$ ions, but with a different combination of mass and velocity, might also follow the ^{14}C ions round the magnets. So a Wien filter (5) is used, which combines both magnetic and electric fields and deflects ions according to their velocity. This ensures that very few ions, other than the ^{14}C ions, traverse both the magnet and the Wien filter. The $^{14}C^{3+}$ ions are finally distinguished from any remaining contaminating ions by a detector (6) which identifies and counts each ion as it enters. The number of ^{14}C ions counted from a given sample (relative to the beam current of ^{12}C ions) depends on the age of the specimen and is compared with

a corresponding measurement from a calibration sample of known age or ^{14}C content (Hedges, 1991).

This method of directly measuring the ^{14}C content of a sample means that its age can be determined in only a few minutes, rather than measuring the decay of the radioactive isotope which takes considerably longer. Even though only about 3% of the ^{14}C content of a sample is detected by AMS, the equivalent time to measure this by beta counting would be about 250 years. Therefore the amount of material necessary to accurately date an artefact by AMS is much smaller than that needed for techniques such as scintillation counting and quantities as low as about 50 μg of carbon are sufficient to produce reasonably accurate dates.

Radiocarbon dating either by scintillation counting or AMS, is a reliable method for determining the age of peat deposits, as long as the sample size is adequate for the chosen method and contains little or no carbon contamination. Radiocarbon dating can be used reliably for samples that are up to 100,000 years old, but it is more commonly used for samples that are no older than 40,000 years. Therefore for Holocene deposits of peat (<14,000 y) radiocarbon dating is an ideal method for age determination.

Uranium-series dating - This encompasses a range of dating methods, all based on various decay products of ^{235}U or ^{238}U (Fig. 1.8). In a system containing uranium, which is undisturbed for a long period of time (~10^6 y), a dynamic equilibrium will prevail in which each daughter product will be present in such an amount that it is decaying at the same rate as it is formed by its parent isotope (Broecker and Bender, 1972). The ratio of one isotope to another will be essentially constant. However, if the system is disturbed, this balance of production and loss will no longer prevail and the relative proportions of different isotopes will change. By measuring the degree to which a disturbed system of decay products has returned to a new equilibrium, an assessment of the amount of time elapsed since disturbance can be made. In natural systems, disturbance of the decay series is common, because of the different physical properties of the intermediate decay series products. Most important of these is the fact that ^{230}Th and ^{231}Pa are virtually insoluble in water. In natural waters these isotopes are precipitated from solution as the uranium decays, and collect in sedimentary deposits.

Radionuclide	Half Life
Uranium 238	$4.5x10^9$ y
↓	
Thorium 234	24.1 day
↓	
Protactinium 234	1 min
↓	
Uranium 234	$2.45x10^5$ y
↓	
Thorium 230	$7.6x10^4$ y
↓	
Radium 226	1600 y
↓	
Radon 222	3.8 day
↓	
Polonium 218	3 min
↓	
Lead 214	27 min
↓	
Bismuth 214	20 min
↓	
Polonium 214	160 μs
↓	
Lead 210	22 y
↓	
Bismuth 210	5 day
↓	
Polonium 210	138 day
↓	
Lead 206	Stable

Figure 1.8 Uranium 238 series - including daughter isotopes

As the isotope is buried beneath subsequent sedimentary accumulations, it decays at a known rate, "unsupported" by further decay of the parent isotopes (^{234}U and ^{235}U respectively) from which it has been separated. Thus, in a sediment which has been deposited at a uniform rate, the ^{230}Th and ^{231}Pa concentrations decrease exponentially with depth. Providing that this initial concentration of the isotopes is known, the extent to which they have decayed in sediment beneath the surface can be related to the amount of time elapsed since the sediment was first deposited. Isotopic decay is expressed in terms of the activity ratio of $^{230}Th/^{234}U$ and $^{231}Pa/^{235}U$; for the former, the useful dating range is 10,000-350,000 y Before Present (y BP), and for the latter 5,000-150,000 y BP. It is assumed that the oceanic uranium isotope composition in the past has been invariant, which is a reasonable assumption for the deep oceans but very unlikely for closed inland basins, making the technique inapplicable in such areas.

^{210}Pb dating - On a much shorter timescale, unsupported ^{210}Pb may also be used as a chronological aid. ^{210}Pb is derived from the decay of ^{222}Rn following the decay of ^{226}Ra from ^{230}Th. Both ^{226}Ra and ^{222}Rn escape from the Earth's surface and enter the atmosphere, where the ^{210}Pb is eventually produced. ^{210}Pb is then washed out of the atmosphere by precipitation or settles out as dry fall-out, where it accumulates in sedimentary deposits and decays (with a half-life of 22 years) to stable ^{206}Pb. Assuming that the atmospheric flux of ^{210}Pb is constant, the decay rate of ^{210}Pb to ^{206}Pb with depth can be used to date sediment accumulation rates (e.g. Koide *et al.*, 1973). It is of value only in dating sediments over the last 200 years, but this may be of particular value in isolating core-top floral and faunal elements for calibration with instrumental climatic data, to derive accurate transfer functions for palaeoclimatic reconstructions. It has also proved useful in dating the upper sections of ice cores and hence allowing estimates of long-term accumulation rates to be made (Crozaz and Langway, 1966; Crozaz *et al.*, 1964). More recently ^{210}Pb dating has been used to determine the accumulation rates of ombrotrophic peat bogs (Aaby *et al.*, 1979; Appleby *et al.*, 1988; El-Daoushy *et al.*, 1982).

1.4.2 Chemical dating methods

Amino acid dating - Virtually all amino acids in living organisms occur in the L configuration (apart from those produced by bacteria) and the interconversion to the D configuration takes place by racemisation. The extent of the racemisation increases with time after death of the organism. This can be measured by gas or liquid chromatographic methods. Unfortunately, unlike radionuclide decay rates, racemisation rates are sensitive to a number of environmental factors, particularly temperature and pH (Hare and Mitterer, 1968). Also the contribution of D-amino acids from bacterial proteins, common to peatlands, make it hard to determine the degree of interconversion. However, if the proteins are purified prior to the analysis of constituent amino acids, bacterial inputs can be eliminated. The presence of amino acids in peat would suggest that this technique could be used for assessment of its age. However, the uncertainty of many environmental factors would exacerbate the uncertainty in the date.

Tephrochronology - Tephra is a general term for the airborne pyroclastic material ejected during the course of a volcanic eruption (Thorarinsson, 1981).

Extremely explosive eruptions may produce a blanket of tephra covering vast areas and therefore form regional isochronous stratigraphic markers. Tephras themselves may be dated directly, by potassium-argon or fission-track methods, or indirectly by closely bracketing radiocarbon dates on organic material above and below the tephra layer. The incorporation of tephra in peat is common and if these particles can be linked to specific volcanic eruptions, accurate dating of peat horizons can be made (e.g. Gillespie *et al.*, 1992).

1.4.3 Biological dating methods

Biological dating methods generally use the size of an individual species of plant as an index of the age of the substrate on which it is growing. They may be used to provide minimum age estimates only, since there is inevitably a delay between the time a substrate is exposed and the time it is colonized by plants, particularly if the surface is unstable. Fortunately this delay may be short and not significant, particularly if the objective is simply relative age dating.

Dendrochronology - Dendrochronology is the dating of past events (climatic changes) through study of tree ring growth. Each year a tree adds a layer of wood to its trunk and branches thus creating the annual rings seen when a cross section is viewed (Fig. 1.9). New wood grows between the old wood and the bark. In the spring, when moisture is plentiful, the tree devotes its energy to producing new growth cells. These first new cells are large, but as the summer progresses their size decreases until, in the autumn, growth stops and cells die, with no new growth appearing until the next spring. The contrast between these smaller old cells and next year's larger new cells is enough to establish a ring, thus making counting possible.

The climatic changes or patterns in specific geographic areas can be traced by the study of old living trees. Samples taken from trees of unknown age can then be studied for matches with samples from trees with known sequences of growth. Using this process, when the rings 'match' or are found to be overlapping in age, the record can be continued further back in time.

Figure 1.9 Photograph of tree rings showing different annual cycles.

Dendrochronology has raised questions regarding radiocarbon dating methods and has been use to recalibrate the ^{14}C process. Each ring dated by dendrochronology can have its radiocarbon content measured and small fluctuations in the production of ^{14}C over time be estimated. The Irish oaks used for the production of the radiocarbon calibration curve, were in part themselves preserved in peat bogs (Pilcher *et al.*, 1984). Therefore any tree growing on a peat bog and subsequently preserved so that the remains contain a record of its rings can be compared with existing records to establish a date for the surrounding peat.

1.5 Application of Dating Techniques for the Age Determination of Peat Deposits

As discussed above, tephrochronology, dendrochronology, amino acid, ^{210}Pb and radiocarbon dating can all be used to determine the age of peat deposits. However, to provide meaningful age determinations the correct technique must be selected. For peat deposits that are thought to be less than 200 years old, techniques such as ^{210}Pb dating would be most beneficial as they would provide contrasting results for horizons that had been deposited seemingly close together. However, most peat deposits found in the northern hemisphere have accumulated during the Holocene and the use of ^{210}Pb dating is therefore restricted to the top few centimetres where peat has only recently

accumulated. Peat deposits can also be dated by tephrochronology and where this can be used, very reliable dates can be inferred, but the use of this technique is subject to several provisos. Tephrochronology can only be applied to peat dating if the horizon to be dated contains sufficient Tephra particles and that these particles can be identified. The process of obtaining Tephra from peat is a laborious one, with the continual acid digestion of material from chosen horizons until all that remains are the particles. Even when this has been done there is no guarantee that the particles will be present and identifiable. The most widespread technique for the age determination of Holocene peat deposits is radiocarbon dating. However, the organic matter contained in peat has been found to be one of the least desirable materials for radiocarbon dating and studies of peat deposits of 12,000 y BP and older, have been found to be contaminated with younger, more mobile carbon material, such as fulvic and humic acid fractions (Hammond *et al.*, 1991). Therefore in order to produce reliable radiocarbon dates from peat, only the material present at the deposition of the horizon should be dated.

Studies tackling some of the problems of sediment dating including the radiocarbon dating of different peat components have been performed. Some of these studies have involved the radiocarbon dating of macrofossils, amino acids, cellulose and total lipid extracts (Fowler *et al.*, 1986a; Fowler *et al.*, 1986b) and others have concentrated on specific lipid subfractions (Bol *et al.*, 1996; Huang *et al.*, 1996).

One study examined the effectiveness of 14 chemical pre-treatment methods on the radiocarbon determination of peat and organic silt samples (Hammond *et al.*, 1991). The authors identified a Tephra layer dated as 22,580 ± 230 y BP which was contained within a peat deposit. Peat and organic silt samples from immediately above and below the Tephra were removed and portions of these were subjected to different chemical pre-treatments before being radiocarbon dated. The pre-treatments included the separation of humic constituents (fulvic acids, humic acids and residual fractions) with NaOH, pre-treatment with HCl/HF (yielding fulvic acids, humic acids and residues), separation of the lipid fraction with organic solvents, separation of the lipid fraction with chloroform alone, hydrolysis with HCl and the residues and hydrolysates produced from heating with HNO_3. Extraction of cellulose with $NaClO_2$ was also performed, but the amount extracted was insufficient for dating. All of the fractions and residues were dated by AMS and the ^{14}C content compared with that of the untreated portions. In general, it was found that the ^{14}C dates of the untreated samples were significantly younger than those that had been treated, with the greatest difference occurring in the residues of the

samples that had been treated with HNO_3. Separation of the humic constituents revealed that the residue yielded a considerably older date than the corresponding fulvic acids. This was expected as the solubility of fulvic acids in water makes them mobile and more likely to be leached through the peat. The lipid fractions from the samples were also found to be older than the untreated peat with the lipids extracted with organic solvents and those separated with chloroform alone, yielding ^{14}C dates of 2650 and 1900 y, respectively, older than the untreated peat (12,550 y BP). The difference in radiocarbon determination of the two lipid samples was attributed to retention of organic solvents in the fraction after extraction.

Other studies which have compared different pre-treatments of peat for radiocarbon dating have used more conventional fractions for comparisons with lipid fractions (Fowler *et al.*, 1986b). In this study 5 peat samples (3 from a Scottish freshwater bog SM1, SM2 and SM3 and 2 from an English palaeochannel overlain by a clay deposit RB1 and RB2) were separated into 9 different fractions for radiocarbon dating. Figure 1.10 shows the different dating fractions obtained.

The total crude lipid extracts were further separated into two fractions, one containing alkanes, fatty acids and sterols and the other, more polar lipids. The radiocarbon dates of the separate components revealed that in two of the three samples from the freshwater peat (SM1 and SM2) the total crude lipid extract I (SM1 10,580 ± 245 and SM2 10,330 ± 165 y BP) and polar lipids (SM1 10,580 ± 245 and SM2 10,180 ± 165 y BP) were found to give significantly older dates than the corresponding humic acids (SM1 9180 ± 215 and SM2 8730 ± 195 y BP) and those dates provided by conventional preparation (SM1 9200 ± 215 and SM2 9630 ± 195 y BP). However, the total crude lipid extract II provided the oldest radiocarbon determination in the third sample (SM3 10,100 ± 180 y BP) with all of the other components producing similar dates (8160-8820 y BP). Analysis of the lipid extracts revealed that all of the samples were dominated by higher plant material, but this was least so in the first extract of SM1 and the second extract of SM3 where increased algal/bacterial components were discovered. None of the radiocarbon dates of the components from the palaeochannel peat deposit (RB1 and RB2) were found to be significantly different (2350-2700 y BP) and it was suggested that the deposit was a simple sedimenting system with a major terrestrial higher plant carbon source.

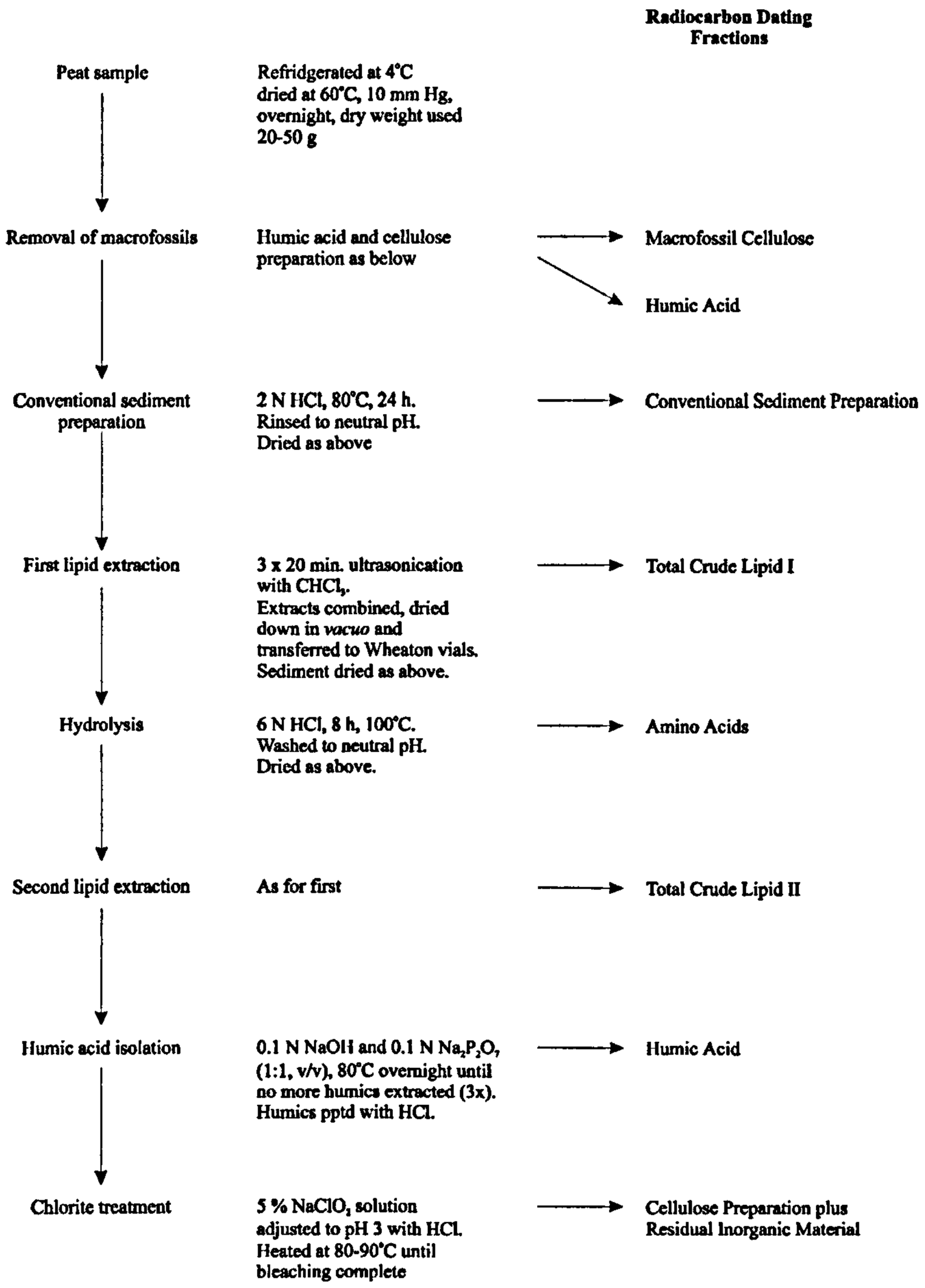

Figure 1.10 Sample preparation procedures used for the comparison of ^{14}C contents of different peat fractions (Fowler *et al.*, 1986b).

In a more recent study of the radiocarbon ages of organic matter and lipid constituents in soil, specific lipid subfractions were radiocarbon dated (Bol *et al.*, 1996). This study compared ^{14}C contents of aliphatic hydrocarbon and carboxylic acid fractions, HCl hydrolysis residues and total soil of stagnohumic gley soil. The soil samples (2 cm contiguous slices) were taken from a 28 cm soil core and contained slightly decomposed mosses and grasses in the top 3.5 cm, humified peat between 3.5 and 12.5 cm, organic rich clay loam between 12.5 and 16.5 cm and a mineral clay loam below this. Lipid extracts were obtained by repeated sonication of the soil samples using a solvent system of increasing polarity. The total fraction was further separated using

solid-phase extraction to isolate acids, followed by silica-gel column chromatography of the neutral fractions such that the aliphatic hydrocarbons could be isolated. The lipid fractions of samples 3.5-5.5 cm, 12.5-14.5 cm and 21.5-24.5 cm were then radiocarbon dated and compared to HCl hydrolysis residues and total soil dates. The aliphatic hydrocarbons were found to be the oldest components of the soil, exhibiting ^{14}C dates up to 3260 y BP older than the corresponding total soil sample. However, the carboxylic acid fraction was found to be the youngest component with radiocarbon dates equivalent to modern sources. This was attributed to the vertical mobility of this fraction within the soil, resulting in the addition of young material from overlying horizons. This fraction was identified by GC and GC/MS and found to be dominated by C_{14} to C_{34} *n*-acids and hydroxy acids, but the authors suggested that it might also have contained amino acids and carbohydrates bearing carboxylic groups, that were not seen on gas chromatograms under the analytical conditions used. If these compounds were from 'recent' plant and organic debris that had leached down the soil profile and been incorporated into the carboxylic fraction, then this could be a possible explanation of the encountered ^{14}C enrichment.

The variations seen in the radiocarbon determinations of the different components in these studies reaffirm the problems associated with the dating of sedimentary systems and the necessity to only date the carbon indigenous to the horizon in question. Therefore proper identification of the dateable material must be performed so that any contamination from extraneous sources can be eliminated. Investigations into the isolation of single lipid compounds in quantities sufficient for their radiocarbon determination by AMS have been performed (Eglinton *et al.*, 1996). This study used preparative capillary GC (PCGC) to concentrate single compounds from lipid extracts of samples which were selected to cover a range of radiocarbon dates and yield a variety of compound classes representative of the types encountered in geochemical samples. These included petroleum samples with infinite radiocarbon age, modern plant samples and a sample of oil independently dated at 1498 BC. The lipid fractions obtained from these samples were identified by GC/MS and selected compounds were isolated by repeated automated injection on a PCGC system. The *n*-alkanes, C_{15}, C_{20}, C_{22}, C_{25} and C_{30} where separated from the petroleum sample and radiocarbon dated. Similarly, C_{29}, C_{31} and C_{33} *n*-alkanes were isolated from modern plants (*Crassula argentea* and *Agave americana*) along with $C_{16:0}$ and $C_{18:1}$ fatty acids and a $C_{29:1}$ sterol. Six fatty acids and 2 unknown compounds were separated from the oil sample and the radiocarbon dates of

each compound compared with the assumed date of the originating matrix. The authors found that using the PCGC system it was possible to isolate >250 μg of carbon by the repeated injection of the sample mixture and that there was minimal ^{14}C contamination from the process. It was found that the alkanes separated from the petroleum sample had an infinite age which suggests that the single compounds were free from ^{14}C contamination. The ^{14}C ages of the individual compounds from the oil sample closely bracketed that of the bulk sample, although one of the fatty acids ($C_{21:0}$) was found to be of modern origin. However, this fatty acid was a standard that was added to oil prior to separation of the single compounds and was used to assess the validity of recovering compounds with variable and distinct radiocarbon signatures within a heterogeneous matrix. The modern plant lipids from *C. argentea* were found to give radiocarbon dates that were older than modern (1530-1650 y BP) and this was attributed to the plant specimens being grown in a greenhouse which was heated by burners fuelled with natural gas. The resulting CO_2 produced from these burners was incorporated into the plants during photosynthesis, giving rise to the anomalously old ^{14}C ages observed. The fatty acids and sterol from *A. americana* were found to give modern radiocarbon dates which was consistent with the bulk material and history of the plant. In general, the use of PCGC for the isolation and AMS radiocarbon dating of single compounds was found to be an excellent tool for the ^{14}C-based age determinations of matrices containing inputs of unknown source.

This technique has been applied to selected hydrocarbon compounds from marine sediments (Eglinton *et al.*, 1997). Here the PCGC and AMS approach to radiocarbon determination of single compounds was applied to marine sediments where organic material from various sources and with different ages are deposited concurrently. Two marine sediments were studied, one from the Black Sea and the other an Arabian Sea deposit. The natural ^{14}C content of specific biomarker compounds chosen to reflect both autochthonous and allochthonous inputs were measured and the magnitude and source of age variation evaluated. The following biomarkers were chosen: long chain alkenes (C_{37-39}) for marine photoautotrophy, C_{29} and C_{31} alkanes for allochthonous inputs of C_3 vascular plants and shorter chain *n*-alkanes (C_{23-27}) of unknown source (Black Sea), two sterenes for marine primary production, highly branched isoprenoid (HBI) alkenes for diatoms, hopanoid alkenes as bacterial biomarkers and shorter chain *n*-alkanes (C_{23-29}) of unknown source (Arabian Sea). The long chain alkenes from the Black Sea were found to have comparable dates (950 ± 100

y BP) with the total organic carbon (TOC) in the sediments (880 ± 25 y BP) as would be expected from an autochthonous source. The C_{29} and C_{31} alkanes also had similar dates (610-500 ± 100 y BP) and it was suggested that, although these compounds were from allochthonous sources, they indicate a relatively fresh terrestrial input incorporated into the sediment. However, the C_{23-27} *n*-alkanes had radiocarbon determinations 1130-1340 y BP suggesting that they had more than one source. It was proposed that they were from both higher plants and fossil hydrocarbons and an isotopic mass balance approach was used to determine the contribution of each source to these compounds. This was found to correspond to a 9% input of fossil hydrocarbons. Such a small contribution would not have noticeably affected carbon number distributions or $\delta^{13}C$ values but is clearly revealed by the ^{14}C analysis. The Arabian Sea samples were found to encompass a greater range of carbon dates (225-10,300 y BP). The sterenes were found to have a younger date than that of the TOC (680 and 890 y BP, respectively) and the authors suggested that as sterenes are generic markers for phytoplankton and some zooplankton that older organic carbon inputs have been incorporated into the sediment. The hopanoid alkenes were found to have ^{14}C ages of about 300-400 y older than the sterenes and their marine origin was indicated by their relatively uniform $\delta^{13}C$ compositions (-20.5 to -23.9‰). However, the increased age of these compounds was attributed, in part, to the incorporation of fossil hydrocarbons. The ^{14}C dates of HBI alkenes were found to be substantially younger (280 y BP) than both the sterenes and TOC and their presence was attributed to mixing of modern surficial material in the sediment. Similarly to the Black sea samples, a high odd-over-even predominance of C_{25} to C_{31} *n*-alkanes suggested that these compounds were from higher plants and their ^{14}C determinations (7,200-10,300 y BP) were found to be considerably older than the TOC of the sediment. Sources of plant detritus were believed to be dust plumes from desiccated lacustrine sediments formed about 6000 y ago when the eastern African environment was less arid and this is consistent with the age of the alkanes.

This study has shown that the individual lipids even from a homologous series of compounds can have very different ^{14}C contents and therefore different sources not revealed by other methods. Therefore, the radiocarbon dating of lipid fractions or sub-fractions is not always sufficient in elucidating the ^{14}C content of a single source. However, the ^{14}C ages of individual compounds whose structures indicate an unmistakable link to a known precursor can be used to provide accurate age

determinations of specific sources where other methods include uncertainties associated with extraneous carbon.

1.6 Aims of Thesis

Previous studies relating past environments to lipid stratigraphy in peat bogs have had limited success. Studies involving the correlation of pollen and lipid records have been found to be hampered by the allochthonous presence of pollen which does not reflect the sources of lipids contained within peat samples (Farrimond and Flanagan, 1996). Other studies have concentrated on *n*-alkane, *n*-alkanol and *n*-alkanoic acid distributions in peat and plant samples which were related to expected results based on macrofossil analyses (Ficken *et al.*, 1998). However, this approach provided only limited agreement and did not include specific biomarker compounds for the peat inputs.

The present study investigates the composition of Bolton Fell Moss (BFM) peat on a molecular scale at different depths and tries to identify their origins with respect to plant material present in the peat. The organic geochemistry of peat lipids has not been fully investigated in the past and this investigation encompasses a much more comprehensive study that relates compounds found in peat to precursors present in the input material. Where macrofossil data is unobtainable it is hoped reconstruction of the peat components can be deduced and that early stages of peat bog development be determined on a molecular level.

The radiocarbon dating of peat to fix timescales for proxy-climate records has many complications. Most studies of peat samples encounter isotopically and chemically heterogeneous matrices which complicate ^{14}C-based age determinations. The radiocarbon content of bulk organic carbon in peat is assumed to reflect the age of the horizon from which it was taken. A major uncertainty in these organic carbon-based measurements is the unknown proportion of reworked carbon within the peat. Even with purified subfractions of organic matter from the peat it is still not possible to directly equate these ages with a specific source. It is only on a molecular level that ^{14}C ages can be related to individual compounds whose structures indicate an unmistakable link to a known precursor (Eglinton *et al.*, 1996). These biomarkers can be any organic compound whose carbon skeleton can be unambiguously linked with a known natural product from a single source. The application of PCGC and AMS methods for the age determination of individual compounds from sedimentary deposits has only included

compounds that do not need derivatisation prior to chromatographic separation (Eglinton *et al.*, 1997). In the present study, compounds that contain functional groups (often more indicative of specific source) that prevent their chromatographic separation without derivatisation were isolated using a PCGC system and radiocarbon dated by AMS.

The main aims of this study were to:

I. Identify lipids from peat corresponding to major excursions in the macrofossil record. These profiles including specific biomarker compounds can then be used to determine inputs to the peat in other horizons where macrofossil data are not well defined.
II. Establish changes in the lipid composition over an depth of peat where a major transition in peat-forming plants is observed in macrofossil records.
III. Characterise lipids from peat deposited during the earliest phase of bog development where macrofossil data is absent due to extensive humification. Use this information to establish the plant inputs and determine whether the formation of Bolton Fell Moss is typical of raised bogs.
IV. Produce methods for the separation of specific biomarker peat lipids using preparative capillary gas chromatography (PCGC) in quantities suitable for radiocarbon dating by AMS. Identify sources and quantities of extraneous carbon associated with the technique. Compare bulk and single compound radiocarbon determinations so that more reliable radiocarbon dates can be inferred. Such compounds should therefore be well resolved on the gas chromatography column, from a known source within the peat, present throughout samples being analysed and in quantities sufficient for the analytical process.

2. BOLTON FELL MOSS

2.1 Geographical Setting of Bolton Fell Moss

Bolton Fell Moss (BFM), Cumbria, England (National Grid reference NY495695, Fig. 2.1) is a large, raised ombrotrophic mire covering an area of 365 ha with a maximum depth in excess of 10 m on the rand (raised central dome) and an average depth in excess of 6 m (Barber, 1998). Presently, the bog is dominated by *Sphagnum* moss and previous detailed work on the peat suggested that this mire was particularly responsive to climatic change (Barber *et al*., 1994b).

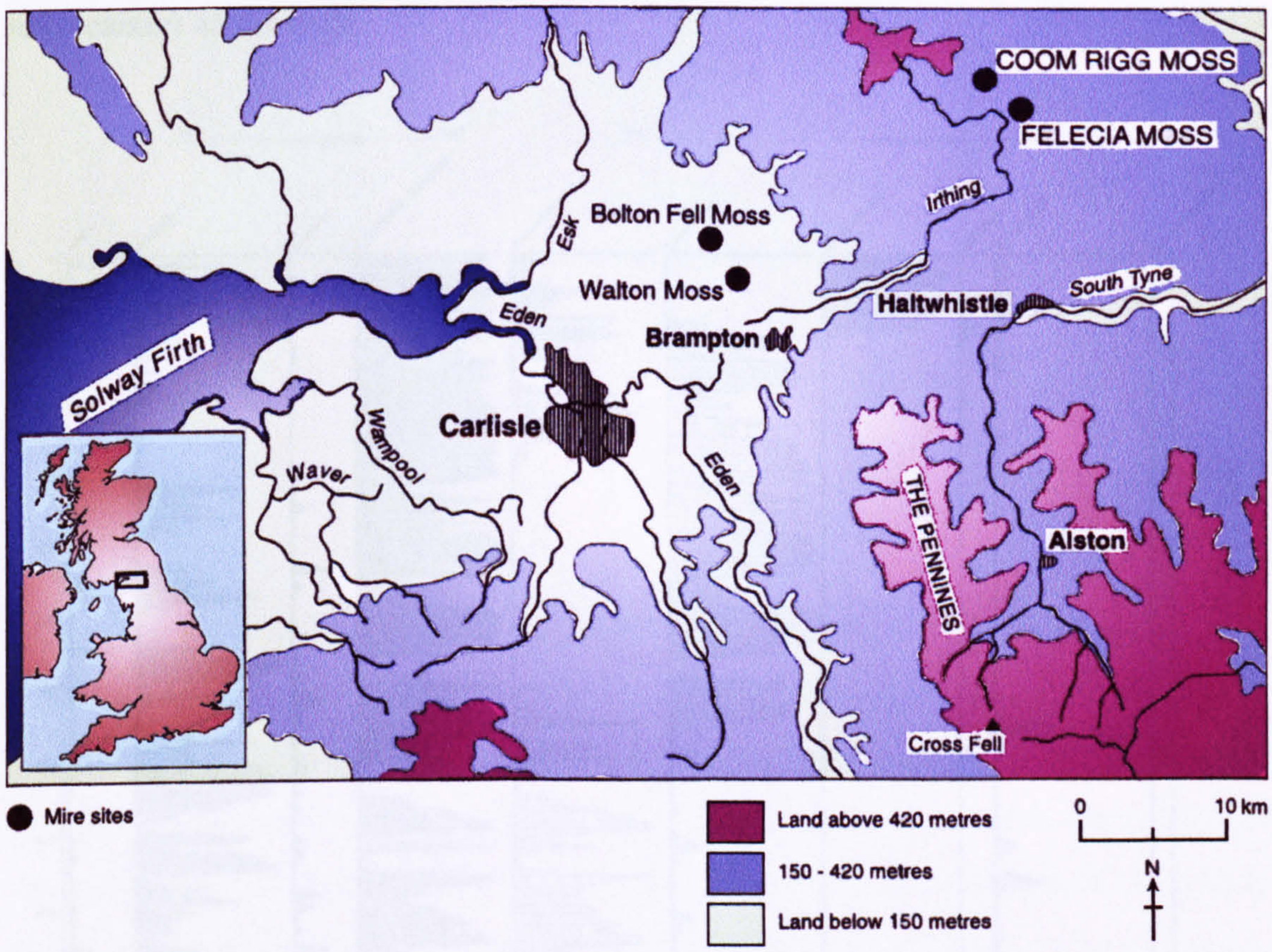

Figure 2.1 Location of Bolton Fell Moss.

2.2 Previous Studies of Bolton Fell Moss

The utilisation of records detailing plants preserved in peat bogs has proved to be productive in the reconstruction of past climates, especially during the Holocene, and such techniques were applied to peat extracted from BFM (Barber *et al.*, 1994b). A 8.3 m peat profile was taken from the bog and 1 × 1 × 4 cm samples of the peat remains were examined under a microscope at ×10 magnification. *Sphagnum*, Monocotyledons, unidentifiable organic matter and Ericaceous remains were identified and the proportion of individual taxa of *Sphagnum* estimated at high magnification (×400). These macrofossil diagrams are shown in Figures 2.2 and 2.3 and indicate the wide variation in plant input to the peat, arranged from the driest-indicator (unidentifiable organic matter) on the left, through to the wettest indicators (*Sphagnum* species *S. cuspidata* and *S. subsecunda*) on the right.

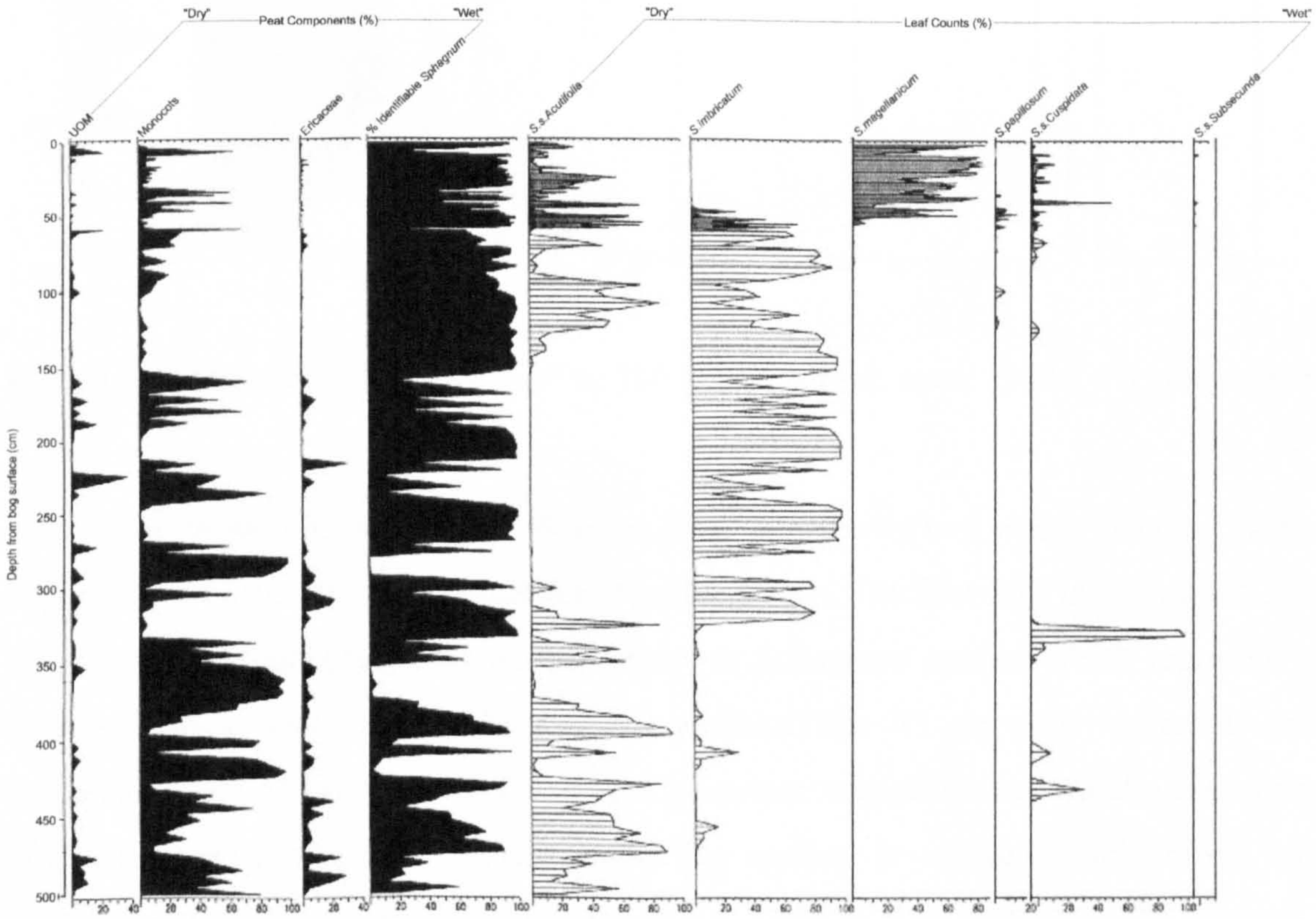

Figure 2.2 Macrofossil diagram of a 0-500 cm peat core. UOM - Unidentified Organic Matter

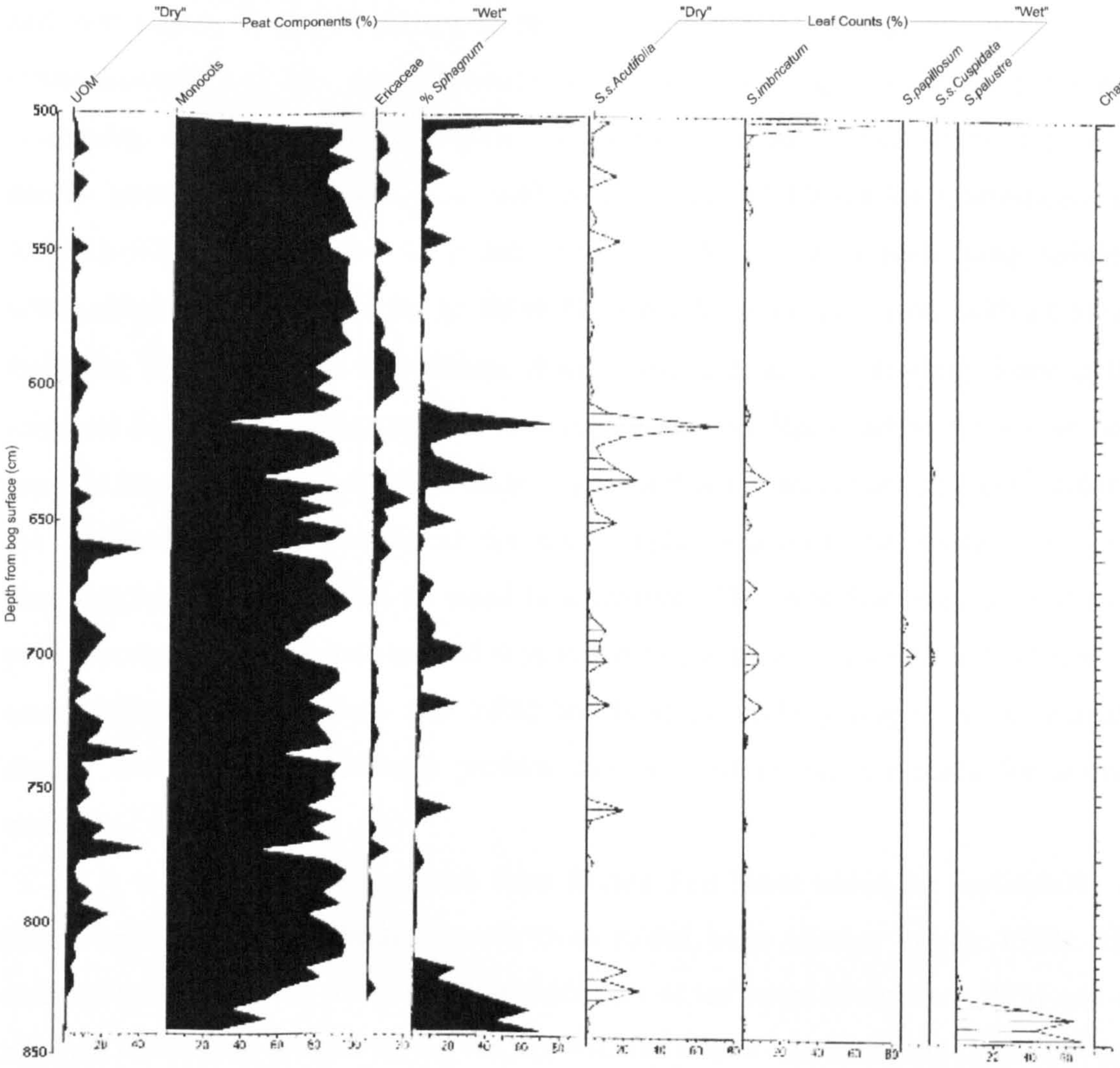

Figure 2.3 Macrofossil diagram of a 500-850 cm peat core. UOM - Unidentified Organic Matter

The 0-500 cm macrofossil diagram (Fig. 2.2) shows two major changes in the bog ecology, occurring at approximately 45 and 332 cm. The first shift in ecology at 332 cm was from Monocotyledons and Ericaceae, to *Sphagnum* species which represent a change from a relatively dry to wet bog surface. The 45 cm shift represents the succession from *Sphagnum imbricatum* to *Sphagnum magellanicum*, which indicates a further increase in the water content of the bog surface. A calibrated radiocarbon age estimate of the peat in this horizon placed this event to 880 y BP (Before Present), which coincides with other proxy-climate records indicating the Little Ice Age. The humification was also measured using a modified version of the Bahnson colorimetric method of humus determination, developed at Keele by Blackford and Chambers (1991). This method bases the humification of peat on its colour, with light coloured peat displaying decreasing humification, i.e. lower temperature or higher precipitation,

and dark coloured peat displaying increasing humification, i.e. higher temperature or lower precipitation. The humification record was then compared with a previously determined hydrological index (Dupont, 1986). Both techniques were found to produce similar proxy-climate signals. The authors then applied Detrended Correspondence Analysis (DCA) to the macrofossil data in order to determine the underlying variables which affect the plant succession on BFM. DCA results and comparisons with a Climate Response Model revealed that climate change was, indeed, a controlling factor in the temporal dominance of plant species growing on the bog. Radiocarbon dates from peat samples suggested that the accumulation of peat at this site was about 12 y cm^{-1} and that the accumulation rate was linear for the samples analysed. Therefore, any equal sampling interval represented an equal time interval. This was then used to produce a proxy-record of surface wetness and was found to compare well with the humification record. These analyses show that BFM has been particularly responsive to climatic change and that its macrofossil profiles can be used as proxy-records for surface wetness.

A more recent study of peat from Bolton Fell Moss tested the replicability of macrofossil and proxy-climate records from raised bogs (Barber *et al.*, 1998). The authors investigated the macrofossil assemblages of ten cores taken from BFM and an adjacent raised bog, Walton Moss (WLM), with the aim of corroborating climatic events recorded in the profiles. These cores were complemented with previous information derived from a total of 16 peat cores, 21 macrofossil profiles from monoliths, 14 peat sections and 3 major pollen diagrams. Each of the BFM cores taken for this study, exhibited a three-stage sequence of deposits which contained:

1. Reedswamp and fen peat, which was dated in one core to be from 10250 to 9650 y BP.
2. Highly humified raised bog peat containing the remains of *Eriophorum vaginatum*, *Calluna vulgaris*, and *Sphagnum* section *Acutifolia*. This was dated from 9650 to 7500 y BP.
3. Fresh *Sphagnum* peat with *E. vaginatum* inputs.

Pollen diagrams constructed from the base of a BFM core and a core taken from WLM were found to be remarkably similar, such that the pollen zones revealed differed by no more than 5-10 cm in depth. This allowed radiocarbon dates performed on the BFM core to be "transferred" to the WLM core. The "transfer" of these dates showed that the transition of fen peat to ombrotrophic peat and then to fresh *Sphagnum* peat, at

both sites occurred at more or less the same time (9850 and 7400 y BP, respectively). Comparison of the different cores taken from BFM revealed similar patterns in the succession of different species of *Sphagnum*, of which a *Sphagnum* section *Cuspidata* phase between 34 and 22 cm depth is the most pronounced feature. This phase has been estimated as occurring during 1650-1770 AD, which corresponds to a cool wet period during the Little Ice Age. The present study attempts to provide a more reliable timescale for these and other events, apparent from macrofossil and lipid stratigraphy.

The extinction of the dominant Holocene peat-forming moss, *S. imbricatum*, varies between 1300 and 1800 AD over both bogs and the variation has been attributed to microtopographical positioning of the bog surface i.e. hummocks containing species flourishing under drier conditions and hollows, species that prefer a wetter environment. However, the data produced from carefully sampled cores were found to be relatively reproducible. The absence of sufficient numbers of radiocarbon dates for the profiles, produced inadequate chronologies. This hampered the correlation of events recorded in the peat cores, although accumulation rates were fairly uniform (10-15 y cm^{-1}). The authors also suggested that for a 5 m core at least 10 radiometric dates would be required to produce a general age/depth model and that significant stratigraphic events would require 30 or more AMS assays to establish accurate dates. The overall conclusion of this study was that considerable effort should be put into field work to ensure that only representative cores are extracted for time-consuming quantitative macrofossil analysis so that valuable proxy-climatic data can be produced.

2.3 Present Study

Two 5 m profiles (BFM1 and BFM2) were extracted from the centre of the bog using 50 cm monolith tins for the first 50 cm and then a 9 cm (30 cm length) bore Russian Corer (Barber, 1984). A 10 m core (BFMN) was also extracted using a 5 cm (30 cm length) bore corer. The cores were taken from a location close to previously examined profiles (Barber, 1998; Barber *et al.*, 1994a) and the exact position was chosen to maximise the likelihood that the plant records contained within the peat would show the most response to changing climate (D. Maddy, personal communication.).

2.4 Sampling Strategy

The main aim of this study was to correlate lipid profiles of BFM peat with plant input related to climate change, as revealed by macrofossil data; to investigate organic geochemical processes related to climate change and produce radiocarbon dates of specific compounds. It is hoped that these dates will be useful for the bracketing of specific climatic events revealed in macrofossil and lipid stratigraphy. This was attempted by the investigation of various peat horizons:

(i) Bulk peat sampled from a monolith at approximately 32 cm depth, used to establish quantities, mobility and identification of lipids

(ii) Low resolution study of 5 m profiles, relating biomarker composition of peat to 7 major excursions in the macrofossil record

(iii) High resolution study of a major transition in peat-forming plants including 30 × 1 cm samples at 419-448 cm depth

(iv) Determination of lipid components of 6 peat samples deposited during the earliest phase of bog development between 8-10 m depth

The low resolution study included 6 × 0.5 cm peat samples from core BFM1 and 1 × 1 cm peat sample from core BFM2. Macrofossil analysis of peat is a time-consuming operation and as such, specific data for these peat profiles could not be acquired until 18 months into the study. Therefore, peat samples were selected based on previous macrofossil data (compiled by D. Mauquoy and D. Maddy at Cheltenham and Gloucester College for Higher Education) to try and produce representative peat samples containing the major plant inputs. The 7 samples together with depth and major plant contributions, are summarised in Table 2.1.

Table 2.1 Major contributing plant inputs to peat samples based on available macrofossil data.

Lab Code	Depth cm	Input Species	% contribution
BFM2-25	25.0-25.5	*S. magellanicum*	60
BFM2-205	205.0-205.5	*S. imbricatum*	95
BFM2-330	330.0-330.5	*E. vaginatum*	64
BFM2-359	359.0-359.5	*S. imbricatum*	32
BFM2-425	425.0-425.5	*S. imbricatum*	81
BFM1-470	470.0-471.0	*E. vaginatum*	37
BFM2-485	485.5-486.0	Monocotyledons	25

2.5 Macrofossil Data

4 cm^3 sub-samples at 4 cm intervals between 250-500 cm were removed from the wet peat and macrofossil analysis was performed by D. Mauquoy and D. Maddy at Cheltenham and Gloucester College for Higher Education (Fig. 2.4). This was carried out by examination of the peat remains under a microscope at x10 magnification and identification of individual taxa of *Sphagnum* at high magnification (x400).

The macrofossil record shows that BFM2-25 also contained 35% *S. s. Acutifolia*. BFM2-330 also contained 15% *Sphagnum* and 20% undifferentiated Monocotyledons. BFM2-359, 25% *E. vaginatum*, 22% undifferentiated Monocotyledons, 4% Ericaceous remains, 13% *S. s. Acutifolia* and 4% fungal sclerotia. BFM2-425, 4% Ericaceous remains, 2% *E. vaginatum* and 8% *S. s. Acutifolia*. BFM2-425 also contained 7% Ericaceous remains and 6% *S. s. Acutifolia*. BFM1-470, 14% Ericaceous remains, 30% unidentified organic matter (UOM) and 9% Fungal sclerotia. BFM2-485, 15% UOM, 16% Ericaceous remains, 20% *E. vaginatum*, 7% *Sphagnum*, 2% *Cenococcum* spp. and 11% fungal sclerotia. Therefore out of all the samples analysed, BFM2-330 contains the most *E. vaginatum*, BFM2-425, *S. imbricatum* and BFM2-485, Ericaceous remains. Samples BFM2-25 and BFM2-205 are assumed to be predominantly *S. magellanicum* and *S. imbricatum*, respectively. Although there is no direct macrofossil data for this part of the core (0-250 cm), matching of the two data sets suggests these plants being the most likely contributors. These samples were solvent extracted and the lipids identified and quantified. The results are presented in Chapter 3.

At approximately 430 cm the macrofossil data shows a sharp change in peat input from predominantly *E. vaginatum*/Monocotyledons to *S. imbricatum* (Fig. 2.4, Table 2.2). Peat from 419-448 cm sampled at 1 cm intervals was solvent extracted and the lipids identified and quantified (Chapter 3). From this data set, 10 samples at 3 cm intervals between 420 and 447 cm were used in a radiocarbon dating study (Chapter 6).

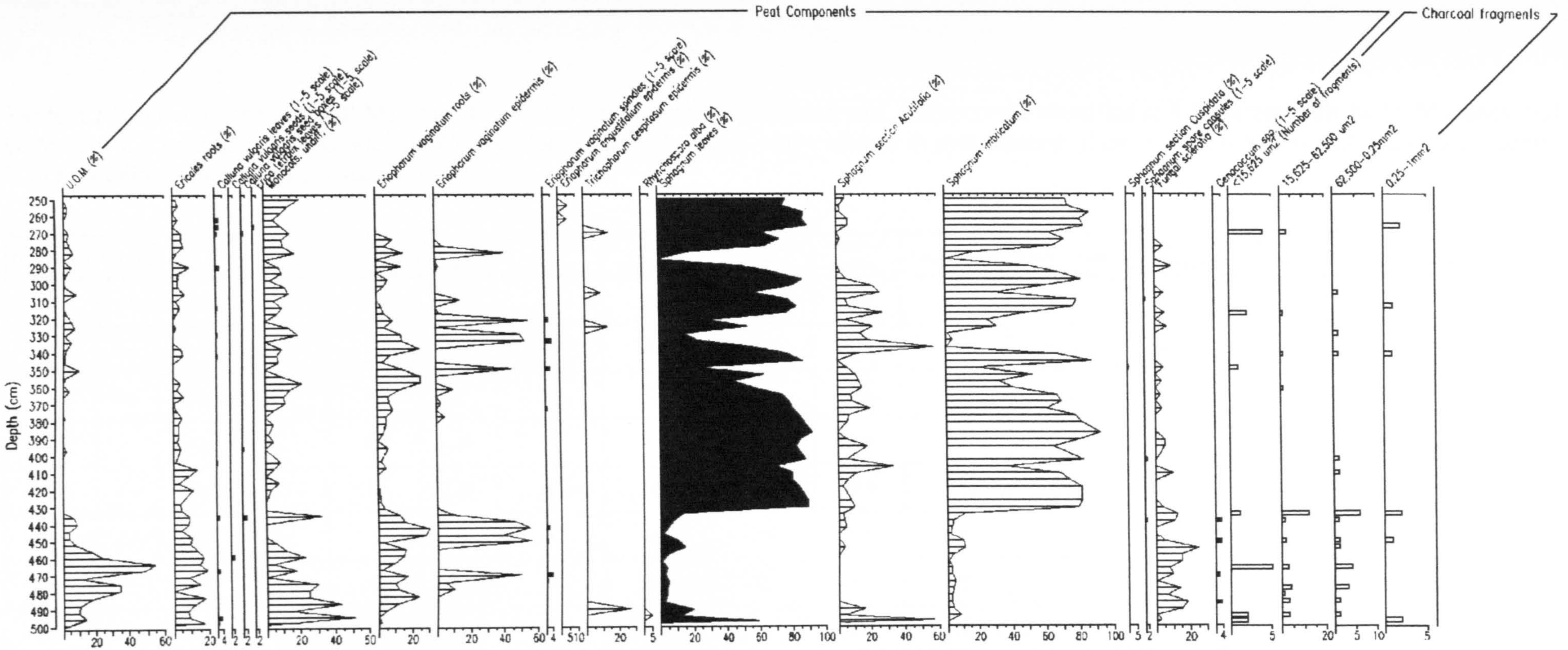

Figure 2.4 Bolton Fell Moss plant macrofossil stratigraphy 250-500 cm for core BFM1. Peat components represent averaged quadrat counts and are plotted as percentage total peat composition. Components identified at 4-8 cm intervals by D. Mauquoy and D. Maddy at Cheltenham and Gloucester College for Higher Education.

Table 2.2 Plant components of BFM1 from 416 to 452 cm as percentage of total peat. Components identified at 4-8 cm intervals by D. Mauquoy and D. Maddy at Cheltenham and Gloucester College for Higher Education. Major change in peat forming plants occurs between 432 and 436 cm depth. U.O.M. - unidentified organic matter.

Depth (cm)	U.O.M.	Ericales roots	*C.vulgaris* leaves	*C.vulgaris* seed boxes	Monocots undiff.	*E.vaginatum* roots	*E.vaginatum* epidermis	*E.vaginatum* spindles	*Sphagnum* leaves	*S.s.Acutifolia*	*S.imbricatum*	*Sphagnum* spore capsules	Fungal sclerotia	Cenococcum spp.	Total *Eriophorum*
416.0	1.0	3.0	0.0	0.0	8.0	0.0	0.0	0.0	80.0	6.0	74.0	0.0	0.0	0.0	0.0
420.0	0.0	12.0	0.0	0.0	3.0	1.0	0.0	0.0	84.0	3.0	81.0	0.0	0.0	0.0	1.0
428.0	0.0	4.0	0.0	0.0	0.0	2.0	0.0	0.0	89.0	8.0	81.0	0.0	0.0	0.0	2.0
432.0	0.0	5.0	0.0	0.0	0.0	4.0	0.0	0.0	89.0	10.0	79.0	0.0	4.0	0.0	4.0
436.0	8.0	10.0	2.0	2.0	33.0	13.0	10.0	0.0	14.0	3.0	11.0	0.0	13.0	0.0	23.0
440.0	10.0	9.0	0.0	0.0	0.0	16.0	46.0	0.0	8.0	4.0	4.0	1.0	11.0	3.0	62.0
444.0	5.0	5.0	0.0	0.0	0.0	30.0	55.0	2.0	5.0	5.0	3.0	0.0	0.0	0.0	87.0
448.0	5.0	11.0	0.0	0.0	0.0	28.0	39.0	0.0	2.0	0.0	2.0	0.0	0.0	0.0	67.0
452.0	9.0	10.0	0.0	0.0	6.0	3.0	56.0	1.0	11.0	1.0	10.0	0.0	5.0	3.0	60.0

2.6 Peat Samples from Earliest Phase of Bog Development

Due to the extensive humification in the lower 2 m of core BFMN, macrofossil analysis proves to be of little value; identifiable leaves, etc. have been destroyed. However, the 2 m core section comprises 5 distinct horizons, which are clearly visible on inspection (Figs. 2.5 and 2.6). Six 2 cm peat samples were taken, so that at least one sample was present from each visible horizon (Fig. 2.7). Two were taken from the thickest peat layer to compare the conditions at the top and bottom of the layer. These were then solvent extracted and the lipids identified and quantified (Chapter 4).

Figure 2.5 Photograph of 5 cm diameter peat section from 980-950 cm depth in Russian type corer. The mineral layer is clearly visible to the left of the core.

Figure 2.6 Photograph of 5 cm diameter peat section from 975-1004 cm depth in Russian type corer. The clay layer is clearly visible on the right of the core.

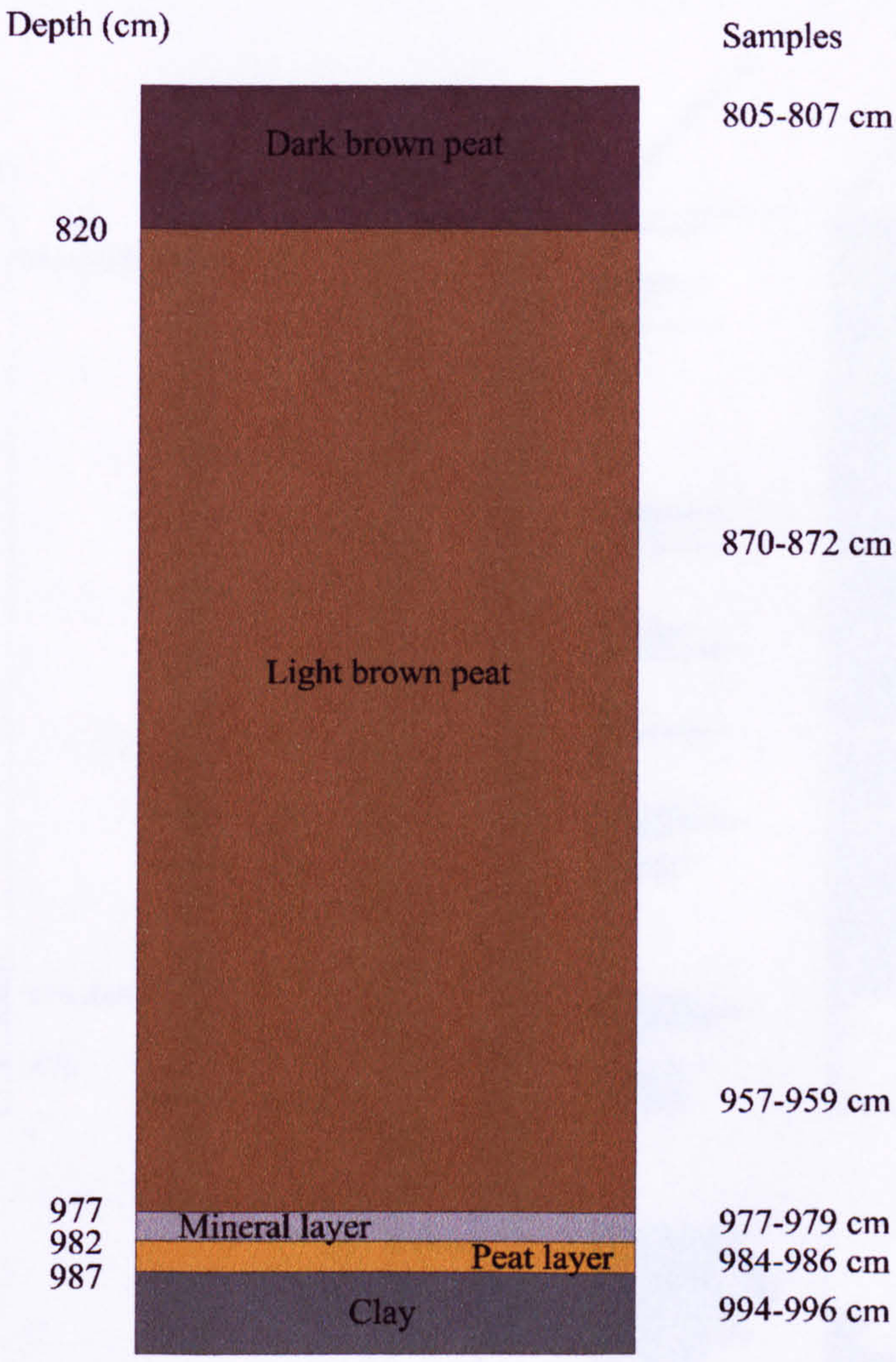

Figure 2.7 Diagram showing visible peat horizons and extracted samples from core BFMN.

A summary of all of the peat samples studied is shown in Figure 2.8. This diagram includes the major plant inputs to the peat where available.

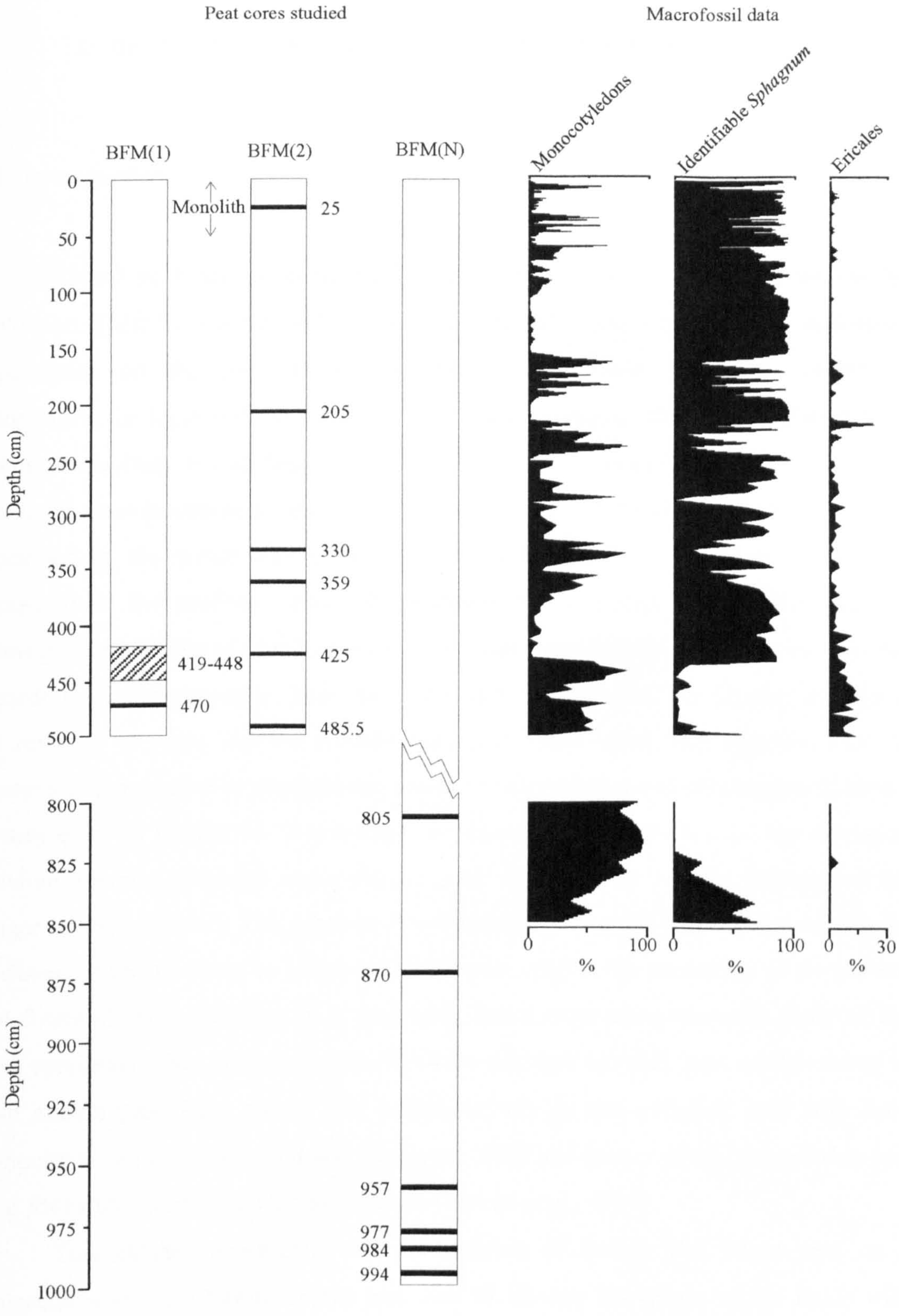

Figure 2.8 Diagram showing peat horizons extracted from cores BFM(1), BFM(2) and BFM(N), together with Monocotyledon, *Sphagnum* and Ericaceous macrofossil data, where available. Horizon 419-448 from BFM(1) consists of 30 x 1 cm continuous samples. Macrofossil data is the combination of previous results performed on adjacent peat profiles (Barber *et al.*, 1994b) and data obtained for BFM1 (250-500 cm) and BFMN (500-850 cm).

3. BIOMARKER STRATIGRAPHY IN BOLTON FELL MOSS

3.1 Introduction

Raised peat bogs contain the best records for climatic variations during the Holocene. Their high accumulation rates, exceptional preservation qualities and direct dependence on the surrounding environment make them excellent sources of information for local and more widespread climatic changes. Their accumulation from almost exclusively autochthonous inputs provides more simplified records than those produced from lacustrine or marine sediments, where terrestrial runoff and diagenetic processes in the water column affect the resulting sedimentary layers. However, compared to the uniform sediments produced in lakes and ocean sediments, the heterogeneous nature of peat bog surfaces requires synchronicity in order to correlate records in microtopography. Lake and ocean deposits can hold environmental records for millions of years, but the records contained within most peat deposits, such as changes in evaporation or precipitation, microbial populations and pH changes, (Chapter 1) only exist for the last 11-13 millennia, as glaciation during the last ice age destroyed previous records (although some tropical peat deposits may contain information for longer periods of time). The relatively short timescale covered by peat bog records is, however, of great interest as Holocene records are used in the prediction of the present and future climate. Therefore it is surprising that a more comprehensive study of the lipid stratigraphy has not been made. Previous attempts to relate past environments to lipid stratigraphy, have shown that pollen records do not correlate well with lipid components in peat (Farrimond and Flanagan, 1996) and studies of macrofossil data and lipid distributions have had limited success (Ficken *et al.*, 1998).

This chapter investigates the composition of Bolton Fell Moss peat on a molecular scale at different depths and tries to identify the origin of the lipids with respect to visible plant material present in the peat. The organic geochemistry of peat lipids has not been fully investigated in the past and this investigation presents the results of a much more comprehensive study which relates compounds found in peat to precursors present in the input material.

The main objectives of this chapter were:

(I) To determine the relative solubilities of different classes of lipid so that any movement of these lipids with the peat water table can be established.

(II) To identify lipids in the organic solvent extracts from Bolton Fell Moss peat with the aim of relating biomarker composition to 7 major excursions in the macrofossil record.

(III) To establish changes in the lipid composition on a high resolution scale, over a depth of peat where a major transition in peat-forming plants is observed in macrofossil records (419-448 cm depth).

3.2 Lipid Mobility in Bog Water

Lipids, by definition have a high degree of hydrophobicity and therefore when deposited in a sediment they would be expected to remain immobile with respect to the matrix in which they are deposited. Throughout the year the water table in a peat bog rises and falls with increasing and decreasing precipitation. This flow transports the dissolved matter in the water throughout the bog. Therefore, if the lipids are to be used to produce accurate representations of macrofossil data, they must remain in the same horizon as the material from which they are derived and not be affected by changes in the water table.

A previous study investigating the solubility of lipids in the drainage water from peatlands discovered that the amount of water-soluble lipids depended on peat type and humification (Lehtonen *et al.*, 1991). The authors investigated 3 *Carex* and 2 *Sphagnum* peats with different degrees of humification and compared their organic solvent extracts with those extracted with water. It was found that the amount of water-soluble lipid matter varied between 0.021 and 0.083% of dry peat and, as humification increased, solubility increased in the *Sphagnum* peat and decreased in *Carex* peat. It was also discovered that the lipids from the most humified *Sphagnum* peat were nearly three times as soluble as those from the most humified *Carex* peat. The authors then concentrated on water-soluble lipid components from the least humified *Carex* sample and it was discovered that *n*-fatty acids were the major components consisting of 58% of the total lipid monomers, with ω-hydroxy acids, α,ω-alkanedioic acids, *n*-alcohols and

sterols contributing 19, 8, 7 and 4%, respectively. The organic extracts were found to contain a much higher contribution of ω-hydroxy acids (43%), with *n*-fatty acids, α,ω-alkanedioic acids, and sterols contributing 2, 7 and 4%, respectively. Shorter chain homologues ($<C_{22}$) of *n*-fatty acids, ω-hydroxy acids and *n*-alcohols predominated the water extracts, comprising 63, 74 and 46%, respectively, much higher proportions than those in the organic solvent extracts (31, 25, and 21%, respectively). This was attributed to the higher solubility of more polar, shorter-chain, acidic compounds in water.

As the above previous investigation into the solubility of peat lipids in water found that the solubility of different classes of compounds varied with the type and humification of the peat (Lehtonen *et al.*, 1991), a study of the water-solubility of BFM peat lipids was carried out. This study was to ensure that lipids used for radiocarbon dating and the determination of different inputs would provide an accurate representation of the horizon in which they were formed.

3.2.1 Results

To estimate the relative mobility/solubility of the lipids, a peat sample was extracted with water as in the study described above (Lehtonen *et al.*, 1991) such that the dry peat/water ratio was about 1:60 w/w and the lipid profile of the resulting extract compared to that of organic solvent extracted peat (Fig. 3.1). Although this was only done for one sample, the aim of this experiment was to quickly verify that peat lipids are relatively immobile within the peat matrix.

The total lipid extracts (TLE) of water (20 h) and organic solvent (9:1 v/v DCM/acetone, 24 h) extracted peat from the 32 cm depth horizon were compared. The major components present in both extracts were: C_{22}, C_{24}, C_{26} and C_{28} *n*-alkanols, $C_{20:0}$, $C_{22:0}$, $C_{24:0}$ and $C_{26:0}$ *n*-fatty acids, β-sitosterol, 3-stigmastanol and a series of wax esters (C_{34}-C_{50}, even carbon numbered homologues). The amount of TLE obtained from each extraction was 98.8 mg g^{-1} of dry peat by DCM/acetone extraction and 2.35 mg g^{-1} with water. As the extraction with water only yielded 2.4% TLE of that with DCM/acetone this shows that the lipids are relatively insoluble in water, as expected. Relative abundances of identified lipids were measured and the contribution of each compound normalised to the β-sitosterol/3-stigmastanol abundance determined (Table 3.1).

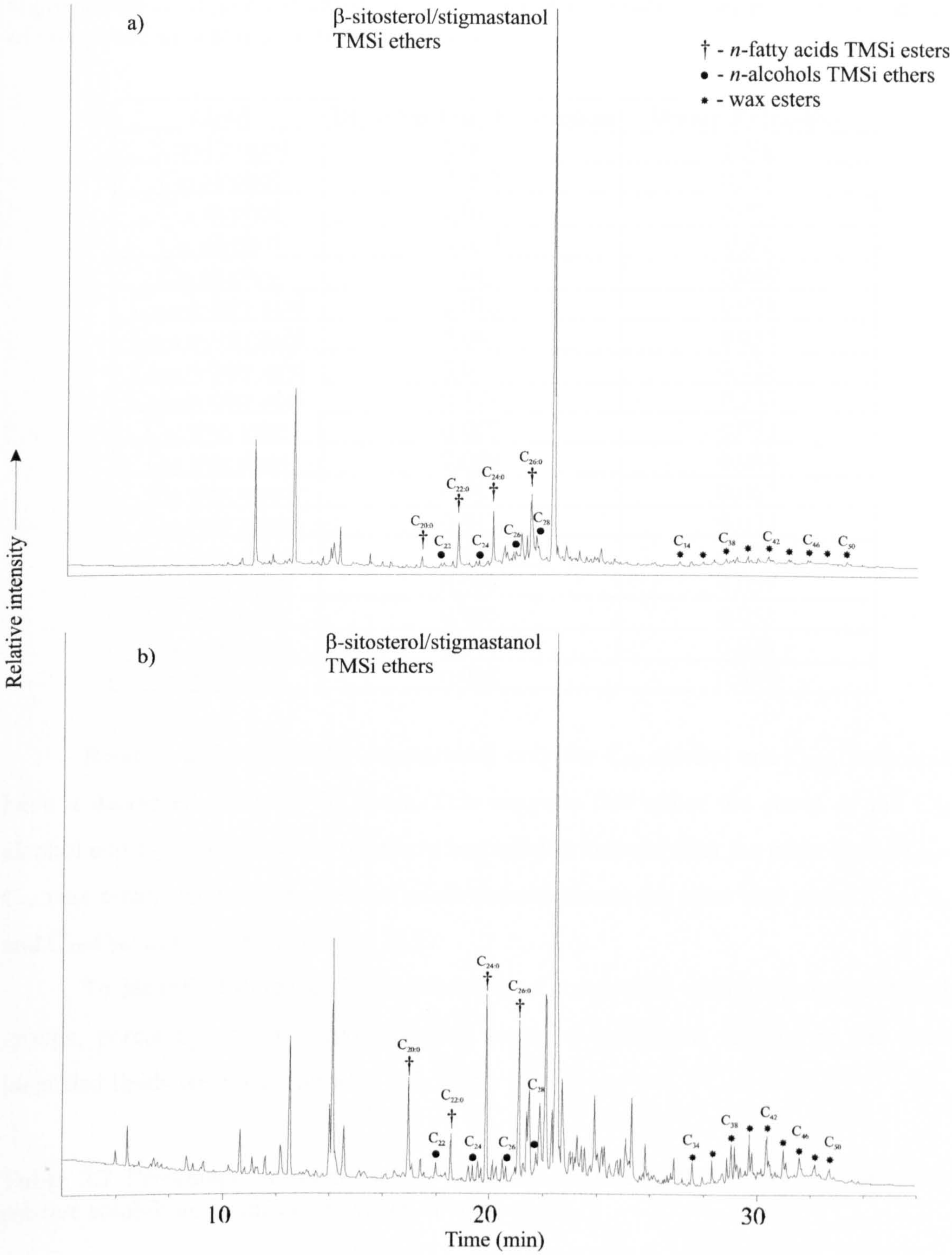

Figure 3.1 Partial gas chromatograms of the TLE from peat monolith at 32 cm depth; 15 m DB-1, 50°C (2 min), 50-350°C @ 10°C min^{-1}, 350°C (10 min): a) 9:1 v/v DCM/acetone (24 h) and (b) water (20°C, 20 h) extracted peat.

Table 3.1 Contributions of lipids to total identified lipids normalised to β-sitosterol/3-stigmastanol combined abundance, to determine relative solubilities of different classes of compound in peat monolith at 32 cm depth.

Lipid	DCM/acetone Extraction	Water Extraction
Sterol/Stanol	1.000	1.000
C_{22} alcohol	0.007	0.026
C_{24} alcohol	0.011	0.021
C_{26} alcohol	0.039	0.02
C_{28} alcohol	0.041	0.069
$C_{20:0}$ *n*-fatty acid	0.016	0.021
$C_{22:0}$ *n*-fatty acid	0.062	0.055
$C_{24:0}$ *n*-fatty acid	0.085	0.221
$C_{26:0}$ *n*-fatty acid	0.171	0.237
C_{34} wax ester	0.008	0.033
C_{36} wax ester	0.008	0.034
C_{38} wax ester	0.013	0.067
C_{40} wax ester	0.013	0.077
C_{42} wax ester	0.019	0.091
C_{44} wax ester	0.008	0.059
C_{46} wax ester	0.005	0.053
C_{48} wax ester	0.004	0.021
C_{50} wax ester	0.008	0.027

Relative to β-sitosterol/3-stigmastanol only the C_{26} alcohol and $C_{22:0}$ fatty acid have a decreased solubility in water. This suggests that either the sterol or the C_{26} alcohol and $C_{22:0}$ fatty acid are relatively less soluble in water than the other lipids. C_{40}-C_{46} wax esters also have an elevated relative abundance to the other wax esters (C_{34}-C_{38} and C_{48}-C_{50}) in the water extracted TLE.

To identify differences in the solubility of compounds with different functional groups, percentage contributions of each class of compound relative to the total identified lipids were determined (Table 3.2).

Table 3.2 Percentage contributions of lipids to total identified lipids, to determine relative solubilities of different classes of compounds.

Compound Type	DCM/acetone Extraction	Water Extraction
n-Alkanols	6.4%	6.4%
n-Fatty Acids	21.9%	25.1%
Sterol/Stanol	65.7%	47.0%
Wax Esters	5.7%	21.6%

This suggests that, of the identified compounds, sterols seem to be the least water soluble lipids relative to the other components within the peat. An increase in the

relative abundance of wax esters in the water extract is again observed. However, the increase from 5.7 to 21.6%, is in part, due to the decrease in sterol solubility. Octanol/water partition coefficients (log k_{ow}) for the free lipids are displayed in Table 3.3. Octanol/water partition coefficients were used as they could be readily estimated for all lipid compounds encountered in peat extracts.

Table 3.3 Calculated octanol/water partition coefficients (log k_{ow}) of selected lipids (Meylan and Howard, 1995) found in peat at 32 cm depth.

Compound	log k_{ow}
C_{20} *n*-fatty acid	8.93
β-sitosterol	9.65
C_{24} *n*-alkanol	9.68
3-stigmastanol	9.73
C_{22} *n*-fatty acid	9.91
C_{26} *n*-alkanol	10.66
C_{24} *n*-fatty acid	10.89
C_{28} *n*-alkanol	11.65
C_{26} *n*-fatty acid	11.87
C_{30} *n*-alkanol	12.63
C_{34} wax ester	15.60
C_{36} wax ester	16.58
C_{38} wax ester	17.56
C_{40} wax ester	18.54
C_{42} wax ester	19.53
C_{44} wax ester	20.51
C_{46} wax ester	21.46
C_{48} wax ester	22.47
C_{50} wax ester	23.45

This shows that short chain fatty acids (C_{20}-C_{22}), β-sitosterol, 3-stigmastanol and C_{24} *n*-alkanol are the most water soluble compounds in the absence of a matrix such as peat. Long chain wax esters are the most water insoluble moieties identified. Therefore the elevated abundance of wax esters in the water extracts must be governed by another factor other than just solubility in water.

The average chain lengths of the different homologues of *n*-alkanols, *n*-fatty acids and wax esters were compared in the water and organic solvent extracts (Table 3.4). Therefore the elevated relative abundance of wax esters in the water extracts suggests that another factor is involved in the increase. Wax esters have been found to be major components of plant epicuticular waxes and act as barriers between plant cells

and the outside environment (Baker, 1982). The presence of wax esters on the exterior surfaces of plant leaves may make them more susceptible to dissolution in water, than those lipids contained within plant cells. As this peat is composed of relatively intact *Sphagnum* leaves, the occurrence of elevated abundance of wax esters in the water extracts suggest that they come from the surface of the plant remains whereas other lipids remain within. This is concurrent with the relatively non-destructive extraction method which was unlikely to disrupt the plant cells (see Experimental, Chapter 8).

Table 3.4 Average chain lengths of lipid homologues in organic solvent and water extracts of peat.

Compound Type	DCM/acetone Extraction	Water Extraction
n-Alkanols	26.3	25.9
n-Fatty Acids	24.5	24.5
Wax Esters	41.2	41.5

This shows that there is little difference in the average chain lengths of *n*-fatty acids and wax esters, but there is a slight decrease in the *n*-alkanol chain length in water extracts. This is likely to be an effect of the higher polarity of shorter-chain compounds, which increases their solubility in water. However, this would also have been expected to affect the average chain length of the relatively polar *n*-fatty acids (Table 3.3).

This suggests that there are some differences in the water-solubility of different lipid components but overall lipids have a low solubility in water. The ratio of dry peat to water in the catotelm at BFM was found to be about 1:23 w/w. This is a lower ratio than that used in this experiment and even at the experimental level the water extract was saturated with lipidic matter. Therefore transfer of free lipids between horizons with changes in water table level is likely to be minimal.

3.3 Relating Biomarker Composition of Peat to Major Excursions in the Macrofossil Record

Peat samples were taken from 7 depths, (Table 2.1) corresponding to the major plant inputs in the macrofossil data, in order to produce representative peat samples for each input. These samples contained either *S. magellanicum* (BFM2-25), *S. imbricatum* (BFM2-205, BFM2-359 and BFM2-425), *E. vaginatum* (BFM2-330 and BFM1-470) or undifferentiated Monocotyledons (BFM2-485) as the major input species. BFM2-485

also had the highest content of Ericaceous remains (16%) of those horizons studied. These samples were extracted with organic solvent and the lipids identified by GC and GC/MS.

In order to assess the composition in more detail, the solvent extractable lipids were separated into six fractions for identification and quantification. This included hydrocarbons, aromatics, ketones/wax esters, alcohol/steroid, polar and acid fractions. In all samples the aromatic and polar fractions contained no GC identifiable material and have not been included in this study. The ketones/wax esters, alcohol/steroid and acid fractions were derivatised with *N,O*-bis(trimethylsilyl)trifluoroacetamide (BSTFA) prior to GC analysis. The identification of lipids was performed either by comparison of GC retention times, comparison of mass spectrum data with library data or by coinjection with authentic compounds of known structure.

3.4 Hydrocarbons

Generally the hydrocarbon (hexane) fraction was dominated by *n*-alkanes displaying an odd-over-even predominance ranging in carbon number, from C_{19} to C_{35} (Fig. 3.2). The distributions maximised at the C_{23}, C_{31} or C_{33} homologue. Other compounds included C_{31} 17α(H), 21β(H) 29-methyl hopane (Fig. 3.3a), C_{31} 17β(H), 21β(H) 29-methyl hopane, an unidentified $C_{30}H_{50}$ hopane (Appendix II), taraxer-14-ene, urs-12-ene, hop-17(21)-ene and taraxast-20-ene (Fig. 3.3b).

3.4.1 BFM2-25

The hydrocarbon fraction of this relatively immature *S. magellanicum* predominant peat, is dominated by *n*-alkanes. These alkanes display an odd-over-even predominance (CPI = 9.5) ranging in carbon number from C_{19} to C_{35} (Fig. 3.4a) with a maximum at the C_{31} homologue (96.6 μg g^{-1} dry peat). Other components of this fraction are tarax-14-ene (6.8 μg g^{-1} dry peat), urs-12-ene (1.5 μg g^{-1} dry peat), 17β(H), 21β(H) 29-methyl hopane (1.9 μg g^{-1} dry peat) and 17α(H), 21β(H) 29-methyl hopane (32.7 μg g^{-1} dry peat).

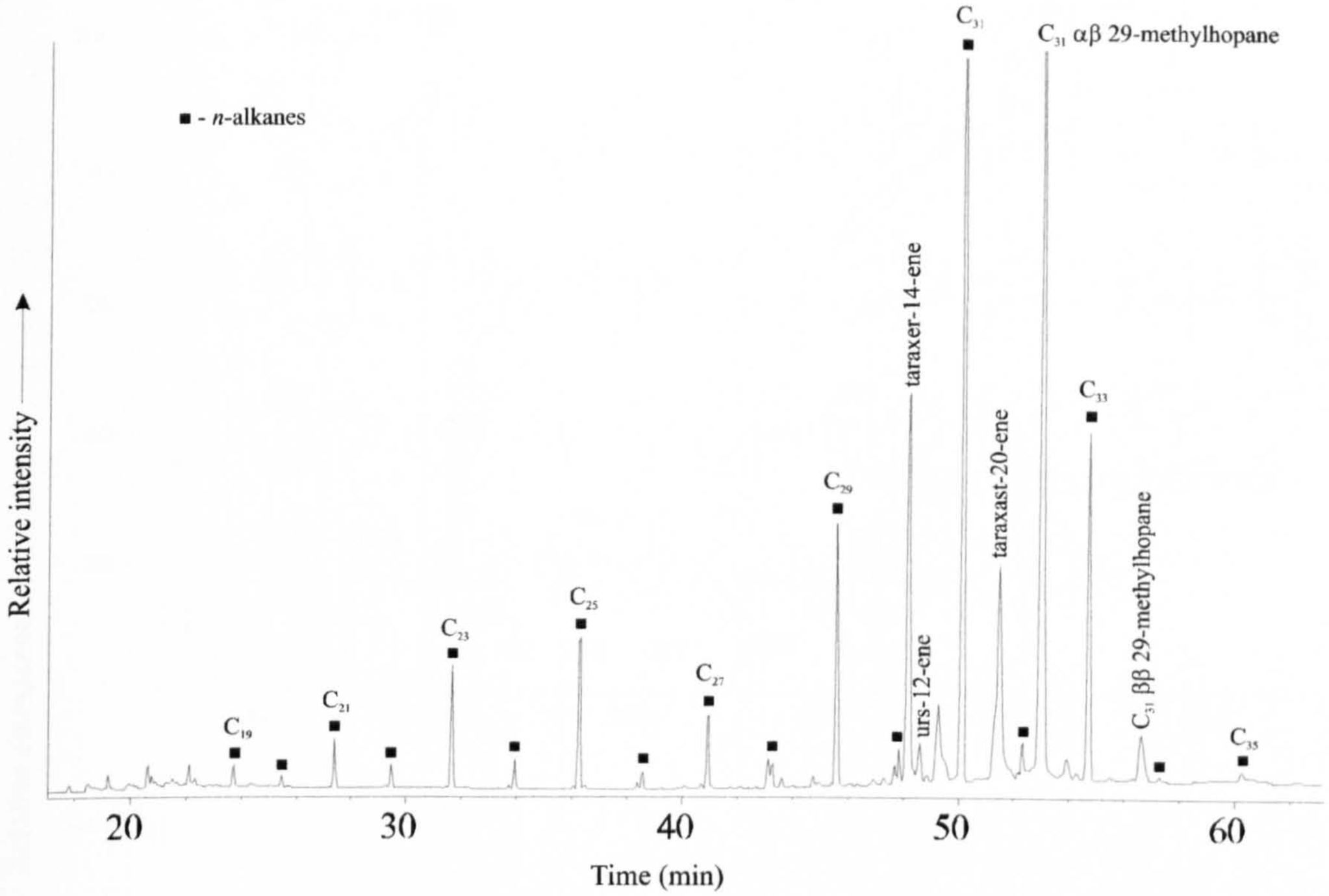

Figure 3.2 Partial gas chromatogram of hydrocarbon fraction from monolith peat at 32 cm depth; 50 m CPSil-5CB, 50-200°C @ 12°C min^{-1}, 200-300°C @ 3°C min^{-1}, 300°C (20 min).

3.4.2 BFM2-205

This peat sample is thought to be almost completely composed of *S. imbricatum* remains (95%). The hydrocarbon fraction is dominated by *n*-alkanes, which display an odd-over-even predominance (CPI = 9.9) and ranged in carbon number from C_{19} to C_{35} (Fig. 3.4b) with a maximum at the C_{31} homologue (96.1 μg g^{-1} dry peat). Other components of this fraction are tarax-14-ene (32.5 μg g^{-1} dry peat), urs-12-ene (1.3 μg g^{-1} dry peat), ββ 29-methyl hopane (5.0 μg g^{-1} dry peat) and αβ 29-methyl hopane (79.3 μg g^{-1} dry peat).

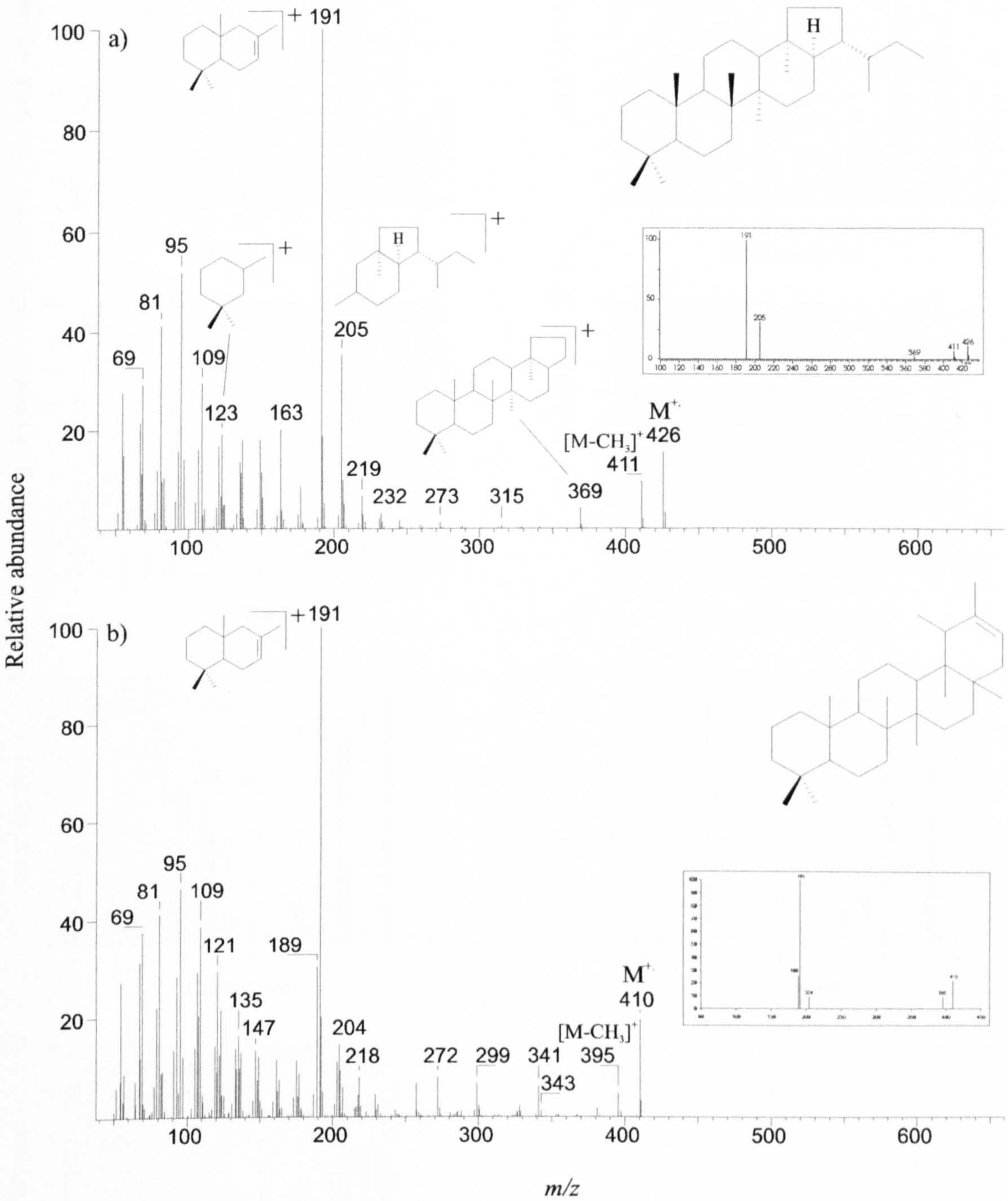

Figure 3.3 Mass spectra of components identified as (a) C_{31} 17α(H), 21β(H) 29-methyl hopane and (b) taraxast-20-ene in hydrocarbon fraction of peat core BFM2, 485.5 cm depth. Assigned by comparison with library spectra (inserts, NST MS library).

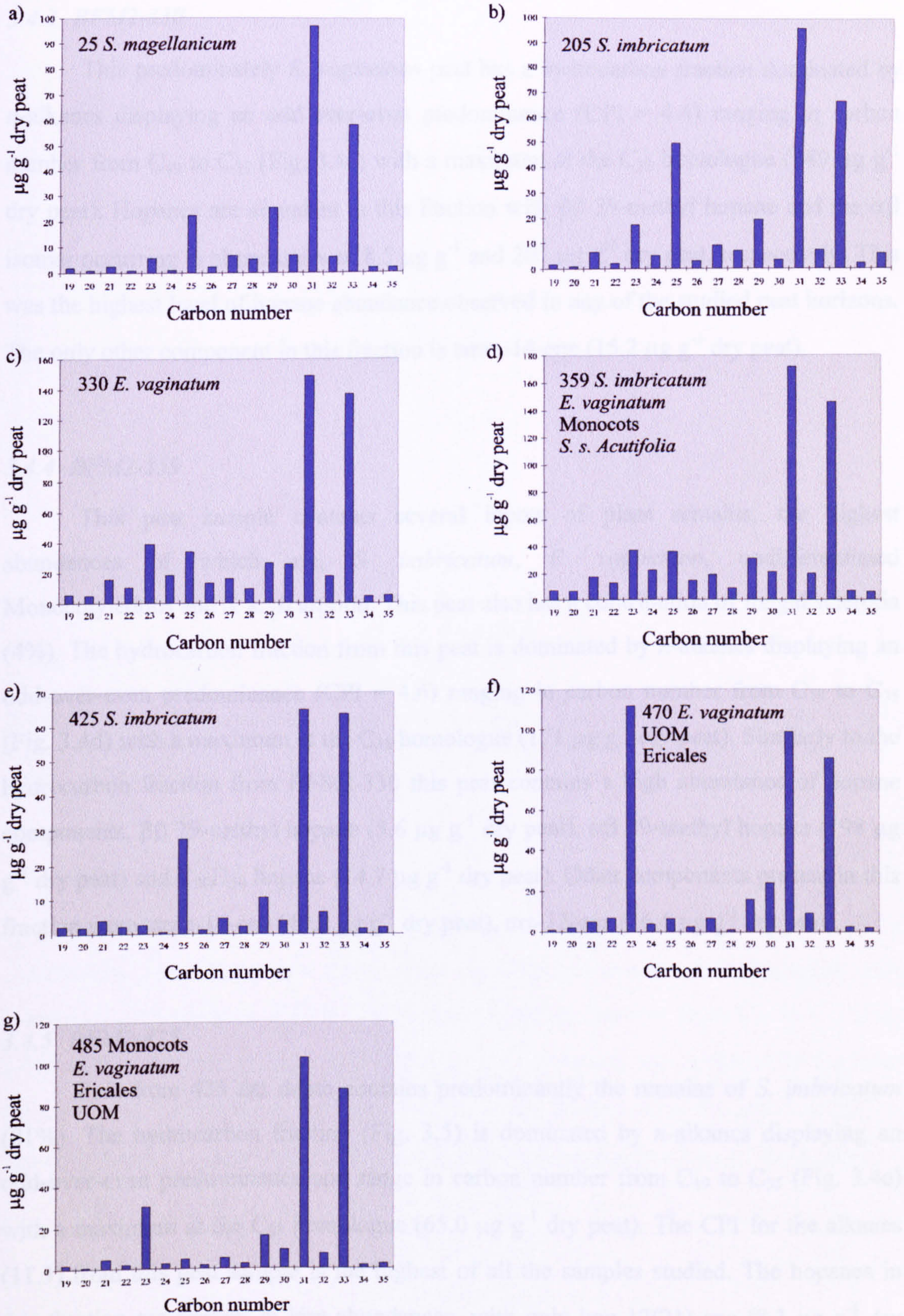

Figure 3.4 Histograms of distributions of *n*-alkane homologues (µg g^{-1} dry peat) from: (a) BFM2-25, (b) BFM2-205, (c) BFM2-330, (d) BFM2-359, (e) BFM2-425, (f) BFM1-470 and (g) BFM2-485.

3.4.3 BFM2-330

This predominately *E. vaginatum* peat has a hydrocarbon fraction dominated by *n*-alkanes displaying an odd-over-even predominance (CPI = 4.4) ranging in carbon number from C_{19} to C_{35} (Fig. 3.4c) with a maximum at the C_{31} homologue (149 μg g^{-1} dry peat). Hopanes are abundant in this fraction with ββ 29-methyl hopane and the αβ isomer occurring at abundances of 8.5 μg g^{-1} and 201 μg g^{-1} dry peat, respectively. This was the highest level of hopane abundance observed in any of the studied peat horizons. The only other component in this fraction is tarax-14-ene (15.2 μg g^{-1} dry peat).

3.4.4 BFM2-359

This peat sample contains several inputs of plant remains, the highest abundances of which are, *S. imbricatum*, *E. vaginatum*, undifferentiated Monocotyledons and *S. s. Acutifolia*. This peat also has a contribution of fungal sclerotia (4%). The hydrocarbon fraction from this peat is dominated by *n*-alkanes displaying an odd-over-even predominance (CPI = 4.6) ranging in carbon number from C_{19} to C_{35} (Fig. 3.4d) with a maximum at the C_{31} homologue (171 μg g^{-1} dry peat). Similarly to the hydrocarbon fraction from BFM2-330 this peat contains a high abundance of hopane components, ββ 29-methyl hopane (5.6 μg g^{-1} dry peat), αβ 29-methyl hopane (198 μg g^{-1} dry peat) and $C_{30}H_{50}$ hopane (14.7 μg g^{-1} dry peat). Other components present in this fraction were tarax-14-ene (49.2 μg g^{-1} dry peat), urs-12-ene (36.6 μg g^{-1} dry peat),

3.4.5 BFM2-425

Peat from 425 cm depth contains predominantly the remains of *S. imbricatum* (81%). The hydrocarbon fraction (Fig. 3.5) is dominated by *n*-alkanes displaying an odd-over-even predominance and range in carbon number from C_{19} to C_{35} (Fig. 3.4e) with a maximum at the C_{31} homologue (65.0 μg g^{-1} dry peat). The CPI for the alkanes (11.3) from this peat sample is the highest of all the samples studied. The hopanes in this fraction are present in low abundances, with only hop-17(21)-ene (8.3 μg g^{-1} dry peat), ββ 29-methyl hopane (0.3 μg g^{-1} dry peat) and αβ 29-methyl hopane (7.1 μg g^{-1} dry peat) being detected.

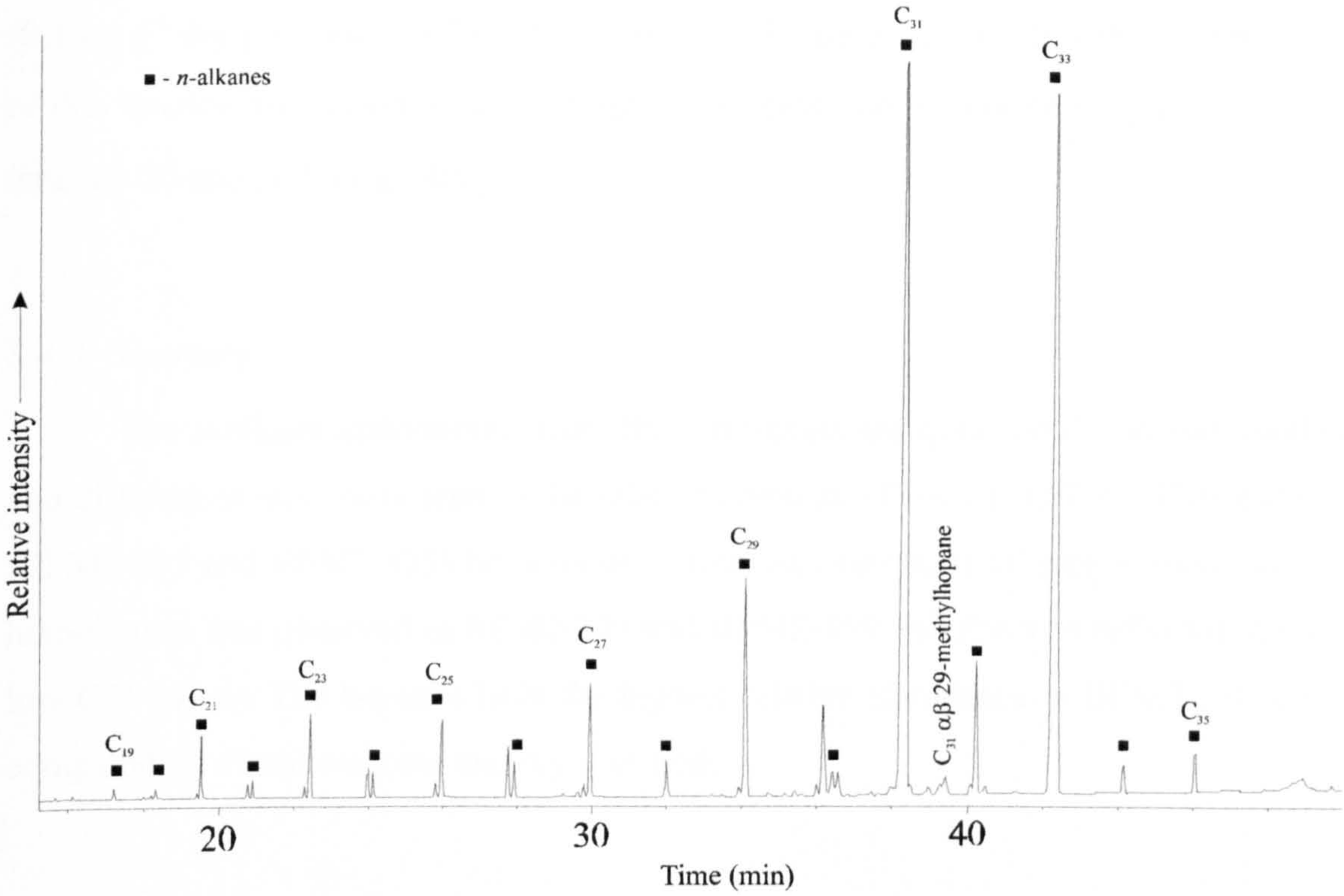

Figure 3.5 Partial gas chromatogram of hydrocarbon fraction from peat sample BFM1-425 at 425 cm depth; 50 m CP-Sil5CB, 50 m CPSil-5CB, 50-200°C @ 12°C min^{-1}, 200-300°C @ 3°C min^{-1}, 300°C (20 min).

3.4.6 BFM1-470

This sample had 4 major inputs of which *E. vaginatum* and UOM were the main contributors. The hydrocarbon fraction was dominated by *n*-alkanes displaying an odd-over-even predominance (CPI = 7.1) ranging in carbon number from C_{19} to C_{35} (Fig. 3.4f). In this sample the C_{23} *n*-alkane (98.8 μg g^{-1} dry peat) was found to be the most abundant. The only other components present in this fraction were the hopanes; ββ 29-methyl hopane (0.1 μg g^{-1} dry peat) and αβ 29-methyl hopane (43.3 μg g^{-1} dry peat).

3.4.7 BFM2-485

Of all the peat samples investigated in this study, the peat from this depth contains the most Ericaceous remains (16%), but its greatest identified input is undifferentiated Monocotyledons (25%). The hydrocarbon fraction is dominated by *n*-alkanes displaying an odd-over-even predominance (CPI = 9.9) and ranged in carbon number from C_{19} to C_{35} (Fig. 3.4g) with a maximum at the C_{31} homologue (103 μg g^{-1}

dry peat). This fraction also contains low abundances of hopanes: ββ 29-methyl hopane (0.1 μg g^{-1} dry peat) and αβ 29-methyl hopane (13.7 μg g^{-1} dry peat). Other components of this fraction are tarax-14-ene (19.5 μg g^{-1} dry peat), urs-12-ene (8.3 μg g^{-1} dry peat), taraxast-20-ene (4.9 μg g^{-1} dry peat).

3.4.8 Summary

The *n*-alkane distributions from the 7 horizons are quite similar to one another and differences were only seen in the relative amounts of the C_{23} (BFM1-470) and C_{25} (BFM2-205 and BFM2-425) homologues. However, elevation of even carbon number homologues was observed in BFM2-330 and BFM2-359 and this was reflected in their low CPI values. The hopanes have the highest relative abundance in BFM2-330 when compared on a total *n*-alkane and dry peat basis.

3.5 Ketones and Wax Esters

Wax esters eluted in the DCM fraction and are depicted in Figure 3.6. The observed distribution range from C_{26} to C_{52} in a bimodal pattern with the components of chain length C_{28} and C_{42} predominating, both of which are based on a C_{26} alkanol moiety. Also present are methyl ketones; these are in low abundances relative to the wax esters and range from C_{17} to C_{27} with maxima at the C_{19} and C_{25} homologue.

In order to elucidate some of the unidentified components, the fraction was further simplified by urea adduction to separate cyclic and acyclic compounds. This revealed that some of the compounds were unidentified triterpenoid acetates. However, the presence of high molecular weight compounds in both the adduct and non-adduct, precluded the use of this fraction for separation of single compounds by PCGC. Thick film columns, such as those used in PCGC systems cannot be used to isolate high molecular weight compounds in the short timescale required for PCGC-AMS analysis. Therefore the ketone and wax ester fraction was not studied further.

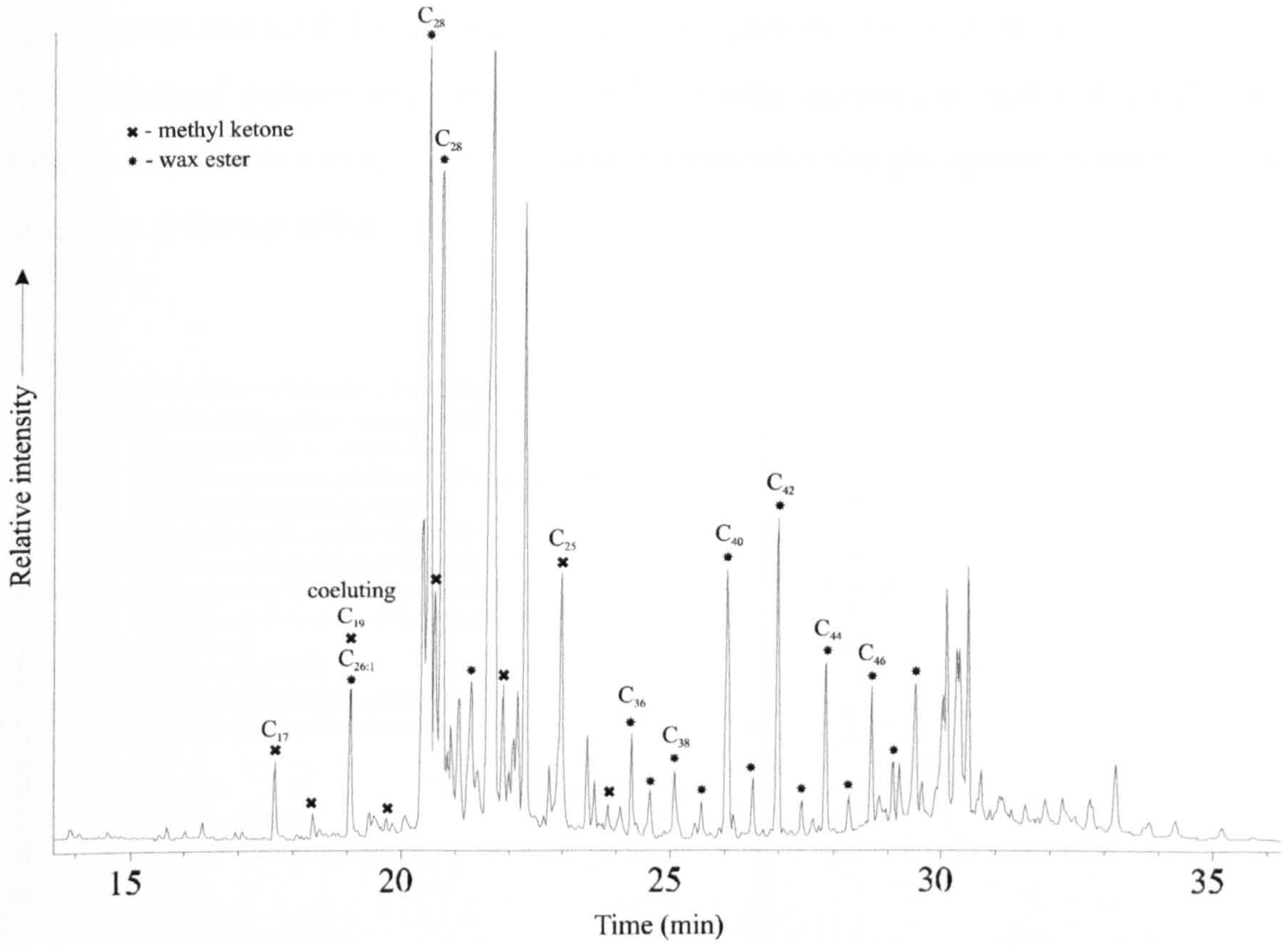

Figure 3.6 Partial gas chromatogram of ketone/wax ester fraction from monolith peat at 32 cm depth; 15 m DB-1, 50°C (2 min), 50-350°C @ 10°C min^{-1}, 350°C (10 min).

3.6 Alcohol and Steroid Fraction

The alcohol/steroid fraction is dominated by sterols (Fig. 3.7), 24*R*-ergost-5-en-3β-ol (campesterol), 24*R*-ergostan-3β-ol (campestanol), 22*E*, 24*R*-stigmasta-5,22-dien-3β-ol (stigmasterol), 22*E*, 24*R*-stigmast-22-en-3β-ol, 24*R*-stigmast-5-en-3β-ol (β-sitosterol, Fig. 3.8a) and 24*R*-stigmastan-3β-ol (3-stigmastanol). Campesterol or β-sitosterol are the most abundant sterols in the upper peat and 3-stigmastanol became dominant at increased depth. Steroidal ketones, 24-methyl-5α-cholestan-3-one (campestanone), 24*R*-stigmastan-3-one (sitostanone, Fig. 3.8b) and 24*R*-stigmast-4-en-3-one (stigmasterone, Fig. 3.8c) are also present. The *n*-alkanols present range from C_{20} to C_{30} displaying an even-over-odd predominance. The distributions maximised at the C_{22} or C_{24} homologue with peripheral components describing a monomodal pattern. A range of *n*-alkyl resorcinols ranging from C_{25}-C_{31} including a C_{15} homologue is also present in varying relative abundance (Fig. 3.9a). These have a maximum at C_{27} with a high odd-over-even predominance. Other compounds that occur in this fraction are

cycloartenol and methyl cycloartenol, which are present in peat at the top of the core. Two hopanoid compounds, 17α(H),21β(H)-bishomohopan-32-ol and 17β(H),21β(H)-bishomohopan-32-ol (Fig. 3.9b) are also present with the ββ epimer being the most abundant at the top of the core.

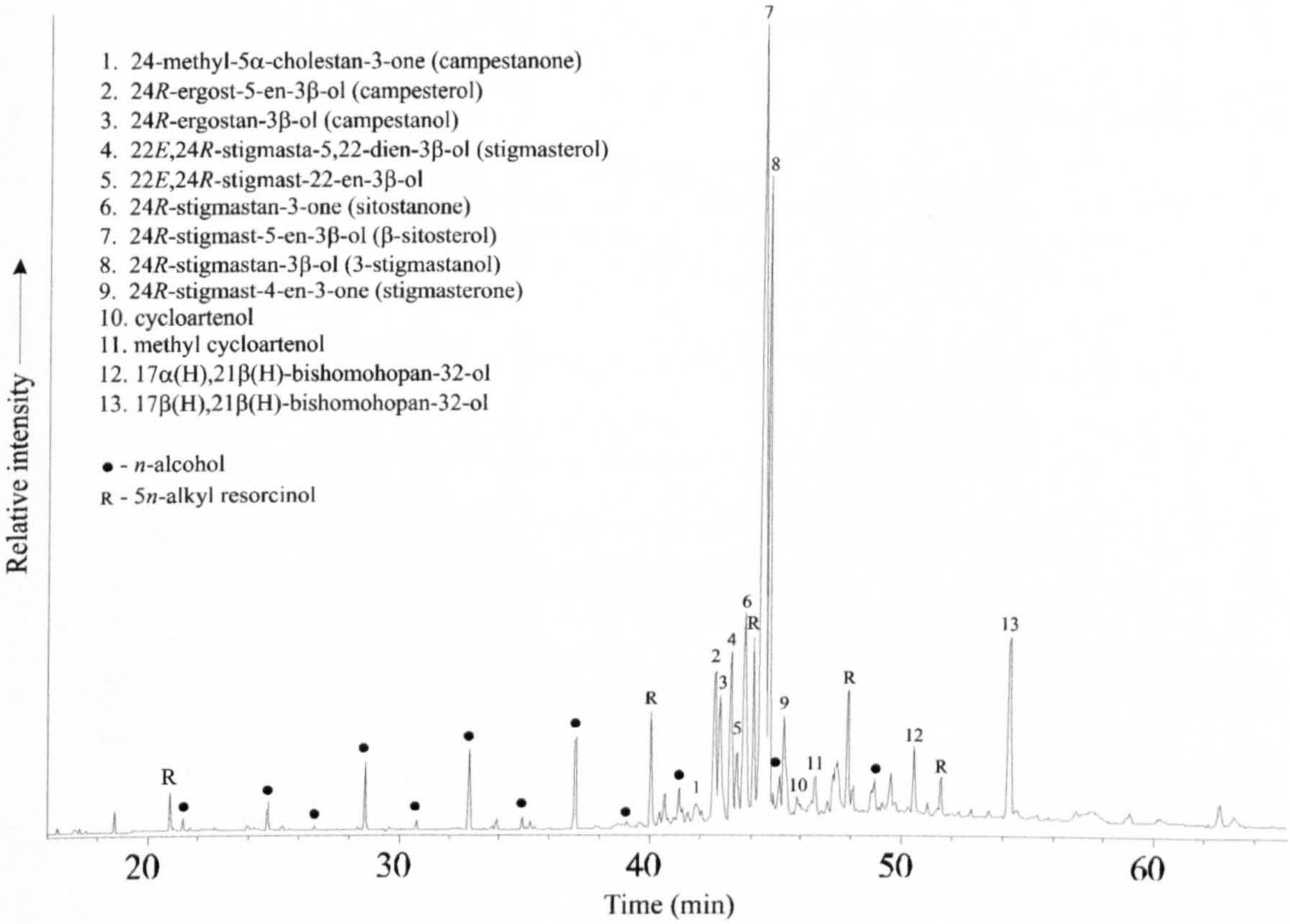

Figure 3.7 Partial gas chromatogram of alcohol/steroid fraction as TMS ethers from monolith peat at 32 cm depth; 50 m CP-Sil5CB, 50-200°C @ 12°C min^{-1}, 200-300°C @ 3°C min^{-1}, 300°C (20 min).

Also present in this fraction at depths greater than 3 m is a group of oxygenated compounds with the androstane skeleton. These include 3α-hydroxy-5α-androstan-17-one (androsterone), 5α-androstan-3,17-dione, 3β-hydroxy-5α-androstan-17-one (epiandrosterone), 5α-androstan-3α,17β-diol and 5α-androstan-3β,17β-diol. These are discussed further in Chapter 4.

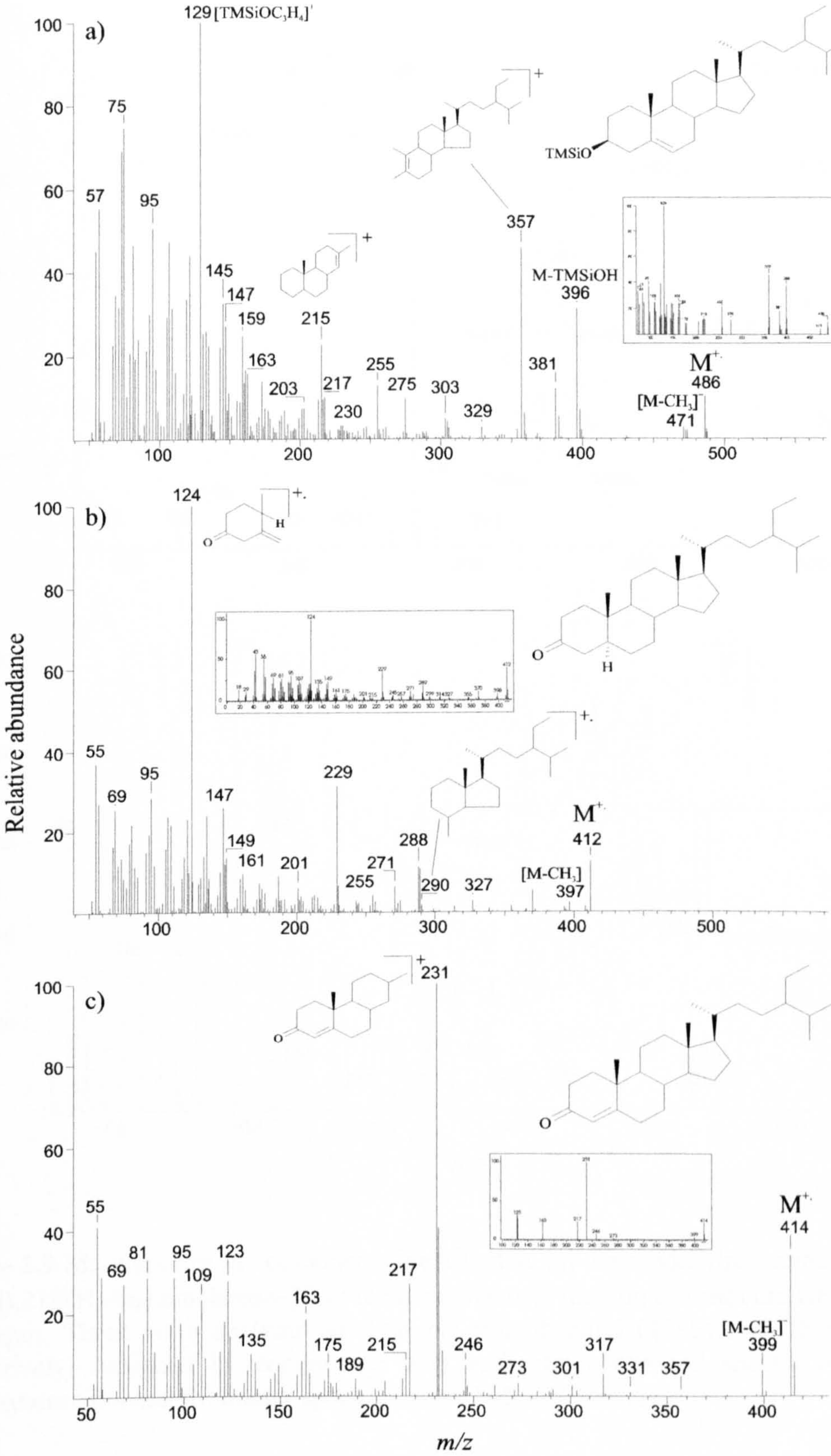

Figure 3.8 Mass spectra of components identified as (a) 24*R*-stigmast-5-en-3β-ol (β-sitosterol), (b) 24*R*-stigmastan-3-one (sitostanone) and (c) 24*R*-stigmast-4-en-3-one (stigmasterone) in alcohol/steroid fraction of peat core BFM2, 25 cm depth. The sterol was analysed as its TMS ether. Assigned by comparison with library spectra (inserts, NIS MS library).

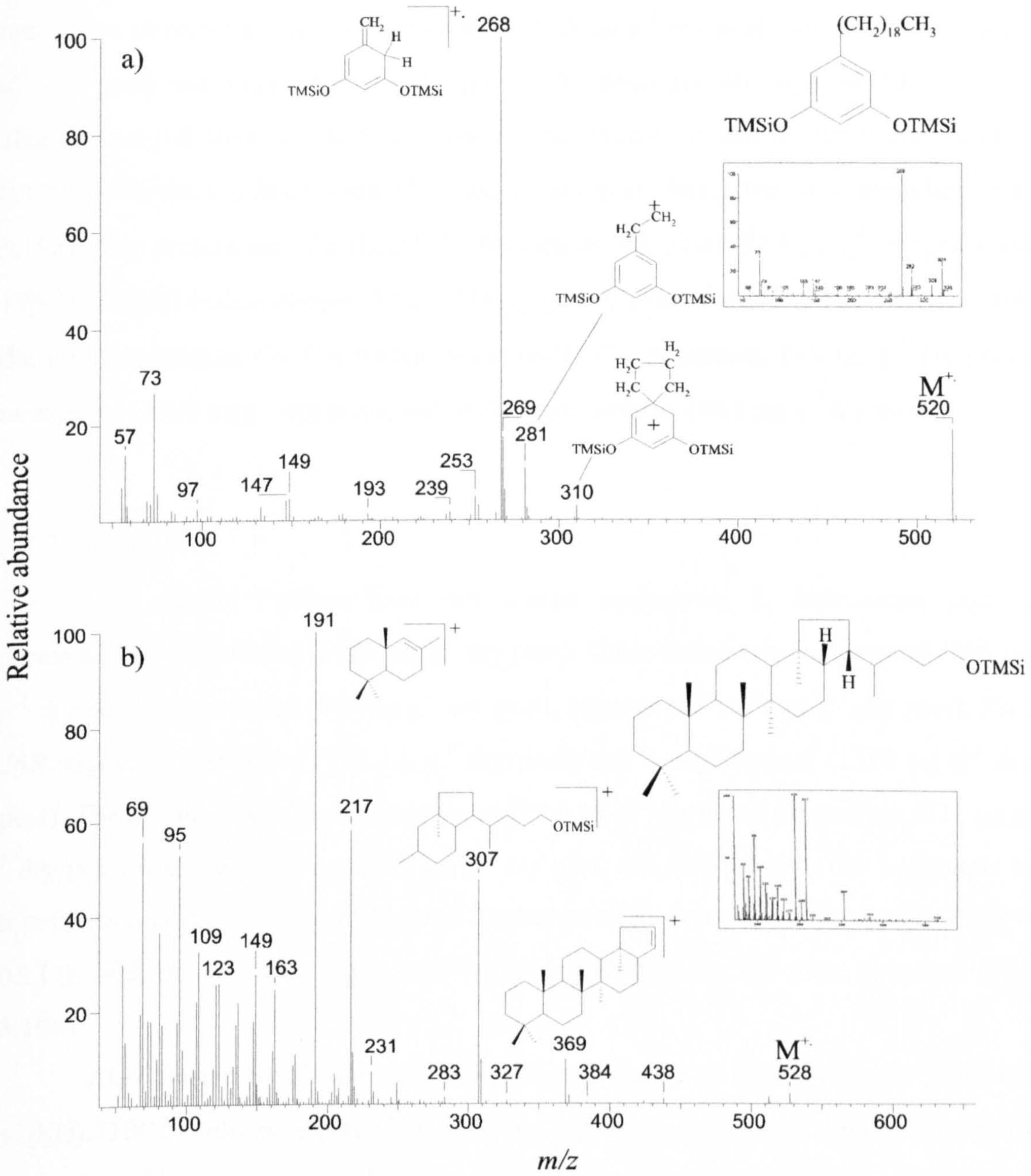

Figure 3.9 Mass spectra of components identified as (a) 5-nonadecylresorcinol and (b) 17β(H),21β(H)-bishomohopan-32-ol in alcohol/steroid fraction of peat core BFM2, 359 cm depth. These were analysed as their *bis* trimethylsilyl (TMS) and TMS ethers, respectively. Assigned by comparison with authentic compound spectra of (a) 5-pentylrescorcinol and (b) library spectra (insert, NIS MS library).

3.6.1 BFM2-25

The alcohol fraction of this *S. magellanicum* peat is dominated by the sterols, campesterol (3363 μg g^{-1} dry peat) and β-sitosterol (3290 μg g^{-1} dry peat). Other sterols present are campestanol (1500 μg g^{-1} dry peat), stigmasterol (552 μg g^{-1} dry peat), 22*E*,

24*R*-stigmast-22-en-3β-ol (440 μg g^{-1} dry peat) and 3-stigmastanol (1010 μg g^{-1} dry peat). The steroidal ketones, campestanone (28.5 μg g^{-1} dry peat), sitostanone (75.3 μg g^{-1} dry peat) and stigmasterone (112 μg g^{-1} dry peat) are also present. Identified *n*-alkanols ranged from C_{20} to C_{30} displaying an even-over-odd predominance (CPI = 0.129), with the C_{22} homologue (184 μg g^{-1} dry peat) being the most abundant (Fig. 3.10a). Also present are 17α(H),21β(H)-bishomohopan-32-ol (65.4 μg g^{-1} dry peat) and 17β(H),21β(H)-bishomohopan-32-ol (334 μg g^{-1} dry peat). Other lipid components are: the odd homologues C_{25}-C_{31} *n*-alkyl resorcinols (C_{25} maximum, 142 μg g^{-1} dry peat), taraxerone (2920 μg g^{-1} dry peat), and methyl cycloartanol (54.1 μg g^{-1} dry peat).

3.6.2 BFM2-205

The alcohol fraction from this almost exclusively *S. imbricatum* peat is dominated by β-sitosterol (1140 μg g^{-1} dry peat). Other sterols are campesterol (196 μg g^{-1} dry peat) campestanol (445 μg g^{-1} dry peat), stigmasterol (373 μg g^{-1} dry peat), 22*E*, 24*R*-stigmast-22-en-3β-ol (130 μg g^{-1} dry peat) and 3-stigmastanol (1320 μg g^{-1} dry peat). The steroidal ketones, campestanone (17.6 μg g^{-1} dry peat), sitostanone (221 μg g^{-1} dry peat) and stigmasterone (122 μg g^{-1} dry peat) are also present. The *n*-alkanols in this fraction range from C_{20} to C_{30} and display an even-over-odd predominance (CPI = 0.117), with the C_{22} homologue (138 μg g^{-1} dry peat) being the most abundant (Fig. 3.10b).

Also present are 17α(H),21β(H)-bishomohopan-32-ol (215 μg g^{-1} dry peat) and 17β(H),21β(H)-bishomohopan-32-ol (285 μg g^{-1} dry peat). Other lipid components were: the odd carbon number homologues C_{25}-C_{31} *n*-alkyl resorcinols (C_{29} maximum, 230 μg g^{-1} dry peat) and taraxerone (396 μg g^{-1} dry peat).

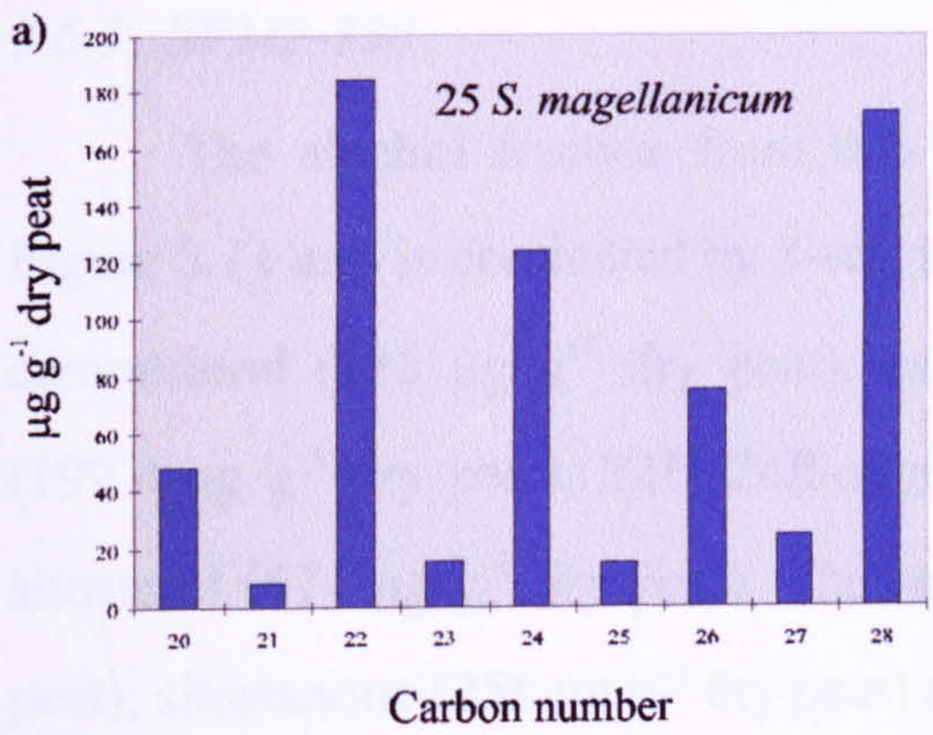

Figure 3.10 Histograms of distributions of *n*-alkanol homologues (µg g^{-1} dry peat) from: (a) BFM2-25, (b) BFM2-205, (c) BFM2-330, (d) BFM2-359, (e) BFM2-425, (f) BFM1-470 and (g) BFM2-485.

3.6.3 BFM2-330

The alcohol fraction from this predominantly *E. vaginatum* peat is shown in Figure 3.11 and is dominated by 3-stigmastanol (1280 μg g^{-1} dry peat). Other sterols are campesterol (126 μg g^{-1} dry peat), campestanol (219 μg g^{-1} dry peat), stigmasterol (199.4 μg g^{-1} dry peat), 22*E*, 24*R*-stigmast-22-en-3β-ol (58.7 μg g^{-1} dry peat) and β-sitosterol (674 μg g^{-1} dry peat). The steroidal ketones, campestanone (43.3 μg g^{-1} dry peat), sitostanone (258 μg g^{-1} dry peat) and stigmasterone (48.0 μg g^{-1} dry peat) are also present. The *n*-alkanols within this peat range from C_{20} to C_{30} and display an even-over-odd predominance (CPI = 0.155), with the C_{22} homologue (230.3 μg g^{-1} dry peat) being the most abundant (Fig. 3.10c).

Also present are 17α(H),21β(H)-bishomohopan-32-ol (141 μg g^{-1} dry peat) and 17β(H),21β(H)-bishomohopan-32-ol (101 μg g^{-1} dry peat). Other lipid components are the odd carbon number homologues C_{25}-C_{31} *n*-alkyl resorcinols (C_{29} maximum, 341 μg g^{-1} dry peat) and taraxerone (88.0 μg g^{-1} dry peat).

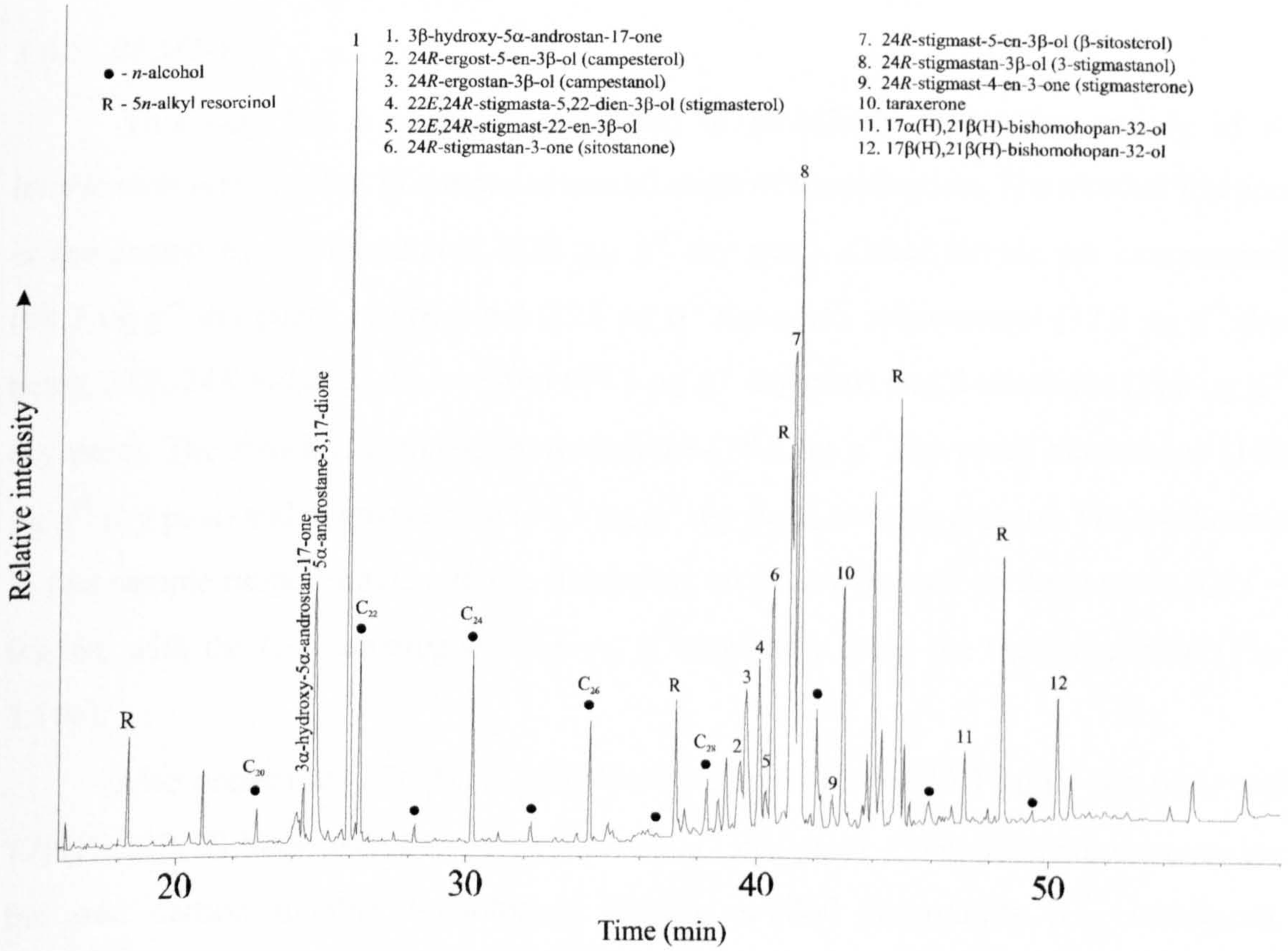

Figure 3.11 Partial gas chromatogram of alcohol/steroid fraction as TMS ethers from peat sample BFM2-330 at 330 cm depth; 50 m CPSil-5CB, 50-200°C @ 12°C min^{-1}, 200-300°C @ 3°C min^{-1}, 300°C (20 min).

3.6.4 BFM2-359

Peat from 359 cm depth contain macrofossil evidence of several inputs, of which *S. imbricatum* was the most abundant. The alcohol fraction from this peat is dominated by 3-stigmastanol (299.7 μg g^{-1} dry peat). Other sterols are campesterol (45.9 μg g^{-1} dry peat) campestanol (155.4 μg g^{-1} dry peat), stigmasterol (72.8 μg g^{-1} dry peat), 22*E*, 24*R*-stigmast-22-en-3β-ol (29.7 μg g^{-1} dry peat) and β-sitosterol (195.1 μg g^{-1} dry peat). The *n*-alkanols present range from C_{20} to C_{30} displaying an even-over-odd predominance (CPI = 0.127), with the C_{24} homologue (71.6 μg g^{-1} dry peat) being the most abundant (Fig. 3.10d).

Also present are 17α(H),21β(H)-bishomohopan-32-ol (40.8 μg g^{-1} dry peat) and 17β(H),21β(H)-bishomohopan-32-ol (37.5 μg g^{-1} dry peat). Other lipid components are the odd carbon number homologues C_{25}-C_{31} *n*-alkyl resorcinols (C_{29} maximum, 151.1 μg g^{-1} dry peat), taraxerone (129.7 μg g^{-1} dry peat), campestanone (12.3 μg g^{-1} dry peat), sitostanone (76.5 μg g^{-1} dry peat) and stigmasterone (39.8 μg g^{-1} dry peat).

3.6.5 BFM2-425

This peat has a similar composition to BFM2-205 consisting mainly of *S. imbricatum* remains, but in a more advanced stage of humification. The alcohol fraction is dominated by 3-stigmastanol (238 μg g^{-1} dry peat). Other sterols are campesterol (68.7 μg g^{-1} dry peat), campestanol (121 μg g^{-1} dry peat), stigmasterol (37.2 μg g^{-1} dry peat), 22*E*, 24*R*-stigmast-22-en-3β-ol (19.8 μg g^{-1} dry peat) and β-sitosterol (210 μg g^{-1} dry peat). The steroidal ketones, campestanone (18.4 μg g^{-1} dry peat), sitostanone (104 μg g^{-1} dry peat) and stigmasterone (34.3 μg g^{-1} dry peat) are also present. The *n*-alkanols in this sample range from C_{20} to C_{30} displaying an even-over-odd predominance (CPI = 0.116), with the C_{22} homologue (76.6 μg g^{-1} dry peat) being the most abundant (Fig. 3.10e).

Also present are 17α(H),21β(H)-bishomohopan-32-ol (30.3 μg g^{-1} dry peat) and 17β(H),21β(H)-bishomohopan-32-ol (47.3 μg g^{-1} dry peat). Other lipid components are the odd carbon number homologues C_{25}-C_{31} *n*-alkyl resorcinols (C_{25} maximum, 55.7 μg g^{-1} dry peat) and taraxerone (137 μg g^{-1} dry peat).

3.6.6 BFM1-470

The alcohol fraction of this humified peat is dominated by 3-stigmastanol (307 μg g^{-1} dry peat). Other sterols are campesterol (90.8 μg g^{-1} dry peat), campestanol (70.1 μg g^{-1} dry peat), stigmasterol (73.3 μg g^{-1} dry peat), 22*E*, 24*R*-stigmast-22-en-3β-ol (52.3 μg g^{-1} dry peat) and β-sitosterol (199.7 μg g^{-1} dry peat). The *n*-alkanols present range from C_{20} to C_{30} displaying an even-over-odd predominance (CPI = 0.143), with the C_{22} homologue (99.9 μg g^{-1} dry peat) being the most abundant (Fig. 3.10f).

Also present are 17α(H),21β(H)-bishomohopan-32-ol (68.5 μg g^{-1} dry peat) and 17β(H),21β(H)-bishomohopan-32-ol (81.3 μg g^{-1} dry peat). Other lipid components are: the odd carbon number homologues C_{25}-C_{31} *n*-alkyl resorcinols (C_{29} maximum, 212 μg g^{-1} dry peat), taraxerone (19.3 μg g^{-1} dry peat), campestanone (6.2 μg g^{-1} dry peat), sitostanone (271 μg g^{-1} dry peat) and stigmasterone (34.0 μg g^{-1} dry peat).

3.6.7 BFM2-485

This peat sample is most representative of Ericaceous input and the alcohol fraction is dominated by 3-stigmastanol (310 μg g^{-1} dry peat). Other sterols are stigmasterol (73.0 μg g^{-1} dry peat), 22*E*, 24*R*-stigmast-22-en-3β-ol (34.2 μg g^{-1} dry peat) and β-sitosterol (190.5 μg g^{-1} dry peat). Steroidal ketone components are sitostanone (115.9 μg g^{-1} dry peat) and stigmasterone (70.9 μg g^{-1} dry peat). The *n*-alkanols present range from C_{20} to C_{30} displaying an even-over-odd predominance (CPI = 0.106), with the C_{22} homologue (85.3 μg g^{-1} dry peat) being the most abundant (Fig. 3.10g).

Also present are 17α(H),21β(H)-bishomohopan-32-ol (19.7 μg g^{-1} dry peat) and 17β(H),21β(H)-bishomohopan-32-ol (22.1 μg g^{-1} dry peat). Other lipid components are the odd carbon number homologues C_{25}-C_{31} *n*-alkyl resorcinols (C_{27} maximum, 177 μg g^{-1} dry peat) and taraxerone (149 μg g^{-1} dry peat).

3.7 Carboxylic Acids

The *n*-alkanoic acid distributions of all the samples studied showed a monomodal even-over-odd predominance over the range C_{20} to C_{32} (Fig. 3.12) with a maximum at C_{24} or C_{26}. ω-Hydroxy acids ranging from C_{22} to C_{28} were also observed in this fraction along with some unidentified terpenyl acids.

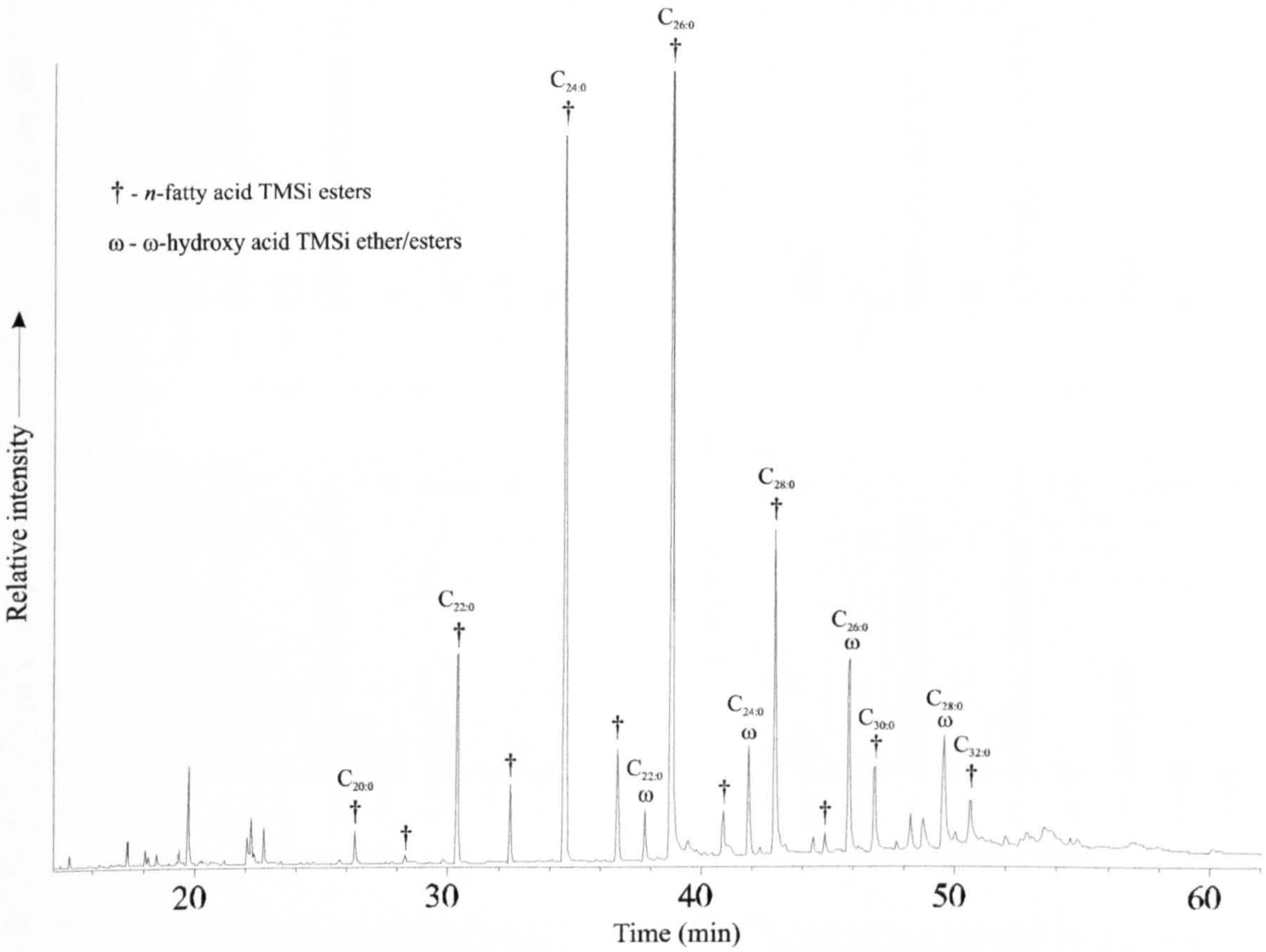

Figure 3.12 Partial gas chromatogram of acid fraction from monolith peat at 32 cm depth; 50 m CPSil-5CB, 50-200°C @ 12°C min^{-1}, 200-300°C @ 3°C min^{-1}, 300°C (20 min). Analysed as TMS ester/ethers.

3.7.1 BFM2-25

The *n*-alkanoic acid distribution of this *S. magellanicum* peat sample show a monomodal even-over-odd predominance (CPI = 0.122) over the range C_{20} to C_{32} (Fig. 3.13a) with a maximum at C_{26} (998.2 μg g^{-1} dry peat). The abundance of the C_{26} acid is relatively high compared to the other acids (next highest abundance acid C_{24}; 771 μg g^{-1} dry peat). Also present in this fraction is a series of even carbon numbered ω-hydroxy acids ranging from C_{22} to C_{28} with a maximum at C_{26} (128.9 μg g^{-1} dry peat).

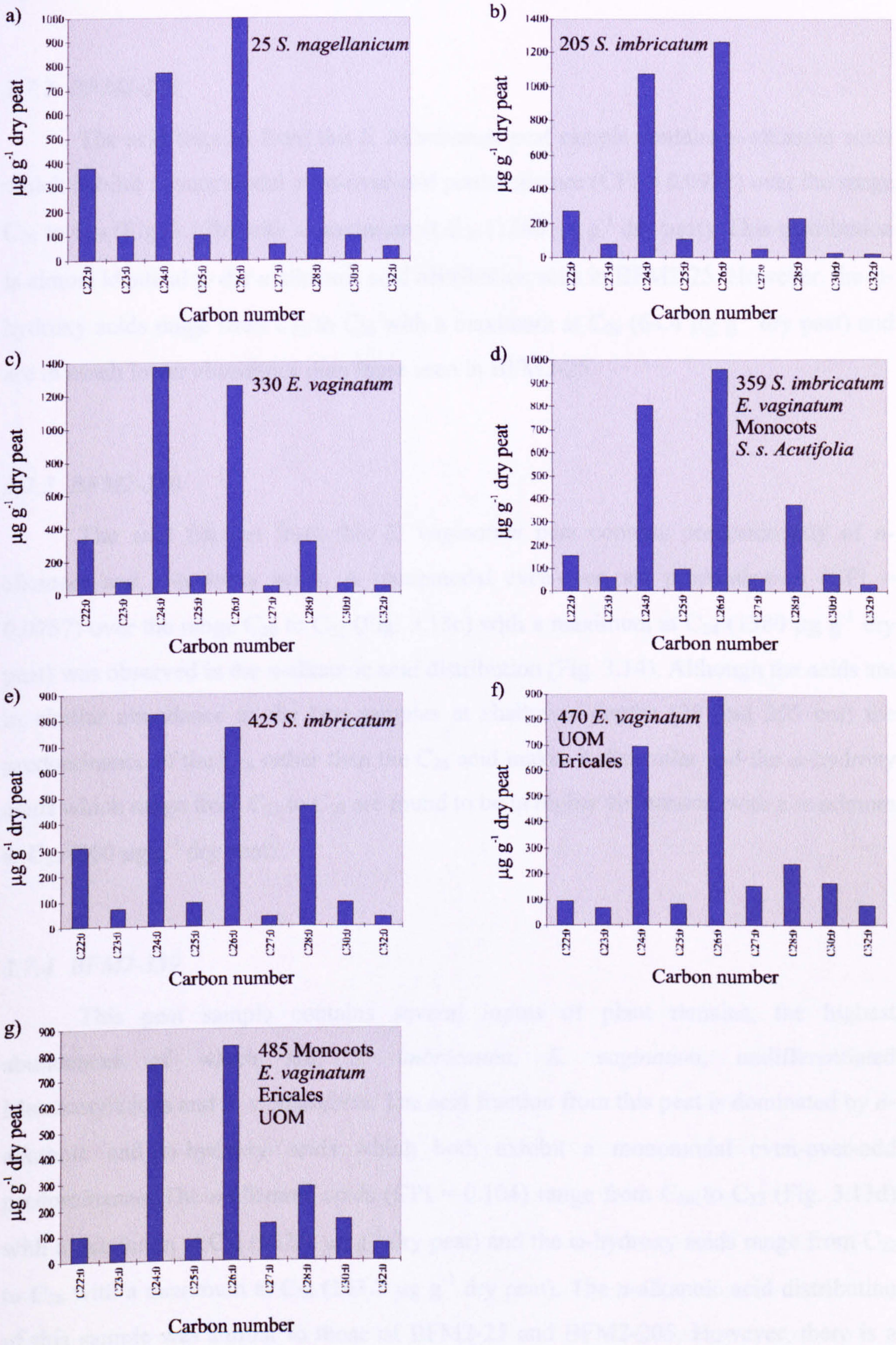

Figure 3.13 Histograms of distributions of *n*-acid homologues (µg g^{-1} dry peat) from: (a) BFM2-25, (b) BFM2-205, (c) BFM2-330, (d) BFM2-359, (e) BFM2-425, (f) BFM1-470 and (g) BFM2-485.

3.7.2 BFM2-205

The acid fraction from this *S. imbricatum* peat sample contains *n*-alkanoic acids which exhibit a monomodal even-over-odd predominance (CPI = 0.0932) over the range C_{20} to C_{28} (Fig. 3.13b) with a maximum at C_{26} (1260 μg g^{-1} dry peat). This distribution is almost identical to the *n*-alkanoic acid distribution seen in BFM2-25. However, the ω-hydroxy acids range from C_{22} to C_{26} with a maximum at C_{22} (64.4 μg g^{-1} dry peat) and are in much lower abundance than those seen in BFM2-25.

3.7.3 BFM2-330

The acid fraction from this *E. vaginatum* peat consists predominantly of *n*-alkanoic and ω-hydroxy acids. A monomodal even-over-odd predominance (CPI = 0.0757) over the range C_{20} to C_{32} (Fig. 3.13c) with a maximum at C_{24} (1380 μg g^{-1} dry peat) was observed in the *n*-alkanoic acid distribution (Fig. 3.14). Although the acids are in similar abundance to the two samples at shallower depths (25 and 205 cm) the predominance of the C_{24} rather than the C_{26} acid makes it dissimilar and the ω-hydroxy acids which range from C_{22} to C_{28} are found to be in higher abundance, with a maximum at C_{24} (260 μg g^{-1} dry peat).

3.7.4 BFM2-359

This peat sample contains several inputs of plant remains, the highest abundances of which are, *S. imbricatum*, *E. vaginatum*, undifferentiated Monocotyledons and *S. s. Acutifolia*. The acid fraction from this peat is dominated by *n*-alkanoic and ω-hydroxy acids which both exhibit a monomodal even-over-odd predominance. The *n*-alkanoic acids (CPI = 0.104) range from C_{20} to C_{32} (Fig. 3.13d) with a maximum at C_{26} (962.4 μg g^{-1} dry peat) and the ω-hydroxy acids range from C_{22} to C_{28} with a maximum at C_{26} (143.7 μg g^{-1} dry peat). The *n*-alkanoic acid distribution of this sample was similar to those of BFM2-25 and BFM2-205. However, there is a higher abundance of longer chain homologues (average chain length = 25.5, *cf.* BFM2-25 = 25.3, BFM2-205 = 25.1).

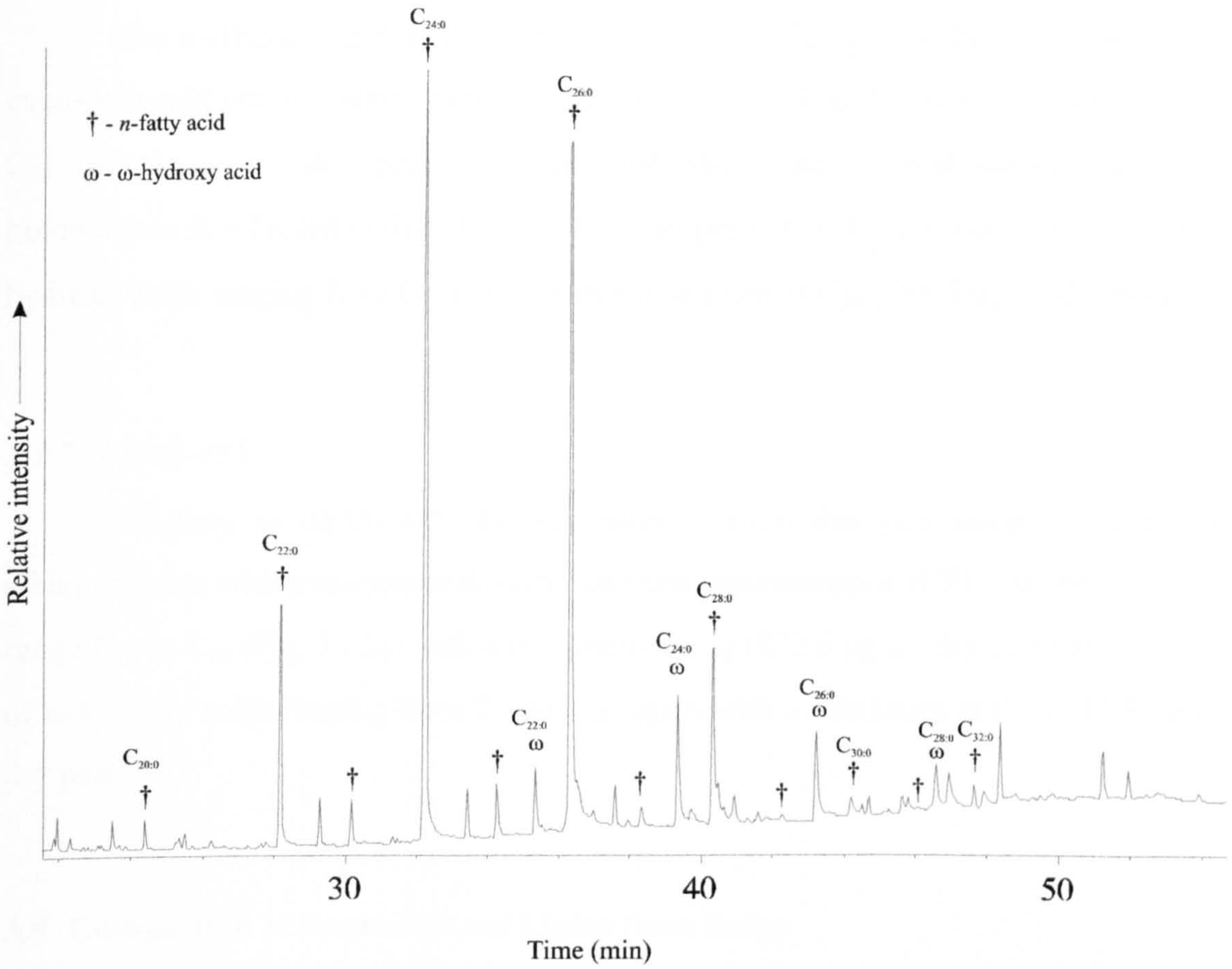

Figure 3.14 Partial gas chromatogram of acid fraction from peat sample BFM1-330 at 330 cm depth; 50 m CPSil-5CB, 50-200°C @ 12°C min^{-1}, 200-300°C @ 3°C min^{-1}, 300°C (20 min). Analysed as TMS ester/ethers.

3.7.5 BFM2-425

Although this peat sample has very similar macrofossil composition (*S. imbricatum*) to BFM2-205, differences in the acid fraction are observed. The *n*-alkanoic acid distribution for this sample shows a monomodal even-over-odd predominance (CPI = 0.101) over the range C_{20} to C_{32} (Fig. 3.13e) with a maximum at C_{24} (821.4 μg g^{-1} dry peat). Also present in this fraction is a series of ω-hydroxy acids ranging from C_{22} to C_{28} with a maximum at C_{24} (460.4 μg g^{-1} dry peat). A higher abundance of longer chain *n*-alkanoic acid (average chain length = 25.4) components and shorter chain ω-hydroxy acids were present in this peat than those found in BFM2-205 (average chain length = 25.1).

3.7.6 BFM1-470

The *n*-alkanoic acid distribution from this humified peat exhibits a monomodal even-over-odd predominance over the range C_{20} to C_{32} (Fig. 3.13f) with a maximum at C_{26} (889.5 μg g^{-1} dry peat). The elevated abundance of odd carbon numbered homologues is reflected in the CPI = 0.174. Also present in this fraction is a series of ω-hydroxy acids ranging from C_{22} to C_{28} with a maximum at C_{26} (394.5 μg g^{-1} dry peat).

3.7.7 BFM2-485

Similarly to BFM1-470 the acid fraction from this peat sample contains *n*-alkanoic acids with a monomodal even-over-odd predominance (CPI = 0.166) over the range C_{20} to C_{32} (Fig. 3.13g) with a maximum at C_{26} (832.6 μg g^{-1} dry peat) and a series of ω-hydroxy acids ranging from C_{22} to C_{28}, again with a maximum at C_{26} (443.5 μg g^{-1} dry peat).

3.8 Comparison of Root and Leaf Lipids from Sedge

Long roots (up to 2 m) from the sedge (*Eriophorum*) species found at Bolton Fell Moss, were found in some of the peat samples analysed. The extraneous lipids from these roots may influence the observed lipid profiles from horizons and include a signal of material not present at the deposition of these horizons. This is particularly important where the radiocarbon dating of specific lipids is concerned, as these lipids would produce younger dates than the true date for the horizon (Chapter 6). Suberin, a component of root material has been found to consist mainly of hydroxy alkanoic acid polymers (Kolattukudy *et al.*, 1976; Walton, 1990). Therefore to get a better understanding of the origin of the hydroxy acids found in the peat samples, a comparison of lipids from sedge roots and leaves was made as below.

Suberin, the woody material which is the major structural component in roots, is composed of a polyester of hydroxy fatty acids (Walton, 1990). Characteristic ω-hydroxy acids range from C_{16} to C_{26} and have been extracted from suberin from apples (*Malus pumilla*) and maize (*Zeamays*). However, $C_{16:0}$ and $C_{18:1}$ components are often found to be major components. If the ω-hydroxy acids found in the peat in the present

study had *Eriophorum* roots as their source, then their inclusion in a lipid stratigraphy would produce misleading results.

To determine if ω-hydroxy acids were predominantly present in the roots of sedge species, the saponified acidic lipids of the leaves and roots of *E. vaginatum* and *E. angustifolium* were studied. Intact *E. vaginatum* and *E. angustifolium* plants were obtained from the surface of Bolton Fell Moss and divided into leaves and roots. Free lipids were then removed from the plants by Soxhlet extraction with 9:1 DCM/acetone (24 h) and the resulting plant material was saponified with methanolic NaOH (0.5 M, 2 h). The organic extracts were separated into neutral and acidic fractions and the acidic fractions studied by GC and GC/MS. Distributions of the major ω-hydroxy and *n*-alkanoic acids are displayed in Figure 3.15.

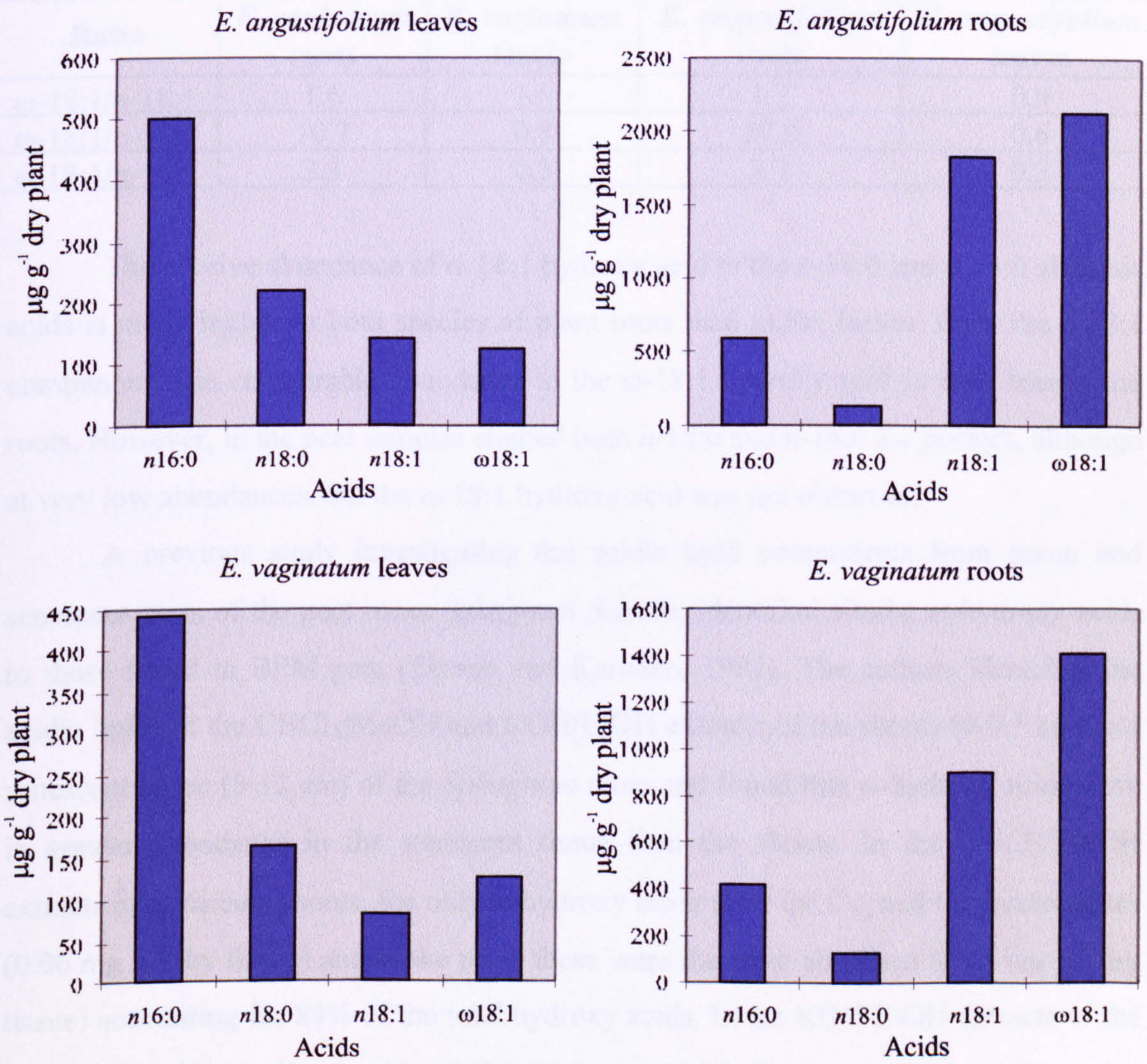

Figure 3.15 Hydroxy and normal acid components of leaves and roots of sedges in µg g $^{-1}$ of plant material.

The ω-18:1 hydroxy acid is the major homologue present in the roots and leaves. The ω-16:0 component is also present in very small abundance in the roots but absent in the leaves. The major *n*-alkanoic acids are *n*-16:0 which is the predominant acid in the leaves, *n*-18:1 which is the predominant acid in the roots and *n*-18:0. Other minor components are the alkanoic acids *n*-14:0, *n*-15:0 and *n*-18:2 of which the *n*-18:2 is found to be in quite high abundance in the roots. Higher chain length acids were not observed. The ratio of the ω-18:1 hydroxy acid to the other major acids is shown in Table 3.5.

Table 3.5 Ratios of ω-18:1 hydroxy acid to other acids in sedge leaves and roots.

Ratio	***E. vaginatum* roots**	***E. vaginatum* leaves**	***E. angustifolium* roots**	***E. angustifolium* leaves**
ω-18:1/*n*-18:1	1.6	1.5	1.2	0.9
ω-18:1/*n*-18:0	10.7	0.8	17.0	0.6
ω-18:1/*n*-16:0	3.3	0.3	3.7	0.2

The relative abundance of ω-18:1 hydroxy acid to the *n*-18:0 and *n*-16:0 alkanoic acids is much higher in both species of plant roots than in the leaves. Only the *n*-18:1 component is in comparable abundance to the ω-18:1 hydroxy acid in both leaves and roots. However, in the peat samples studied both *n*-18:0 and *n*-16:0 are present, although at very low abundances, but the ω-18:1 hydroxy acid was not observed.

A previous study investigating the acidic lipid components from green and senescent parts of the peat moss *Sphagnum fuscum*, identified similar ω-hydroxy acids to those found in BFM peat (Ekman and Karunen, 1982). The authors identified the acidic lipids in the $CHCl_3$/MeOH and KOH/EtOH extracts of the shoots (0-0.5 cm) and senescent tissue (9-12 cm) of the *Sphagnum* moss and found that ω-hydroxy acids were in greater abundance in the senescent tissue than the shoots. In the $CHCl_3$/MeOH extracts of *S. fuscum* shoots, the only ω-hydroxy acids were the C_{22} and C_{24} homologues (0.06 mg g^{-1} dry tissue) and in the roots these were the most abundant (0.16 mg g^{-1} dry tissue) accounting for 84% of the total hydroxy acids. In the KOH/EtOH extracts of the shoots, the ω18:1 hydroxy acid and C_{16} 9,16- and 10,16-dihydroxyacids were the major components (0.21 mg g^{-1} dry tissue). The senescent tissue yielded a greater proportion of the ω18:1 hydroxy acid (1.03 mg g^{-1} dry tissue) but there was also a considerable

contribution from the C_{22} (0.28 mg g^{-1} dry tissue) and C_{24} (0.20 mg g^{-1} dry tissue) ω-hydroxy acids. This suggests that the ω-hydroxy acids found in BFM peat are likely to be the products of senescent *Sphagnum* remains which have been shown to contain the longer chain components (C_{22-26}). As the senescent parts of moss do not protrude below the horizon in which they are formed, they are unlikely to contribute 'young', extraneous lipids to lower peat horizons. However, the absence of these compounds in extracts of sedge roots does not mean that they are not a possible source. By analogy with the findings of Ekman and Karunen (1982), the absence of longer chain ω-hydroxy acids in the roots of sedge may be related to the extraction method employed, where the authors found that $CHCl_3$/MeOH extraction favoured longer chain saturated compounds (ω-22:0 and ω-24:0) from *Sphagnum* and the KOH/EtOH extraction favoured shorter chain unsaturated components (ω-18:1). The absence of longer chain compounds detectable by GC and GC/MS in the sedge roots extracts, however, suggests that these are not the main source of ω-hydroxy acids in BFM peat.

3.9 Discussion

3.9.1 Hydrocarbons

<u>*n*-Alkanes</u> - Except for the relative quantities of the C_{23} and C_{25} homologues the *n*-alkane distributions from the 7 samples were similar to each other. A previous investigation of modern bog vegetation from Bolton Fell Moss revealed that *Sphagnum* species display an enhanced abundance of lower chain length *n*-alkane homologues (C_{21}-C_{25}), where other plants revealed typical higher plant distributions (Nott *et al.*, 2000). Over a 40 cm peat profile the varying abundance of the *n*-C_{23} homologue appeared to be related to vegetation change. Typically the abundances of these are normalised against the C_{31} homologue and the ratios of the C_{23} and C_{25} *n*-alkanes from the present study are displayed in Figure 3.16.

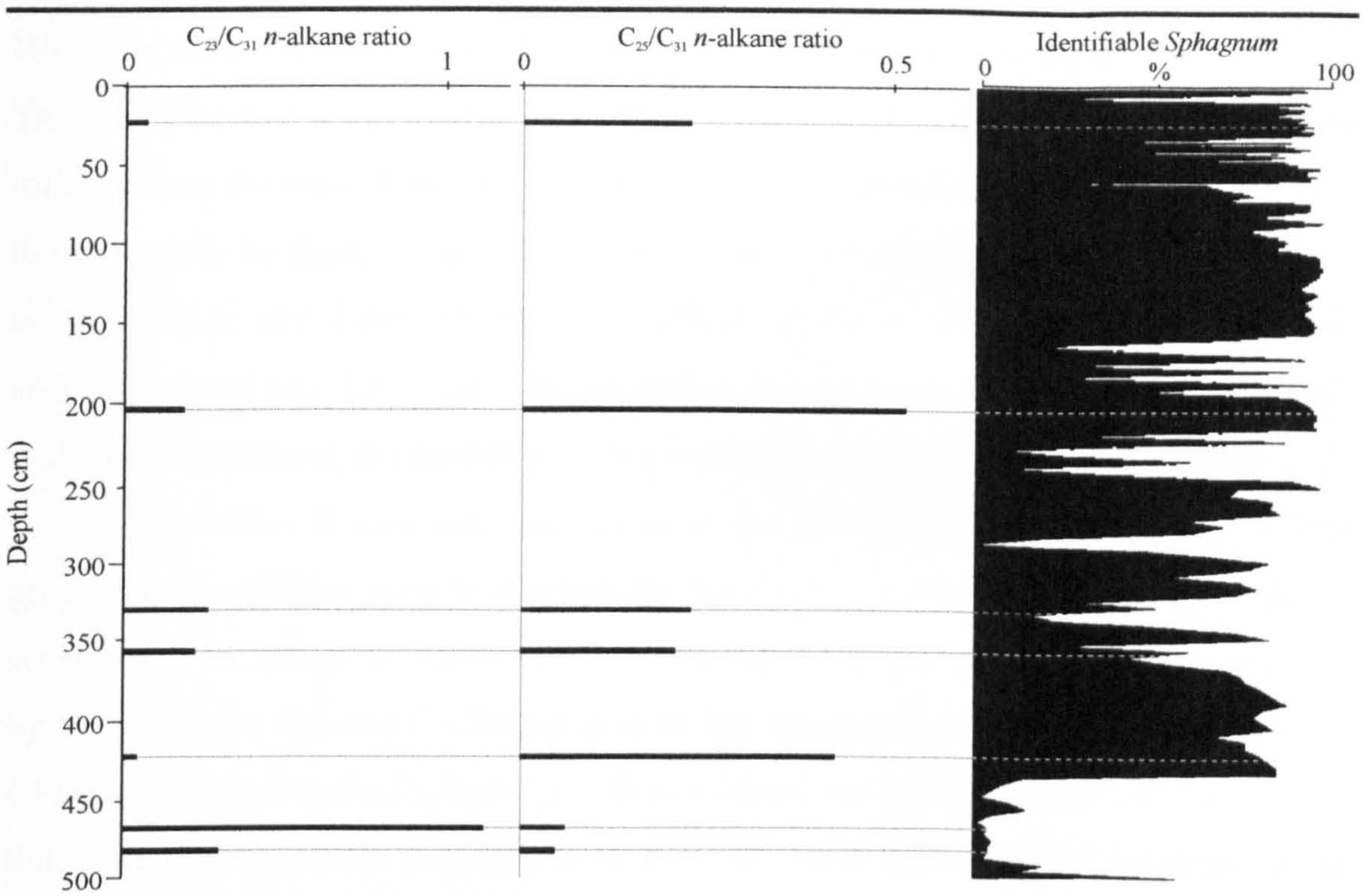

Figure 3.16 Plot of the ratios of *n*-C_{23} and *n*-C_{25} to *n*-C_{31} alkane together with total identified *Sphagnum* in the 0-500 cm peat core.

Lipid profiles have been determined for *S. magellanicum, S. imbricatum, S. capillifolium, S. cuspidatum, S. palustre, S. papillosum, S. recurvum, S. sub-nitens, Polytrichum* species, *Aulacomnium palustre, Hypnum cupressiforme, E. vaginatum, E. angustifolium, Trichophorum cespitosum, Rhynchospora alba, Empetrum nigrum, Vaccinium oxycoccus, Erica tetralix, Calluna vulgaris, Andromeda polifolia* and *Cladonia* species (Nott, 2000). An elevated abundance of the C_{23} alkane relative to the C_{31} homologue observed in BFM1-470 is also in the hydrocarbons of *S. papillosum, S. recurvum, S. imbricatum, S. capillifolium, S. cuspidatum*, and *S. palustre*. The high abundance of the C_{23} alkane in BFM1-470 and BFM2-485 is completely contrary to the macrofossil data (e.g. Fig. 3.16) which indicates few *Sphagnum* macrofossils and *E. vaginatum* as the major input at 470 cm. This horizon, however, contains 30% unidentified organic matter (Fig. 2.4), which could possibly be the remains of decayed *Sphagnum*, or another input with an elevated C_{23} content. A high abundance of the C_{25} alkane relative to the C_{31} homologue in samples BFM2-205 and BFM2-425 is also observed in the hydrocarbon fraction from *S. magellanicum, S. capillifolium* and *S. imbricatum*. This correlates with macrofossil data where BFM2-205 and BFM2-425 contain 95% and 81% *S. imbricatum*, respectively. Figure 3.16 appears to show a relationship between the C_{25}/C_{31} *n*-alkane ratio and the *Sphagnum* content of the peat.

However, the C_{25}/C_{31} ratio for BFM2-25 does not correlate as well as the other samples. This could be a result of an inaccuracy in the macrofossil data as the top 250 cm were inferred from the macrofossil record of a nearby core. Therefore the *Sphagnum* record in the peat could be displaced and the peat at 25 cm depth could have a similar *Sphagnum* contribution to peat from 330 cm depth. Discrepancies between *n*-alkane distributions and macrofossil data have been reported before. Ficken *et al*. (1998) found very similar *n*-alkane distributions in peat samples with quite different known biological inputs.

The Carbon Preference Index of the *n*-alkanes is presented in Figure 3.17. This graph shows a similar trend to that seen for the C_{25}/C_{31} *n*-alkane ratio and may also be an indicator of *Sphagnum* contribution to peat. To determine if the CPI was influenced by the increased C_{23} and C_{25} abundances in the *Sphagnum* dominated peat samples, a CPI graph excluding the C_{23} and C_{25} *n*-alkane values was plotted (Fig. 3.18). This shows the same odd-over-even predominance, indicating that the original CPI graph is not heavily influenced by increases in the C_{23} and C_{25} homologues.

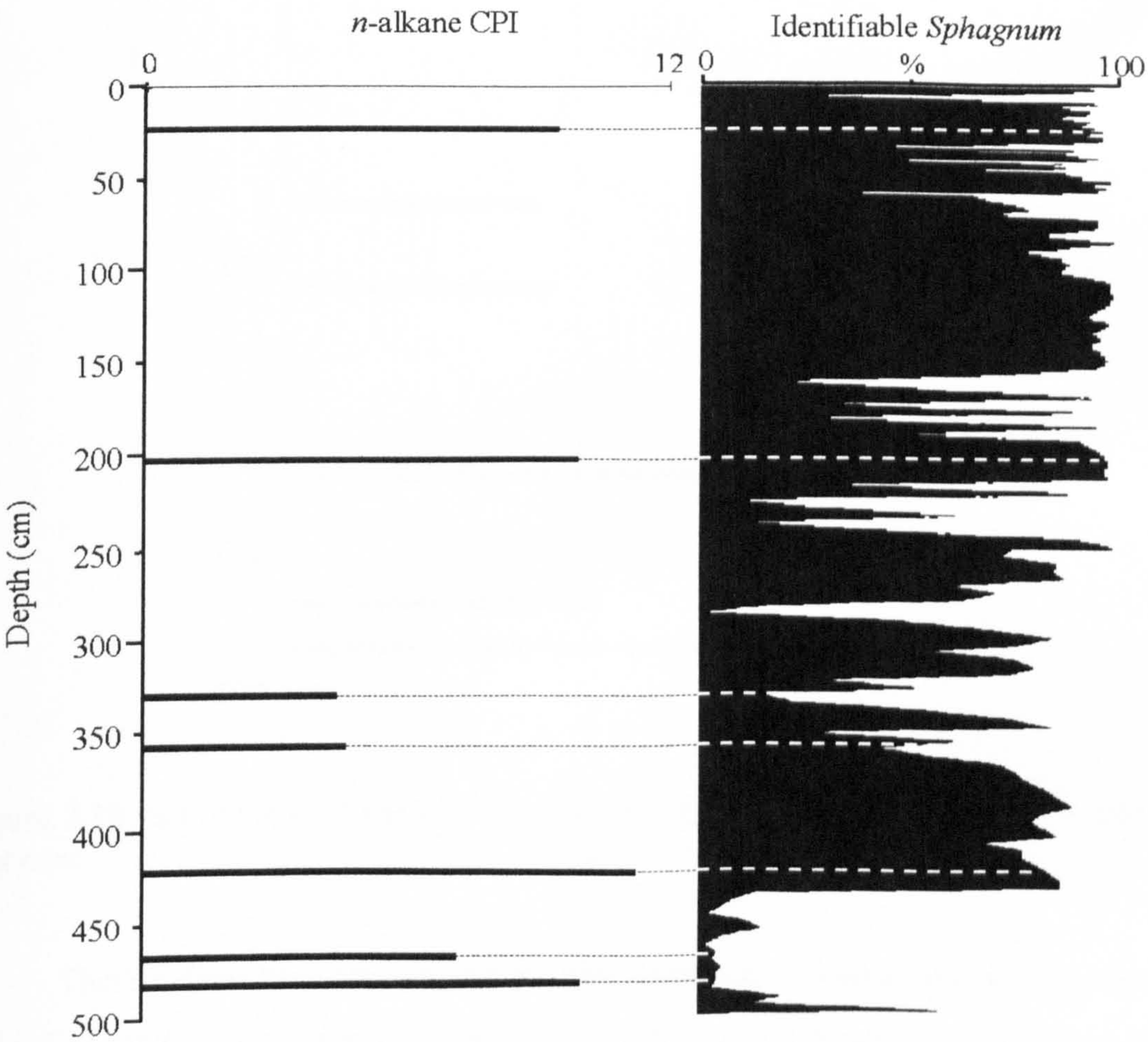

Figure 3.17 Plot of the *n*-alkane Carbon Preference Index (CPI) together with total identified *Sphagnum* in the 0-500 cm peat core.

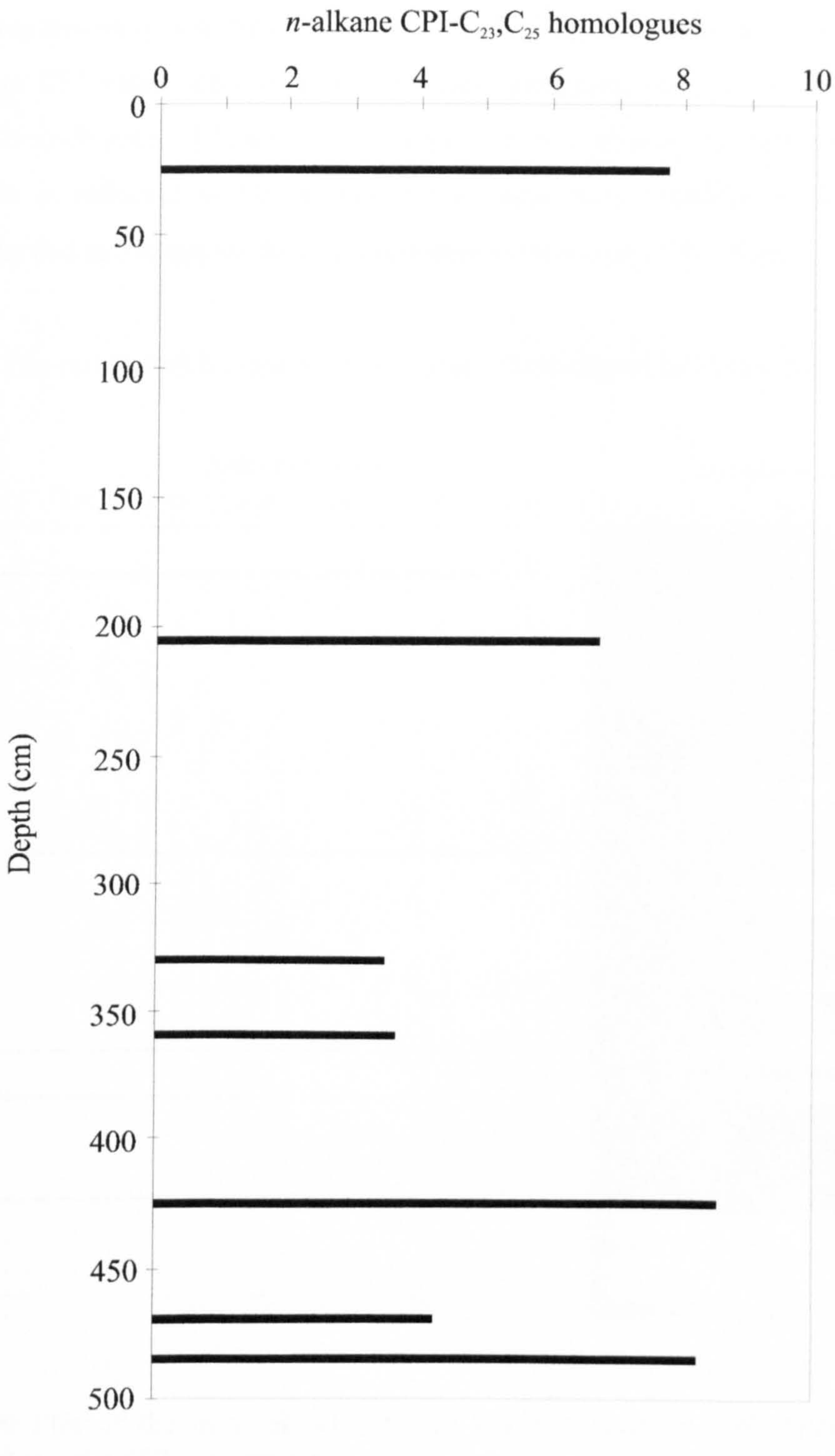

Figure 3.18 Plot of the *n*-alkane CPI excluding C_{23} and C_{25} homologues in the 0-500 cm peat core.

These indices have previously been used to indicate possible inputs in a sediment and a CPI greater than 5 for *n*-alkanes has been found to indicate a major higher plant input (Brooks *et al.*, 1976). Therefore, the low CPI values for BFM2-330 and BFM2-359 could represent an alkane input from non-higher plant material not revealed by

macrofossil analyses. Alternatively, the CPI values could also reflect changes in higher plants. Comparisons of *n*-alkane CPI values (C_{19}-C_{33}) for different peat types has found that average CPI values decreased in the range *Sphagnum* (8.1, n = 3) > *Carex* (6.1, n = 4) > *Carex-Bryales* (4.5, n = 6) > *Bryales* (3.8, n = 4) peat (Lehtonen and Ketola, 1993). This is reflected in the present study where high abundances of *Sphagnum* species recorded in the macrofossil data correspond with high CPI values.

Hopanes - The ratio of ββ hopane to total hopanes is displayed in Figure 3.19.

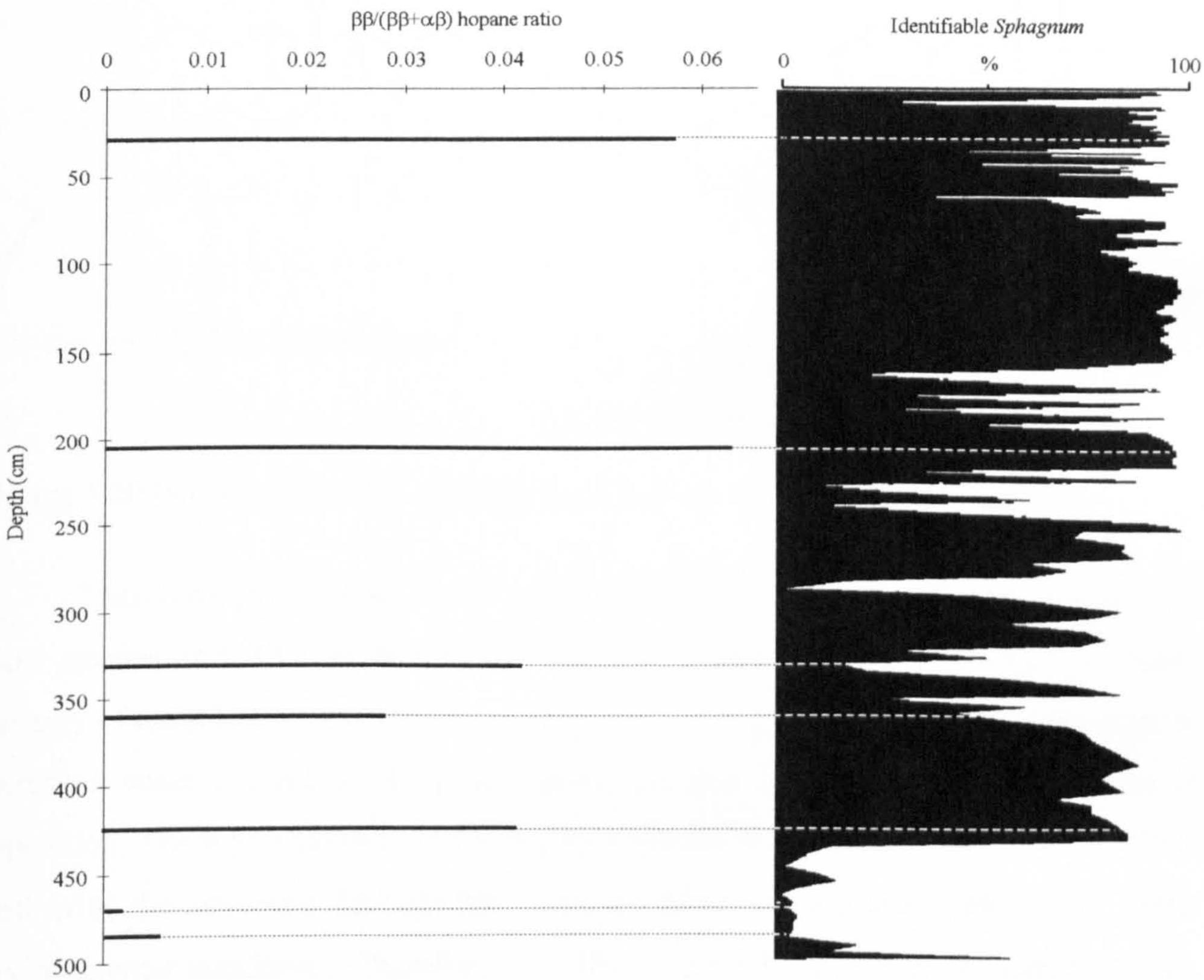

Figure 3.19 Plot of the ratio of ββ/(ββ+αβ) hopanes together with total identified *Sphagnum* down the 500 cm peat core.

Extended hopanoids of the ββ series, when found in sediments are normally regarded as being derived from aerobic bacteria (e.g. Ourisson *et al.*, 1979; Rohmer *et al.*, 1980) and it is likely that the αβ-hopane derives from isomerisation of ββ-hopane, facilitated by acidic bog conditions (Quirk *et al.*, 1984). The epimerisation of 17β(H),21β(H) hopanes to their αβ and βα analogues has long been known and is used

as a maturity indicator for oils and bitumen (reviewed by Farrimond *et al.*, 1998). The isomerisation is temperature driven and as the temperature rises during catagenesis the available energy becomes sufficient so that the energy barrier for conversion of the ββ and αβ forms can be overcome, (Peters and Moldowan, 1993). It is unlikely for this isomerisation to occur in peat as the temperature is not normally sufficient for these processes. However, previous studies of peat environments have suggested that the ββ to αβ isomerisation is acid-catalysed (Fig. 3.20, van Dorsselaer *et al.*, 1977).

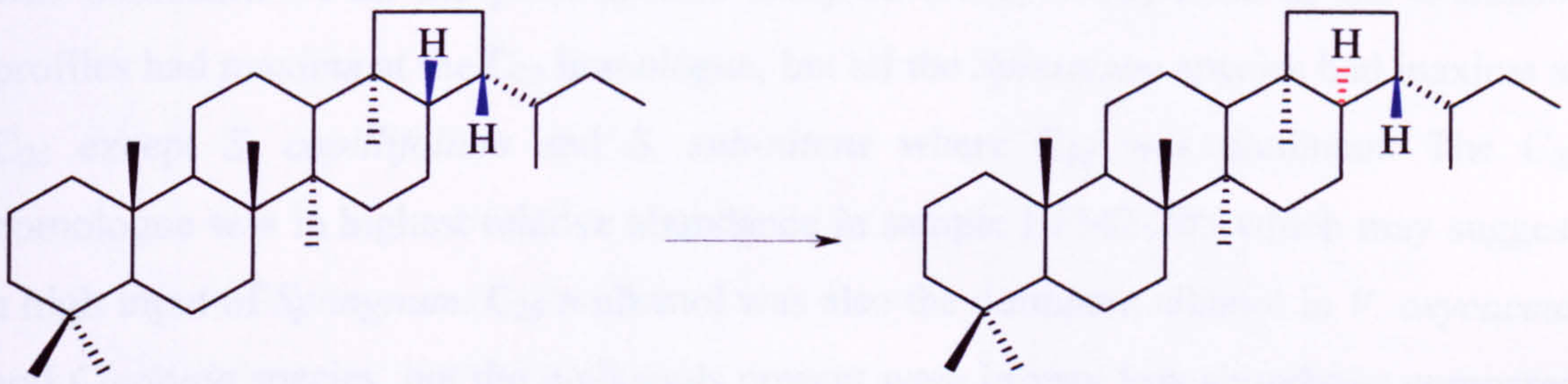

29-methyl-17β(H),21β(H)-hopane

29-methyl-17α(H),21β(H)-hopane

Figure 3.20 Isomerisation of a 17β(H),21β(H) hopane to 17α(H),21β(H) hopane.

Therefore, ββ/(αβ+ββ) ratios could reflect pH, which is affected by changing plant species and dilution factors due to water content of the peat. The increased quantity of the ββ-hopane relative to the αβ isomer in BFM2-425 could be a result of an increased water content of the peat making the peat less acidic around the time of deposition. The high abundance of *Sphagnum* species in the macrofossil data correlates well with the observed ββ/(αβ+ββ) ratio, as these species are markers for wetter environmental conditions. Therefore it is likely that where *Sphagnum* species thrive, higher water content conditions prevail, thus increasing pH levels and lowering the ββ to αβ isomerisation. Where high abundances of C_{23} *n*-alkane and UOM are present (e.g. BFM1-470, Fig. 3.16) but *Sphagnum* species are not detected in the macrofossil record the ββ/(αβ+ββ) ratio is low. This could be a result of *Sphagnum* input to the peat occurring where unusually dry conditions prevail, causing the rapid decay of the *Sphagnum* macrofossils and increasing the UOM content. This in turn would increase the pH, increasing the isomerisation of the ββ hopane, hence lowering the ββ/(αβ+ββ)

ratio. The overall increase in the αβ hopane in the 0-500 cm core is likely to be a result of the gradual transformation of the ββ isomer with time.

3.9.2 Alcohols and Steroids

<u>*n*-Alkanols</u> - The *n*-alkanol distributions remained similar over the 7 samples, with the maximum homologue being C_{22} in all cases except for BFM2-359 where C_{24} was dominant. Of all the plant species analysed (Nott, 2000) none of the *n*-alkanol profiles had maxima at the C_{22} homologue, but all the *Sphagnum* species had maxima at C_{26} except *S. capillifolium* and *S. sub-nitens* where C_{24} was dominant. The C_{26} homologue was in highest relative abundance in sample BFM2-205 which may suggest a high input of *Sphagnum*. C_{26} *n*-alkanol was also the dominant alkanol in *V. oxycoccus* and *Cladonia* species, but the *n*-alkanols present were in very low abundance compared to other compounds found in this fraction.

The Carbon Preference Index of the *n*-alkanols is presented in Figure 3.21. This graph shows that the highest CPI (greatest proportion of odd numbered homologues) occurs in samples BFM2-330 and BFM1-470 where macrofossil analyses reveal low abundances of *Sphagnum*. The CPI values for *n*-alkanols are dependent on the distributions of all of the peat inputs, as all of the plant species have been shown to contain these compounds to some extent. Therefore it is difficult to elucidate input species based on CPI values alone, as where more than two plant species are present this can dramatically change the CPI as a composite value is produced. The observed difference between samples BFM1-470 and BFM2-485 may be a result of this as they both contain a similar *Sphagnum* composition (4-7%). This is very low and other differences, including UOM (30-16%) and *E. vaginatum* (20-37%) compositions, are likely to alter the values.

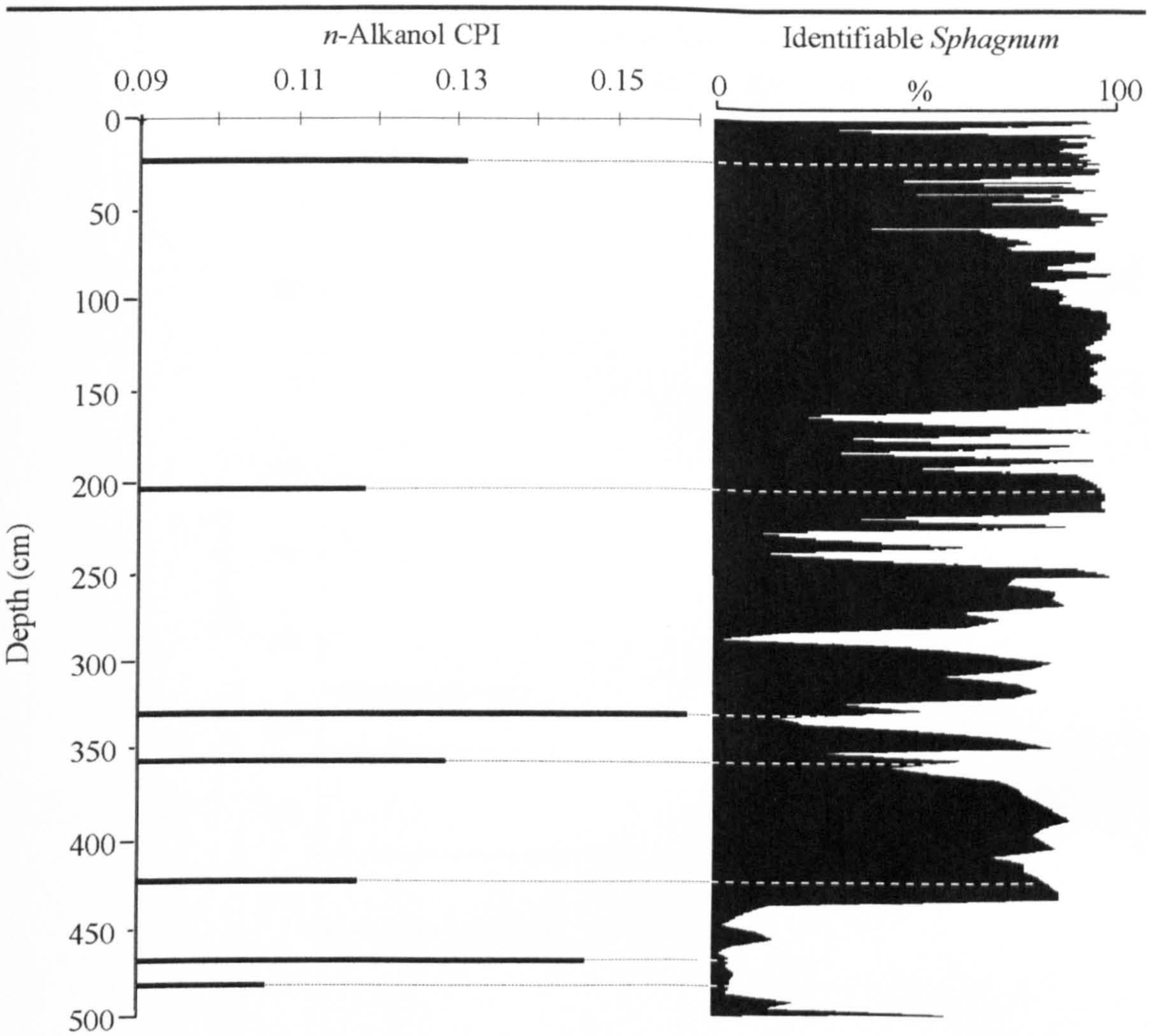

Figure 3.21 Plot of the *n*-alkanol CPI together with total identified *Sphagnum* in the 0-500 cm peat core.

Sterols - The sterol contents of different types of peat and lignite deposits have been studied widely and reduction of double bonds, believed to occur through sterone intermediates has been reported (Evershed and Connolly, 1994; Ives and O'Neil, 1958). The β-sitosterol/(β-sitosterol+3-stigmastanol) ratio is displayed in Figure 3.22.

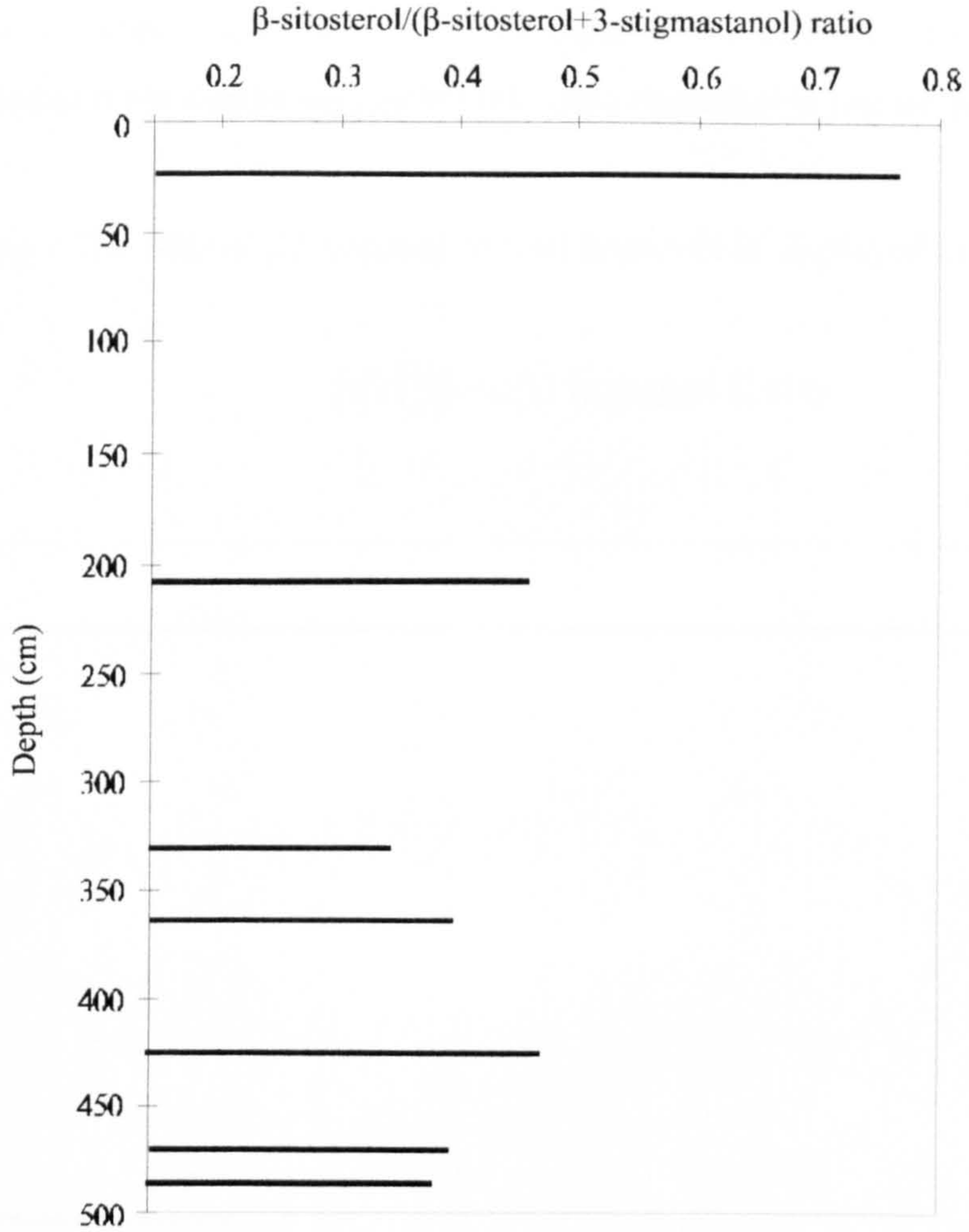

Figure 3.22 Plot of the ratio of β-sitosterol/(β-sitosterol+3-stigmastanol) in the 0-500 cm peat core.

The relative abundance of β-sitosterol to the stanol shows a general decrease with depth as expected with ongoing reduction of the sterol. The increase in this ratio around BFM2-359, BFM2-425, and BFM1-470 could be attributed to the further degradation of 3-stigmastanol to other products (see Chapter 4), therefore elevating the relative abundance of the sterol. It is unlikely that this ratio is directly affected by plant input as 3-stigmastanol was found not to be present in any of the plant species analysed (Nott, 2000) and therefore, is most probably, solely derived from β-sitosterol. The ratio of stanols to Δ^5-sterols has been measured for different peat types with differing humification (Lehtonen and Ketola, 1993). This revealed that the ratio seemed to reflect the aerobic/anaerobic microbial conditions in the peat, where the stanol/sterol ratio increased with increasing minerotrophic and decreasing ombrotrophic nature. Nutrients obtained from flowing waters of the environment (minerotrophic) increased the aerobic nature of the peat. Therefore the increase of β-sitosterol at ~ 420 cm may reflect less

aerobic conditions. This is consistent with the macrofossil data where an absence of UOM is recorded at these depths suggesting that little degradation has occurred.

Hopanols - The ratio of ββ hopanol to total hopanols is displayed in Figure 3.23.

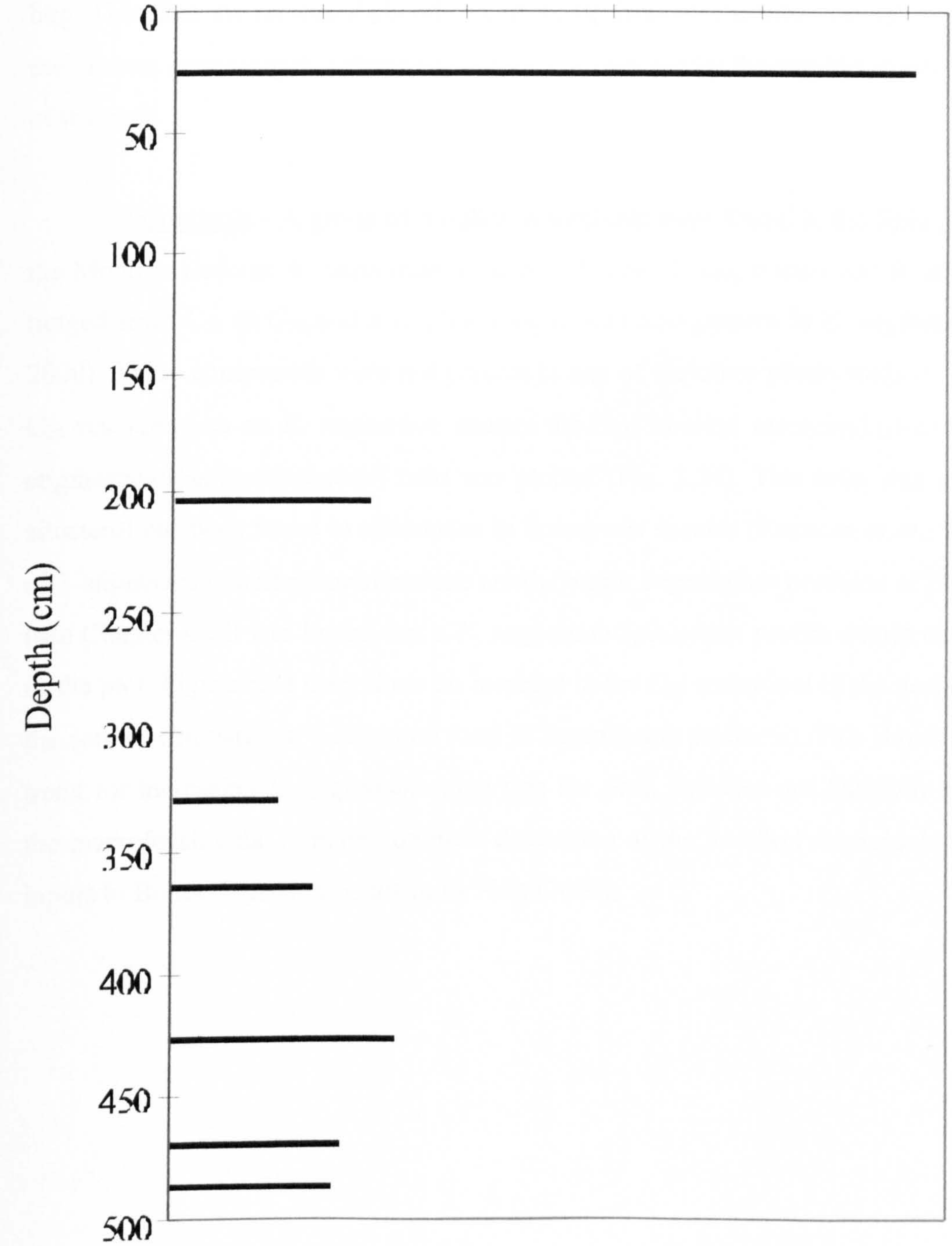

Figure 3.23 Plot of the ratio of ββ/(ββ+αβ) hopanol down the 500 cm peat core.

Similarly to the hopanes identified in the peat, the hopanols have a higher relative abundance of the ββ isomer at the top of the core and a general decrease as isomerisation takes place and the αβ epimer is formed. Interestingly, this ratio has an almost identical trend to the β-sitosterol/(β-sitosterol+3-stigmastanol) ratio (Fig. 3.22) and an increase in the ratio at BFM2-425 is also seen. The sterol/stanol ratio suggests that at ~ 420 cm depth there is an increase in the ombrotrophic/anaerobic nature of the bog. Therefore the increased abundance of the ββ isomer relative to the αβ suggests that the process governing this change is likely to be affected by the aerobic/anaerobic nature of the peat.

Resorcinols - A group of 5*n*-alkyl resorcinols were found in the lipid profiles of the Monocotyledons: *E. vaginatum*, *E. angustifolium*, *T. cespitosum* and *R. alba*. These ranged from C_{27} to C_{33} and a C_{25} homologue was also present in *E. vaginatum* (Nott, 2000). These compounds were not present in any of the other plants studied. Using the C_{25} resorcinol as an *E. vaginatum* marker the C_{25} 5*n*-alkyl resorcinol/(β-sitosterol+3-stigmastanol+epiandrosterone) ratio was plotted (Fig. 3.24). This ratio was used as β-sitosterol has been found in abundance in *Sphagnum* species (Karunen *et al.*, 1983) and as 3-stigmastanol and epiandrosterone are the major degradation products of β-sitosterol (see Chapter 4), it was hoped that a *E. vaginatum*/*Sphagnum* profile would be reflected in the plot. Figure 3.24 does show an increase in the C_{25} resorcinol in the deeper part of the core as compared to β-sitosterol (and its degradation products). This shows a general trend for increasing *E. vaginatum* input into the peat, but does not faithfully reproduce the macrofossil data. A more complete discussion of the 5*n*-alkyl resorcinols and plant inputs to Bolton Fell Moss is given by Nott (2000).

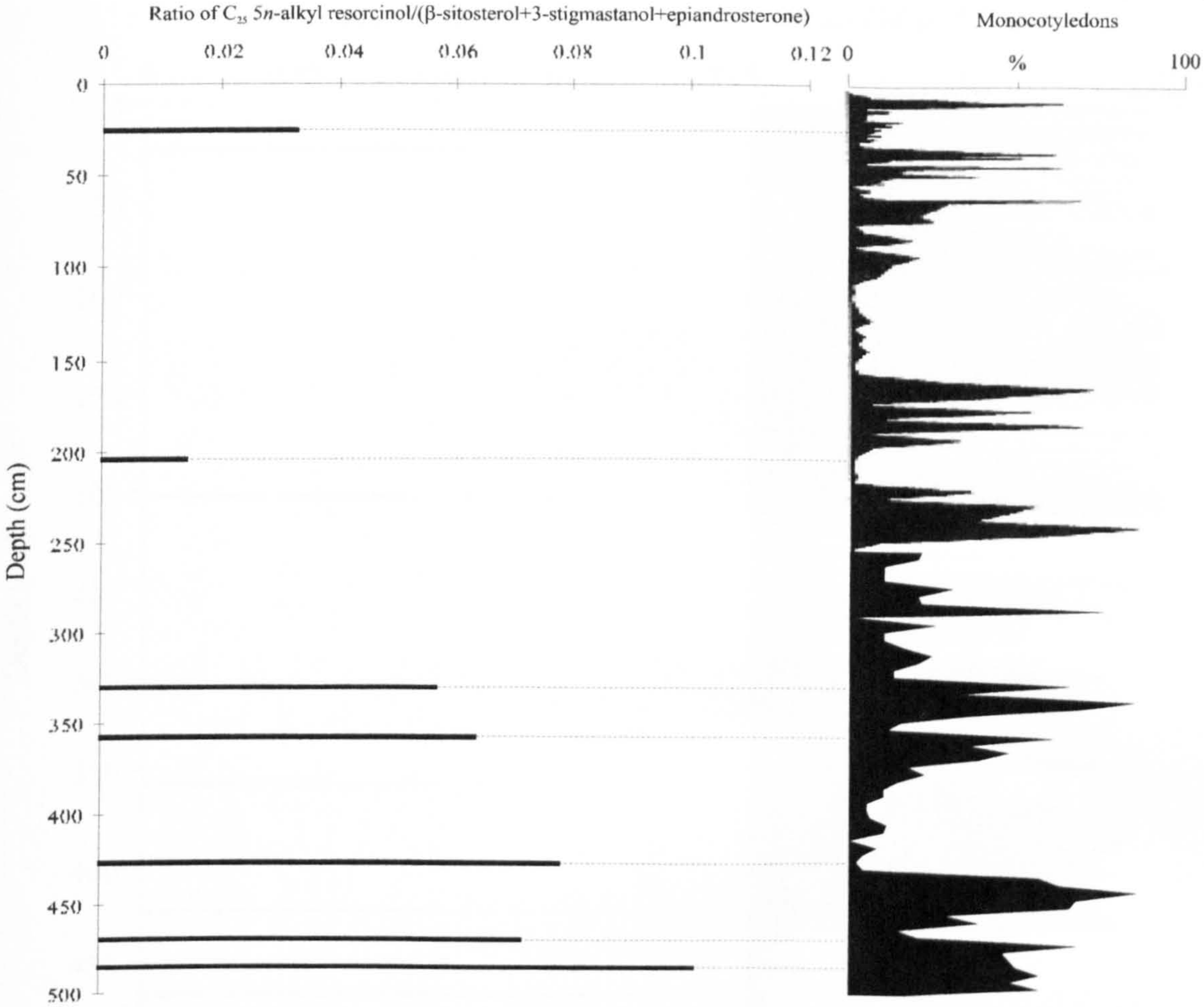

Figure 3.24 Plot of the ratio of C_{25} 5*n*-alkyl resorcinol/(β-sitosterol+3-stigmastanol+epiandrosterone) together with total identified Monocotyledons in the 0-500 cm peat core.

3.9.3 Carboxylic Acids

n-Alkanoic acids - The *n*-alkanoic acid distributions of the plants from Bolton Fell Moss (Nott, 2000) indicate that most of the species display bimodal distributions with C_{16} and even numbered C_{20} to C_{28} homologues being predominant. Although *n*-hexadecanoic acid (C_{16}) was seen in all peat samples, it was only detected at very low abundances compared to higher homologues. *Sphagnum* species had either C_{24} or C_{26} as the predominant acid components, but *Polytrichum* species, *A. palustre* and *E. angustifolium* also contained these acids in high abundance. The CPI for the *n*-alkanoic acids is presented in Figure 3.25.

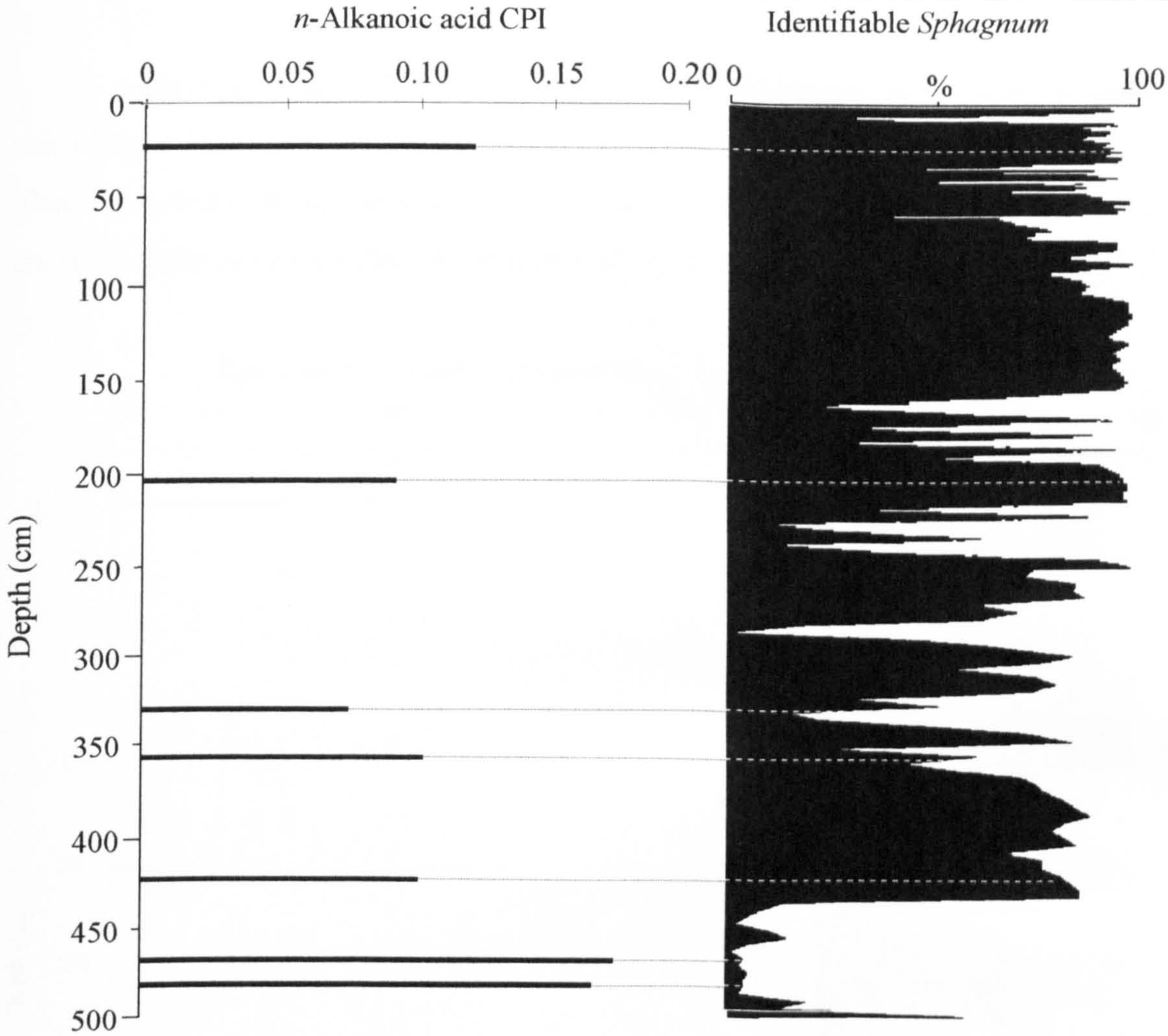

Figure 3.25 Plot of the *n*-alkanoic acid CPI together with total identified *Sphagnum* in the 0-500 cm peat core.

Similarly to the *n*-alkane and *n*-alkanol CPI the *n*-alkanoic acids exhibit an increased odd numbered carbon abundance with increased *Sphagnum* input. However, where *Sphagnum* is low in abundance (BFM1-470 and BFM2-485) the CPI is shown to increase. Again, this is likely to be due to the inputs of other plant species (e.g. Ericales) other than Monocotyledons which are the second most abundant species in the upper 4 m of the peat. Previous studies have seen little variation in the alkanoic acid distributions of peats (Ficken *et al.*, 1998; Lehtonen and Ketola, 1993), however, the abundance of *n*-hexadecanoic acid has been shown to rapidly decrease in the senescent parts of *Sphagnum* moss, such that it is almost absent when compared with the longer chain compounds (Karunen and Salin, 1980). The rapid degradation of the abundant alkanoic acids of plant species (e.g. C_{16}) in peat samples makes this fraction unsuitable for the determination of peat components.

ω-Hydroxy acids - The ratio of C_{22}-C_{28} ω-hydroxy acids to C_{22}-C_{28} *n*-alkanoic acids (Fig. 3.26) shows a marked increase with depth. This could be a result of changing plant input, but as these compounds are not seen in any of the plants as free lipids they are more likely to be a product of decay of *n*-alkanoic acids.

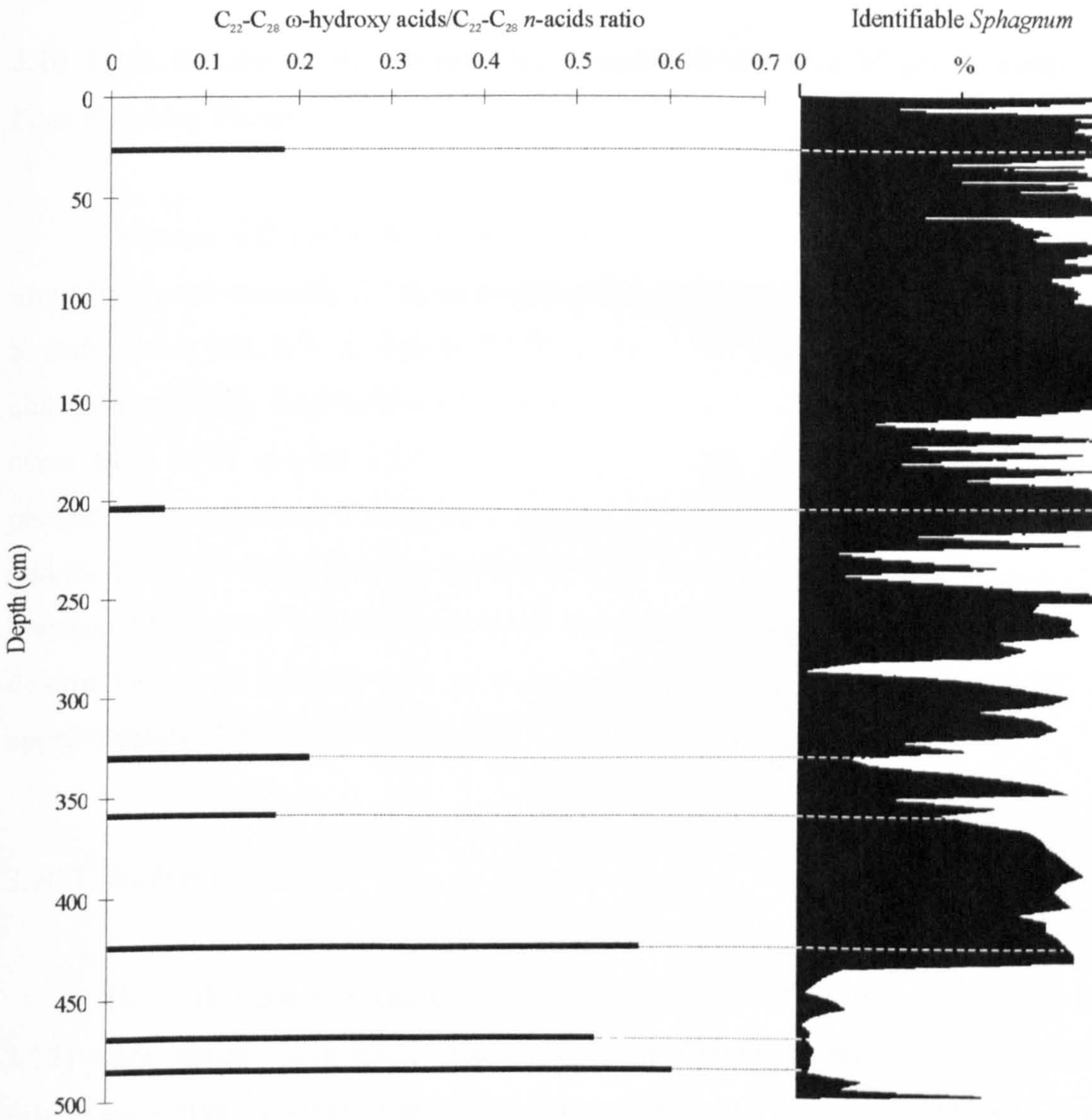

Figure 3.26 Plot of the ratio of C_{22}-C_{28} ω-hydroxy acids/C_{22}-C_{28} *n*-acids together with total identified *Sphagnum* in the 0-500 cm peat core.

Previous studies have shown that C_{22}-C_{26} ω-hydroxy acids occur in the senescent parts of *S. fuscum* (Ekman and Karunen, 1982). The correlation between the relative abundances of ω-hydroxy acids and identified *Sphagnum* (Fig. 3.26) shows that in samples BFM2-330, BFM2-359 and BFM2-425 that the amounts of *Sphagnum* could be related to the quantities of the acids. Although macrofossil data for BFM2-25 and

BFM2-205 is taken from an adjacent core and may not truly represent peat components in these samples it is unlikely to greatly differ and *Sphagnum* species are probably the most abundant peat input in these samples. The abundance of C_{22}-C_{26} ω-hydroxy acids has been shown to increase with increasing humification (Lehtonen and Ketola, 1993). This may therefore be just a senescence indicator of the degradation of peat components.

3.10 High Resolution Biomarker Stratigraphic Study of a Major Transition in Peat-Forming Plants

Between 432 and 436 cm the macrofossil data shows a sharp change in peat input from predominantly *E. vaginatum*/Monocotyledons (56-4%) to *Sphagnum* species *S. imbricatum* and *S. s. Acutifolia* (14-89%, Table 2.2, Fig. 2.4). This represents the change from highly humified raised bog peat to *Sphagnum* peat previously seen in other cores from BFM and the nearby peat deposit, Walton Moss (Barber, 1998). In the present study, peat from 419-448 cm sampled at 1 cm intervals was solvent extracted and the lipids identified and quantified. From this data set, 10 samples at 3 cm intervals between 420 and 447 cm were used in the radiocarbon dating study (Chapter 6) and ^{14}C determinations of the bulk peat revealed that the 30 cm interval accumulated over approximately 300 y (4800-4500 y BP).

3.10.1 Hydrocarbons

The hydrocarbon fractions of the 30 samples, BFM1-419 to BFM1-448 (Fig. 3.27) were almost exclusively dominated by *n*-alkanes in the C_{19} to C_{35} range, displaying a high odd-over-even predominance (highest CPI = 16.8, BFM1-440, lowest CPI = 7.5, BFM1-420, average CPI = 13.0, Fig. 3.28). The *n*-alkanes had maxima at the C_{31} (73.3-246.9 μg g^{-1} dry peat) or C_{33} (72.3-223.6 μg g^{-1} dry peat) homologues, with C_{31} being dominant in samples BFM1-421-428 and BFM1-435-445. The ββ and αβ 29-methyl hopanes were detected at low abundances (αβ 3.11-12.9 μg g^{-1} dry peat, ββ 0.38-1.60 μg g^{-1} dry peat) and the ββ/(αβ+ββ) ratio showed a slight decrease with increasing depth. Other compounds present in low abundance were, taraxer-14-ene, taraxast-20-ene and $C_{30}H_{50}$ hopane (Appendices II+III).

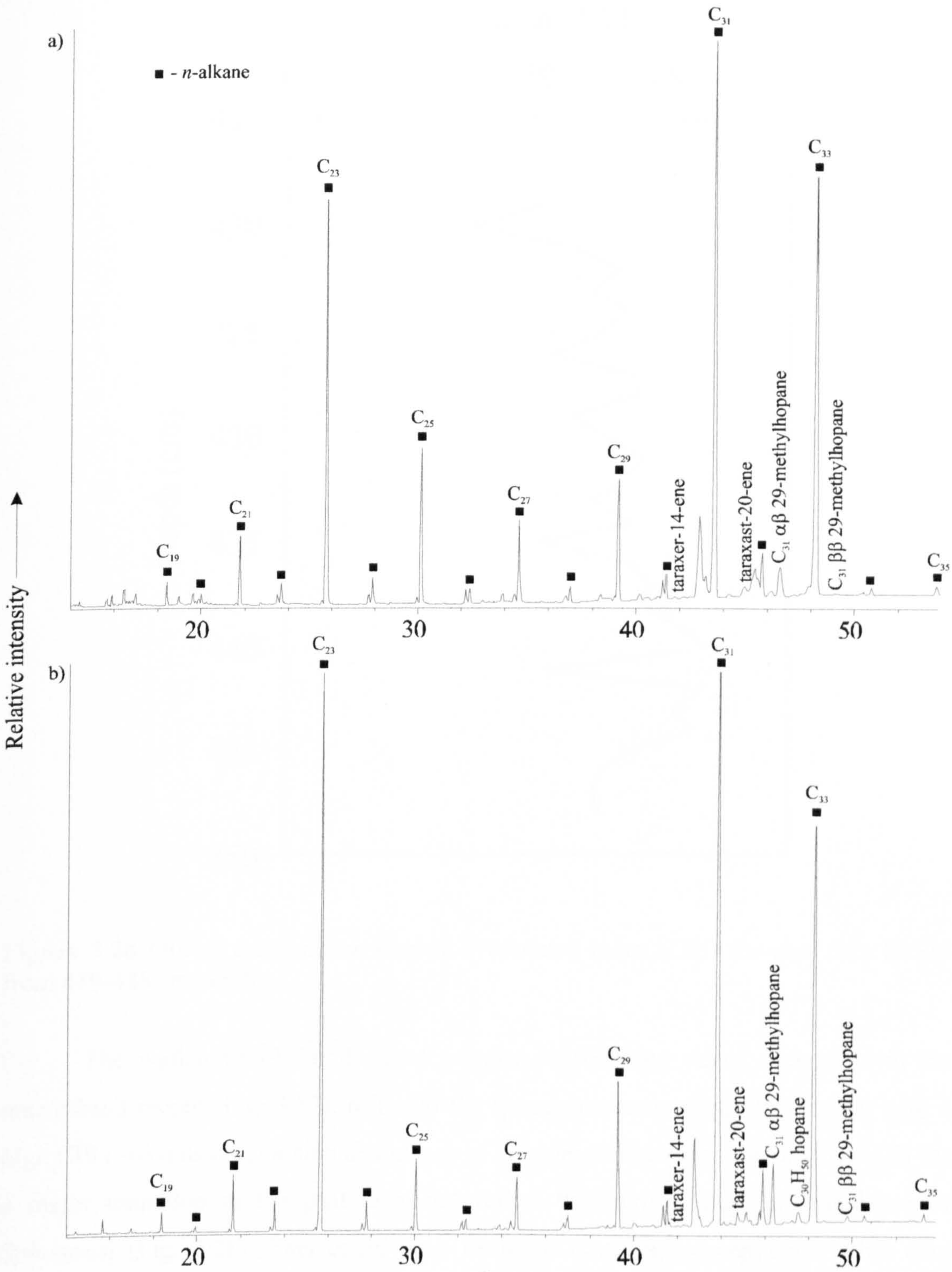

Figure 3.27 Partial gas chromatograms of hydrocarbon fraction from peat core BFM1 at (a) 428 cm and (b) 442 cm depth; 50 m CPSil-5CB, 50-200°C @ 12°C min^{-1}, 200-300°C @ 3°C min^{-1}, 300°C (20 min).

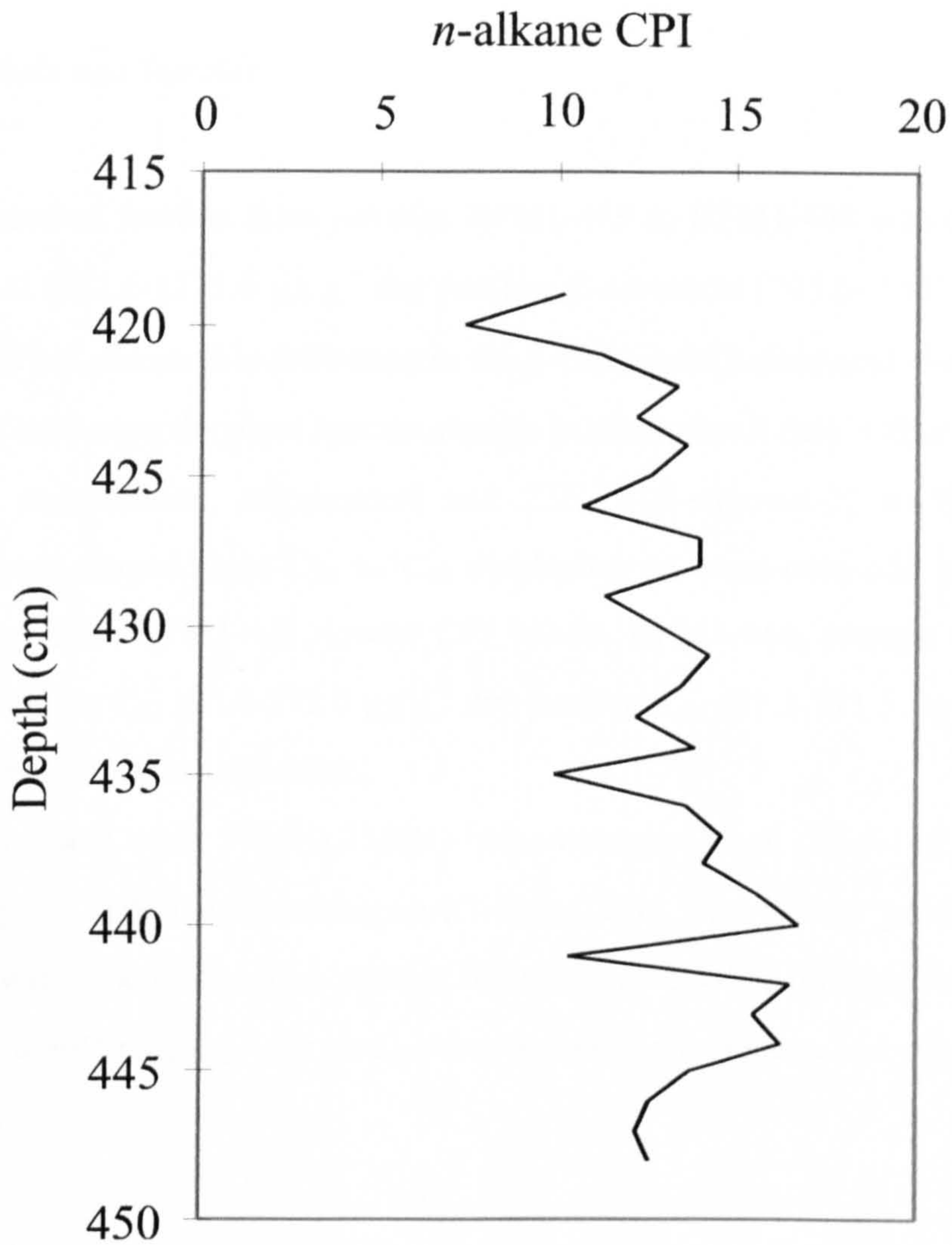

Figure 3.28 Plot of the *n*-alkane Carbon Preference Index (CPI) for peat core BFM1 from 419-448 cm depth.

The *n*-alkane CPI for the peat samples representing major excursions in the macrofossil record (Fig. 3.17), reflected the *Sphagnum* composition of the peat with a high CPI (>6) indicating a high abundance of *Sphagnum*. However, the *n*-alkane CPI for a major transition in the peat does not reflect the same change in abundance of *Sphagnum* (Fig. 3.28). This could be a result of other peat components other than *Sphagnum* influencing the CPI. Over the 420-452 cm depth peat profile there is a 3-12% contribution of Ericales roots (Table 2.2) and these might be involved in obscuring a *Sphagnum* abundance signal in the *n*-alkane CPI. Where the roots are most abundant (420, 436 and 448 cm) the *n*-alkane CPI shows a low odd-over-even predominance.

3.10.2 Alcohols and Steroids

The alcohol fraction from samples BFM1-419 to BFM1-448 was dominated by 3-stigmastanol (582.6-1131.6 μg g^{-1} dry peat) or β-sitosterol (705.6- 1511.1 μg g^{-1} dry peat, Fig. 3.29). A discernible difference in the β-sitosterol/(β-sitosterol+3-stigmastanol) ratio was not seen over the plant species change in macrofossil data. Other sterols were, campesterol, campestanol, stigmasterol and 22*E*, 24*R*-stigmast-22-en-3β-ol. The *n*-alkanols present ranged from C_{20} to C_{30} displaying an even-over-odd predominance (highest CPI = 0.36, BFM1-421, lowest CPI = 0.06, BFM1-444, average CPI = 0.186, Fig. 3.30), with the C_{22} (95.0-272.0 μg g^{-1} dry peat) or C_{24} (81.2-211.5 μg g^{-1} dry peat) homologue being the most abundant.

Also present were 17α(H),21β(H)-bishomohopan-32-ol (17.6-140.7 μg g^{-1} dry peat) and 17β(H),21β(H)-bishomohopan-32-ol (11.3-51.3 μg g^{-1} dry peat). Other lipid components were: the odd carbon number homologues C_{25}-C_{31} *n*-alkyl resorcinols (C_{27} maximum, 176.4-458.7 μg g^{-1} dry peat), campestanone, sitostanone and stigmasterone.

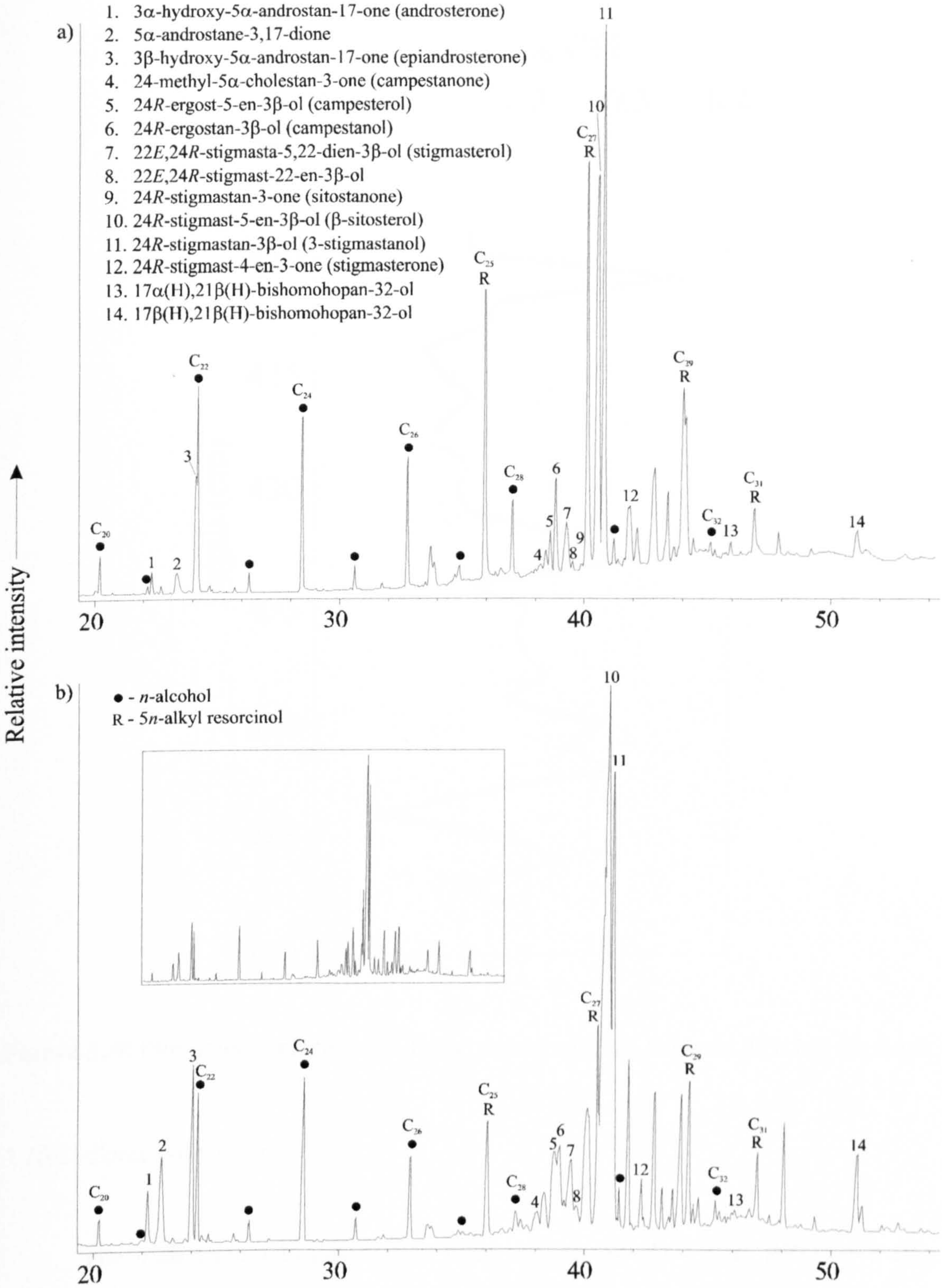

Figure 3.29 Partial gas chromatograms of alcohol/steroid fraction from peat core BFM1 at (a) 428 cm and (b) 442 cm depth (The major components have been overloaded to reveal those at lower abundance, insert shows non-overloaded chromatogram); 50 m CPSil-5CB, 50-200°C @ 12°C min^{-1}, 200-300°C @ 3°C min^{-1}, 300°C (20 min). Analysed as TMS ethers.

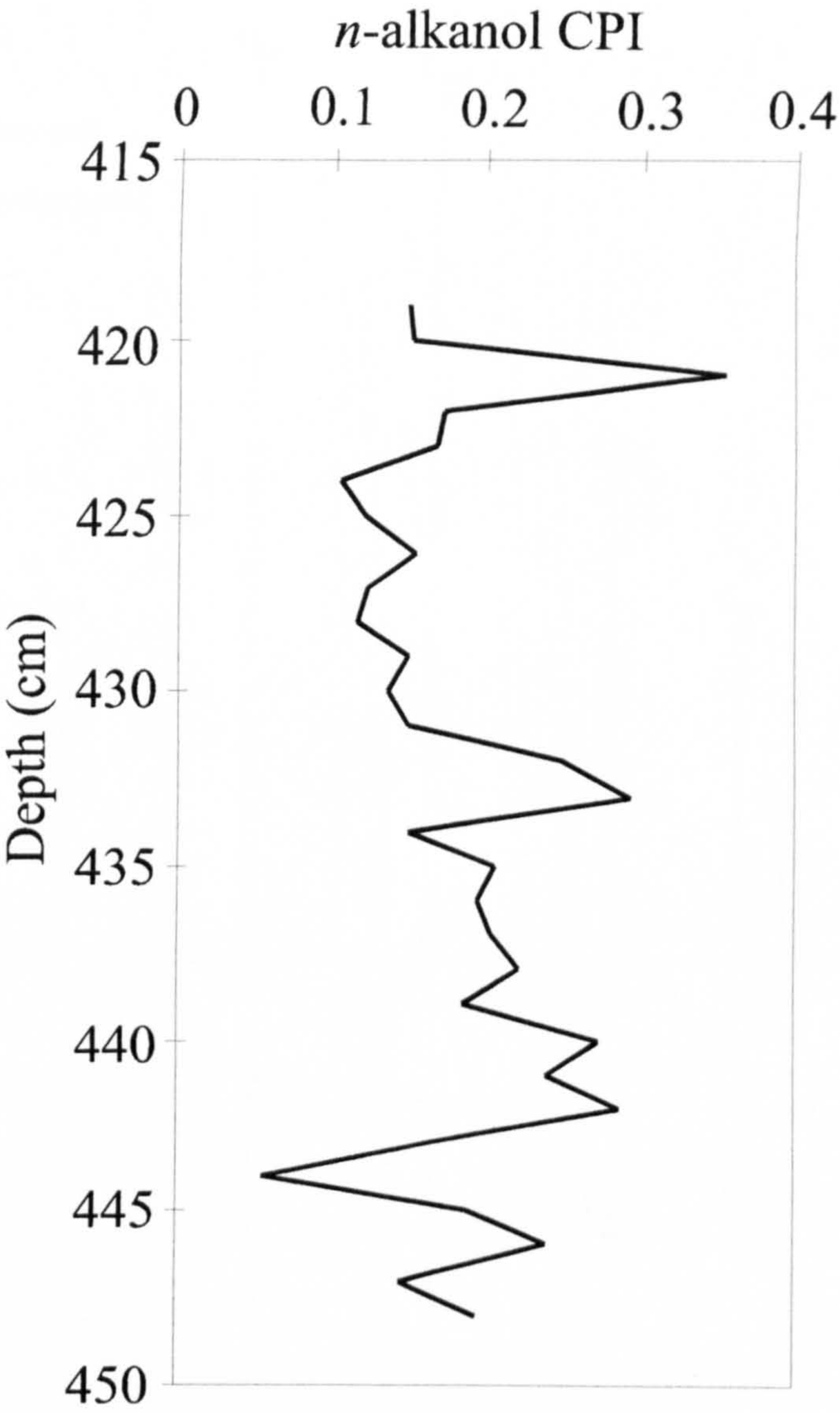

Figure 3.30 Plot of the *n*-alkanol CPI from peat core BFM1 between 419-448 cm depth.

3.10.3 Carboxylic Acids

The *n*-alkanoic acid distribution from samples BFM1-419 to BFM1-448 (Fig. 31) was observed to show a monomodal even-over-odd predominance (highest CPI = 0.15, BFM1-435, lowest CPI = 0.09, BFM1-428, average CPI = 0.11, Fig. 3.32) over the range C_{20} to C_{32} with a maximum at C_{24} (766.8-1622.7 μg g^{-1} dry peat) or C_{26} (698.0-1687.2 μg g^{-1} dry peat). Also present in this fraction is a series of ω-hydroxy acids ranging from C_{22} to C_{28} with C_{26} being the most abundant component in most samples (120.1-692.4 μg g^{-1} dry peat).

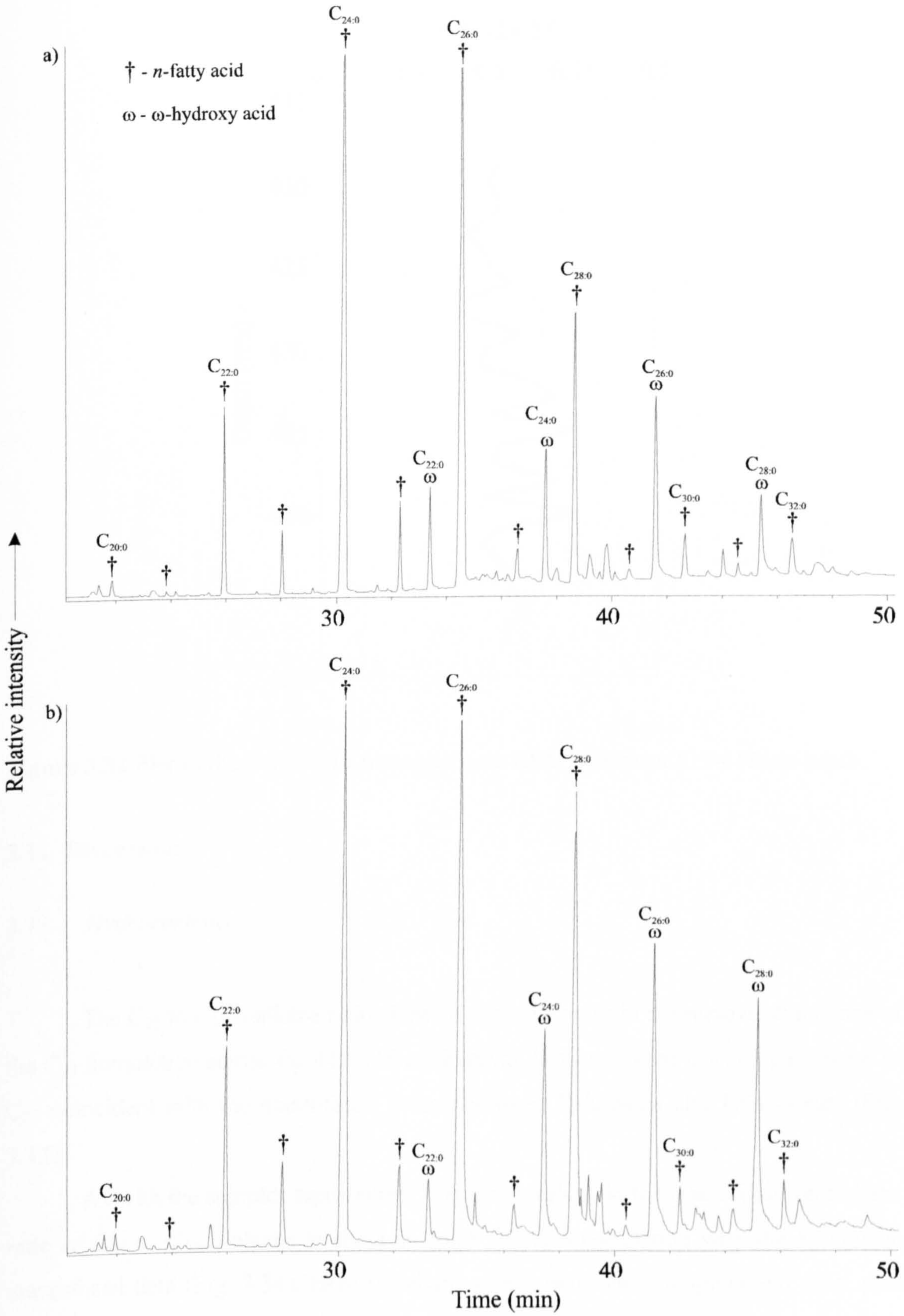

Figure 3.31 Partial gas chromatograms of acid fraction from peat core BFM1 at (a) 428 cm and (b) 442 cm depth; 50 m CPSil-5CB, 50-200°C @ 12°C min^{-1}, 200-300°C @ 3°C min^{-1}, 300°C (20 min). Analysed as TMS esters/ethers.

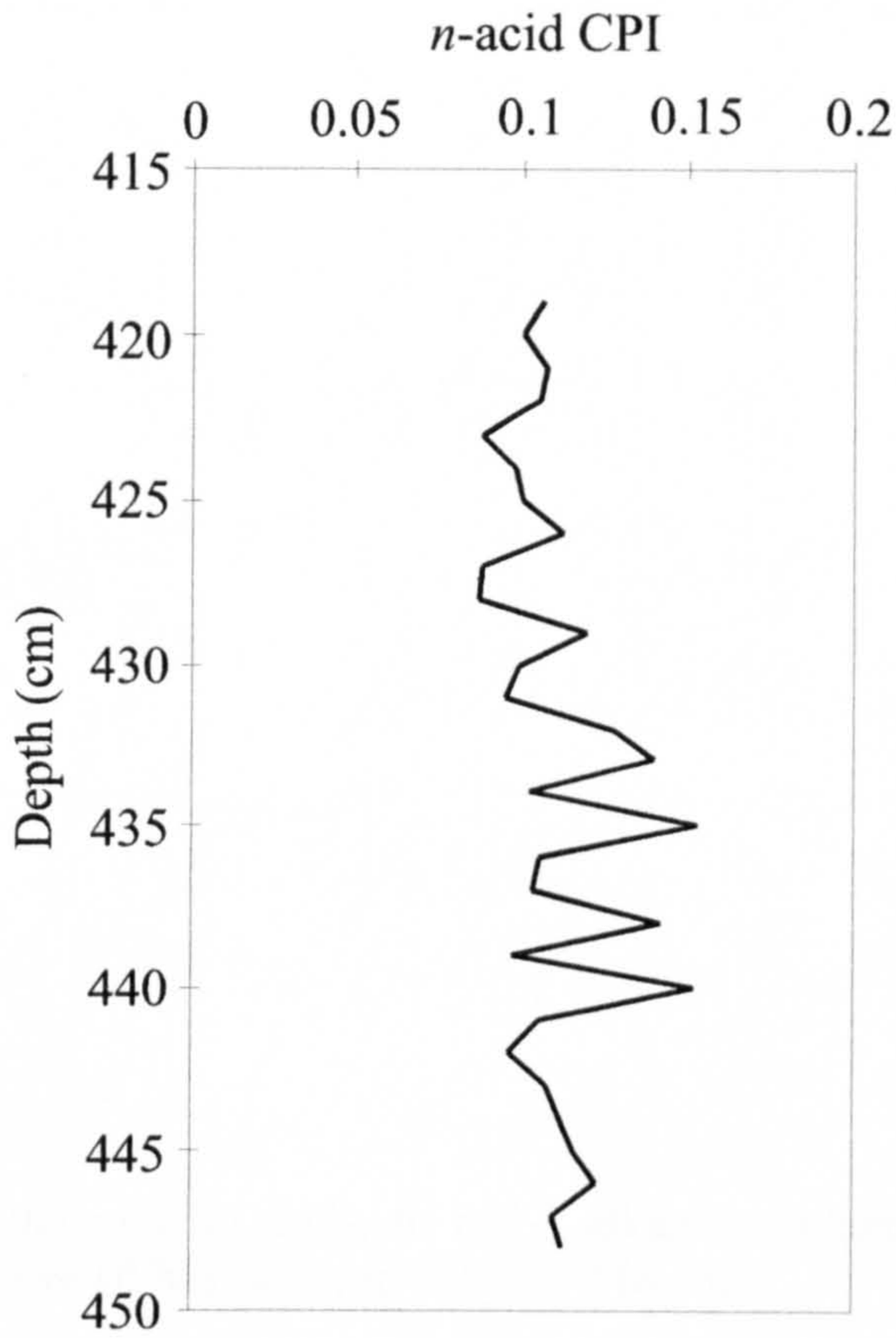

Figure 3.32 Plot of the *n*-acid CPI from peat core BFM1 between 419-448 cm depth.

3.11 Discussion

3.11.1 Hydrocarbons

The C_{23} to C_{31} *n*-alkane ratio shows a slight increase in the relative abundance of the C_{23} homologue across the 419-448 cm interval, however there is a sharp decrease in C_{23} coincident with the macrofossil switch between *Sphagnum* and *Eriophorum* (Fig. 3.33).

As with the samples representing major excursions in the macrofossil record, the ratio of C_{25} to C_{31} *n*-alkane in these samples shows a correlation with the *Sphagnum* macrofossil data (Fig. 3.34). Here the sharp switch between *Sphagnum* and other peat components, occurs between 432 and 433 cm using lipid data.

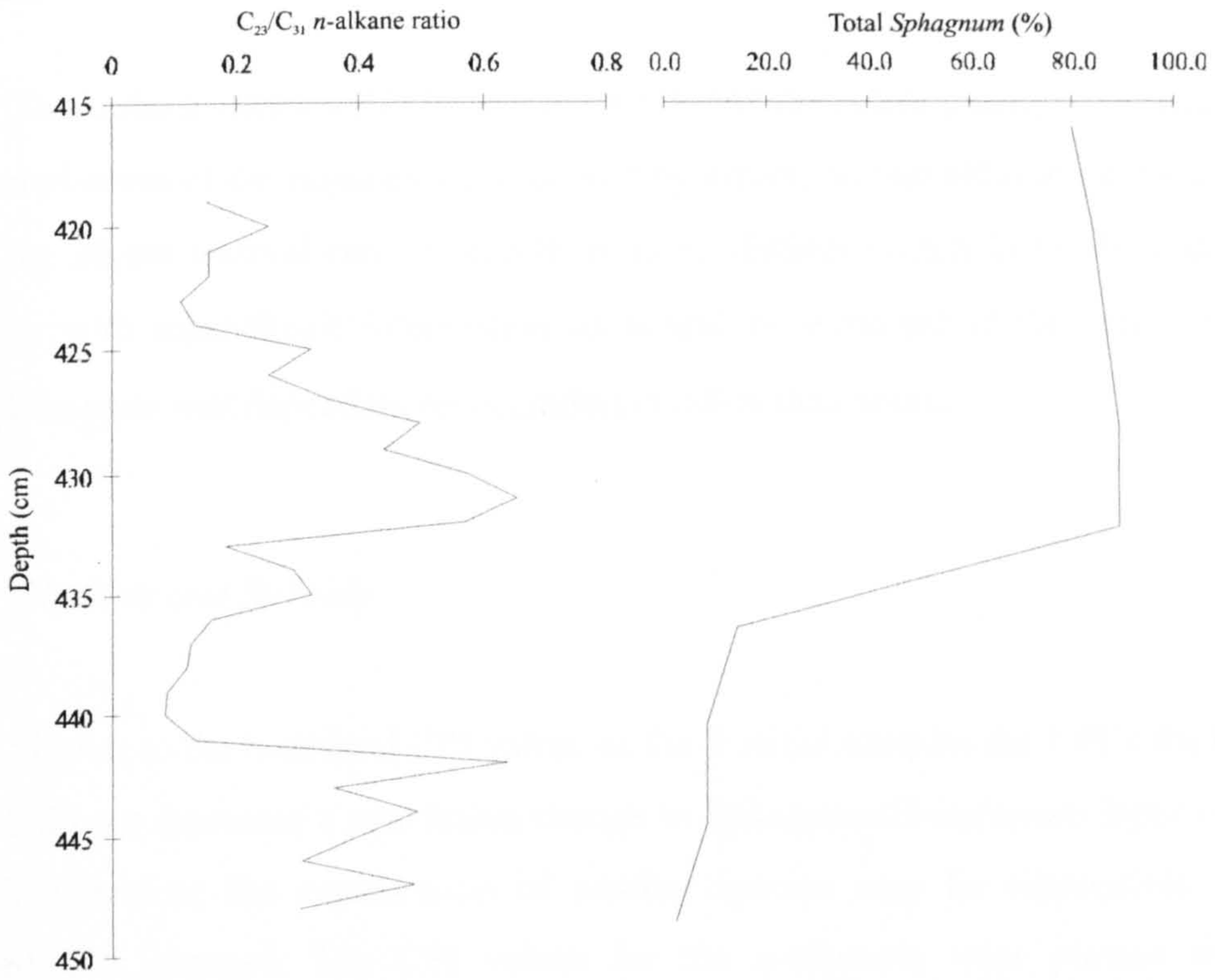

Figure 3.33 Plot of the ratio of *n*-C_{23} to *n*-C_{31} alkane together with total identified *Sphagnum* from peat core BFM1 between 419 and 448 cm.

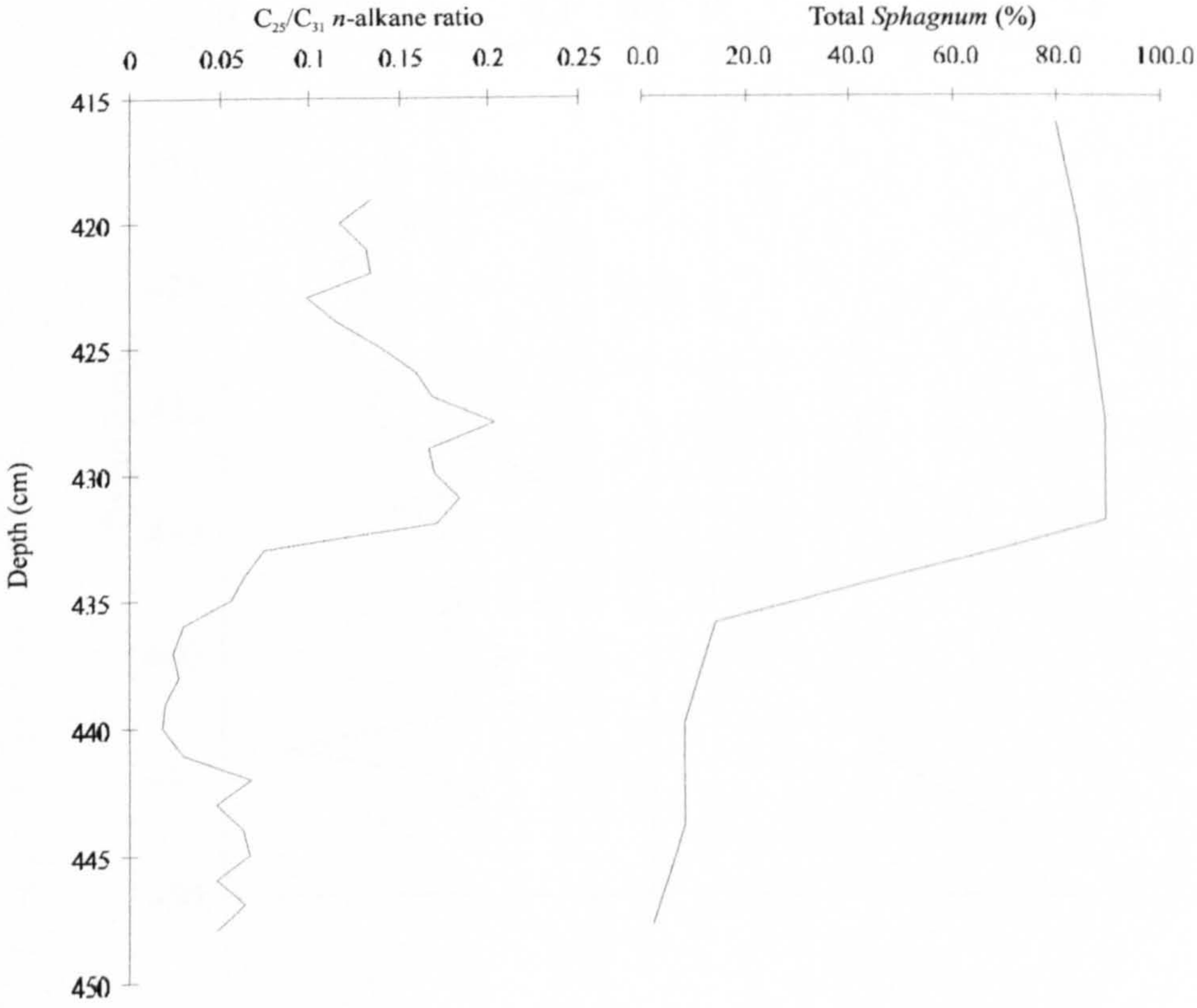

Figure 3.34 Plot of the ratio of *n*-C_{25} to *n*-C_{31} alkane together with total identified *Sphagnum* from peat core BFM1 between 419 and 448 cm.

Throughout samples BFM1-419 to BFM1-448 the subtle changes that occur with the isomerisation of the hopanes are obscured by errors, so that although general trends across the 30 cm interval can be seen there is no distinct switch in the lipid data that coincides with macrofossil information as would be expected if the ratio of ββ to (ββ+αβ) hopane was dependant on degradation rather than source.

3.11.2 Alcohols and Steroids

Similar to the *n*-alkanol CPI values of the 7 initial samples the CPI's for BFM1-419-448 do not represent a conclusive change in *Sphagnum/Eriophorum* input over the interval. Therefore the contribution of another species may be responsible for the observed CPI changes. The CPI values for the *n*-alkanols were plotted with the macrofossil Ericales abundance in Figure 3.35.

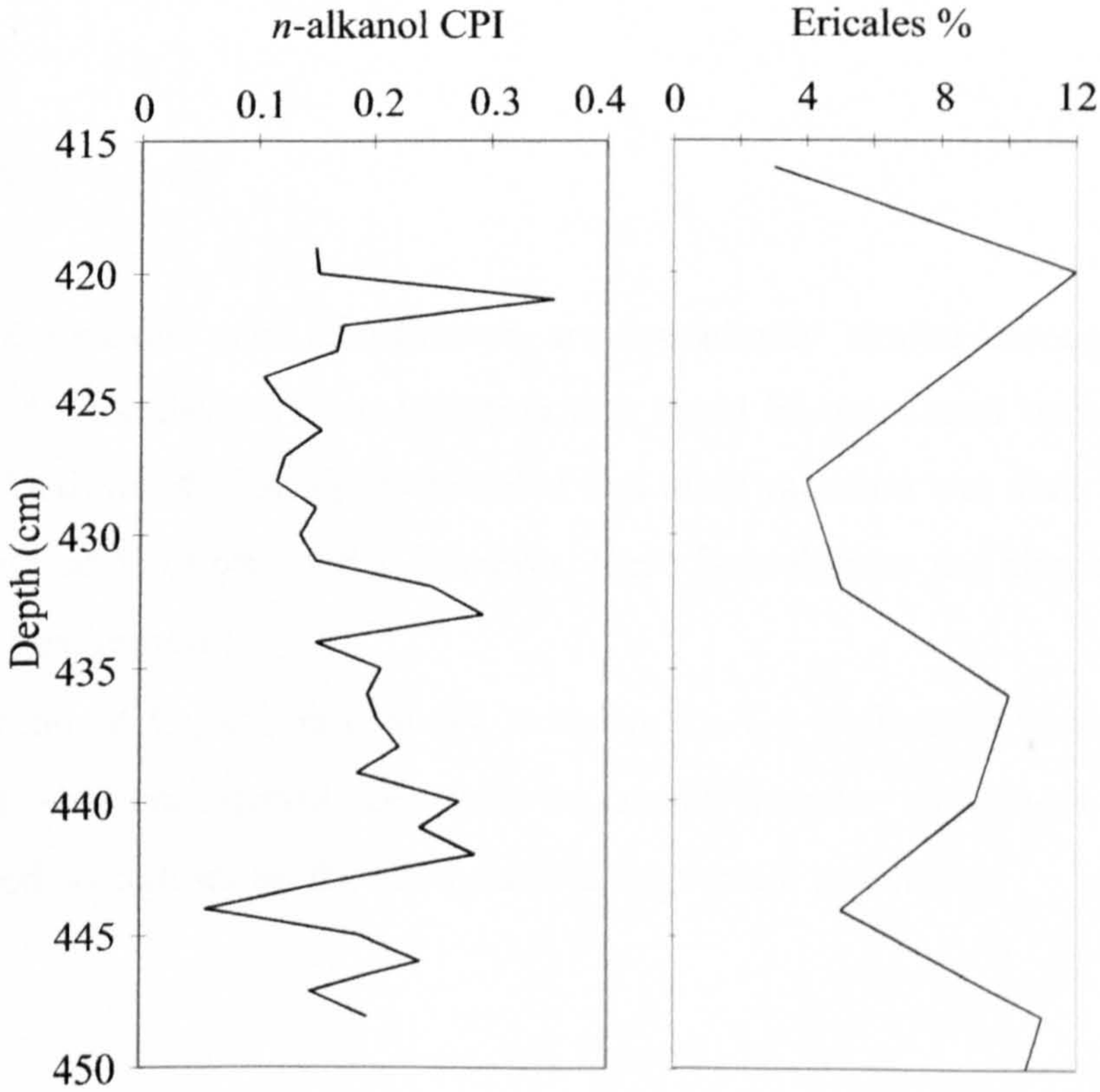

Figure 3.35 Plot of the *n*-alkanol CPI together with the total identified Ericaceous material from peat core BFM1 between 419 and 448 cm.

The *n*-alkanol distributions from the Ericaceous plant species *E. nigrum*, *V. oxycoccus*, *C. vulgaris* and *A. polifolia* have previously been determined (Nott, 2000) revealing that *E. nigrum*, *C. vulgaris* and *A. polifolia* all contain almost exclusively even numbered *n*-alkanols. However, *V. oxycoccus* was found to contain only C_{22}-C_{30} *n*-alkanols and the C_{23}, C_{25} and C_{27} homologues were in high relative abundance, increasing its CPI value. Although *C. vulgaris* leaves were identified at 436 cm depth (2%, Table 2.2), the Ericales were not identified on a taxa basis in the macrofossil record as only their roots remained. Therefore the CPI values could represent an input of *V. oxycoccus* in the peat as it has a low even-over-odd predominance, where macrofossil data could not distinguish between different species.

Mirroring the hopane results, the progressive hopanol isomerisation was not represented by such a short interval in the diagenetic process. However, a slight decrease in the ββ to (ββ+αβ) hopanol ratio was noted over the 30 samples. Also the β-sitosterol/(β-sitosterol+3-stigmastanol) ratios did not reflect a marked change as would be expected over this time frame.

3.11.3 Carboxylic Acids

The *n*-alkanoic acid distributions are remarkably similar throughout the 30 samples and do not show a clear variation that could be associated with a change in plant input. Analysis of plant lipids revealed that most variation was seen with C_{16} and C_{18} *n*-alkanoic acids (Nott, 2000), however, these homologues are almost completely absent in the peat samples.

The ratio of C_{22}-C_{28} ω-hydroxy acids to C_{22}-C_{28} *n*-alkanoic acids (Fig. 3.36) across the 419-448 cm interval does show an overall increase with depth but does not show a marked change across the *Sphagnum*/*E. vaginatum* switch.

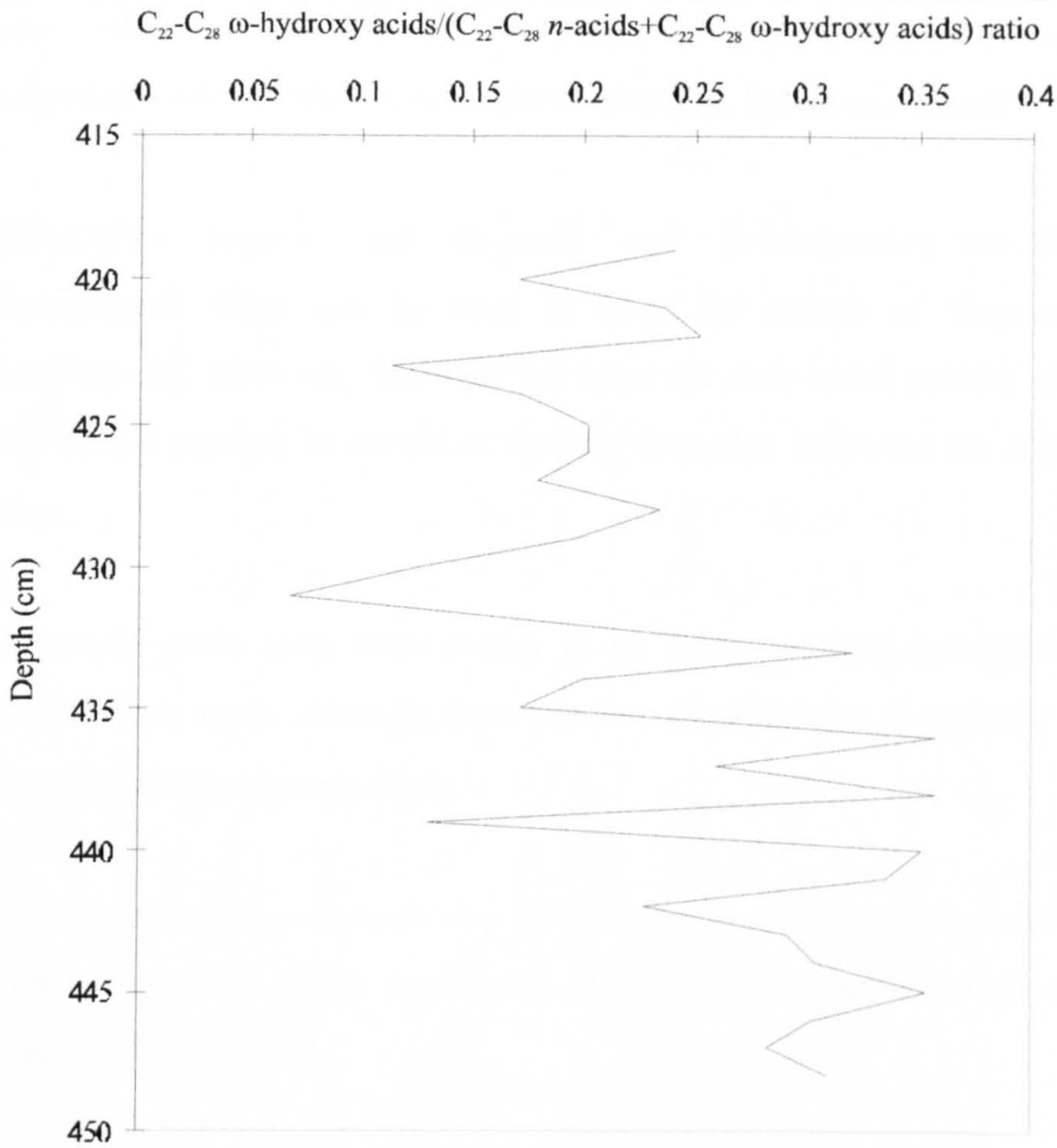

Figure 3.36 Plot of the ratio of C_{22}-C_{28} ω-hydroxy acids/C_{22}-C_{28} *n*-acids from peat core BFM1 between 419 and 448 cm.

3.12 Summary

The main objectives of this chapter were to determine relative mobilities of peat lipids and identify the lipid changes corresponding to plant variation revealed in the macrofossil record. The lipid composition was then determined on a high resolution scale, over an area of peat where a major transition in peat-forming plants occurred. The major findings of this research are:

1. The C_{25} to C_{31} *n*-alkane ratio is a good indicator of the *Sphagnum* input to the peat, a ratio of 0.2-0.5 indicating a high *Sphagnum* contribution. This was also seen with the C_{23} to C_{31} *n*-alkane ratio, but it was not so pronounced.

2. Low CPI values of *n*-alkanes (>5) may reveal non-higher plant peat components not recorded in macrofossil data (e.g. lichen and algae).

3. ββ/(αβ+ββ) hopane and hopanol and β-sitosterol/(β-sitosterol+3-stigmastanol) ratios can be used to trace the extent of diagenesis(or humification). However, these are not apparent over small periods of time (300 y) and changes in the pH of the bog may also influence the hopanoid ratios.

4. *n*-Alkanoic acids have been shown to be fairly uniform throughout the different peat types although their relative abundance to ω-hydroxy acids decreases with increasing depth.

5. The CPI values for *n*-alkanols may be an indicator of the specific Ericaceous plant *V. oxycoccus* which was shown to have a high predominance of odd numbered homologues.

6. Although diagenetic processes are evident throughout the 5 m peat profile, they do not seem to alter lipid distributions over a short timescale. Therefore, where rapid changes in major plant input occurs the lipid profiles should directly reflect the input change. However, changes were only apparent within *n*-alkane distributions, and this is probably because of contributions of inputs other than *S. imbricatum* and *E. vaginatum*. Considerable variations in Ericales, undifferentiated Monocotyledons, *S. s. Acutifolia* and fungal sclerotia (Table 2.2) are all likely to be responsible for the complicated lipid variations and obscure lipid differences.

4. IDENTIFICATION OF NOVEL STEROL DIAGENETIC PRODUCTS IN PEAT

4.1 Introduction

The structural features of sterols, such as double bonds and side-chain alkylation, together with their resistance to degradation in sediments, make them useful as biological markers. However, the ubiquitous nature of some of these compounds in the biosphere complicates the identification of their source.

Pre- and post-burial structural alterations of sterols have been investigated in many sedimentary environments, including marine, lacustrine and terrestrial deposits, and a wide variety of transformations have been recognised. These include low temperature diagenetic reactions such as dehydration to yield sterenes (e.g. Wakeham *et al.*, 1980), reduction to give stanols (e.g. McLean *et al.*, 1958), backbone and other carbocation rearrangements (e.g. Peakman *et al.*, 1984; Rubinstein *et al.*, 1975) and aromatisation (Riolo and Albrecht, 1985). At higher temperatures, reactions lead to further aromatisation (Ludwig *et al.*, 1981; Mackenzie *et al.*, 1981), configurational changes (Mackenzie *et al.*, 1980; Seifert and Moldowan, 1981) and thermal cracking. In recent sediments the steroid components that have been reported include intact sterols and corresponding stanols (e.g. McLean *et al.*, 1958) and ketones and sterenes (e.g. Wakeham *et al.*, 1980). In more mature sediments steranes are usually detected (e.g. Mackenzie *et al.*, 1980; Seifert and Moldowan, 1981) along with their partially or fully aromatised counterparts (e.g. Ludwig *et al.*, 1981; Mackenzie *et al.*, 1981). Most reports of sedimentary steroids relate to components in which the C-17 side chain has remained intact, although hydrocarbons with the androstane skeleton have been reported in ancient sedimentary organic matter and are presumed to originate through side chain cleavage (Matveyeva and Petrov, 1992). The latter compounds were detected in crude oils and were present as regular androstanes or were partially rearranged so that the C-19 methyl group at C-10 had been transferred to the C-5 position. Partially and fully aromatised androstane components have also been found in brown coal deposits (Chaffee and Johns, 1983). It has been proposed that these polyaromatic hydrocarbon compounds may be derived from steroid compounds as there is a similarity in their carbon skeleton. However, direct evidence for this transformation has not yet been obtained.

In a study of unsaturated hydrocarbons of recent sediments from the sea of Norway, Δ^2-sterenes and $\Delta^{13(17)}$-sterenes were discovered (Dastillung and Albrecht, 1977). The authors proposed that the Δ^2-sterenes were diagenetic intermediates between sterols and 5α-steranes and that the $\Delta^{13(17)}$-sterenes were formed from stanols by an acid-catalysed skeletal rearrangement through Δ^2-sterene intermediates (Fig. 4.1):

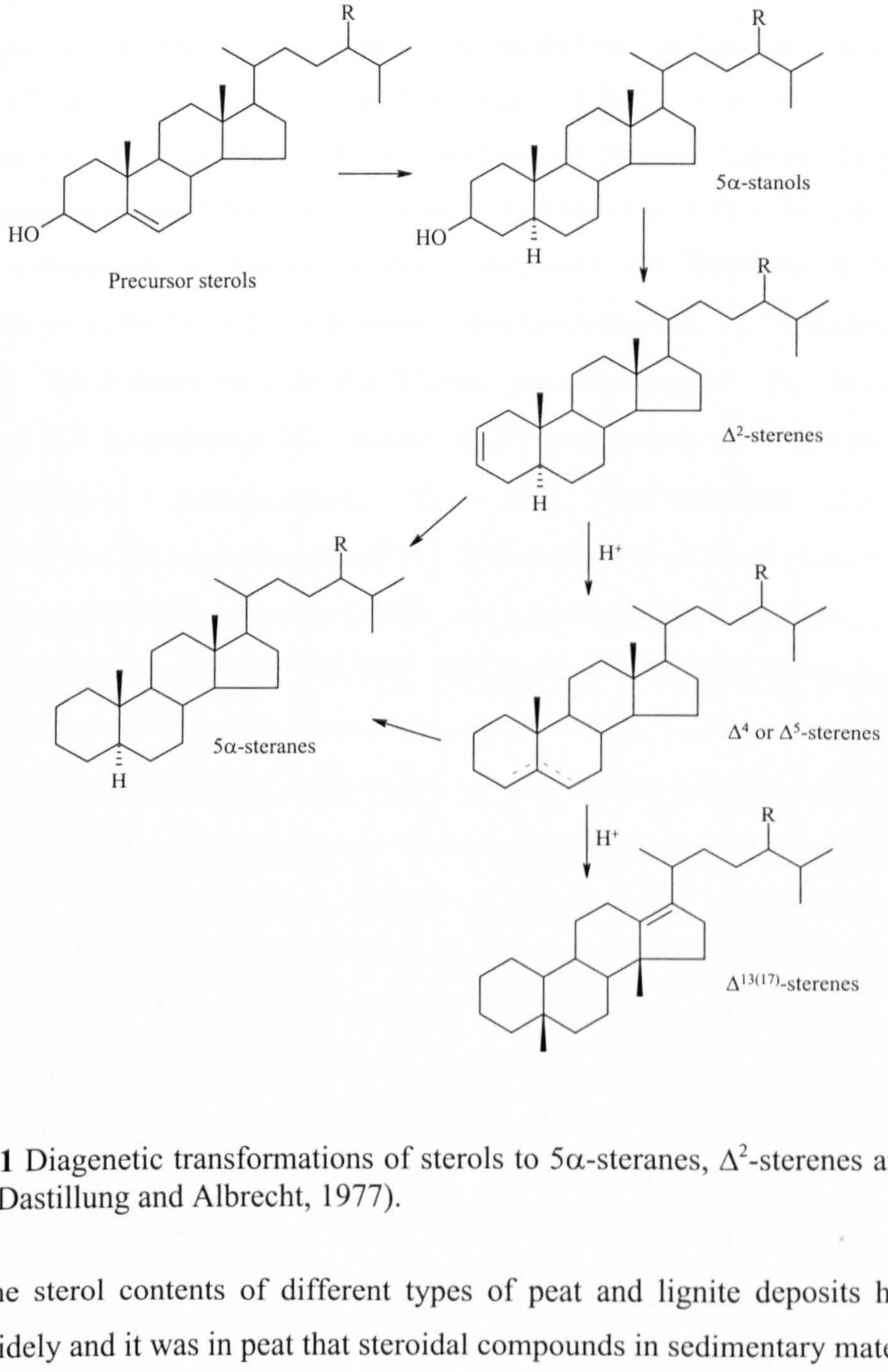

Figure 4.1 Diagenetic transformations of sterols to 5α-steranes, Δ^2-sterenes and $\Delta^{13(17)}$-sterenes (Dastillung and Albrecht, 1977).

The sterol contents of different types of peat and lignite deposits have been studied widely and it was in peat that steroidal compounds in sedimentary material were first confirmed, with the identification of β-sitosterol and β-sitostanol (McLean *et al.*, 1958). The reduction of sterol double bonds, believed to occur through sterone intermediates to give stanols, has also been reported (Evershed and Connolly, 1994; Ives and O'Neil, 1958).

In this chapter the first identification of hydroxy and ketonic androstanes from an immature sediment is reported. The structures of these compounds indicate formation from plant sterols by microbial oxidation of the C-17 side chain.

4.2 Results and Discussion

When examining the components of an alcohol/steroid fraction from samples of Bolton Fell Moss peat below 3 m depth (core BFM2), a group of oxygenated compounds with the androstane skeleton was observed. Figure 4.2 shows the partial gas chromatogram obtained from a steroid fraction. GC/MS (Fig. 4.3) and coinjection with authentic compounds of known structure confirmed the identities of the major components as 3α-hydroxy-5α-androstan-17-one (androsterone, **1**), 5α-androstan-3,17-dione (**2**), 3β-hydroxy-5α-androstan-17-one (epiandrosterone, **3**), 5α-androstan-3α,17β-diol (**4**), 5α-androstan-3β,17β-diol (**5**), 24*R*-ergost-5-en-3β-ol (campesterol, **6**), 24*R*-ergostan-3β-ol (campestanol, **7**), 22*E*, 24*R*-stigmasta-5,22-dien-3β-ol (stigmasterol, **8**), 24*R*-stigmastan-3-one (**9**), 24*R*-stigmast-5-en-3β-ol (β-sitosterol, **10**), 24*R*-stigmastan-3β-ol (stigmastanol, **11**) and 24*R*-stigmast-4-en-3-one (**12**). 3β-Hydroxy-5α-androstan-17-one (**3**) and 24*R*-stigmastan-3β-ol (**11**) are the most abundant compounds in this fraction.

Figure 4.3 shows the EI mass spectra of 5α-androstan-3,17-dione (**2**), and of 3α-hydroxy-5α-androstan-17-one (**1**) and 3β-hydroxy-5α-androstan-17-one (**3**) as their TMS ether derivatives. The mass spectrum of the dione (**2**) is characterised by the molecular ion, $M^{+\cdot}$, at *m/z* 288 (base peak) and ions at *m/z* 273 $[M\text{-}CH_3]^+$, *m/z* 270 $[M\text{-}H_2O]^{+\cdot}$, *m/z* 255 $[M\text{-}H_2O\text{-}CH_3]^+$, *m/z* 244 $[M\text{-}COCH_2]^{+\cdot}$ and *m/z* 217 $[M\text{-}CH_3\text{-}CO(CH_2)_2]^+$. The mass spectra of the epimeric hydroxy-5α-androstan-17-ones (**1, 3**) are clearly distinguishable and both display a molecular ion $M^{+\cdot}$ at *m/z* 362 and several specific fragment ions at *m/z* 347 $[M\text{-}CH_3]^+$, *m/z* 272 $[M\text{-}TMSiOH]^{+\cdot}$, *m/z* 257 $[M\text{-}TMSiOH\text{-}CH_3]^+$, *m/z* 129 $[TMSiOC_3H_4]^+$ and *m/z* 75 $[Si(CH_3)_2OH]^+$. The base peak for the 3α epimer (**1**) is *m/z* 75 with the fragment ion at *m/z* 272 occurring in far greater abundance than for the 3β epimer (**3**) which has a base peak at *m/z* 347. Ions at *m/z* 129, 215 and 257 are also in greater relative abundance in the 3α epimer (**1**).

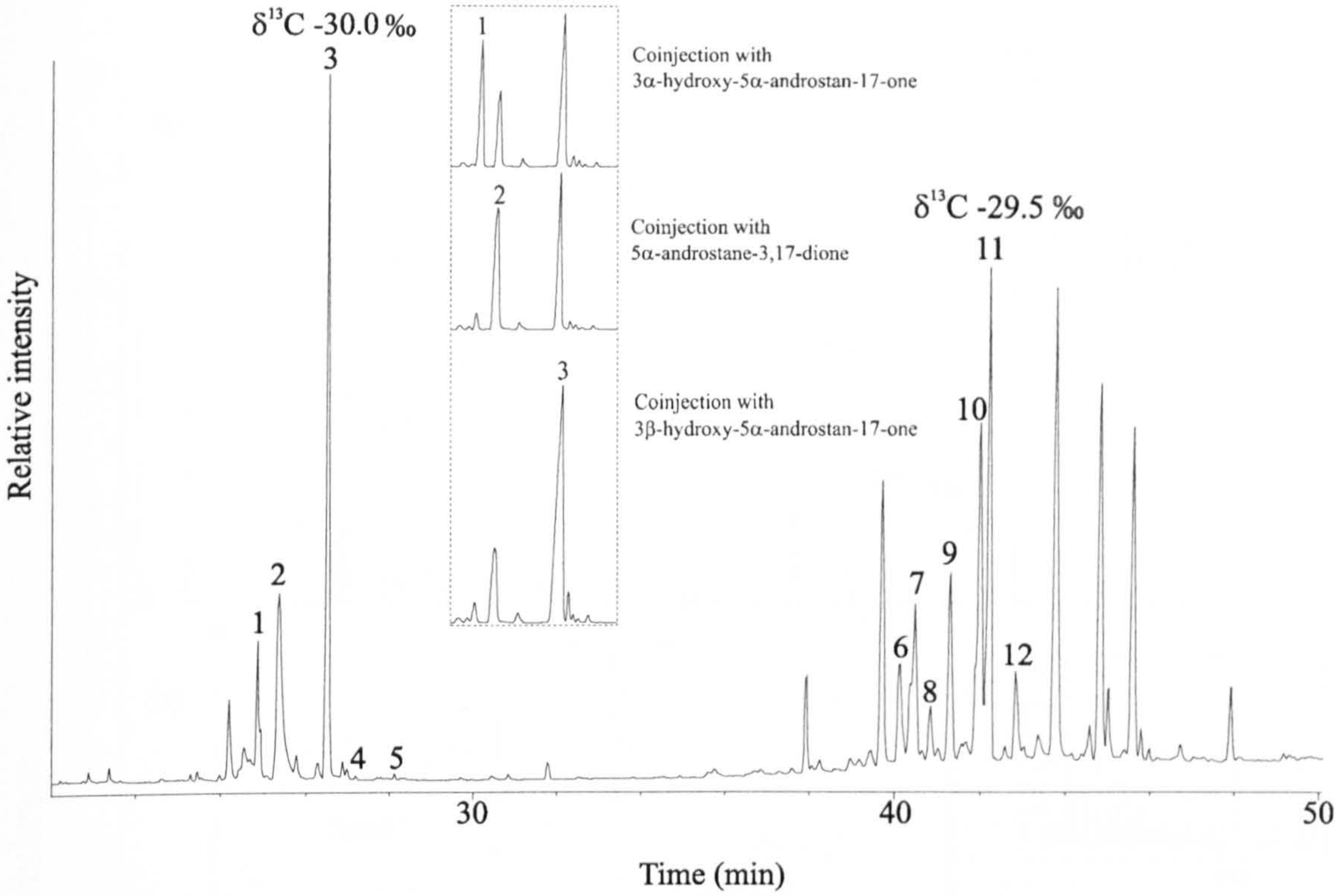

Figure 4.2 Partial gas chromatogram of the trimethylsilylated steroid fraction from peat core BFM2 at 4.25 m depth; 50 m CPSil-5CB, 50-200°C @ 12°C min^{-1}, 200-300°C @ 3°C min^{-1}, 300°C (20 min). Key: **1** = 3α-hydroxy-5α-androstan-17-one, **2** = 5α-androstane-3,17-dione, **3** = 3β-hydroxy-5α-androstan-17-one, **4** = 5α-androstane-3α,17β-diol, **5** = 5α-androstane-3β,17β-diol, **6** = 24*R*-ergost-5-en-3β-ol, **7** = 24*R*-ergostan-3β-ol, **8** = 22*E*, 24*R*-stigmasta-5,22-dien-3β-ol, **9** = 24*R*-stigmastan-3-one, **10** = 24*R*-stigmast-5-en-3β-ol, **11** = 24*R*-stigmastan-3β-ol, **12** = 24*R*-stigmast-4-en-3-one (inserts show coinjection of major androstane compounds with authentic compounds).

GC/MS analyses of shallow samples taken from 25 cm depth showed the most abundant sterols to be 24*R*-stigmast-5-en-3β-ol (**10**) and 24*R*-stigmastan-3β-ol (**11**). The relative abundance of 24*R*-stigmastan-3β-ol (**11**) to 24*R*-stigmast-5-en-3β-ol (**10**) increases with depth, with the related 24*R*-stigmastan-3-one (**9**) and 24*R*-stigmast-4-en-3-one (**12**) remaining in low abundance. Components with the androstane skeleton first appear in the core at a depth of approximately 3 m.

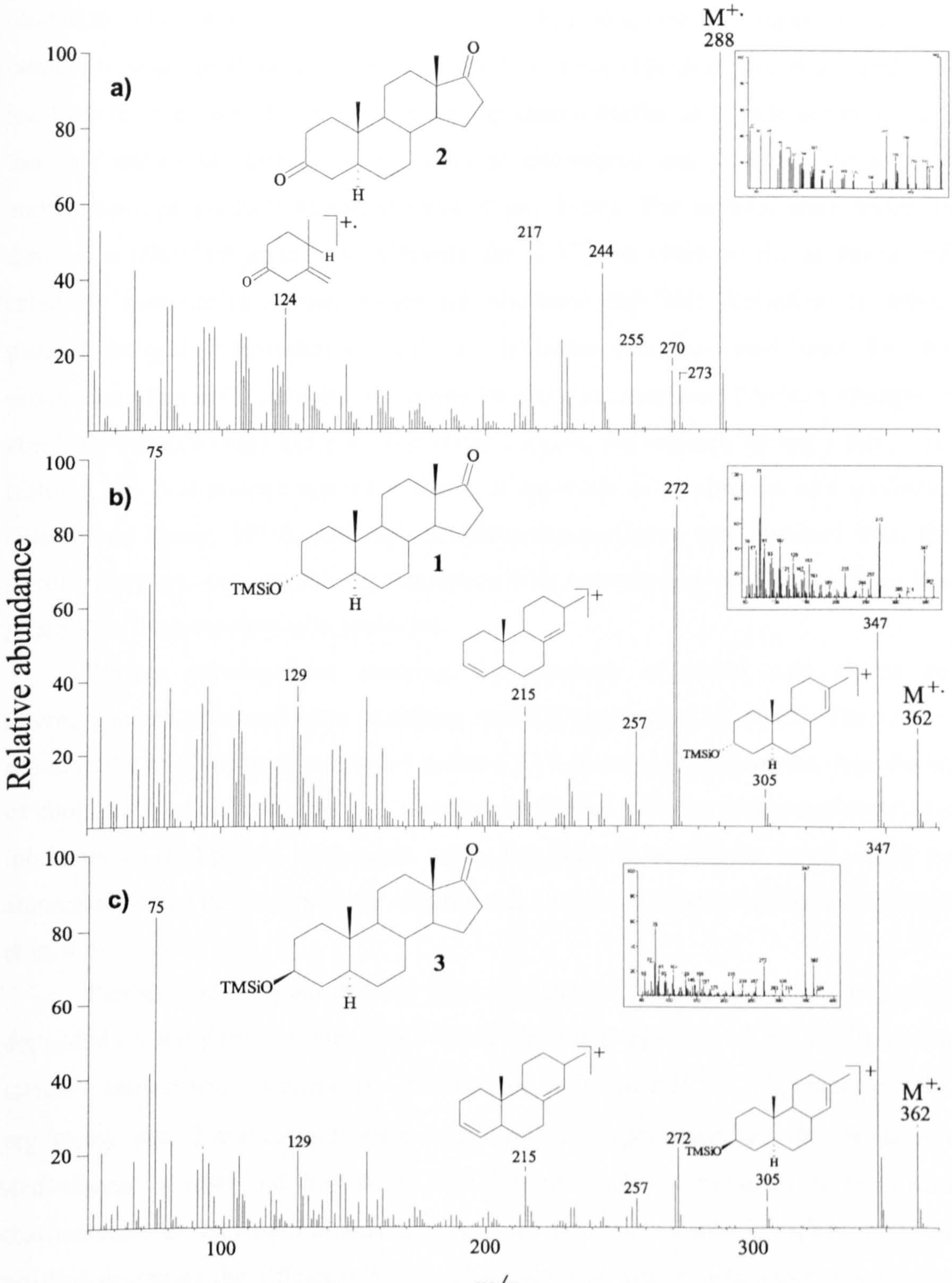

Figure 4.3 Mass spectra of (a) 5α-androstan-3,17-dione, (b) 3α-hydroxy-5α-androstan-17-one and (c) 3β-hydroxy-5α-androstan-17-one. The hydroxyandrostanes were analysed as their TMS ethers (inserts show mass spectra of authentic compounds).

The androstane components have structures reminiscent of the sterols found within the peat but with the C-17 side chain missing, presumably through removal by

oxidation. The sterols of *Sphagnum* mosses, which dominate the input to the peat, contain high concentrations of 24*R*-stigmast-5-en-3β-ol (**10**) (Karunen *et al.*, 1983). It has been reported, based on laboratory biodegradation studies, that bacteria can degrade the side chains of common sterols such as cholesterol and sitosterol, to produce androstane-type products (Bhattacharyya *et al.*, 1984). The authors were trying to develop a microbial process to eliminate the C-17 side chain of the abundant and relatively inexpensive sterols, cholesterol, sitosterol and their derivatives to obtain useful steroidal intermediates, such as 3β-hydroxyandrost-5-en-17-one for the production of anabolic steroids and estrone for oral contraceptives. Previous attempts to eliminate the side chain had met with varied success, the research having a forty year history. The first attempt applied a chemical approach using chromic acid oxidation (Fieser and Fieser, 1959). Although dehydroepiandrosterone was obtained from the sterols, there was considerable contamination with unwanted by-products, making this process far from economically profitable.

Further investigations studying the cleavage of sterol side chains by microorganisms produced more promising results (Nagasawa *et al.*, 1969). The authors reported the production of androsta-1,4-diene-3,17-dione (ADD) from the degradation of cholesterol by certain bacteria. It was also found that, with the addition of metabolic inhibitors (α,α′-dipyridyl or arsenic acid), the degradation of the sterol could be attenuated so that the intermediates with the side chain eliminated could be accumulated (Fig. 4.4).

Further studies found that the yield of ADD and other androstane compounds depended on the particular side chain being cleaved (Nagasawa *et al.*, 1970). Seven sterols, cholesterol, campesterol, β-sitosterol, stigmasterol, 7-dehydrocholesterol, ergosterol and β-cholestanol were subjected to degradation by the bacterium *Arthrobacter simplex* and the amount of ADD produced was measured. It was found that increases in the length of side chain and the introduction of a branch at the C-24 position decreased the efficiency of side chain removal. Other factors that retarded the degradation included the presence of a Δ^7 or Δ^{22}-double bond such that the ease of "cleavability" decreased in the following order: cholesterol > campesterol, β-sitosterol > stigmasterol > 7-dehydrocholesterol > β-cholestanol > ergosterol.

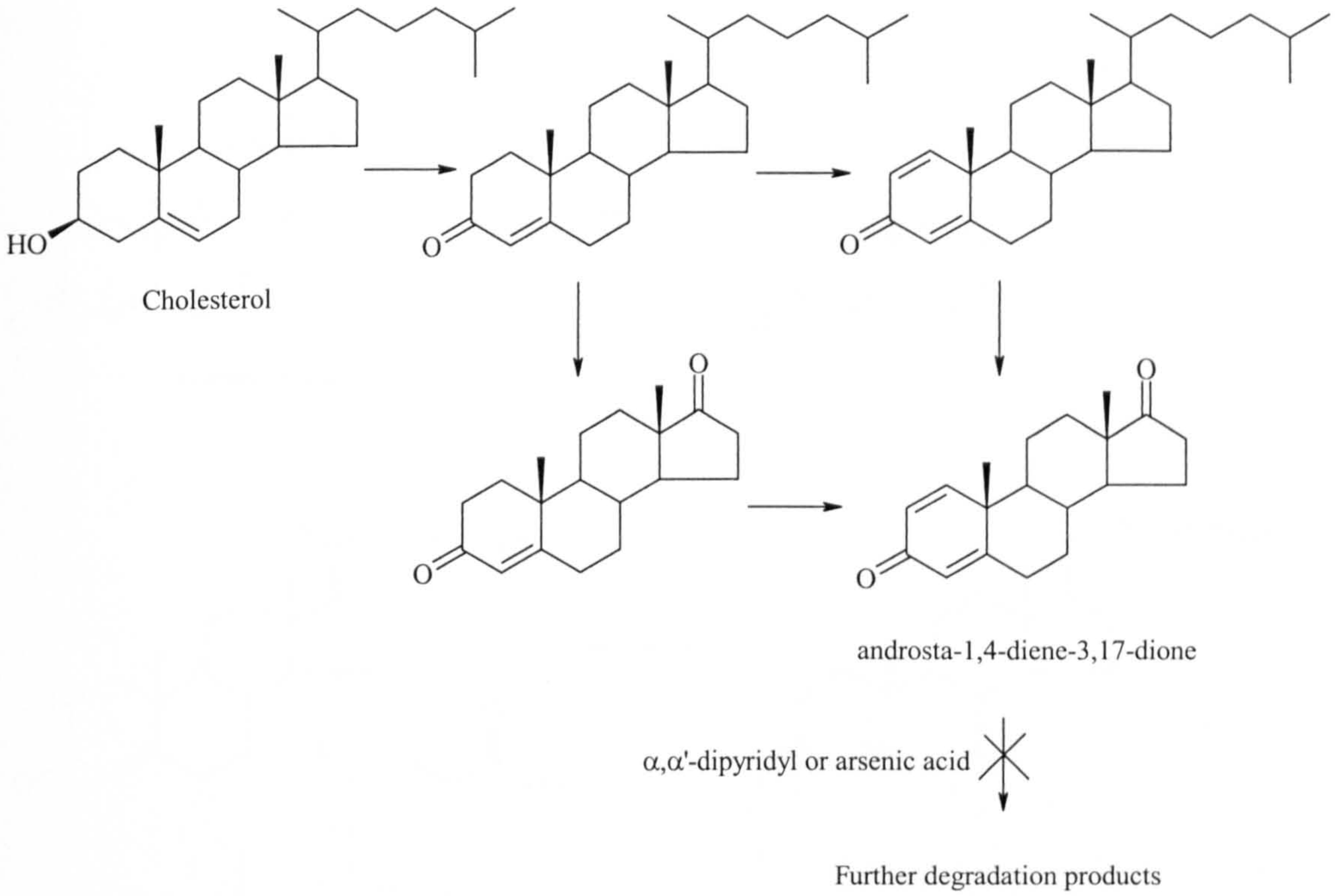

Figure 4.4 Bacterial side chain cleavage of cholesterol to yield androsta-1,4-diene-3,17-dione (Nagasawa *et al.*, 1969).

The high cost involved in the large scale manufacture of estrone for oral contraceptives has prompted research into microbially-mediated synthesis of estrone from sterols which are present in abundance as the by-products from meat, food oil and textile industries. One study using these substrates and common microorganisms isolated from natural sources (e.g. soil, sewage, silage, etc.) has produced androstane compounds in high yield (Bhattacharyya *et al.*, 1984). These experiments have shown that the bacteria which cleave the side chains of sterols do so under anaerobic conditions and that the cleavage occurs by β-oxidation (Fig. 4.5). The first stage of this cleavage involves the hydroxylation at the C-26 position of cholesterone and oxidation to the carboxylic acid. This is followed by the progressive β-oxidation of the C-24 acid and subsequent C-22 acid with elimination of propanoic acid. The final stage involves the elimination of propanoic acid through dehydrogenation at the C-17/C-20 bond.

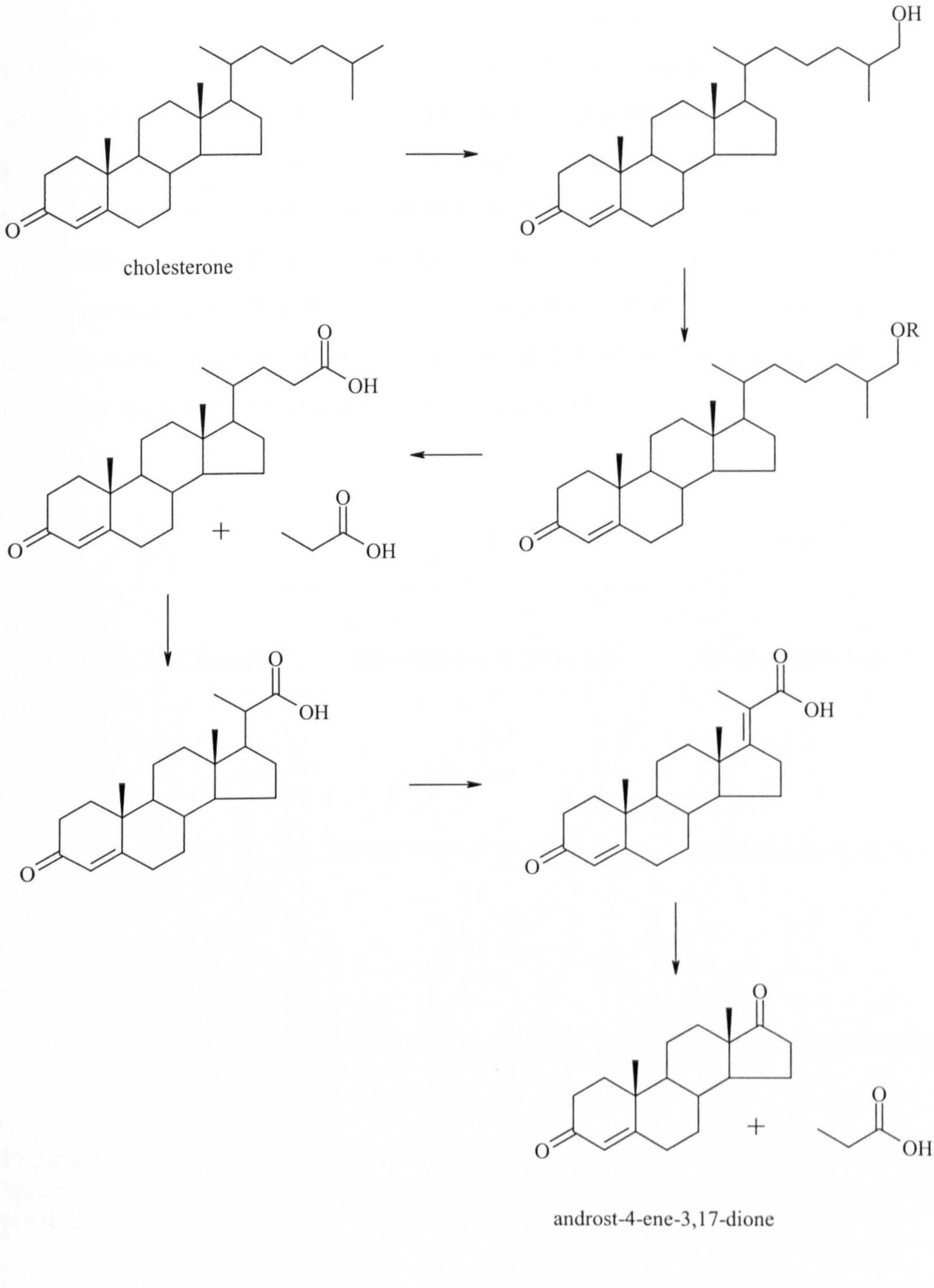

Figure 4.5 Side chain cleavage of cholesterone by microorganisms (Bhattacharyya *et al.*, 1984).

Since the bacteria used in the experiments were isolated from soil, similar microorganisms may be, or may have been, active in the peat. Hence, by analogy with the findings of Bhattacharyya *et al.* (1984) and by comparison of sterol and stanol distributions with those of the androstanes in Bolton Fell Moss peat it appears that 24*R*-

stigmast-5-en-3β-ol (**10**) and other sterols and stanols are transformed in this environment to 3β-hydroxy-5α-androstan-17-one (**3**) *via* the pathways in Figure 4.6. To provide further evidence that the androstane compounds are indeed degradation products of the sterols, $\delta^{13}C$ values of selected components (Fig. 4.2) were measured using isotope ratio monitoring-GC/MS (irm-GC/MS) which gave values of -30.0‰ for 3β-hydroxy-5α-androstan-17-one (**3**) and -29.5‰ for 24*R*-stigmast-5-en-3β-ol (**10**) and 24*R*-stigmastan-3β-ol (**11**). These results are consistent with the compounds originating from the same source, i.e. 3β-hydroxy-5α-androstan-17-one (**3**) is a biotransformation product of the major sterol 24*R*-stigmast-5-en-3β-ol (**10**).

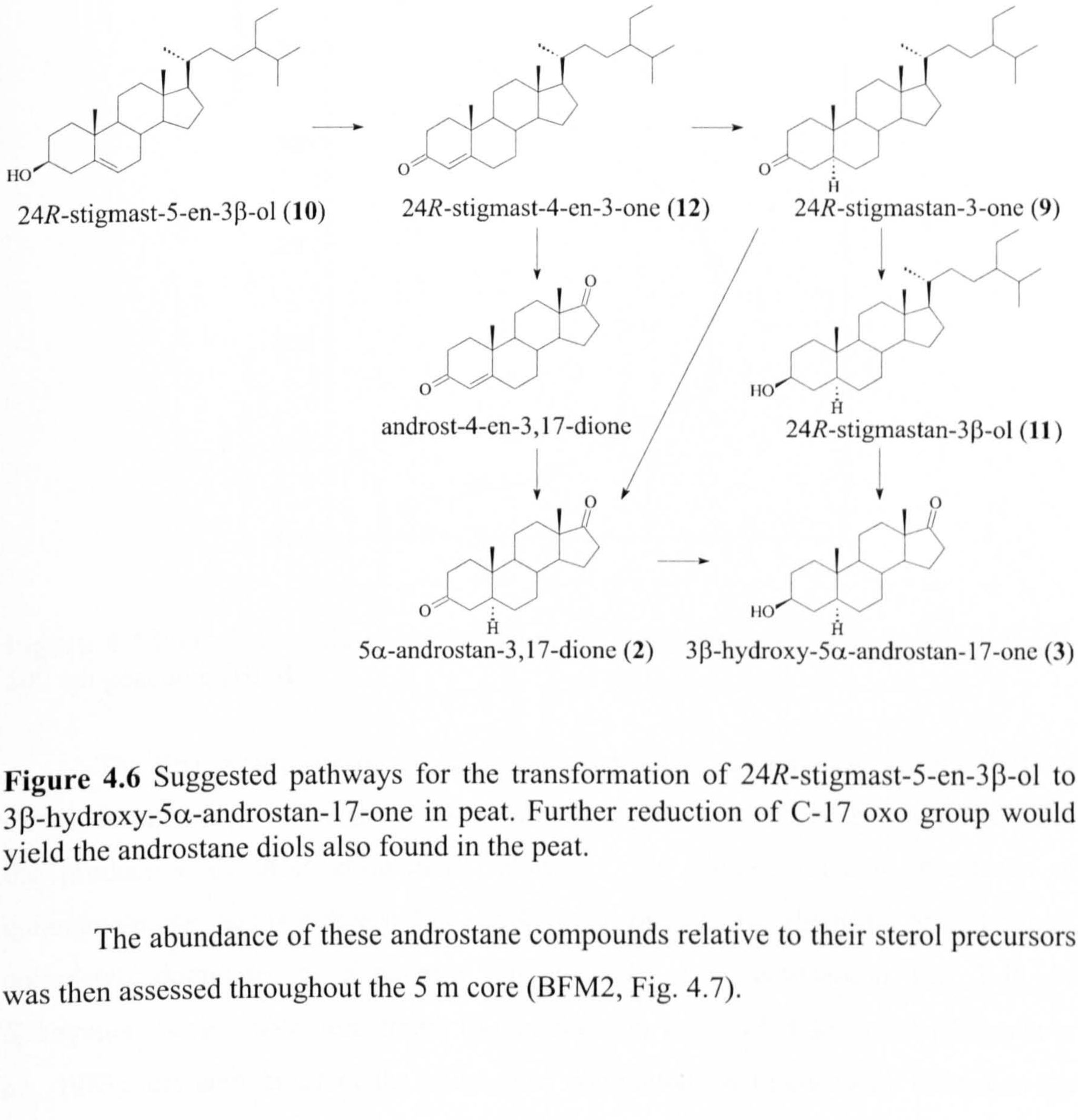

Figure 4.6 Suggested pathways for the transformation of 24*R*-stigmast-5-en-3β-ol to 3β-hydroxy-5α-androstan-17-one in peat. Further reduction of C-17 oxo group would yield the androstane diols also found in the peat.

The abundance of these androstane compounds relative to their sterol precursors was then assessed throughout the 5 m core (BFM2, Fig. 4.7).

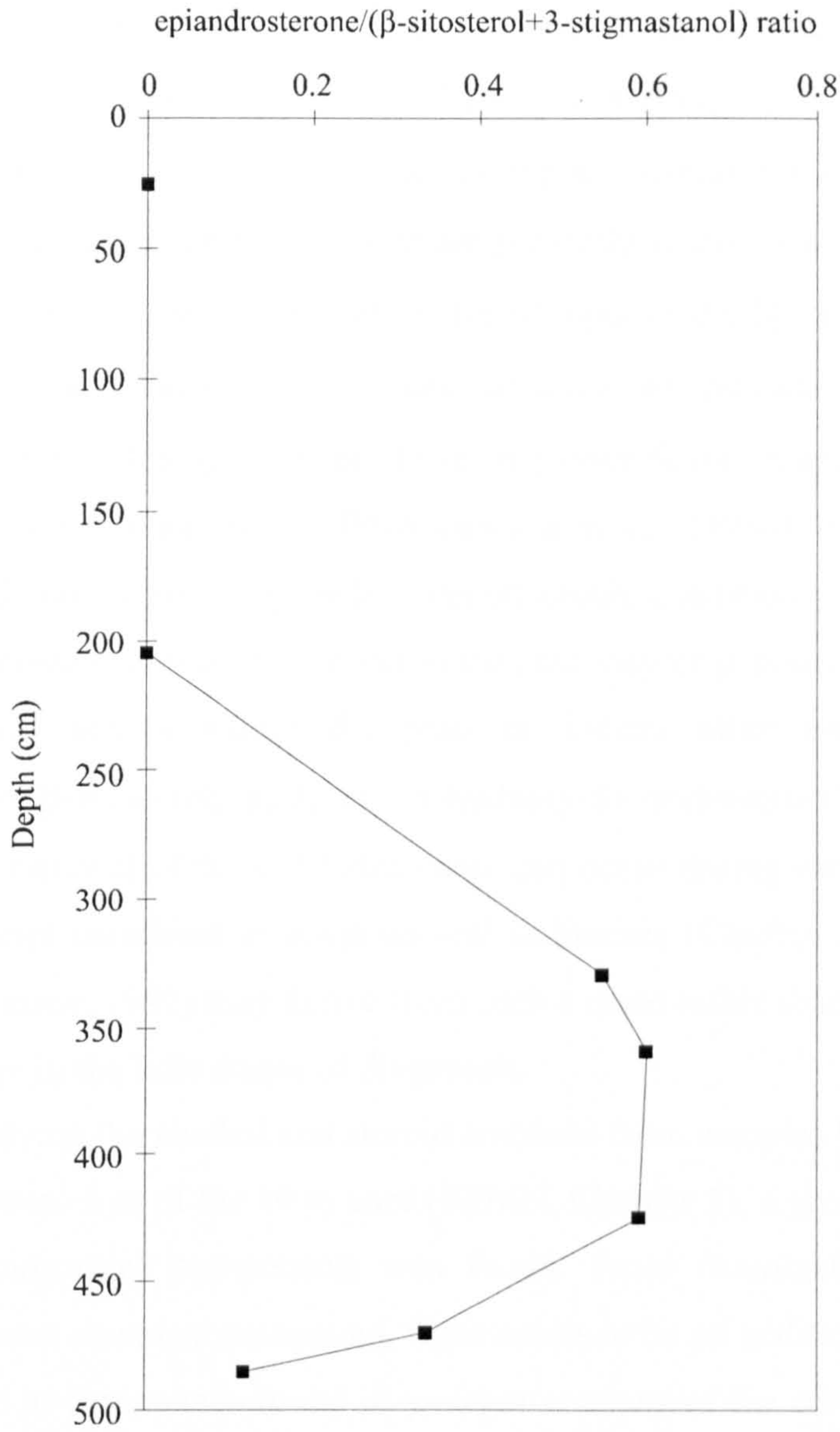

Figure 4.7 Plot of the ratio of epiandrosterone/(β-sitosterol+3-stigmastanol) in the 0-500 cm peat core (BFM2).

The first occurrence of the androstane compounds is between 205 and 330 cm depth, during which period there is no major change in plant input that might relate to the production of these compounds. However, the highest relative abundance of epiandrosterone occurs between 359 and 425 cm, throughout which the peat is almost completely dominated by *Sphagnum* (56-92% total peat composition, Fig. 2.4). As *Sphagnum* species have been found to contain high levels of β-sitosterol (Karunen *et al.*, 1983), the abundance of the androstane compounds is likely to be related to the increased amounts of β-sitosterol/3-stigmastanol within this peat. However, the proposed transformation (Fig. 4.6) of these compounds as bacterially mediated would suggest that the abundance of the compounds is also likely to be related to bacterial

activity. This is reflected in the hopanes (Fig. 3.19) and hopanols (Fig. 3.23) of bacterial origin that were found in the same horizons, by way of the relative abundance of the ββ to αβ epimers being elevated. Possible reasons for an increased abundance of the ββ hopane could be an input from bacteria that are presently active or were recently active within these horizons. This would provide a 'fresh' input of the ββ isomers and elevate the ββ/αβ ratios. These bacteria would then facilitate the increase in the side chain degradation of sterols. Although hopanes have only been found in aerobic bacteria and the peat at this depth is anaerobic, Bhattacharyya *et al.* (1984) found that aerobic bacteria produced androstane compounds under anaerobic conditions.

Other androstane compounds found in the peat may be products of the microbial oxidation of other sterols within the peat- or indeed other products from the transformation of β-sitosterol, such as 3α-hydroxy-5α-androstan-17-one (**1**). These results show that removal of the C-17 side chain can occur during early diagenesis and that the androstanes identified in some ancient sediments (Chaffee and Johns, 1983; Matveyeva and Petrov, 1992) may derive from such a route rather than being formed by a thermal cleavage in the later stages of diagenesis.

When studying the alcohol and steroid fractions from samples 957-959 and 977-979 cm in the bottom 2 m of the 10 m core (BFMN, Chapter 5), a group of compounds similar to the androstane components was found. From examination of the mass spectrum of the most abundant compound, there seems to be an additional methyl group present compared to compounds found in younger sections of the core (Fig. 4.8). Also found in this fraction was a 4-methyl sterol, dinosterol, which has been found to be present in dinoflagellates (Boon *et al.*, 1979) and certain algae (Volkman *et al.*, 1990). The samples in which these compounds are found are from horizons which were stratified at the early stages of peat formation (Fig. 1.1a+b), and it is likely from the presence of dinosterol that these horizons existed at the bottom of a lake. Thus, the presence of a 4-methyl sterol would suggest that the novel methylated androstane compounds are derived from dinosterol and that the methyl group is in the 4 position.

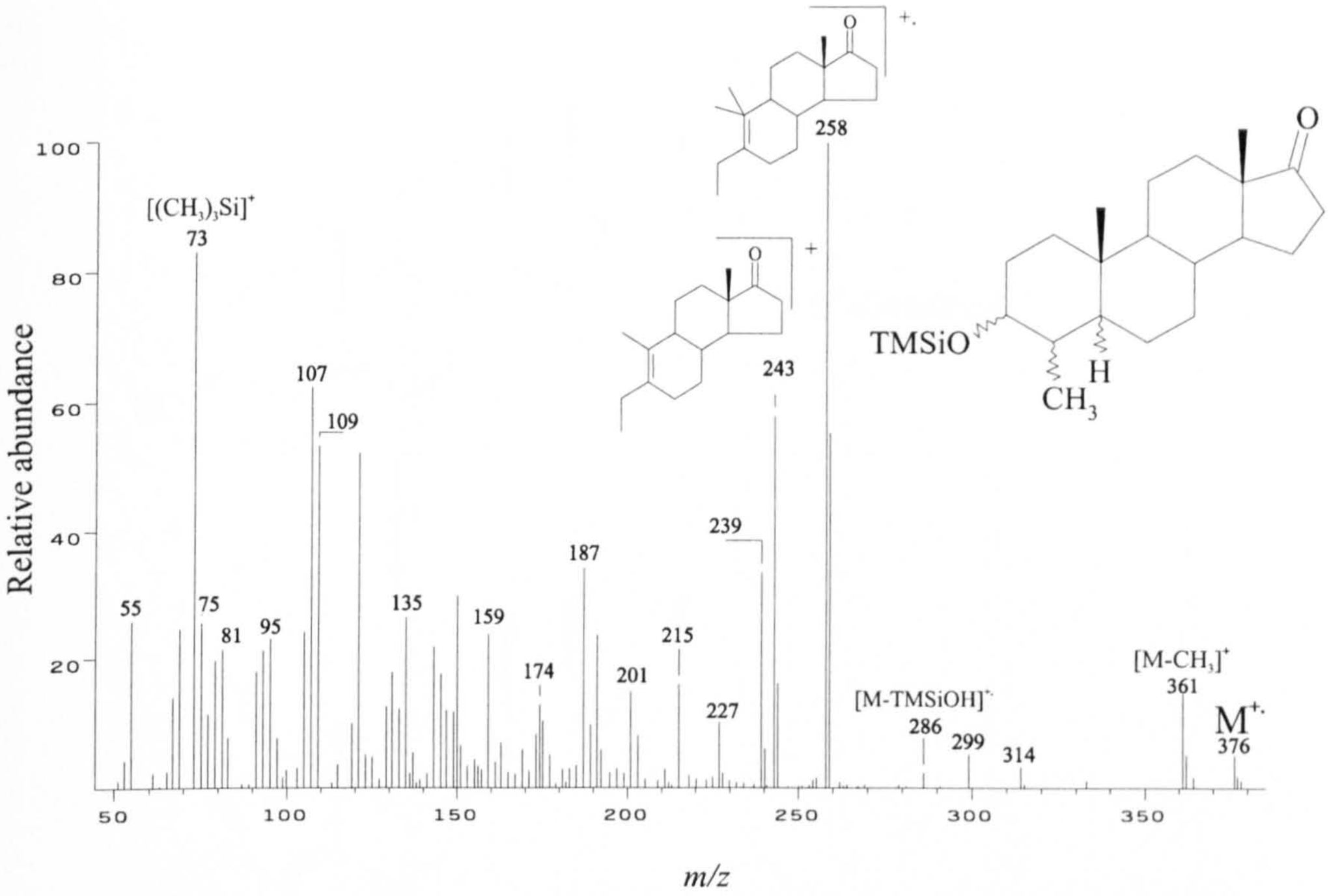

Figure 4.8 Mass spectrum of 3-hydroxy-4-methylandrostan-17-one, as TMS ether.

Figure 4.8 shows the EI mass spectrum of the component assigned as 3-hydroxy-4-methylandrostan-17-one TMS ether. This displays a molecular ion $M^{+\cdot}$ at *m/z* 376 and several fragment ions at *m/z* 361 $[M\text{-}CH_3]^+$, *m/z* 286 $[M\text{-}TMSiOH]^{+\cdot}$, and *m/z* 73 $[(CH_3)_3Si]^+$. The base peak for this compound is *m/z* 258 and is assigned to result from cleavage of the C1-2 and C3-4 bonds.

By analogy with the scheme in Figure 4.6, a diagenetic pathway to the major methylated androstane is proposed in Figure 4.9. Since the bacterially-mediated oxidation of the C-3 alcohol moiety to the ketone appears to require the presence of a Δ^5 double bond (Bhattacharyya *et al.*, 1984) to give the enone, the source of the methylated androstanone component is indicated as Δ^5-dinosterol. Due to the absence of an authentic compound with known structure, the configuration of the 3-hydroxy substituted and 4-methyl group is hard to determine. There are 4 possible epimers; $\alpha\alpha$, $\beta\beta$, $\alpha\beta$ and $\beta\alpha$, but the most abundant epimer is likely to have the hydroxy group in the β conformation and the methyl in the α configuration, as in dinosterol. Unfortunately, however, it was difficult to deduce the number of epimeric components as there was extensive coelution.

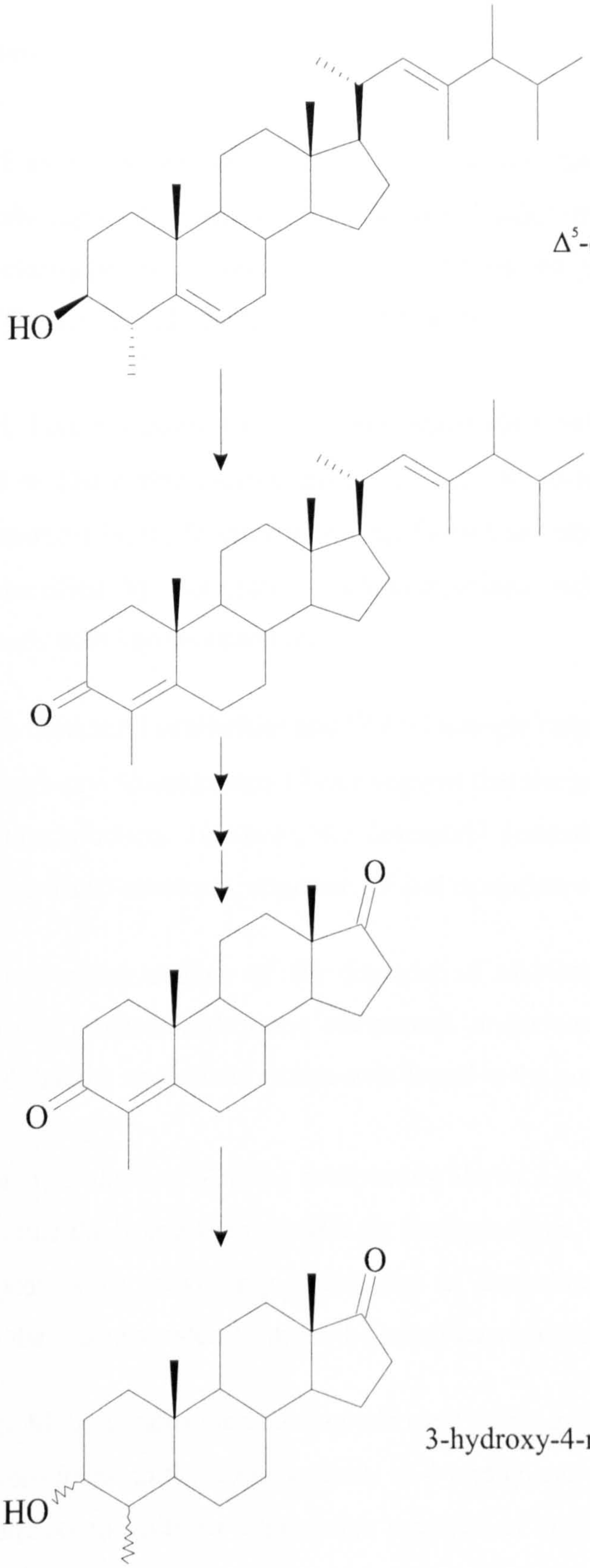

Δ^5-dinosterol

3-hydroxy-4-methylandrostan-17-one

Figure 4.9 Proposed microbially mediated degradation pathway of Δ^5-dinosterol in peat core BFMN between 957 and 979 cm depth.

4.3 Summary

This chapter explored the possible origins of novel androstane compounds not previously reported in peat or other immature sediments. $^{13}C/^{12}C$ isotopic ratios were used to clarify precursors and microbial transformation pathways proposed.

The major findings of this research were:

1. Five compounds with the androstane skeleton were found in peat core BFM2 below 3 m (3α-hydroxy-5α-androstan-17-one, 5α-androstan-3,17-dione, 3β-hydroxy-5α-androstan-17-one, 5α-androstan-3α,17β-diol and 5α-androstan-3β,17β-diol). These were identified by coinjection and comparison with mass spectra of authentic compounds with known structure.

2. Structural similarities and $^{13}C/^{12}C$ isotopic ratios of β-sitosterol/3-stigmastanol and 3β-hydroxy-5α-androstan-17-one suggest that the androstane compounds are sterol degradation products. However, the desmethyl androstanes are likely to derive from several sterols (β-sitosterol, stigmasterol and campesterol).

3. Previous studies of the degradation of sterols have revealed that aerobic bacteria can produce androstane compounds under anaerobic conditions. It has been proposed that the androstane compounds found in the peat have a microbial origin.

4. The absence of these compounds above 3 m and proposed microbial origin suggests that the bacteria responsible for their presence, either only populate those areas of the peat, were active only at the time of deposition of these peat layers or only degrade the precursor sterols under the conditions present at these depths.

5. Methyl androstane compounds were found in the deepest part of the peat core. These were found in the same horizons as 4-methyl sterols and it was proposed that the androstane compounds are degradation products of these sterols and also have a methyl group in the 4 position.

6. Although not fully characterised the 4-methyl group in the major 4-methyl compound, 3-hydroxy-4-methylandrostan-17-one was thought to be in the α configuration.

5. LIPID ORGANIC GEOCHEMISTRY OF PEAT DEPOSITED DURING THE EARLIEST PHASE OF BOG DEVELOPMENT

5.1 Introduction

The formation of raised peat bogs has been discussed in Chapter 1. Three major stages of development have been identified (Fig. 1.1, Foss, 1987).

(I) Lakes - deep hollows or basins with poor drainage

(II) Fens - peatlands containing sedges, *Sphagnum* mosses and other plant species that tolerate low nutrient conditions

(III) Raised bogs - the accumulation of *Sphagnum* remains over hundreds or thousands of years in an anaerobic waterlogged environment

The distinct environments that occur throughout the development of a raised peat bog, with the successions of different plant vegetation, should produce horizons with contrasting stratigraphy. However, the absence of macrofossil data, resulting from extensive humification in part of the peat profile, provides little insight into the species of plant that were present during early bog formation. Although the plant macrofossils cannot be identified, the contrasting stratigraphy produced at the formation of a peat bog may be reflected in the lipid profiles from each distinct horizon (being more resistant to change).

In this chapter, lipid fractions of peat taken from Bolton Fell Moss, were used to determine whether formation of this ombrotrophic mire followed the established model of peat bog development as described by Foss (1987). Lipid extracts of samples taken from the lower 2 m of the 10 m core (BFMN) were studied and compared to the lipid profiles of younger peat samples with for which macrofossil data was available (Chapter 3), enabling determination of the stages of peat development from the study of a humified section.

Hence, the main objectives of this study were:

I. Identification of lipid components from distinct peat horizons present during the early formation of the peat bog.

II. Determination of likely plant taxa present in these horizons, by comparison of lipid records with lipid distributions of previously characterised peat-forming plants.

III. Application of these data to determine if the formation of Bolton Fell Moss followed the bog development model proposed by Foss (1987).

5.2 Peat Horizons

The distinct peat horizons present in the bottom 2 m of the 10 m core (BFMN) from Bolton Fell moss can be seen in Figures 2.5 and 2.6 (Chapter 2). The 5 horizons (Fig. 2.7) consist of a clay layer between 987 and 1004 cm, a very light brown peat layer between 982 and 987 cm, a mineral layer (similar to the clay below 987 cm) between 977 and 982 cm, a light brown peat layer between 820 and 977 cm and above this a dark brown peat layer between 800 and 820 cm depth. Macrofossil data from an adjacent core (500-850 cm depth, Fig. 2.3) were available and suggested that the dark brown peat between 800 and 820 cm has Monocotyledons as the major plant component. The peat present in the top 10 cm of the 820 and 977 cm horizon is likely to be composed predominantly of *Sphagnum* remains. However, replicability studies performed on peat profiles from Bolton Fell Moss have suggested macrofossil data cannot be transferred between different peat cores with a high degree of certainty (Barber, 1998).

Peat samples representative of each of the distinct horizons were taken from the following depths (Fig. 2.7): 805-807 cm (BFMN-805), 870-872 cm (BFMN-870), 957-959 cm (BFMN-957), 977-979 cm (BFMN-977), 984-986 cm (BFMN-984) and 994-996 cm (BFMN-994). Samples BFMN-870 and BFMN-957 were taken from near the top and bottom of the same visible peat layer; this was done to determine if there were any discernible differences in the lipid profiles from these samples as, although they look similar, their time of deposition is likely to be several hundreds of years apart.

As these horizons exhibit a clearly defined stratigraphy their lipid profiles should reflect this. However, it is likely that at their time of deposition, the peat bog had not yet reached an ombrotrophic stage and lacustrine conditions probably prevailed. This could result in the input of allochthonous material which would not be present in samples taken from ombrotrophic peat.

5.3 Lipid Organic Geochemistry of Early Deposited Peat

The very different nature of these sediments (i.e. clay or peat material) made the comparison of absolute lipid abundances on a dry mass basis difficult. Therefore, the total organic carbon content (TOC) of each sample was determined and lipid contents are presented as % TOC.

The total amount of solvent-extractable lipids varied through the core (0.4-4.6% of TOC, Appendix III). The bottom clay layer, BFMN-994, showed the lowest amount with 0.4% and the highest percentage was shown by the top sample (BFMN-805), which contained 4.6% lipid material. The lipid matter content of peat is generally thought to increase with increased humification (Lehtonen and Ketola, 1993). This is apparent within the light brown peat layer (820-977 cm), which shows an increase in lipidic matter with depth (1.9% and 4.0% at BFMN-870 and BFMN-957 cm respectively). The dark brown peat layer contained the highest amount of lipid matter (4.6%), which agrees well with the results from Lehtonen and Ketola (1993) who found *Carex* peat to have a higher lipid content than *Sphagnum* peat. As would be expected, the mineral and clay layers contain very little lipidic matter.

As with the studies carried out on the less mature peat samples (Chapter 3), the solvent extractable lipids were separated into six fractions for identification and quantification: hydrocarbons, aromatics, ketones/wax esters, alcohol/steroid, polar and acid fractions. In all samples the aromatic and polar fractions contained no GC-amenable material and are not reported in this study. The ketones/wax esters, alcohol/sterol and acid fractions were derivatised with *N,O*-bis(trimethylsilyl)trifluoroacetamide (BSTFA) prior to GC analysis. The identification of lipids was performed either by comparison of GC retention times, comparison of mass spectral data with library data or by coinjection with compounds of known structure.

5.4 Hydrocarbons

All samples contain long chain *n*-alkanes with a high odd-over-even carbon preference (Figs. 5.1, 5.2 and 5.3). Most samples range in distribution between C_{19} and C_{33} with only BFMN-957 containing longer chain alkanes (Fig. 5.1). The alkanes had a dominant chain length of either C_{31} (BFMN-994, BFMN-984, BFMN-977, BFMN-805),

or C_{27} (BFMN-957, BFMN-870). Hydrocarbons were most abundant in the peat layer samples, and of these BFMN-870 contained the highest amount with 0.2% of the TOC. Also present in BFMN-994, BFMN-984, BFMN-870 and BFMN-805 was taraxast-20-ene, a compound with a triterpene skeleton (Fig. 5.3).

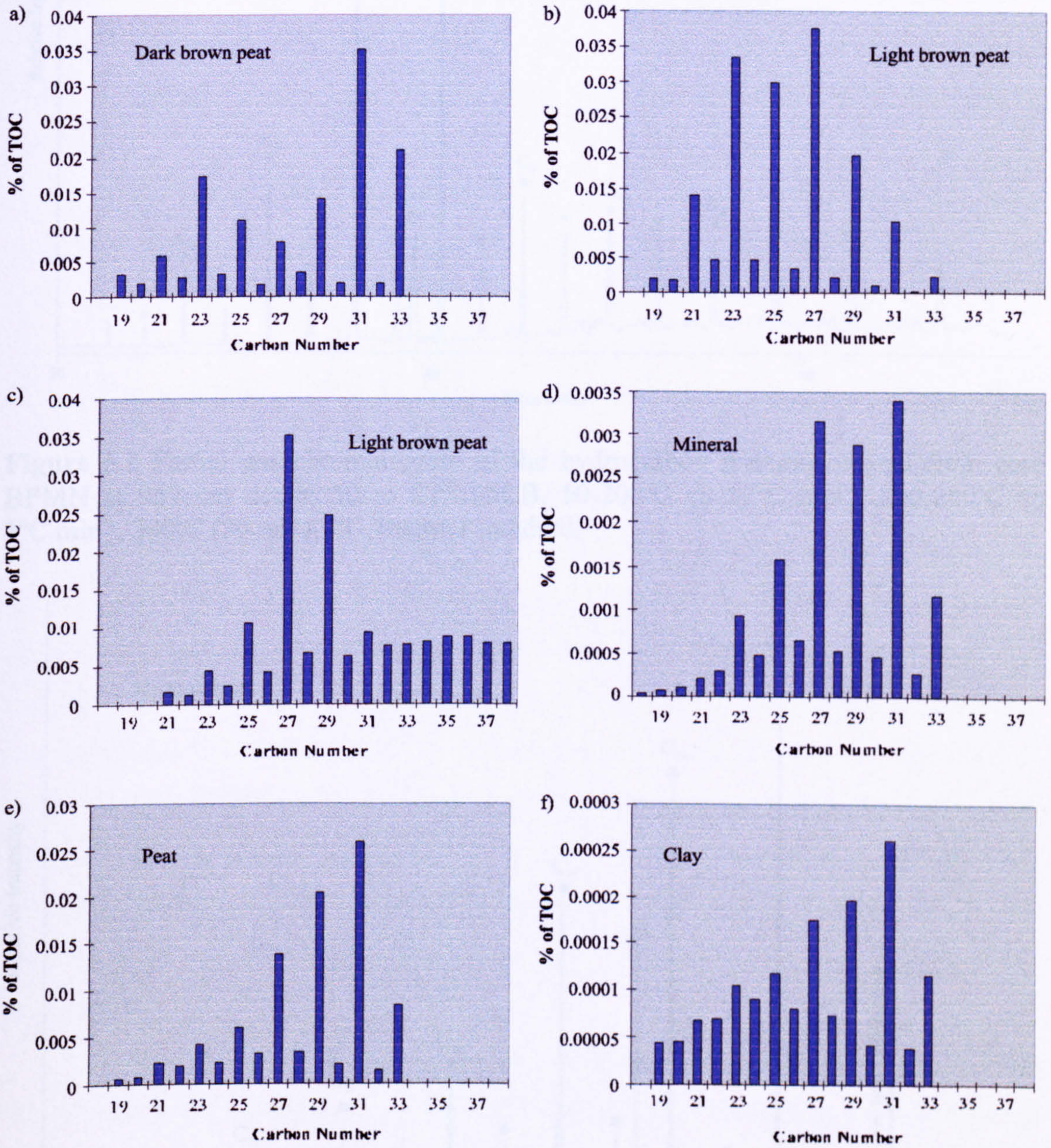

Figure 5.1 Histograms of distributions of *n*-alkane homologues (% of TOC) from (a) BFMN-805, (b) BFMN-870, (c) BFMN-957, (d) BFMN-977, (e) BFMN-984 and (f) BFMN-994.

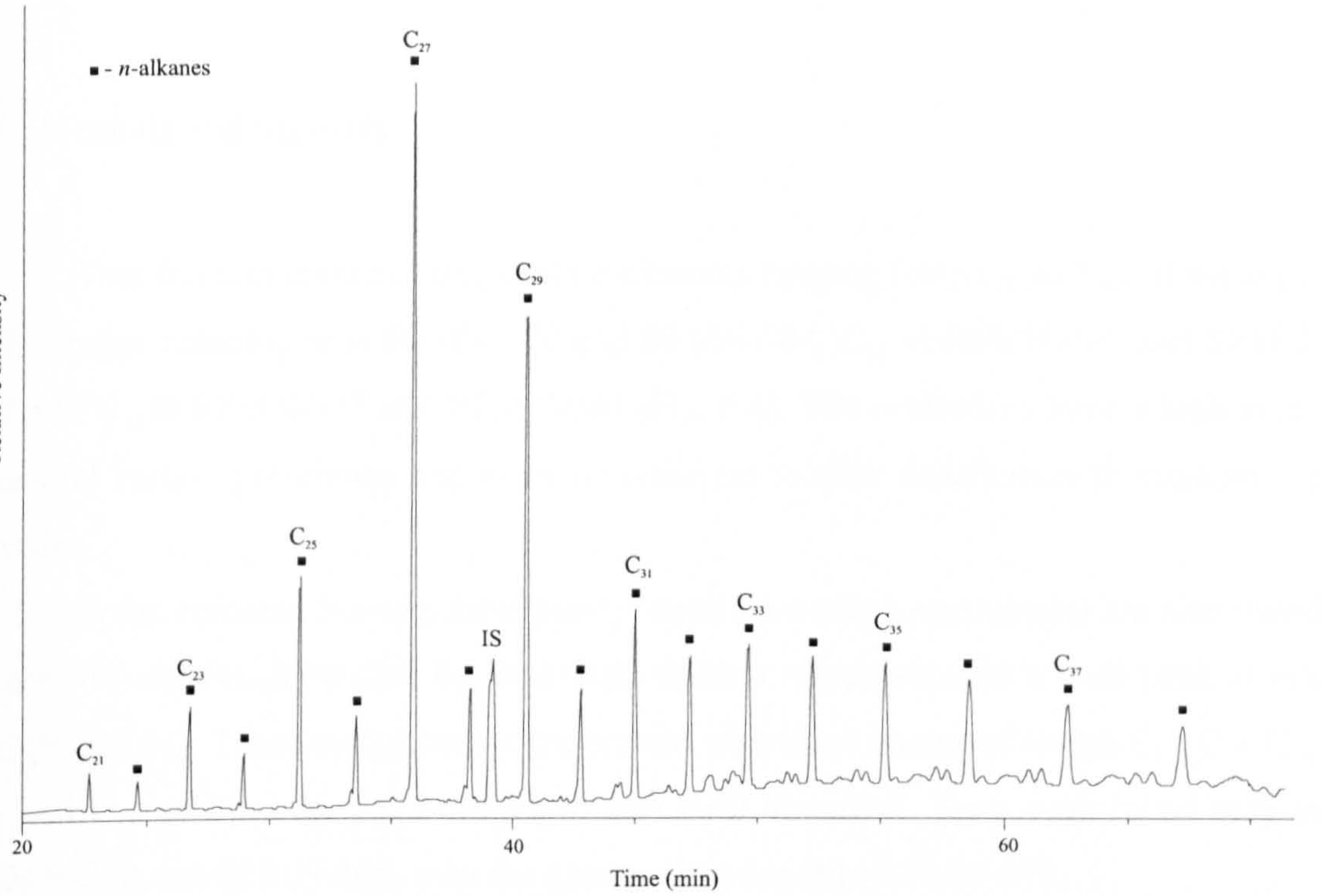

Figure 5.2 Partial gas chromatogram of the hydrocarbon fraction of peat from core BFMN at 957 cm depth; 50 m CPSil-5CB, 50-200°C @ 12°C min^{-1}, 200-300°C @ 3°C min^{-1}, 300°C (20 min). IS - Internal standard.

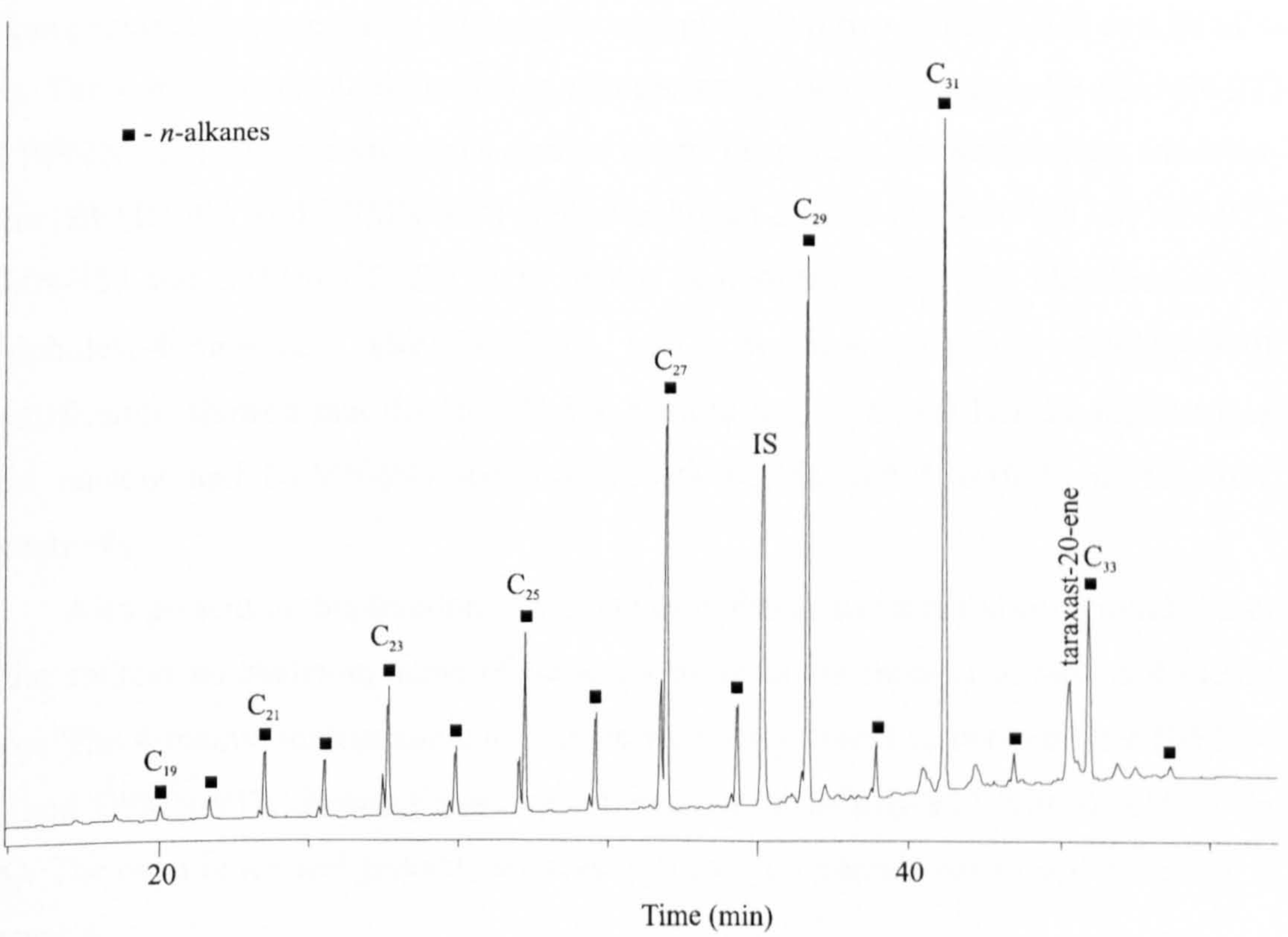

Figure 5.3 Partial gas chromatogram of the hydrocarbon fraction of peat from core BFMN at 984 cm depth; 50 m CPSil-5CB, 50-200°C @ 12°C min^{-1}, 200-300°C @ 3°C min^{-1}, 300°C (20 min).

5.5 Alcohols and Steroids

This fraction contains long chain *n*-alcohols ranging from C_{20} to C_{32}; of these C_{22} is the major homologue in BFMN-870 and BFMN-994, C_{26} in BFMN-805 and BFMN-957 and C_{28} at BFMN-977 and BFMN-984 (Fig. 5.4). The *n*-alcohols have a high even-over-odd carbon preference and show a somewhat similar distribution throughout the samples.

In the fraction, 5-*n*-alkylbenzene-1,3-diols (5-*n*-alkyl resorcinols) are also found in certain samples, identified by their mass spectra which showed a base peak at *m/z* 268 (Fig. 3.9a). These compounds were present with alkyl chains of length C_{11}, C_{17}, C_{19}, C_{21} and C_{23}; of these the C_{21} homologue was most abundant. They were found only in BFMN-870 and BFMN-805, with the greater abundance in BFMN-870.

This fraction contains several sterol compounds and in all samples 24R-ethylcholest-5-en-3β-ol (β-sitosterol) and 24R-ethylcholestan-3β-ol (3-stigmastanol), are present. 24R-methylcholest-5-en-3β-ol (campesterol) and 24R-methylcholestan-3β-ol (campestanol) are present in all samples except the top two (BFMN-870 and BFMN-805). The 4-methyl sterol, dinosterol is also present in two of the samples (BFMN-977 and BFMN-957). Other compounds present in one or more of the samples are friedelan-3-one (BFMN-977 and BFMN-957) and homohopan-30-one (BFMN-994, BFMN-977, BFMN-957 and BFMN-870; Fig. 5.5). Minor components were also identified as 24-ethylcholest-4-en-3-one (BFMN-977) and 5α-cholest-14-ene (BFMN-870). Quantification showed that the BFMN-870 sample from the peat has the highest total sterol content and BFMN-994 the lowest with 0.21% and 5.6×10^{-3}% of the TOC respectively.

Also present in this fraction is a group of hydroxy and ketonic compounds based on the androstane skeleton; some of these compounds are thought to have a 4-methyl group. The 4-methyl androstane compounds were only found in two samples (BFMN-977 and BFMN-957, showing a greater abundance in BFMN-957 with 0.66% of the TOC. The occurrence and possible sources of these compounds have been discussed in Chapter 4.

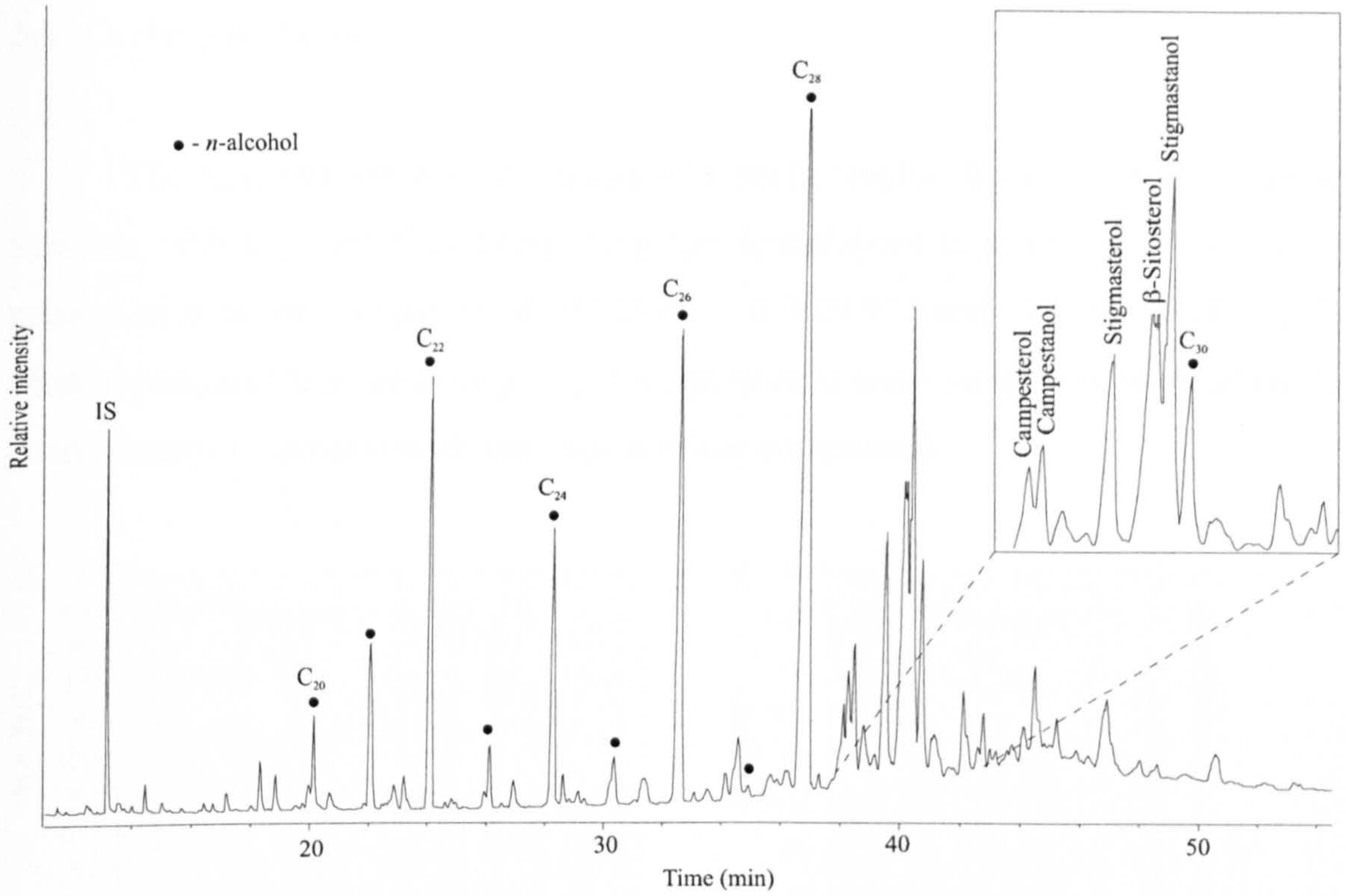

Figure 5.4 Partial gas chromatogram of the alcohol and steroid fraction as TMS ethers of peat from BFMN-984 at 984 cm depth; 50 m CP-Sil5CB, 50-200°C @ 12°C min^{-1}, 200-300°C @ 3°C min^{-1}, 300°C (20 min).

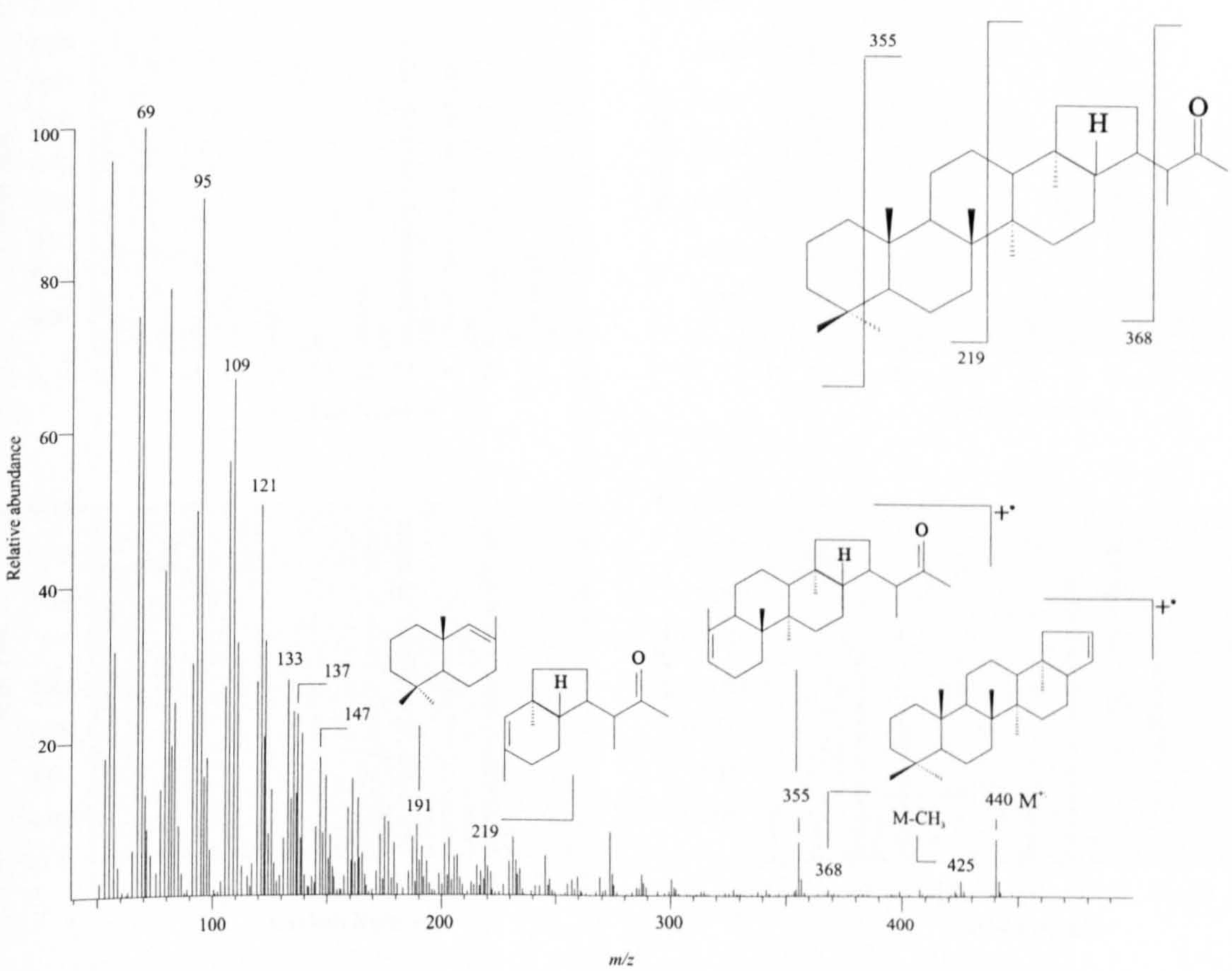

Figure 5.5 Mass spectrum of component identified as 22*R*-homohopan-30-one from peat from core BFMN at 870 cm depth. Assigned by comparison with library spectra.

5.6 Carboxylic Acids

The acid fraction contains saturated *n*-acids ranging from C_{10} to C_{32} over all samples, with $C_{24:0}$ and $C_{26:0}$ being the major homologues in most (Fig. 5.6). $C_{28:0}$ is present as a major component in BFMN-984, BFMN-977 and BFMN-957 (Fig. 5.7). Monounsaturated fatty acids (e.g. $C_{18:1}$) are present in some samples in small amounts. Also present are terpenyl acids but only as minor components.

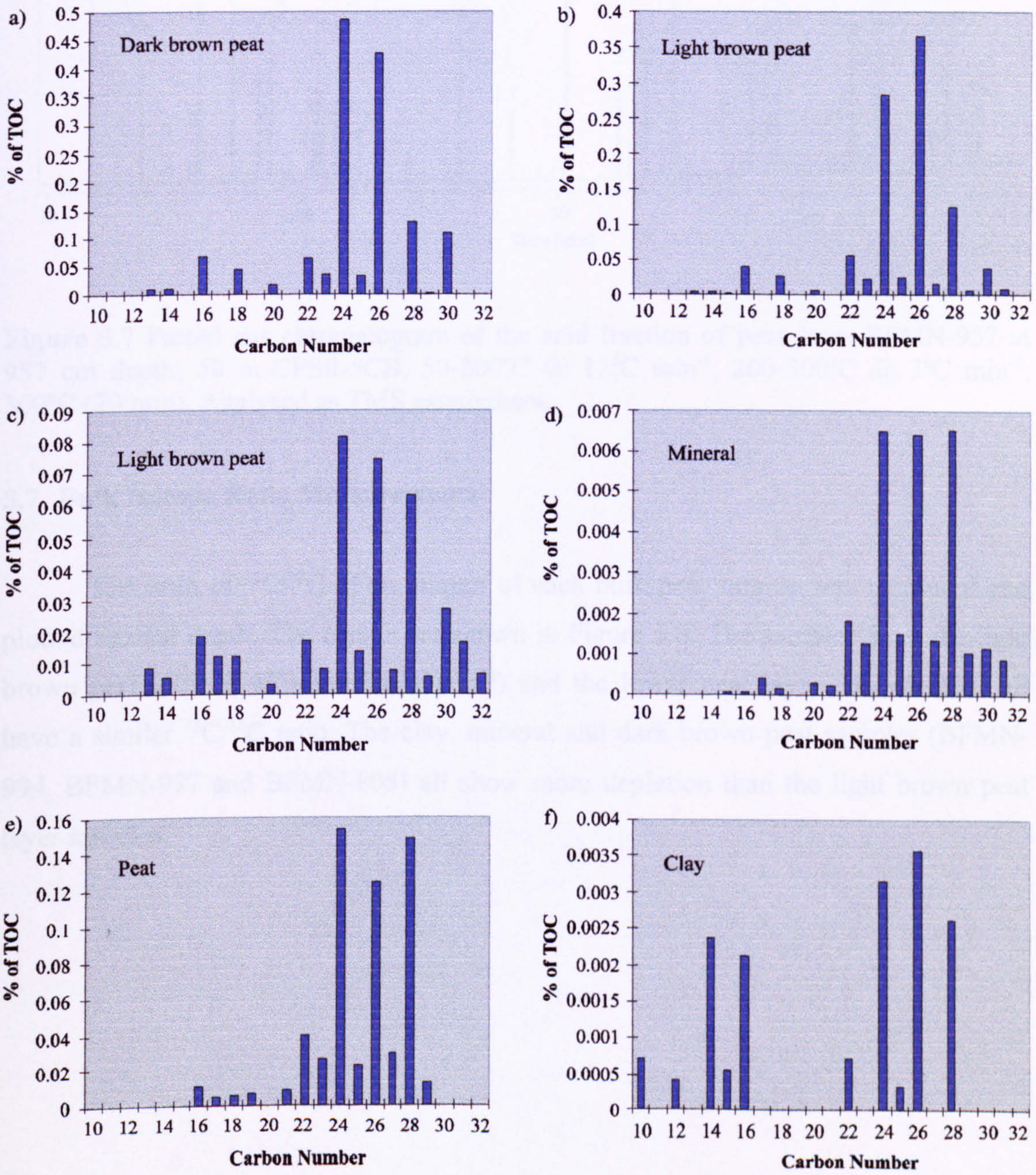

Figure 5.6 Histograms of distributions of *n*-acid homologues (% of TOC) from (a) BFMN-805, (b) BFMN-870, (c) BFMN-957, (d) BFMN-977, (e) BFMN-984 and (f) BFMN-994.

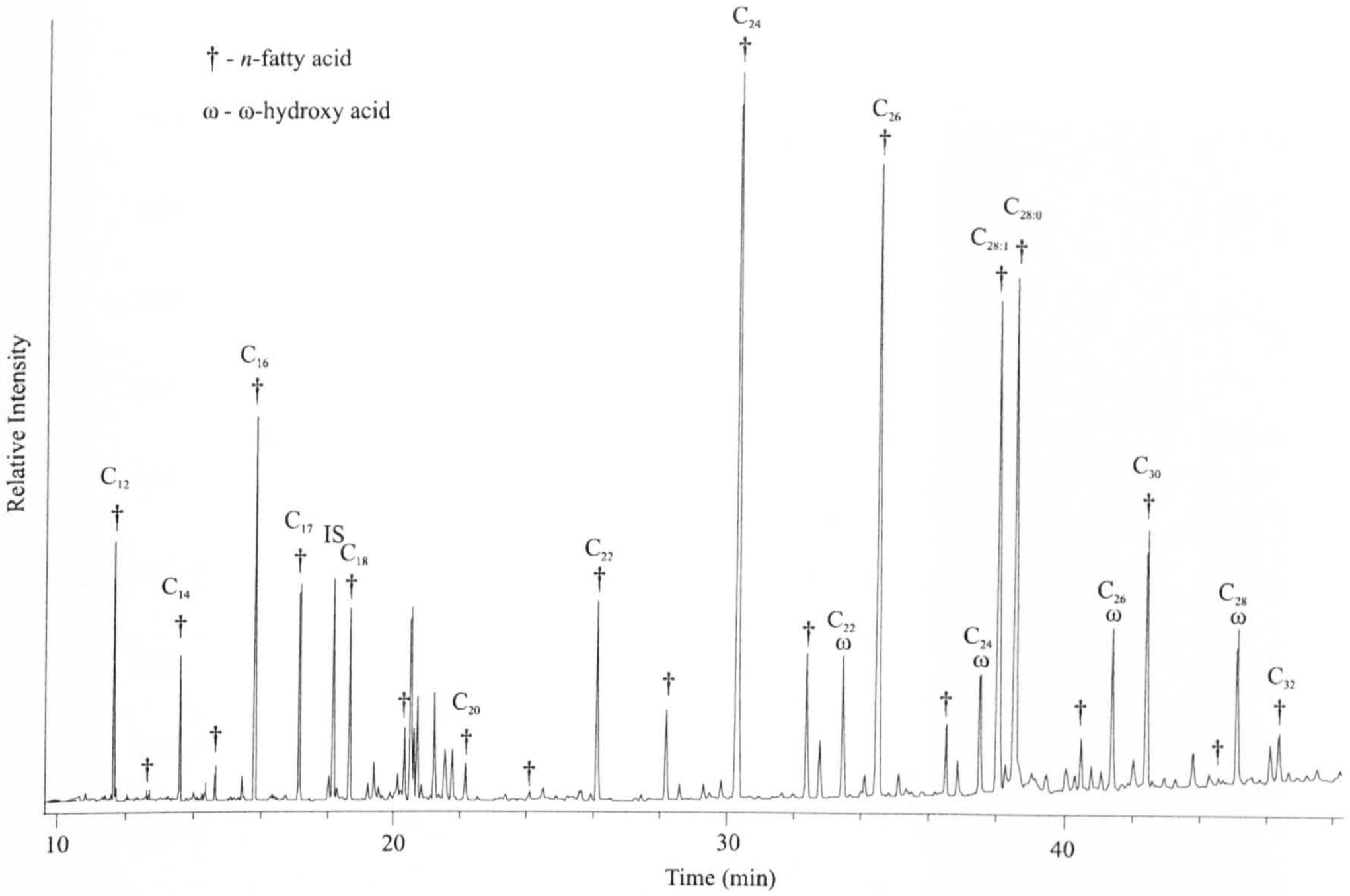

Figure 5.7 Partial gas chromatogram of the acid fraction of peat from BFMN-957 at 957 cm depth; 50 m CPSil-5CB, 50-200°C @ 12°C min^{-1}, 200-300°C @ 3°C min^{-1}, 300°C (20 min). Analysed as TMS ester/ethers.

5.7 Bulk Isotope Ratio Measurements

The ratio of $^{13}C/^{12}C$ of an aliquot of each bulk peat sample was measured and plotted against depth. The results are shown in Figure 5.8. The samples from the light brown peat (BFMN-870 and BFMN-957) and the lower peat layer (BFMN-984) all have a similar $^{13}C/^{12}C$ ratio. The clay, mineral and dark brown peat samples (BFMN-994, BFMN-977 and BFMN-805) all show more depletion than the light brown peat layer samples.

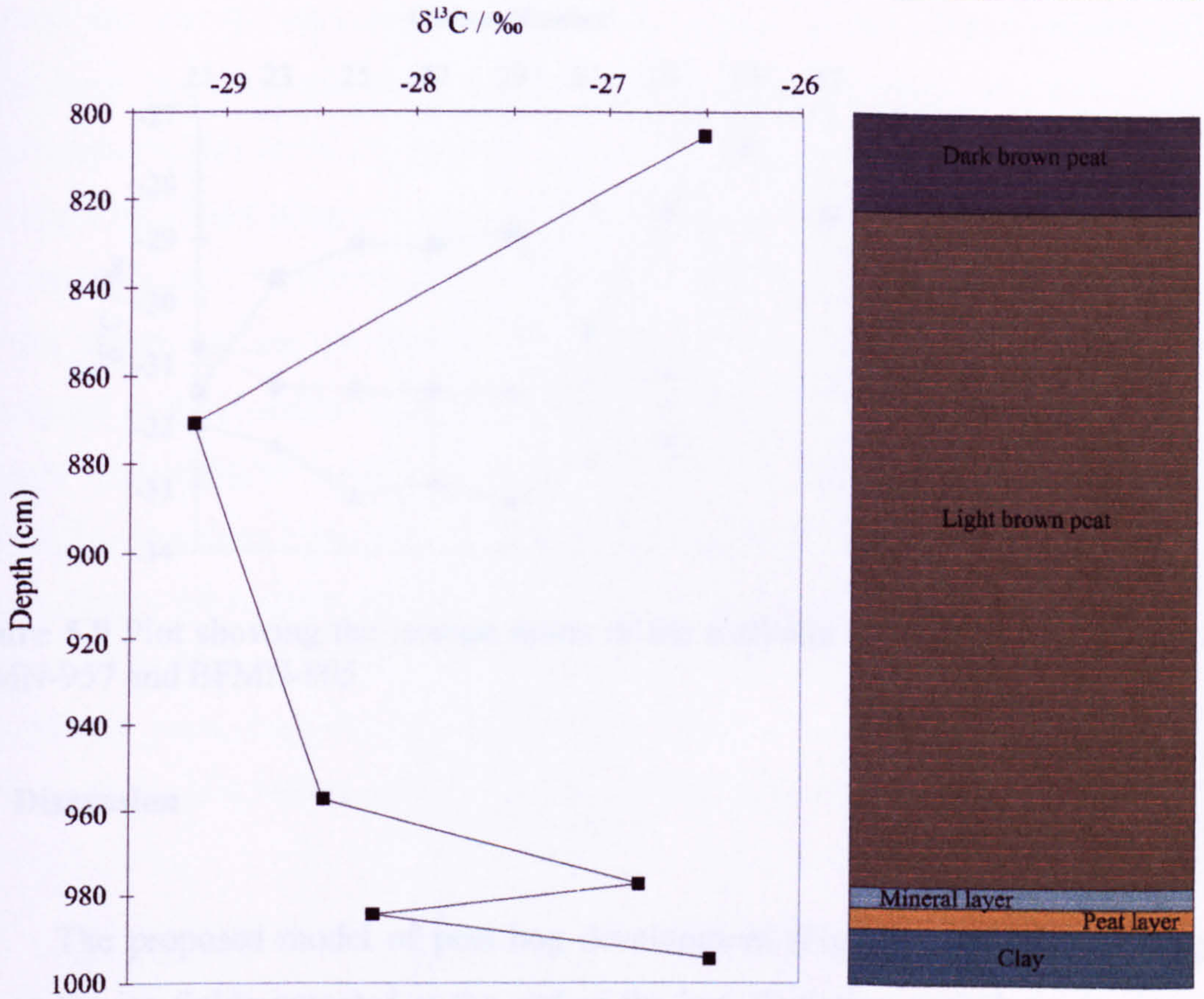

Figure 5.8 Plot to show the change in the bulk isotope ratio with depth.

5.8 irm-GC/MS of 984, 957 and 805 Hydrocarbons

The BFMN-957 hydrocarbon fraction contains unusually long chain *n*-alkanes (Fig. 5.2), it was decided to investigate the isotope ratio of each individual alkane to try to determine the inputs. Sample BFMN-984 is from a corresponding area of peat, i.e. just above a mineral/clay layer and shows a similar bulk isotope value (Fig. 5.8), and should therefore be a good comparison to sample BFMN-957. Sample BFMN-805 consisted completely of peatified remains and was expected to show a different isotope ratio distribution to that of the other two samples (BFMN-984 and BFMN-957). The results are shown in Figure 5.9.

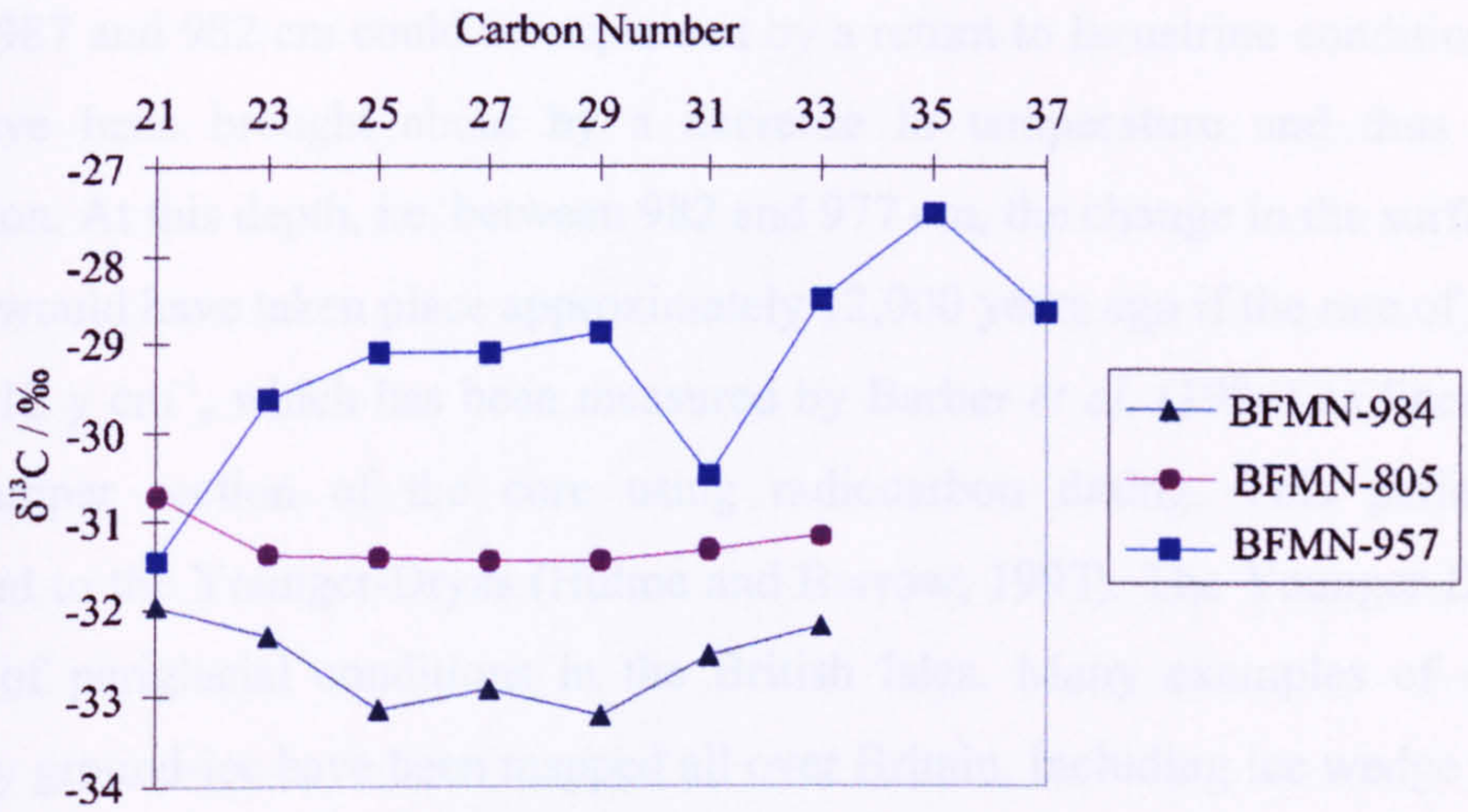

Figure 5.9 Plot showing the isotope ratios of the *n*-alkane homologues of BFMN-984, BFMN-957 and BFMN-805.

5.9 Discussion

The proposed model of peat bog development (Fig. 1.1; Foss, 1987) suggests that as the ice fields retreated at the end of the last glaciation period, a very irregular topography was produced. The undulating landscape had many deep hollows or basins which filled with water due to the poor drainage characteristics of the basin soils. As the climate gradually became warmer, a range of vegetation types grew in these lakes: reeds grew along the margins, water lilies in shallow bays and floating pondweeds on the deeper waters. When these plants died they only partially decayed and their remains accumulated at the bottom of the lakes. Over time the plant residues built up and the lake became shallower and gradually infilled. When fen peatlands formed and their depth increased to the level where the surface vegetation could no longer be influenced by mineral rich ground waters or surface waters, the type of vegetation changed to plant species, such as *Sphagnum* mosses, which grew and tolerated the low nutrient conditions present in rainwaters. The raised bog peats formed when the *Sphagnum* mosses partially decayed and accumulated in annual cycles over hundreds or thousands of years in the anaerobic waterlogged environment.

Therefore, if Bolton Fell Moss followed this model it would be likely that the bottom clay layer (BFMN-994) is composed of both material deposited during glacial retreat and that produced in the water column of the lake. The peat layer immediately above the clay (BFMN-984) may be the remains of plants that infilled from the lake edge and floating species on the surface of the lake. The mineral layer occurring

between 987 and 982 cm could be explained by a return to lacustrine conditions. These could have been brought about by a decrease in temperature and thus a partial reglaciation. At this depth, i.e. between 982 and 977 cm, the change in the surface of the peat bog would have taken place approximately 12,000 years ago if the rate of growth is taken as 12 y cm^{-1}, which has been measured by Barber *et al.* (1994) as linear growth for the upper section of the core using radiocarbon dating. This period would correspond to the Younger-Dryas (Hulme and Barrow, 1997). The Younger-Dryas saw a return of periglacial conditions in the British Isles. Many examples of structures formed by ground-ice have been mapped all over Britain, including ice wedge casts and pingos. Pingos are hillocks that develop when ground-water freezes to form a lens of ice which may be as much as 10 m thick. The ice pushes up the soil above it until the soil slips off the crest, exposing the ice beneath. This usually results in the ice melting, leaving a crater-like hollow with a raised rim (Hulme and Barrow, 1997).

5.9.1 Hydrocarbons

Examination of the distribution of the *n*-alkanes alone has proved to be rather non-diagnostic, the chain lengths indicate simply that the *n*-alkanes are generally from higher plants. The characteristic *n*-alkane distributions of 'pure' *Sphagnum* peat and 'pure' sedge peat illustrated by Lehtonen (1993) for instance, are not apparent in the results of this study. This is perhaps due to mixing of the *Sphagnum* and sedge signals which gives an average of the two, and also *n*-alkane contributions from other species present in the peat.

Isotope data of hydrocarbon fractions has proved to be more useful for the identification of organic matter inputs to sediments. Recent work by Nott (2000) on modern peat-forming plants from Bolton Fell Moss is used as a comparison with the results herein. Nott's work has shown the ^{13}C depletion to be higher in the modern plants than that in the corresponding humified remains in the peat. For *E. vaginatum* (a sedge species) the $\delta^{13}C$ values for the members of the homologous *n*-alkane series remain relatively constant within approximately 1‰, whereas for the *S. papillosum* the fluctuation in $\delta^{13}C$ values is much larger, the trend being for depletion to decrease as chain length increases (Fig. 5.10). Comparing the values with those for the samples in this study (BFMN-984, BFMN-957 and BFMN-805, Fig. 5.9), indicates that the BFMN-984 horizon is dominated by a sedge input of a slightly less depleted nature than the modern plant. The BFMN-805 horizon also appears to be dominated by a sedge

input, which correlates with macrofossil data from Barber *et al.* (1994) and once again the $\delta^{13}C$ values show a lower depletion than the modern plants and are also less depleted than in BFMN-984. The BFMN-957 horizon appears to contain a significant *Sphagnum* input, indicated by the trend for decreased depletion as chain length increases, although the effect is not as great as in the modern *Sphagnum*. Unfortunately, the data for comparison do not have isotopic values for the longer chain lengths, as the compounds were in insufficient abundance for reliable values to be obtained. Distributions of the longer chain length *n*-alkanes ($>C_{35}$) showing little odd-over-even carbon predominance, as found in BFMN-957, have previously been found in recent sediments (e.g. Nichols *et al.*, 1988) and been attributed to a variety of sources including contamination. However, there are several examples which suggest the possibility of a natural source. *n*-Alkane distributions lacking odd-over-even predominance in some freshwater dinoflagellates have been reported (Robinson *et al.*, 1987). Also many examples have been reported from marine environments, (e.g. Bieger *et al.*, (1997) who reported long chain *n*-alkanes with no odd-over-even predominance in spring bloom and sediment samples taken from Conception Bay, Newfoundland and Volkman *et al.*, (1998) who found long chain *n*-alkanes present in microalgae taken from the Huon Estuary, Tasmania). This seems to indicate that the long chain alkanes found in BFMN-957 originate from an algal source, which again supports the hypothesis that lacustrine conditions existed during this period.

The $\delta^{13}C$ values of the peat *n*-alkanes show a lower degree of ^{13}C depletion than the modern plant *n*-alkanes; this seems to be a result of the Holocene period due to changes in the concentration of atmospheric CO_2 during the period of development of the bog (White *et al.*, 1994). A higher concentration of CO_2 in the atmosphere resulting in more discrimination towards ^{13}C in carbon fixation in plants. This discrimination results in the biosynthesis of more depleted lipids.

These results appear to agree quite well with the visual observation of the section, and previous work done on peat. The macrofossil data indicate sedges dominated during deposition of sample BFMN-805 and this is consistent with the $\delta^{13}C$ values of the *n*-alkanes. Sample BFMN-984 shows sedge inputs from the distributions (high relative abundances of C_{23} and C_{25} *n*-alkanes) and $\delta^{13}C$ values of the *n*-alkanes, which agrees with the established model for peat bog formation (Foss, 1987), wherein sedge species at the edges of the lake infill forming the first peat layer. The *Sphagnum* input indicated for BFMN-957 from the *n*-alkanes seems to suggest this peat layer could have been formed by the remains of *Sphagnum* species floating on the water surface.

However, long chain *n*-alkanes (>C_{35}) also suggest other inputs are also present in this peat layer. The peat in the layer from which this sample (BFMN-957) was taken is highly humified and as there is no macrofossil data this indicates indirectly that there is a *Sphagnum* input as *Sphagnum* is humified faster than sedge species (Barber *et al.*, 1994).

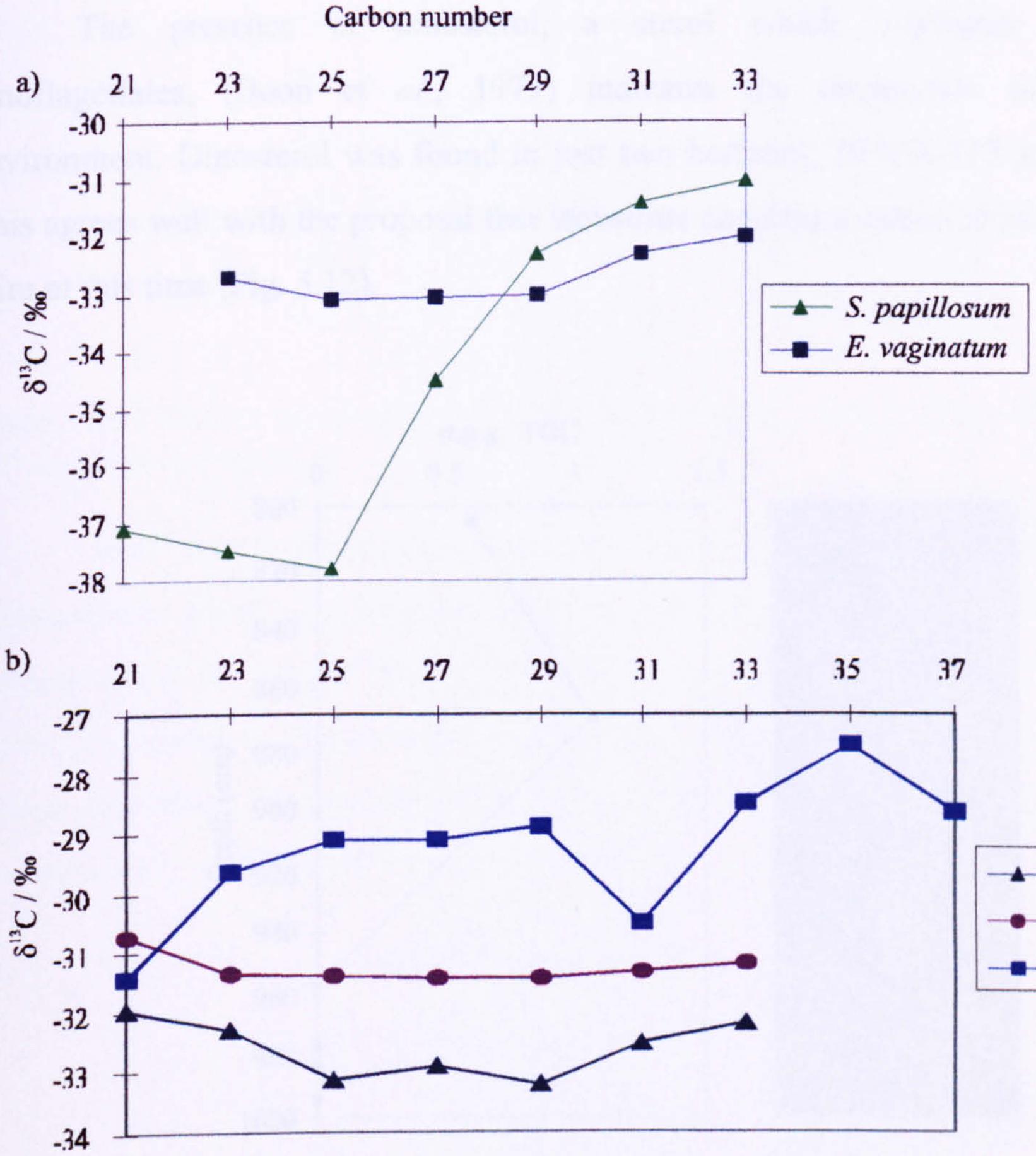

Figure 5.10 Plots to show the carbon isotope ratios of a) C_{21-33} *n*-alkanes from modern *S. papillosum* and *E. vaginatum* plants, (Nott, personal communication) and b) *n*-alkane homologues of BFMN-984, BFMN-805 and BFMN-957.

5.9.2 Alcohols and Steroids

The *n*-alkanol distributions show an even-over-odd carbon preference, which indicates higher plant inputs. However, without further information such as $\delta^{13}C$ values, the *n*-alkanol distributions are not indicative of plant species alone.

The *n*-alkyl resorcinols, which have been proposed as specific biomarker compounds of sedge (Nott, 2000), occur in two of the samples (BFMN-870, BFMN-805), but not in the others (Fig. 5.11). This clearly provides further evidence that these horizons have a sedge input. This would correlate with the Foss model (1987), which indicates that a *Sphagnum* layer (BFMN-957) will be followed by a sedge layer as the infill from the lake margin dominates the input.

The presence of dinosterol, a sterol which originates mainly from dinoflagellates, (Boon *et al.*, 1979) indicates the occurrence of a lacustrine environment. Dinosterol was found in just two horizons, BFMN-977 and BFMN-957. This agrees well with the proposal that lacustrine conditions occurred in this area of the mire at this time (Fig. 5.12).

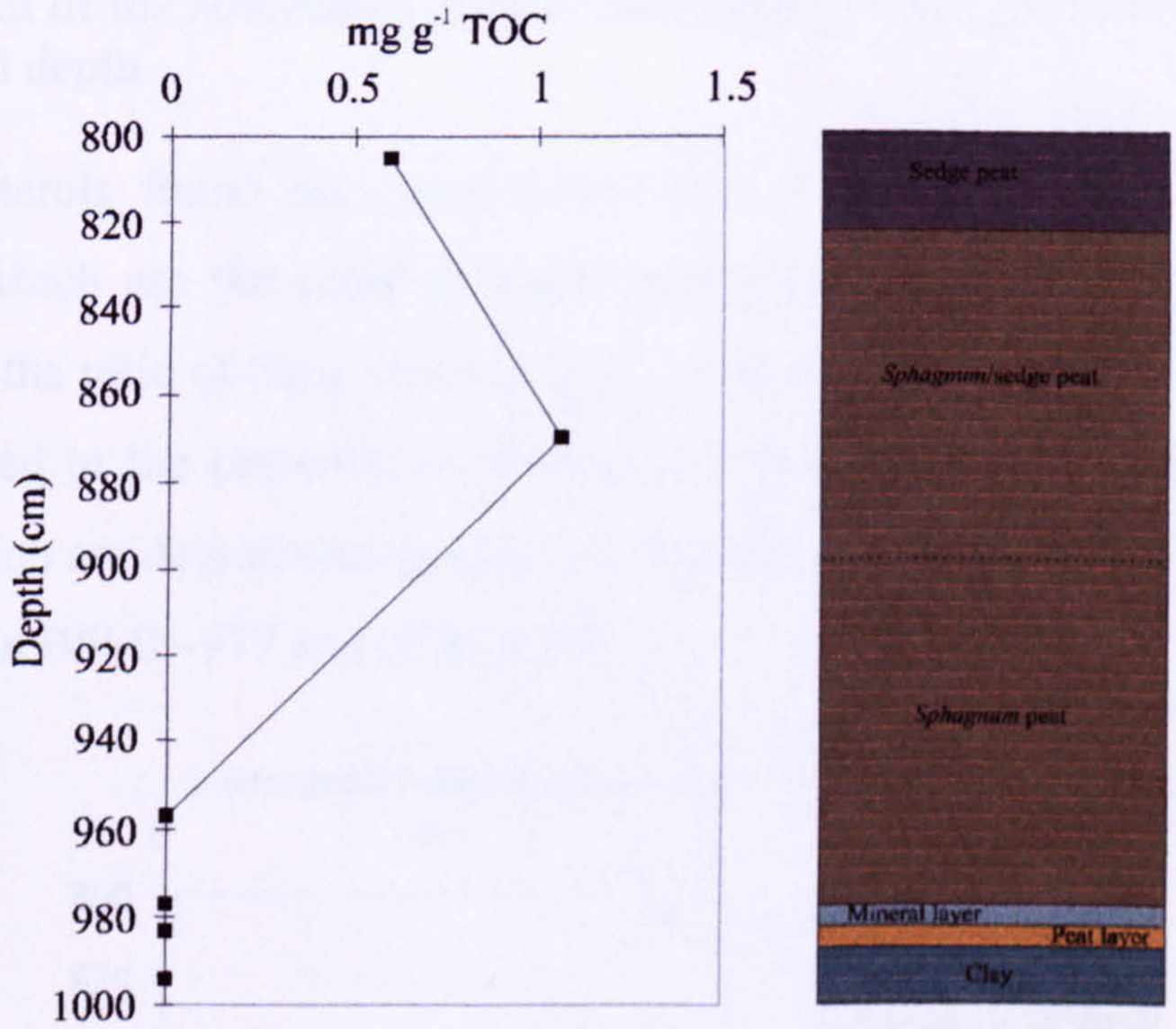

Figure 5.11 Plot of the abundance of total *n*-alkylresorcinols (mg g^{-1} TOC) in core BFMN between 805 and 994 cm depth.

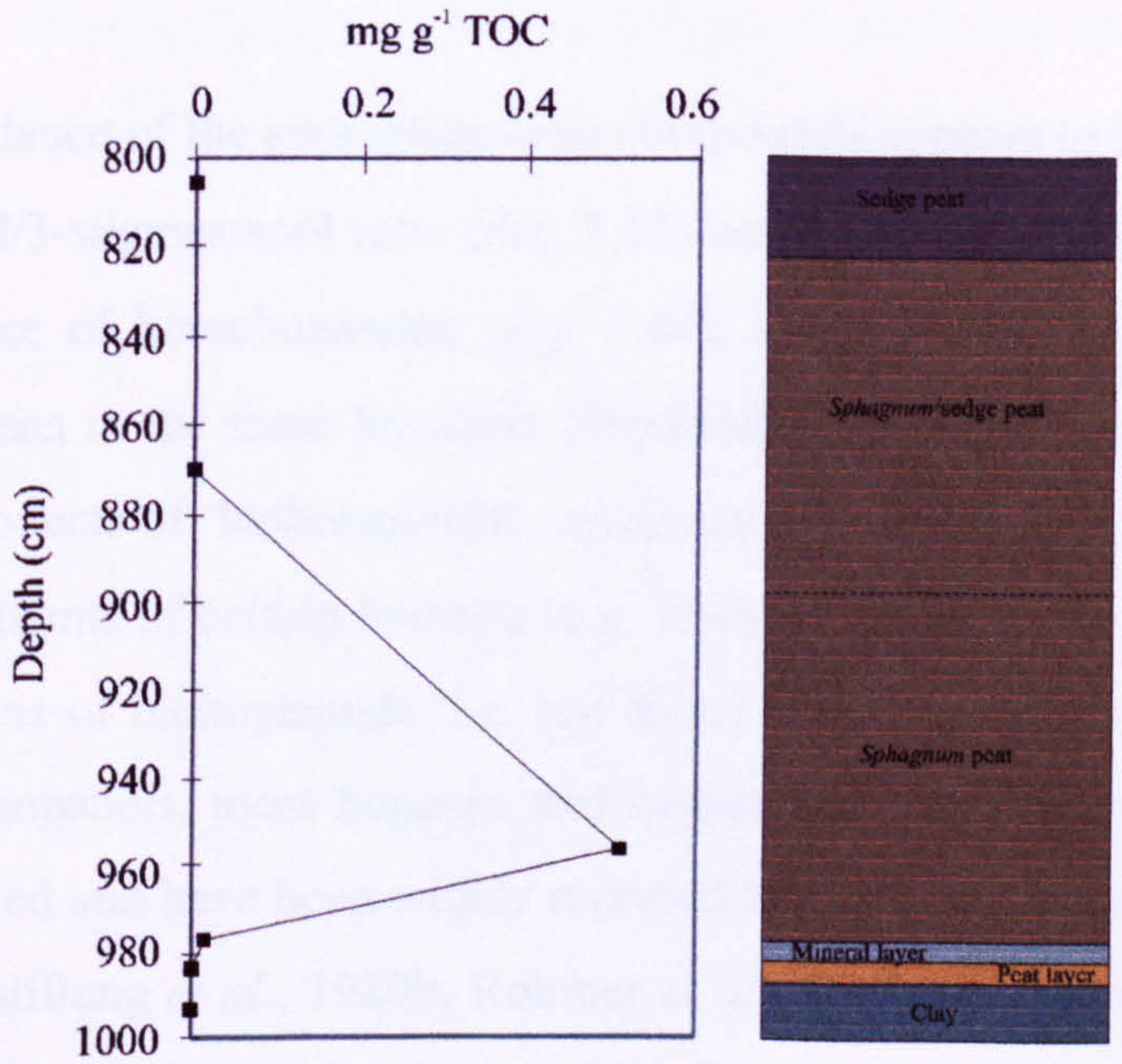

Figure 5.12 Plot of the abundance of dinosterol (mg g^{-1} TOC) in core BFMN between 805 and 994 cm depth.

Other sterols found are listed previously; these include β-sitosterol and 3-stigmastanol, which are the most abundant and present in all horizons investigated. Comparison of the ratio of these two steroidal compounds with depth (Fig. 5.13) can, it seems, be related to the presence or absence of other compounds such as androstane compounds which are degradation products of the sterols and stanols. These compounds are found only in BFMN-977 and BFMN-957.

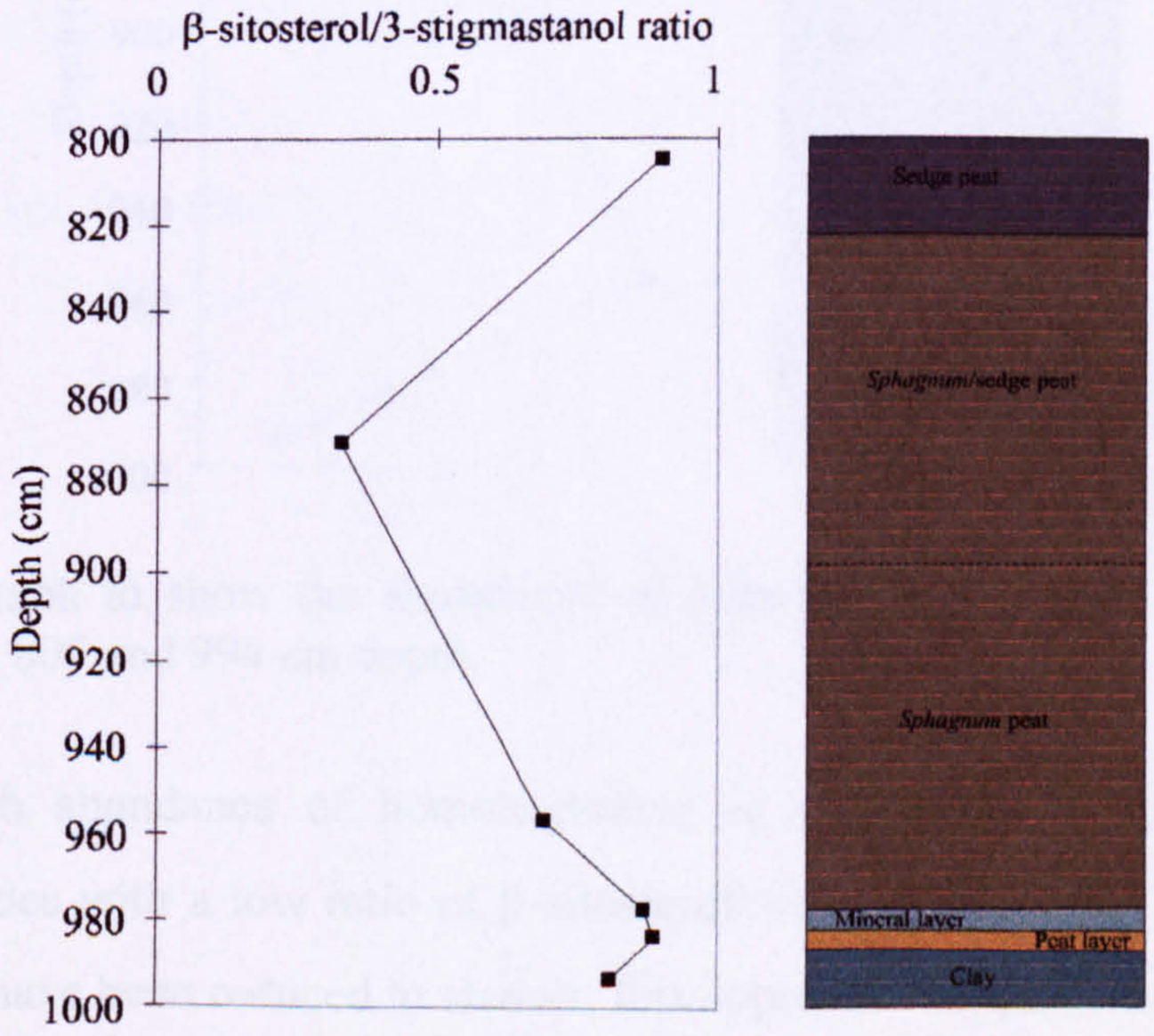

Figure 5.13 Plot of the ratio of β-sitosterol to 3-stigmastanol in core BFMN between 805 and 994 cm depth.

The abundance of the androstane-type compounds appears to be related not only to the β-sitosterol/3-stigmastanol ratio (Fig. 5.13) but also to the presence of dinosterol and the abundance of homohopanone (Fig. 5.14), in that elevated abundances of all compounds are seen in the same horizons. Hopanoids found in geological samples are the diagenetic products of 'biohopanoids', compounds predominantly biosynthesised as membrane constituents of certain bacteria (e.g. Innes *et al.*, 1997); 'geohopanoids' (the diagenetic products of biohopanoids; i.e. not direct products of biosynthesis), such as hopanoic acids, hopanols, most hopenes and hopanoidal aldehydes and ketones have been widely studied and have been widely reported in recent sediments (e.g. Dastillung *et al.*, 1980a; Dastillung *et al.*, 1980b; Rohmer *et al.*, 1980) and peats (Dehmer, 1993; Quirk *et al.*, 1984). The high abundance of the hopanone indicates a large bacterial population which in turn could result in increased bacterial activity at the time of deposition (Fig. 5.14).

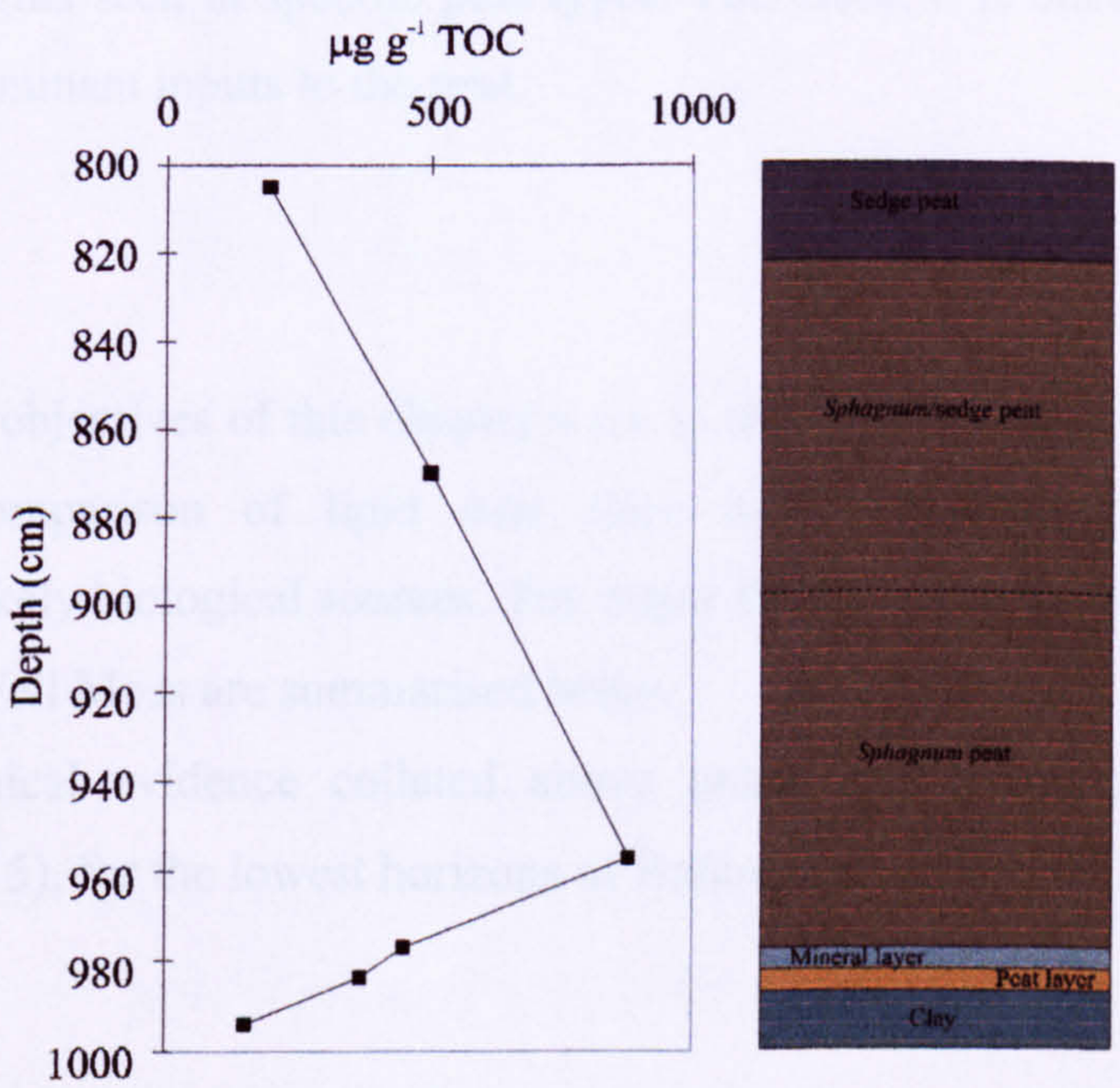

Figure 5.14 Graph to show the abundance of homohopanone (μg g^{-1} TOC) in core BFMN between 805 and 994 cm depth.

The high abundance of homohopanone in the BFMN-957 and BFMN-870 horizons coincides with a low ratio of β-sitosterol/3-stigmastanol, the latter indicating that the sterols have been reduced to stanols; this appears to support, indirectly, the idea that the bacteria suggested by the presence of homohopanone are responsible for the

reduction. It also coincides with the huge abundance of androstane-type compounds in the same horizon whose formation is also thought to be bacterially derived (Chapter 4).

5.9.3 Carboxylic Acids

Fatty acids are abundant in most organisms, and are often the most abundant lipid type in recent sediments. Sources of fatty acids include bacteria, microalgae, and higher plants; each of these types of organism has a distinctive fatty acid profile. However, some fatty acids such as palmitic and stearic acid ($C_{16:0}$ and $C_{18:0}$ respectively) are ubiquitous (Volkman *et al.*, 1998). The distributions of *n*-acids (Fig. 5.6) are bimodal in most samples, centred at C_{14}, C_{16}, C_{18} and C_{24}, C_{26}; this is due to contributions from various anatomical parts of the peat-forming plants and multiple sources (Lehtonen and Ketola, 1993). The distributions shown do not correlate with data from Lehtonen *et al.*, (1993) for other peats; they do not show the longer chain acids, i.e. $>C_{32}$ (C_{38} maximum detectable homologue); nor the same large dominance of certain chain lengths seen in specific peat types. Therefore, it is unclear if they reflect changes in the dominant inputs to the peat.

5.10 Summary

The main objectives of this chapter were to identify the stages of early peat bog formation by comparison of lipid data from humified material with the lipid distributions of likely biological sources. The major findings and proposed development stages of Bolton Fell Moss are summarised below.

The chemical evidence collated above indicates the following stratigraphy shown in (Fig. 5.15), for the lowest horizons of Bolton Fell Moss.

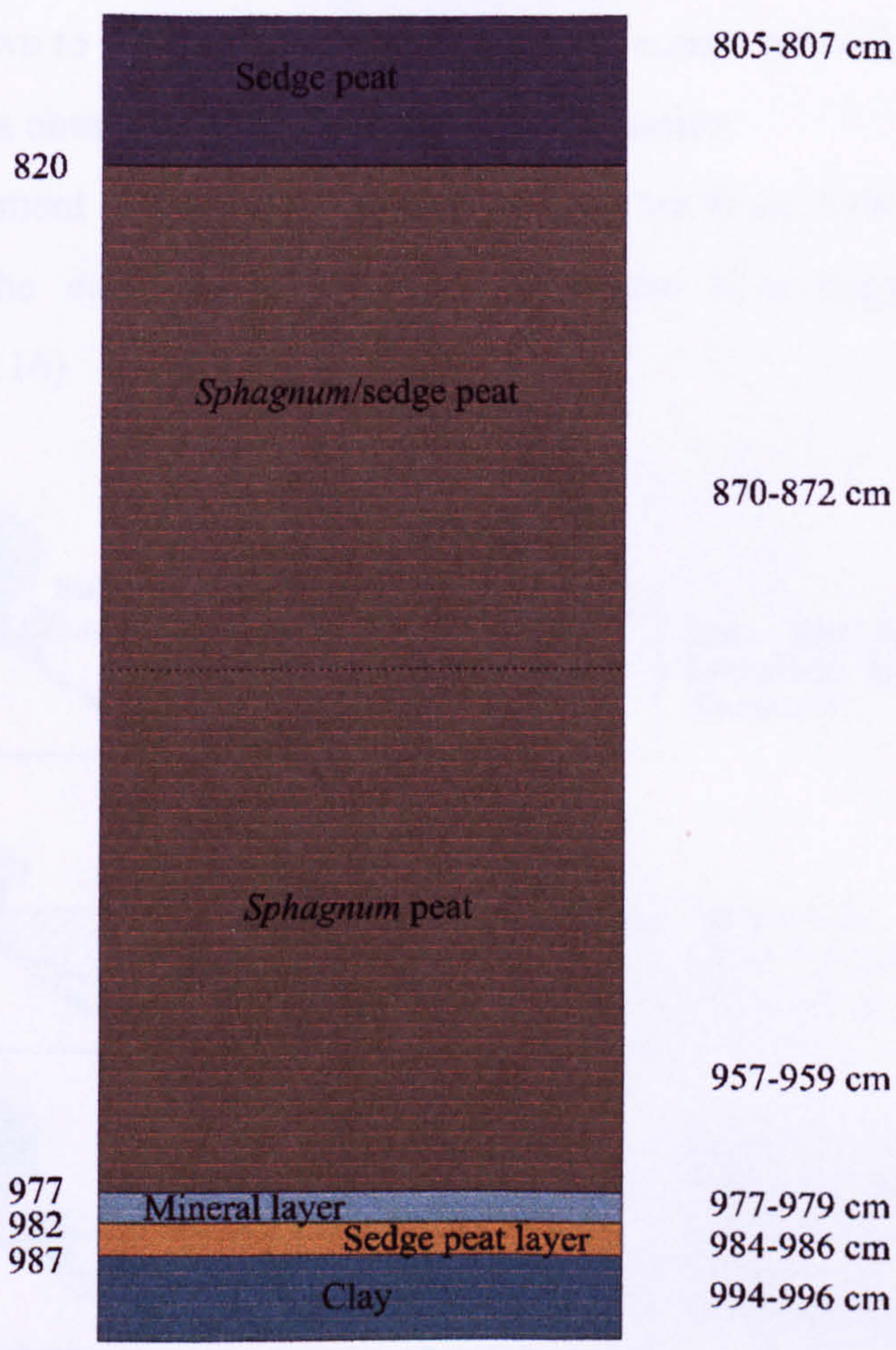

Figure 5.15 Compositional stratigraphy of core BFMN between 800 and 994 cm depth implied by chemical analysis.

Figure 5.15 indicates differences in the peat layers ascribed originally by observation (Fig. 2.7). The peat horizon between 987 and 982 cm is likely to be sedge dominated as indicated by the isotope data obtained from the hydrocarbon fraction (Fig. 5.9). Although resorcinols are not present in this layer, there may be preferential preservation of certain parts of sedge species infilling from the edges of the lake which do not contain resorcinols. The mineral layer is due to a return of a cold lacustrine environment unable to support higher plant growth, evidenced by the dinosterol and possibly also by the very long chain alkanes, as shown previously by Nichols *et al.* (1988). The layer between 977 and 820 cm shows two types of peat, in two indistinct layers. The lower section (BFMN-957) appears to be dominated by *Sphagnum* peat indicated by the isotope data obtained from the hydrocarbon fraction and low abundances of resorcinols. The upper section (BFMN-870) peat contains a high abundance of *n*-alkyl resorcinols which indicates a sedge input. Based on this evidence

it appears that this layer has both sedge and *Sphagnum* inputs. The uppermost horizon (BFMN-805) is shown to be sedge dominated by the presence of *n*-alkyl resorcinols and the isotope ratio data obtained from the hydrocarbon fraction.

The development of the lower section of the core from Bolton Fell Moss only partially follows the established Foss model. Below is a suggested model for development (Fig. 5.16).

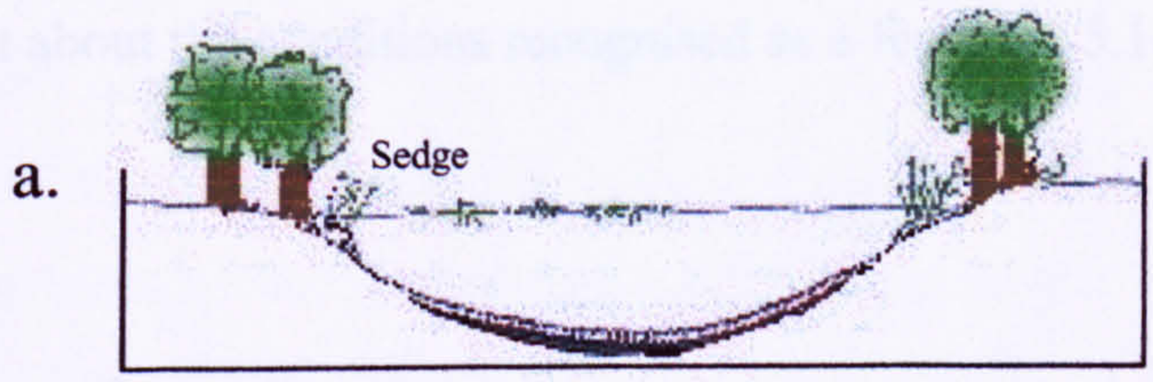

Lake - Samples 994 and 984. Lacustrine inputs such as dinosterol.

Sample 984. Sedge inputs revealed by $\delta^{13}C$ *n*-alkane values.

Samples 977 and 957. High dinosterol abundance - lacustrine environment. Depleted $\delta^{13}C$ *n*-alkane values - *Sphagnum* inputs.

Samples 957 and 870. *Sphagnum* and sedge inputs - high abundances of resorcinols and $\delta^{13}C$ *n*-alkane values reflecting both inputs.

Fen - Samples 870 and 805. Sedge inputs revealed by $\delta^{13}C$ *n*-alkane values and resorcinols.

Figure 5.16 Suggested model for the development of the lower horizons of Bolton Fell Moss.

The retreat of a glacier at the end of the last ice age left irregular topology and the hollows filled with water to create the so-called lake conditions. The peat formed at the bottom of the lake contains floating *Sphagnum* and sedge from the lake margins (Fig. 5.16a). Return of periglacial conditions in the Younger-Dryas led to ice formation and the cessation of peat deposition. Inputs during this time were from organisms in the

water trapped beneath the ice. This deposited a mineral layer comprised of debris in the ice dropping into the lake as the ice melted (Fig. 5.16b). The climate warmed again, the ice retreated and peat development began afresh; *Sphagnum*-dominated peat was formed due to the input of floating *Sphagnum* species on the top of the lake (Fig. 5.16c). The peat development continued with sedge species at the lake margins dominating the input as they grew in towards the centre of the lake (Fig. 5.16d). Sedge species filled in the lake and grew thicker until losing contact with the mineral-rich groundwater. This brought about the conditions recognised as a fen (Fig. 5.16e).

6. RADIOCARBON DATING OF PEAT AND SPECIFIC COMPOUNDS

6.1 Introduction

Carbon has three naturally occurring isotopes, ^{12}C, ^{13}C, and ^{14}C. The ratio of carbon isotopes in the atmosphere is ^{14}C:^{13}C:^{12}C, 10^{-12}:10^{-2}:1 i.e. ^{14}C is present in modern carbon as one part in a million million. Since they are not radioactive the amounts of ^{12}C and ^{13}C remain constant and therefore a measurement of the ^{14}C/^{12}C ratio can be used to estimate the age of an organic sample once the half-life of radiocarbon is known. The modern ratio, defined as that for 1950 AD, is also required, and the time elapsed for exponential decay T is given by

$$T = -\frac{T_{½}}{\ln 2}\ln\frac{A}{A_0} = -8033\ln\frac{a^{14}}{100}$$

where $T_{½}$ is the half-life of ^{14}C (Libby value = 5568 years);

A_0 the present day activity (as measured from an international standard);

A the measured activity of the sample;

$\frac{T_{½}}{\ln 2}$ = 8033 years, the mean lifetime of ^{14}C;

$a^{14} = \frac{A}{A_0}$ and is expressed as a percent.

Therefore a sample with a measured activity of 50% has a conventional age of 5568 years BP.

6.2 Fractionation of Isotopes

Although carbon isotopes are chemically indistinguishable, there is a tendency for the lightest isotope to be taken up preferentially in biological pathways. Therefore when radiocarbon dating a sample, a correction must be applied for 'fractionation' (kinetic isotope effect). It has been calculated that the % depletion of an isotope is proportional to the difference in atomic mass. Therefore the depletion of ^{14}C (with respect to ^{12}C) is double that of ^{13}C. In practice, a standard correction to the value of wood, ^{13}C/^{12}C (δ^{13}C) of -25‰ relative to the Vienna Pee Dee Belemnite (vPDB) standard (a marine carbonate with a δ^{13}C defined as 0‰) is made.

The conventional method of calculating a date is given below:

$$T = 8033 \ln \frac{1}{1+(\mathrm{D}(^{14}\mathrm{C}) \times 10^{-3}} \text{ years BP}$$

This implies a half-life of 5568 years and that 1950 AD is year zero

D the proportion of ^{14}C in a sample relative to ^{12}C and ^{13}C is defined

$$\mathrm{D}(^{14}\mathrm{C}) = \mathrm{d}(^{14}\mathrm{C})\text{-}(^{13}\mathrm{C} \text{ fractionation correction})$$

where $$\mathrm{d}(^{14}\mathrm{C}) = 1000 \times \left\{ \frac{A_{(\text{sample})}}{A_{(\text{standard})} \times F_{(\text{standard})}} - 1 \right\}$$

$A_{(\text{sample})}$ is measured activity, ^{14}C/^{12}C, of sample

$A_{(\text{standard})}$ is measured activity, ^{14}C/^{12}C, of standard

$F_{(\text{standard})}$ is the calibration factor for the particular standard, 0.950 for the National Bureau of Standards Oxalic Acid

The ^{13}C fractionation correction is normalised to -25‰ relative to vPDB.

The correction is assumed to be linear with mass difference

$$\delta^{13}\mathrm{C} = \left[\frac{(^{13}\mathrm{C}/^{12}\mathrm{C})}{(^{13}\mathrm{C}/^{12}\mathrm{C})_{\mathrm{PDB}}} - 1 \right] \times 10^3 \text{ ‰}$$

$$\therefore \text{ Correction factor} = 2 \times (\delta^{13}\mathrm{C} + 25)(1 + \frac{\mathrm{d}(^{14}\mathrm{C})}{1000})$$

Therefore the complete equation for D is:

$$\mathrm{D}(^{14}\mathrm{C}) = \mathrm{d}(^{14}\mathrm{C}) - 2 \times (\delta^{13}\mathrm{C} + 25)(1 + \frac{\mathrm{d}(^{14}\mathrm{C})}{1000})$$

6.3 Associated Errors with Radiocarbon Dates

The error term - When radiocarbon dates are quoted they usually contain an associated error. When the ^{14}C in a sample decays, it does so such that the half life is 5568 years (Libby value, correct value is 5730 years), but when measuring the decay over a short time interval the number of decaying atoms is not exactly predictable. The longer the time interval, the smaller the error, but this can lead to lengthy counting times. This is not such a problem when assessing the ^{14}C content by AMS as it is a direct measurement, but there are still the associated errors (e.g. limits of detection). The uncertainty of the measurement is given by the calculated standard deviation and is quoted as σ. Therefore the likelihood that the true radiocarbon result of a sample is

within the experimental result ±1σ is 68.3%, within ±2σ is 95.4%, and within ±3σ is 99.7%. When applied to a real sample with a radiocarbon determination of 1600±50 BP, this gives dates of 410-540 AD to 1σ and 340-600 AD to 2σ.

6.4 Calibration and Wiggle Matching

The radiocarbon date obtained from a $^{14}C/^{12}C$ measurement is quoted in radiocarbon years and to convert it to calendar years, the date must be corrected for fluctuations in the atmospheric ^{14}C concentration throughout time. The ^{14}C concentration in the atmosphere is affected by several natural factors (de Vries, 1958), and two anthropogenic effects, the use of fossil fuels and nuclear weapons testing.

Controls on the concentration of ^{14}C in the atmosphere:

I. *Geomagnetic field effect* - Variations in the Earth's magnetic moment cause variations in the number of cosmic ray particles that can reach the atmosphere. The greater the magnetic moment, the more that cosmic rays are deflected and less ^{14}C is produced in the upper atmosphere. Geomagnetic changes are the main cause of the long-term slow changes in ^{14}C production (Barbetti, 1980).

II. *Solar activity* - With high solar activity, intensification of the weak interplanetary magnetic field carried by the solar wind occurs and this deflects cosmic rays away from the Earth. These are short-term variations having periods of about 200 years. Sunspot cycles (every 11 years) linked to solar activity are only just detectable as changes in ^{14}C production, but the sunspot number does not correlate precisely with solar activity. Solar flares do not generally influence ^{14}C production, but may be important during periods of high solar activity (Costagnoli and Lal, 1980; Korff and Mendell, 1980; Stuiver and Quay, 1980).

III. *Climate* - The concentration of atmospheric ^{14}C is dependent on reservoir size and exchange rates between compartments. Therefore changes in ocean surface area and the extent of glaciation all serve to alter the atmospheric CO_2 concentration. The colder the climate, the lower the concentration of atmopsheric ^{14}C, as the solubility of CO_2 in water increases as the temperature drops (Siegethaler *et al.*, 1980).

IV. *Fossil fuel effect* - The vast increase in amounts of coal and oil being burnt for industrial purposes from the mid 19th century has significantly lowered the

atmospheric ^{14}C abundance, as ^{14}C depleted CO_2 is released into the atmosphere (Bowman, 1990).

V. *Nuclear weapons testing* - Since 1954, tests carried out in the upper atmosphere have created ^{14}C in the same regions as natural ^{14}C production, as the neutrons produced from such testing, in turn produce ^{14}C from interactions with ^{14}N. This has increased the ^{14}C abundance in present times (Bowman, 1990).

Calibration is performed by matching the measured ^{14}C age of a sample to that obtained from known age samples, such as varves and tree rings which occur annually. The latest calibration curve covers 24,000-0 cal y BP and is based on radiocarbon content of dendrochronologically dated tree rings, uranium-thorium dated corals and varve-counted marine sediment (Stuiver *et al.*, 1998). The dendrochronology that this curve uses is based on Irish Oak (Pilcher *et al.*, 1984), German Oak and pine records (Spurk *et al.*, 1998), which take the curve back 11,857 cal BP with a possible error of 20 cal years. This is further extended with uranium-thorium dated corals (Bard *et al.*, 1998; Burr *et al.*, 1998; Edwards *et al.*, 1993) back to 24,000 cal y BP. This involves a reservoir correction of 509±25 ^{14}C years over the 12,000-10,000 cal y BP interval due to the equilibrium between atmospheric CO_2 and mixed layer ocean bicarbonate. A floating marine varve chronology has also been used to strengthen the coral information over 14,500-11,700 cal y BP. The calibration curve has been further extended to 40,000 cal BP (Bard *et al.*, 1998) using two coral measurements but this points to increasing differences between ^{14}C and calibrated ages.

When dating sediment layers or other materials that are deposited annually it is sometimes possible to use the wiggles that occur on the calibration curve to achieve a more accurate date. This is done by taking a series of samples within a known interval and radiocarbon dating them. Once this is done it is possible to match the small wiggles that occur through the data set with those observed on the calibration curve.

6.5 Hard Water Effect

Another factor that can influence the ^{14}C content of dateable material is the hard water effect. This is a result of infinite age carbon dissolution which can result in living organisms taking up carbon with depleted ^{14}C content and causes the sample to appear

older than expected. It is so called because it is often associated with the presence of calcium ions from calcium carbonate. This can affect the radiocarbon dating of peat as although water is received directly from precipitation in the case of ombrotrophic bogs, surrounding minerals can dissolve into the resulting water.

6.6 Radiocarbon Dating of Peat

Before a sample can be dated using AMS (see Introduction, Chapter 1) it must be pre-treated to remove any contamination to ensure that only the ^{14}C content of organic carbon endogenous to the peat is measured. For samples such as peat the pre-treatment might involve the sample being crushed/dispersed in de-ionised water, then given hot HCl acid washes to eliminate carbonates and alkali washes (NaOH) to remove secondary organic acids. The alkali washes are followed by a final rinse to neutrality prior to drying.

Previous analyses of peat from Bolton Fell Moss have included bulk radiocarbon dates from 3 cores (Barber *et al.*, 1994). The calibrated results are shown in Table 6.1. These results show an almost linear accumulation rate of 15.4 y cm^{-1} over the first core, 11.1 y cm^{-1} over the second and 11.4 y cm^{-1} over the third. The higher accumulation in the upper core has been attributed to shrinkage of the peat bog due to drainage caused by peat cutting (Barber *et al.*, 1994).

For the study reported in this thesis, bulk peat samples (20 mg) from 39-40 cm, and between 420-448 cm depth at 3 cm intervals from core BFM(1) were submitted for pre-treatment and radiocarbon dating at the Oxford Radiocarbon Accelerator (Table 6.2). The latter samples cover a major transition in peat forming plants at Bolton Fell Moss and their bulk dates are used to compare with radiocarbon contents of individual lipids from the same samples

Table 6.1 Radiocarbon data for bulk peat samples. These dates were determined by conventional ^{14}C dating by NERC Radiocarbon Laboratory, East Kilbride (UK). nd - not determined (Barber *et al.*, 1994).

Depth (cm)	$\delta^{13}C$	RC Date (y BP)	Calibrated Range (y BP)
Core 1			
20-22	nd	355±35	307-509
26-28	nd	465±35	480-542
32-34	nd	635±35	545-671
38-40	nd	740±35	666-731
44-46	nd	865±35	691-916
40-42.5	nd	870±35	692-918
56-58	nd	985±35	795-967
Core 2			
63-65	-26.4	1380±40	1267-1347
91-93	-27.3	1550±45	1344-1540
100-108	-25.9	1270±35	1097-1284
134-138	-26.2	1695±45	1521-1716
178-182	-27.6	2435±50	2349-2729
200-207	-26.5	2575±35	2558-2761
235-238	-26.1	3460±45	3629-3848
260-268	-26.9	3370±35	3487-3697
290-294	-27.3	3915±50	4229-4521
330-334	-26.6	4320±50	4734-5031
370-374	-27.9	4580±40	5116-5444
400-407	-26.6	4675±35	5309-5563
439-442	-27.3	4900±45	5493-5729
485-489	-27.6	5315±50	5949-6279
493-500	-27.6	5315±35	5955-6263
Core 3			
400-408	-27.5	3725±45	3960-4240
500-508	-27.4	4575±45	5040-5200
560-568	-28.2	5860±45	6540-6760
620-628	-28.3	6335±50	7150-7420
680-688	-28.6	7005±50	7690-7880
740-748	-28.5	7660±45	8370-8550
800-808	-27.5	8470±50	9420-9550
860-868	-27.5	8840±45	9700-10160
920-928	-28.4	9165±50	10220-10430
970-978	-29.2	9305±45	10360-10600

Table 6.2 AMS radiocarbon data for bulk peat samples from core BFM(1).

Depth	Oxford No.	$\delta^{13}C$	% modern C	Calibrated Range(y BP)
39-40	OxA-9123	-24.1	96.8±0.5	430-150
420-421	OxA-9110	-25.0	58.1±0.4	5030-4850
423-424	OxA-9177	-24.8	60.8±0.3	4520-4410
426-427	OxA-9178	-24.0	61.1±0.3	4520-4300
429-430	OxA-9111	-24.9	58.0±0.3	5030-4860
432-433	OxA-9112	-25.0	59.6±0.3	4830-4580
435-436	OxA-9179	-24.5	59.8±0.3	4820-4550
438-439	OxA-9113	-26.1	60.2±0.3	4790-4440
441-442	OxA-9114	-25.8	57.7±0.3	5210-4870
444-445	OxA-9115	-25.2	59.5±0.4	4830-4620
447-448	OxA-9180	-24.4	60.4±0.4	4790-4420

It follows that after deposition if the peat remains undisturbed, horizons at greater depth will be older than those higher up. Therefore as some of the calibrated given in Table 6.2 do not reflect older dates with increasing depth, the correlation of single radiocarbon determinations to the calibration curve does not necessarily provide correct dates. Small variations in the calibration curve can result in several possible calibrated dates for certain radiocarbon determinations. Therefore, single radiocarbon dates, although statistically most likely to correspond with a calibrated date may actually lie outside the calibrated range when put into context with other data. As the peat horizons dated in Table 6.2 are in increasing depth order, peat at greater depth must be older than shallower horizons, as long as the peat remained undisturbed. Therefore, to place the calibrated dates in context of depth, wiggle matching can be performed. Wiggle matching puts constraints on the data based on known depositional factors. For radiocarbon dates for core BFM(1) at depth 420-448 cm it is assumed that the rate of deposition is relatively uniform and horizons are deposited in chronological order. Previous results from adjacent peat cores indicate an accumulation rate of between 11 and 14 y cm^{-1} (Barber *et al.*, 1994) and a similar accumulation rate is assumed for core BFM(1). Using these constraints it is possible to produce more reliable calibrated dates for BFM(1) peat horizons using wiggle matching.

Although BFM(1) peat samples at depth 420-448 cm were dated at an equal depth interval (3 cm) the exact time interval could not be established using existing data. Therefore a variable time interval of 37.5±8 y was imposed and the peat horizons were placed in chronological deposition order. Using these data and the variable sequence wiggle match facility provided by the Oxcal v3.3 program (Bronk Ramsey, 1995), the calibrated radiocarbon dates were matched to the calibration curve to find the best fit for the data. The results are presented in Figure 6.1.

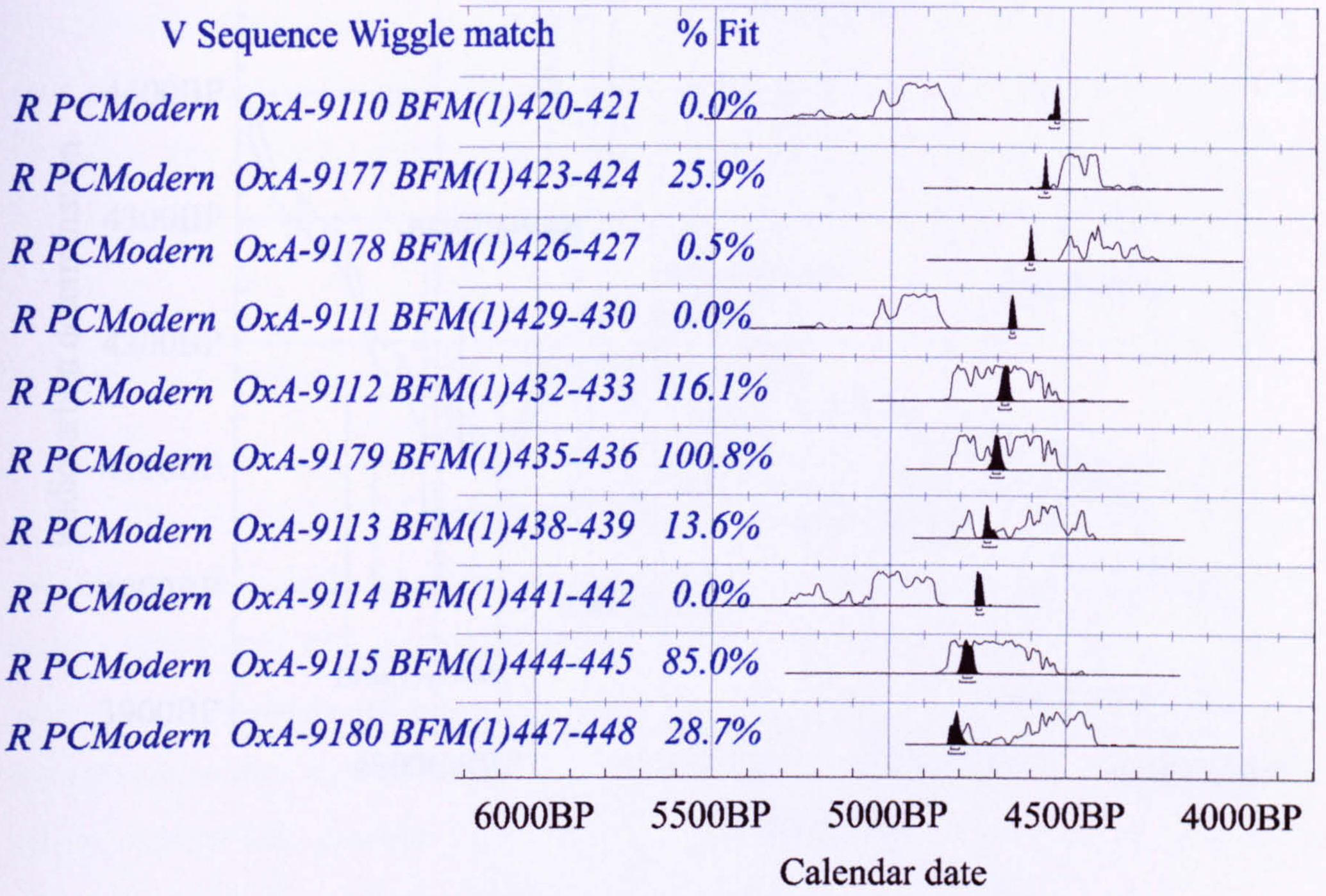

Figure 6.1 Calibrated distributions of bulk peat fitted using OxCal v3.3 with a variable sequence with gap = 37.5±8 y. Open curves represent calibrated radiocarbon date ranges based on single radiocarbon determinations. Filled curves represent best fit calibrated radiocarbon date ranges produced by wiggle matching. % Fit shows how well the wiggle matched data fits with original radiocarbon determinations.

From the calibrated results, three dates stand out as outliers, BFM(1) 420-421, BFM(1) 429-430 and BFM(1) 441-442. These three samples exhibit dates which suggest that the material they contain is older than expected when compared to the others. The presence of younger material in a peat horizon due to the intrusion of roots from above is common, however, the occurrence of older material within a horizon is not so easily explained. One possible explanation for the apparent age difference of these samples to the others could be the absence (or depletion) of younger material which is included in the other seven horizons, effectively increasing their age. The calibration curve with these results is plotted in Figure 6.2, the inner boxes shows a 1σ error and the outer 2σ.

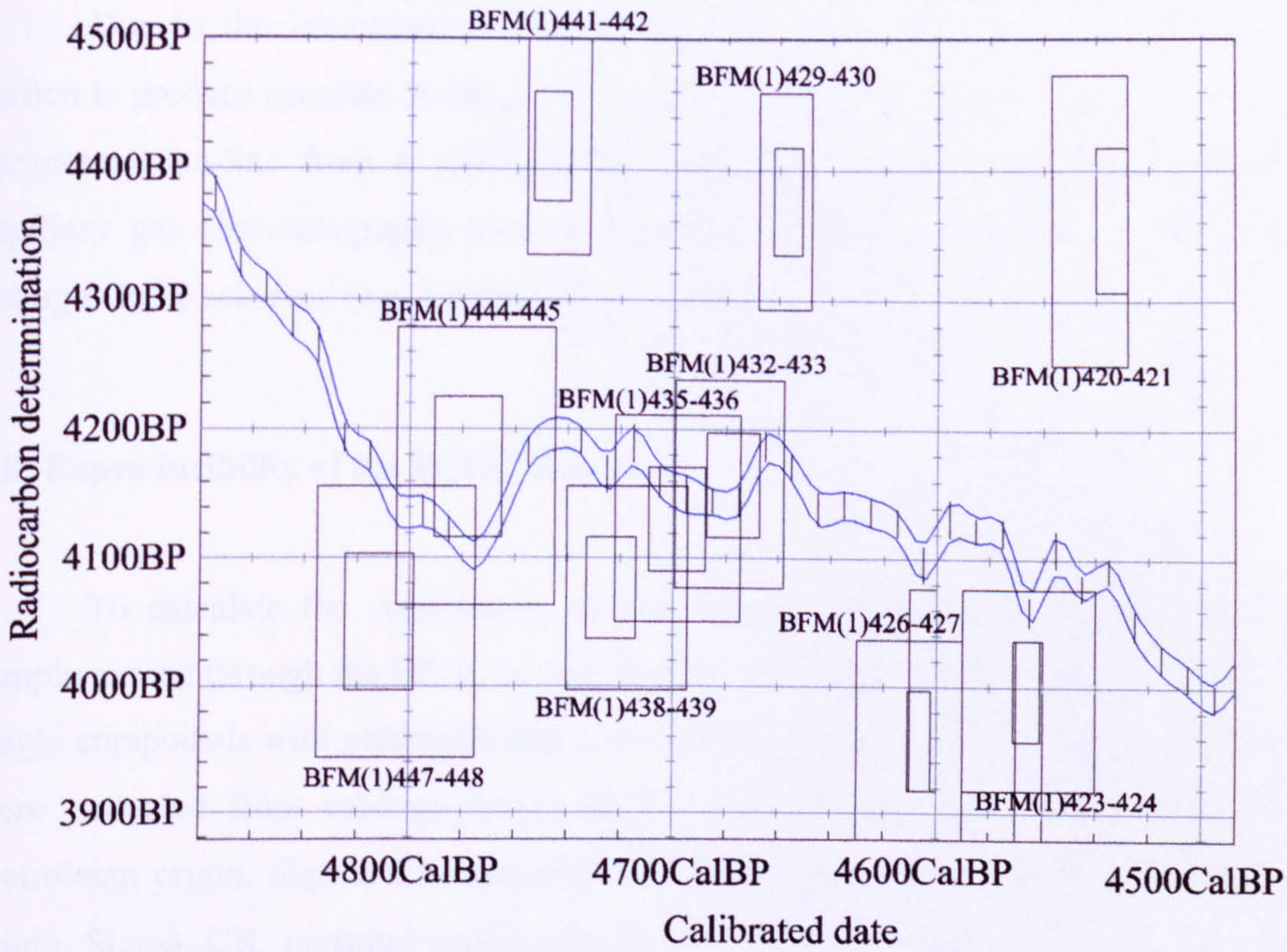

Figure 6.2 Calibrated distributions of bulk peat fitted to the calibration curve based on chronological and relatively uniform deposition (12.5±2.7 y cm^{-1}) parameters.

6.7 Preparative Gas Chromatography

The variations encountered in the radiocarbon determinations of the different components of sedimentary systems reaffirm the necessity to only date carbon indigenous to the horizon in question (Chapter 1.5). Therefore proper identification of the dateable material must be performed so that any contamination from extraneous sources can be eliminated. PCGC isolation of single lipid compounds in quantities sufficient for their radiocarbon determination by AMS have been shown to provide refined radiocarbon dates for samples of known age (Eglinton *et al.*, 1996).

Preparative gas chromatography has been used both as a method to obtain quantities of purified material where relatively difficult separations are involved (Zlatkis and Pretorius, 1971) and to provide quantities of single compounds for identification by off-line analytical techniques. Since the development of suitable interfaces, the identification of compounds arising at the end of a capillary column by techniques such as on-line GC/MS has become commonplace and the use of preparative capillary gas chromatography has declined.

Due to the limitations of AMS, which conventionally requires >100 μg of carbon to produce accurate results, it is currently not possible to radiocarbon date single compounds on-line from a capillary GC column. Therefore automated preparative capillary gas chromatography must be employed if compound specific radiocarbon dating is to be achieved (e.g. Eglinton *et al.*, 1996).

6.8 Reproducibility of the PCGC System

To calculate the contribution of contaminant modern and dead carbon to a sample passed through the PCGC system and the reproducibility of repeated injections, single compounds with predetermined radiocarbon contents were employed. *n*-Alkanes were extracted from cabbage leaves (111.3±1.4% modern) and added to C_{28}, C_{30} (petroleum origin, Sigma, UK, personal communication) and C_{29} *n*-alkanes (unknown origin, Sigma, UK, personal communication, 98.9±1.4% modern) in known quantities so that five 250 μl solutions could be made:

1.00 mg cabbage C_{29} modern alkane (36 × 2μl injections trapped)

1.00 mg Sigma C_{29} modern alkane (26 × 2μl injections trapped)

0.67 mg modern cabbage/0.33 mg Sigma C_{29} modern alkane (30 × 2μl injections trapped)

0.33 mg modern cabbage/0.67 mg Sigma C_{29} modern alkane (30 × 2μl injections trapped)

1 mg cabbage C_{29} alkane spiked with 1 mg C_{28} and C_{30} petroleum derived Sigma alkanes (46 × 2μl injections trapped)

These were then subjected to PCGC and the peak corresponding to the C_{29} alkane trapped. The trapped compounds were then transferred to tin capsules and submitted for radiocarbon dating. A 1 mg sample of unprepped Sigma C_{29} alkane was also submitted as a reference to determine carbon contamination of the PCGC system (Table 6.3).

Table 6.3 PCGC calibration samples corrected for $\delta^{13}C$ values. Cb = cabbage, S = Sigma, U - unprepped.

Compound / Oxford No.	$\delta^{13}C$	% modern	% Expected	C yield
100% Cb C_{29} alkane / OxA-X-21	-35.8	111.3±1.4	111.3	239 μgC
66.7% Cb C_{29} alkane / OxA-X-22	-35.5	107.1±1.4	107.2	186 μgC
33.3% Cb C_{29} alkane / OxA-X-23	-35.1	105.3±1.3	103.0	186 μgC
100% S C_{29} alkane / OxA-X-24	-34.8	97.8±1.3	98.9	132 μgC
U 100% S C_{29} alkane / OxA-X-25	-34.8	98.9±1.4	-	>385 μgC
C_{28} C_{30} spiked Cb C_{29} alkane / OxA-X-26	-35.8	107.5±1.3	111.3	354 μgC

These results have been corrected for the modern carbon content of the tin capsules which adds 2.15 μg of modern carbon to the sample and 0.75 μg for the combustion system giving 2.9±0.2 μg of modern carbon overall. This correction was based on previous radiocarbon determinations using this method and as calculated by the Oxford laboratory (C. Ramsey, personal communication). This correction is applied to all samples submitted in tin capsules and is denoted by OxA-X under the Oxford radiocarbon labelling system. Source information obtained from Sigma (UK) for the C_{28} and C_{30} alkanes found them to be petroleum derived and they are therefore expected to contain no radiocarbon.

C_{29} *n*-alkane (Sigma, UK) was passed through the PCGC system with GC oven conditions: 50°C (2 min)-250°C @ 20°C min^{-1}, 250-300°C @ 5°C min^{-1}, 300°C (5 min), total time 27.0 min. Six preliminary runs were completed to establish the retention time of the C_{29} peak and a further 26 runs were performed trapping the time window 16.4-17.6 min into trap 1. The contents of trap 1 were then transferred to a tin capsule and a further 1 mg of the alkane in another tin capsule were submitted for radiocarbon dating. The radiocarbon contents for these compounds are displayed in Table 6.3. The difference in percentage of modern carbon between the alkane passed through the PCGC system and submitted in a tin capsule is within the error associated with the AMS technique. This suggests that when collecting compounds in quantities greater than 100 μg, only negligible amounts (if any) of contamination are introduced from the PCGC system. However, it is possible that material with a similar percentage of ^{14}C as the alkane could be introduced in the system and not change the subsequent radiocarbon date. This is very unlikely and can be determined by repeating this experiment with a compound with a much lower ^{14}C content (Future work, Chapter 7.6).

The other three samples used to determine the replicability of the PCGC system (100% cabbage C_{29} alkane, 66.7% cabbage C_{29} alkane and 33.3% cabbage C_{29} alkane)

were collected under the same conditions with only the number of runs changing (26-36 runs). The radiocarbon determinations are plotted in Figure 6.3.

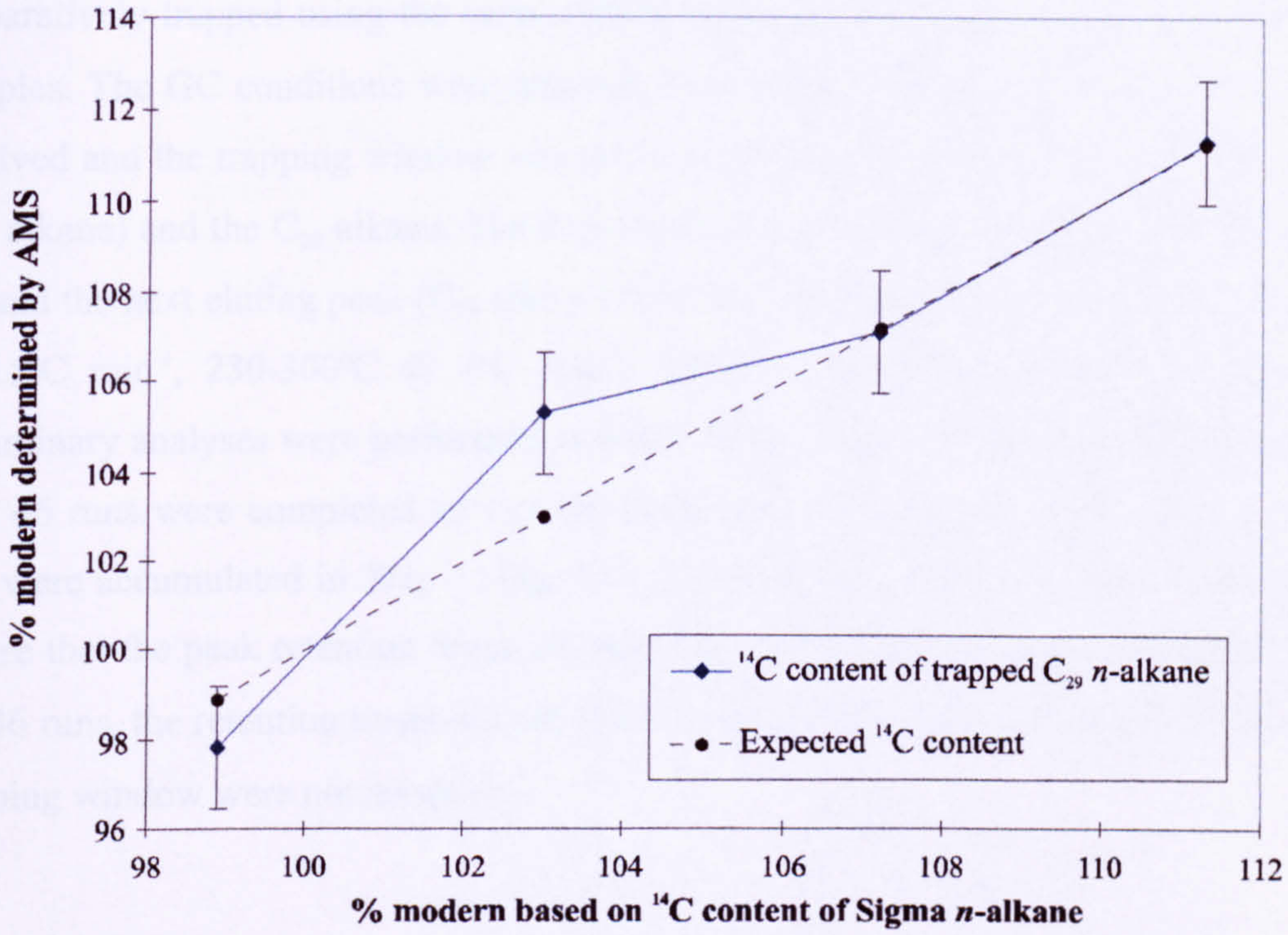

Figure 6.3 Graph showing experimental and expected percentage modern carbon content of prepped C_{29} alkane samples and therefore uncertainties associated with the PCGC process. Error bars contain only the uncertainty of the AMS system.

These results show that when >130 μg of carbon at about 100% modern radiocarbon content is trapped, any contaminant carbon contribution from the system has negligible effect on the radiocarbon determination. Errors associated with the preparation of the C_{29} alkane mixtures have not been included here and would be expected to contribute to the slight discrepancies seen between the radiocarbon dates and those predicted. Therefore when similar conditions to these are employed in the separation of single compounds there need not be any additional correction applied for the PCGC system. Also, this indicates the reproducibility of radiocarbon determinations of compounds subjected to the PCGC technique as the variation from the expected results is very low (<±0.5% modern C). However, to provide a better understanding of extraneous carbon inclusion from the PCGC system and other ^{14}C content altering factors, both smaller quantities of compounds and compounds with more contrasting ^{14}C contents should be isolated to provide a more universal calibration graph.

To assess the efficiency of the separation of a compound from others contained in a fraction, an aliquot containing 1 mg of C_{29} *n*-alkane from cabbage was mixed with 1 mg each of petroleum derived C_{28} and C_{30} alkanes and the C_{29} alkane was preparatively trapped using the same chromatography conditions employed for typical samples. The GC conditions were adjusted so that the peak to be trapped was >100% resolved and the trapping window was set to start halfway between the preceding peak (C_{28} alkane) and the C_{29} alkane. The trap window was then closed halfway between the C_{29} and the next eluting peak (C_{30} alkane). The GC conditions were 50°C (1 min)-230°C @ 15°C min^{-1}, 230-300°C @ 4°C min^{-1}, 300°C (3 min), total time 33.5 min. Six preliminary analyses were performed to establish the width of the trapping window and then 46 runs were completed so that the components eluting in the interval 21.1-22.6 min were accumulated in Trap 1 (Fig. 6.4). The progress of the runs was monitored to ensure that the peak retention times did not drift relative to the trapping window. Over the 46 runs, the retention times did not drift by more than ±1.6 s and adjustments to the trapping window were not necessary.

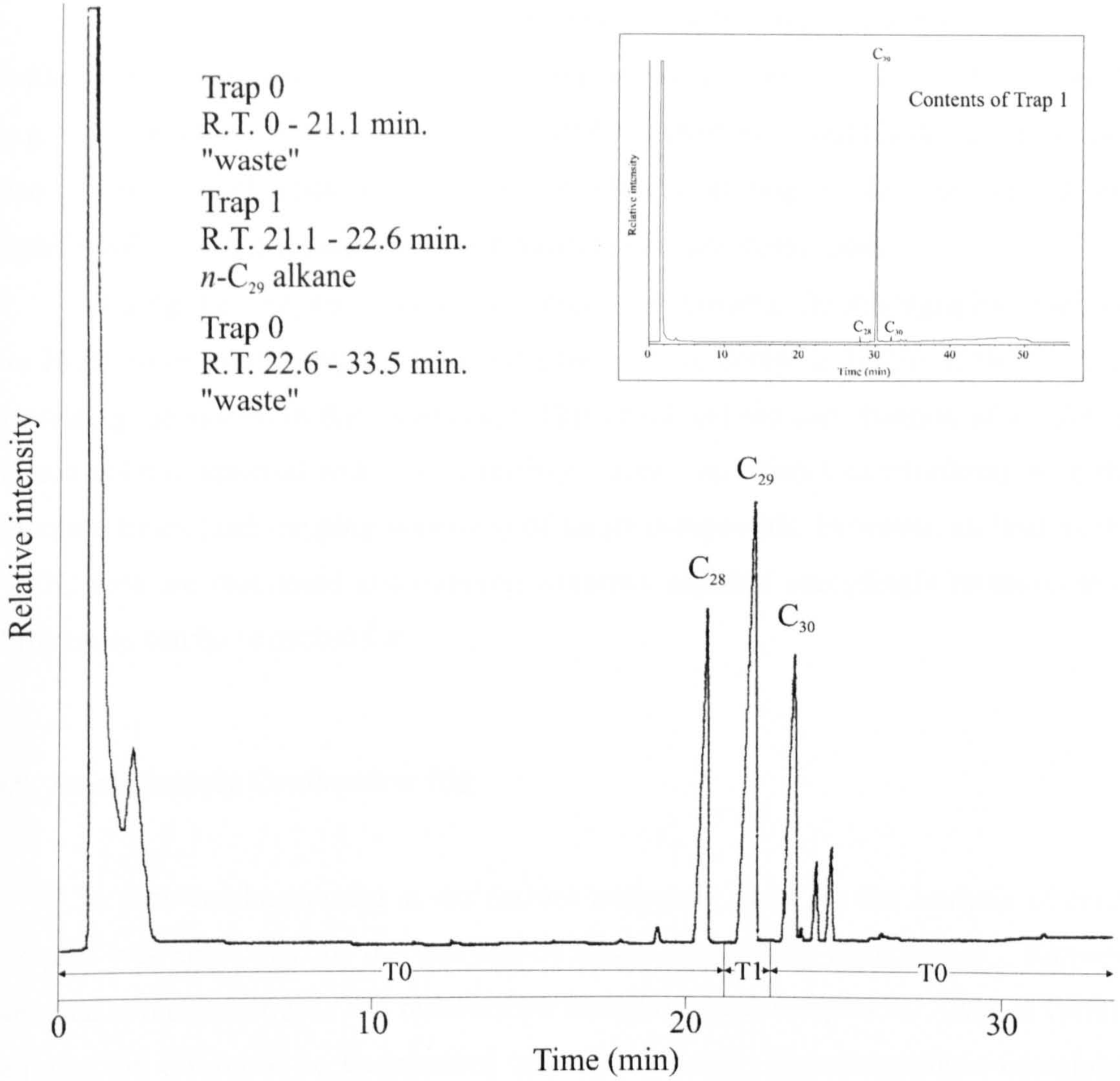

Figure 6.4 PCGC gas chromatogram of hydrocarbon fraction from cabbage with the addition of C_{28} and C_{30} petroleum derived alkanes Insert represents an aliquot of the contents of Trap 1 reanalysed under the same GC conditions.

The C_{29} alkanes separated from the purified hydrocarbon fraction from cabbage and that spiked with C_{28} and C_{30} alkanes were compared by GC and separation efficiency assessed. GC reanalysis of the contents of Trap 1 revealed that the C_{29} alkane was separated with a purity of 96% (based on detection area). This is reflected in the difference of the radiocarbon contents of pure cabbage (111.3±1.4% modern C) and spiked (107.5±1.3% modern C) C_{29} alkane where a 3.5% decrease is observed. Although the radiocarbon contents of the C_{28} and C_{30} alkanes were not measured for this experiment they are likely to have a significantly lower radiocarbon content than the cabbage alkane as they are from a petroleum source (Sigma, UK, personal communication).

Unpolluted sediment horizons for which this technique has been applied are unlikely to contain lipid components which have widely variable radiocarbon contents (e.g. Eglinton *et al.*, 1996; Eglinton *et al.*, 1997). Therefore, should isolated compounds also contain small relative quantities of closely eluting peaks this should not significantly alter the radiocarbon determination of target compounds.

During the analysis of naturally occurring sediments, chromatographic fractions are likely to be more complex, containing many more compounds than those prepared for testing the system in this experiment. This could add the complication of a build up of non-volatile material within the capillary column and therefore interfering with the retention times (and trapping windows) of target compounds. However, as long as the PCGC runs are monitored and trapping windows adjusted accordingly retention time differences can be corrected for.

6.9 Small Sample Combustion Rig

A new combustion rig at the Oxford laboratory used for the analysis of small samples was employed for the analysis of single compounds from peat (C. Ramsey, personal communication). The radiocarbon dating of small samples by AMS at Oxford requires the carbon to be transformed into CO_2. Usually, organic residues containing ~3-5 mg carbon together with a piece of silver wire in a vycor tube are transferred to a large quartz combustion tube which contains CuO. After being sealed the larger tube is evacuated (0.01 torr) and heated at 850°C for two hours. The CO_2 is released by oxidation of the carbon reacting with the CuO. The CO_2 gas is then dried through dry ice/alcohol traps and finally frozen out in a liquid nitrogen cold trap. The CO_2 is expelled from the trap into a storage vessel ready for introduction into the AMS system. However, where quantities are lower than 250 μg, as often seen with PCGC isolated samples, a scaled down version of the above combustion rig was employed. To determine if any extraneous carbon contamination occurs during combustion of the samples, several small samples containing known amounts of compounds were applied to tin capsules and submitted for radiocarbon dating using the small sample combustion rig. Solutions of modern cocoa butter and radiocarbon dead *n*-C_{18} alkane were made up and approximate quantities (in μg carbon) were applied to tin capsules. The samples were as follows: *n*-C_{18} alkane 50 μgC, 75 μgC, 100 μgC and 150 μgC. Cocoa butter 50 μgC, 100 μgC and 150 μgC (Table 6.4).

Table 6.4 Small sample combustion rig results, corrected for $\delta^{13}C$.

Compound	Oxford No.	$\delta^{13}C$	% modern	Carbon yield
n-C_{18} alkane 150	OxA-X-887-29	-33.2	13.0±0.9	140
n-C_{18} alkane 100	OxA-X-887-30	-33.2	9.3±0.4	81
n-C_{18} alkane 75	OxA-X-887-31	-33.2	13.0±0.8	43
n-C_{18} alkane 50	OxA-X-887-32	-33.2	21.4±1.1	29
cocoa butter 150	OxA-X-887-26	-26.0	182.9±1.5	160
cocoa butter 100	OxA-X-887-27	-26.0	184.0±1.2	93
cocoa butter 50	OxA-X-887-28	-26.0	171.0±1.7	53

These results were used to test the 2.9±0.2 μg of modern contamination correction used in samples of this nature. The 150 and 75 μg *n*-C_{18} alkane samples indicate that this correction is about right, but the 100 and 50 μg *n*-C_{18} alkane samples suggest that there may be some variable contamination in either direction. The 50 μg cocoa butter sample suggests that older than modern carbon contamination is also present. From these results it was decided to use the original correction of 2.9±0.2 μg of modern contamination, which should be accurate unless low yields (>50 μg carbon) are obtained.

6.10 Radiocarbon Dating of Specific Compounds

Ideally, a sample for radiocarbon dating should be from a known source and possess a high percentage of organic carbon. It should have obtained this carbon from a single CO_2 reservoir that is in equilibrium with the atmosphere and be in a well preserved state. Unfortunately, peat is a heterogeneous mixture, comprising the remains of many different plants and while maintaining a high level preservation, the exact origin of bulk peat cannot be always determined. Therefore the radiocarbon dating of bulk peat and its sub-fractions cannot be unequivocally linked to an original source with a great deal of certainty. However, on a molecular level the origin of precursors can be assigned and compound specific radiocarbon dating should tie ages to specific sources. Such compounds should therefore be: (i) well resolved on the gas chromatography column, (ii) from a known source within the peat, and (iii) be present throughout the sequence of samples being analysed in sufficient quantities to yield the required dating precision.

6.11 Scale-Up of Analytical Process

For the analysis of peat (*ca.* 0.6 g, Chapters 3-5), 10% of the TLE (~6 mg) obtained was separated using 500 mg aminopropyl Bond Elut columns and then further separated on small silica (0.6 g) columns. The compounds that were then identified using GC and GC/MS were, however, in too low abundance to be collected by PCGC and radiocarbon dated. Therefore the process was scaled up in order to collect compounds from each of the different classes for radiocarbon dating by AMS. The amount of peat that could realistically be obtained from a 1 cm section of core was measured and the process based on this amount of material. Aminopropyl Bond Elut (5 g) cartridges were used to separate the TLE (*ca.* 180 mg) from 1.8 g of peat into acid and neutral fractions. The neutral fraction was derivatised with BSTFA and analysed using HT-GC/MS. The mass chromatogram was then searched for the characteristic ions (*m/z* 117, 132 and 145) of *n*-fatty acids as TMS esters, as these are the most abundant acidic component found in peat lipidic extracts. As none of these compounds were detected it was determined that these Bond Elut cartridges were suitable for the efficient separation of acid and neutral components from quantities of peat required for the radiocarbon dating of single compounds.

To determine the amount of neutral compounds that could be efficiently separated using small silica columns, a mixture of compounds with varying polarity was produced. Ten compounds, *n*-C_{21}, *n*-C_{30} and *n*-C_{35} alkanes, naphthalene, hexadecyl octadecanoate, 10-nonadecanone, *n*-hexadecanol, *n*-octadecanol, dehydroiso-androsterone and stigmasterol (0.1 g of each compound), were chosen, dissolved in DCM/isopropanol (2:1 v/v, 20 ml), and sonicated. The solvent was then removed under a stream of nitrogen to obtain a homogeneous solid. An aliquot (0.1 g, i.e. 10 mg of each compound) of this was then taken and extracted using a small silica column (see Experimental chapter). The fractions were collected and analysed by GC to determine if there was any carry-over of compounds between fractions (Table 6.5). It was found that the fractions were separated efficiently using this column and, although the same solvent system as the original separations was used, the only observed difference was that it took longer for the solvent to pass through the column to complete the separation.

Table 6.5 Compounds separated using small flash column.

Fraction	Compounds Obtained
Hydrocarbon (3 ml Hexane v/v)	*n*-C_{21}, *n*-C_{30} and *n*-C_{35} Alkanes
Aromatic (1.5 ml Hexane/DCM 9:1v/v)	Naphthalene
Ketone/Wax Ester (5.5 ml DCM)	Hexadecyl octadecanoate, 10-Nonadecanone
Alcohol/Sterol (3 ml DCM/MeOH 1:1v/v)	*n*-Hexadecanol, *n*-Octadecanol, Dehydroisoandrosterone, Stigmasterol
Polar (2.5 ml MeOH)	None Present

6.12 Selection Criteria for the Radiocarbon Dating of Single Compounds from Peat

Suitable compounds for radiocarbon dating should reflect the age of their source and be directly related to the horizon in which they occur. Such compounds, therefore, should remain immobile within the peat when water levels rise and fall. A previous experiment to determine the solubility of lipids in water (Chapter 3) revealed that all lipids were only sparingly soluble and thus were good candidates for radiocarbon dating (Fig. 3.1).

A selection of compounds from 444-445 cm depth peat, chosen based on their high abundance, good separation on the GC column and presence throughout the core were trapped, *viz*:

$C_{24:0}$ fatty acid as methyl ester (FAME, Fig. 6.5)

$C_{26:0}$ ω-hydroxy acid as methyl ester acetate (Fig. 6.5)

$C_{28:0}$ ω-hydroxy acid as methyl ester acetate (Fig. 6.5)

C_{22} *n*-alcohol as acetate (Fig. 6.6)

β-sitosterol/stigmastanol as acetates

Compounds containing hydroxyl groups were derivatised using acetic anhydride and pyridine to yield acetates. The acetate derivatives were used in preference to the trimethylsilyl ethers that were produced for identification purposes, because the acetates were found to be stable during long-term storage and PCGC trapping and contain less added carbon than TMS groups. Trimethylsilyl ethers and esters are unsuitable for PCGC trapping since they are unstable, only remaining derivatised for about seven days at room temperature.

Table 6.6 Compound specific radiocarbon dates from BFM(1) 444-445 cm as acetates (except C_{24} FAME). * $\delta^{13}C$ values imposed at Oxford.

Compound	Oxford No.	$\delta^{13}C$	% modern	% purity	C yield
C_{24} FAME	OxA-X-887-21	-25.0*	60.4±0.6	88%	187 μg
C_{26} hydroxy ME	OxA-X-887-22	-25.0*	56.8±0.5	86%	>385 μg
C_{28} hydroxy ME	OxA-X-887-20	-25.0*	57.8±0.6	83%	>385 μg
C_{22} alcohol	OxA-X-887-23	-25.0*	71.9±5.4	92%	15 μg
β-sitosterol/stanol	OxA-X-887-24	-25.0*	58.8±0.5	78%	>385 μg

Due to the low abundance of *n*-alkanes in the peat (<180 μg g dry wt^{-1}), three hydrocarbon fractions were combined (443, 444 and 445 cm) and C_{23}, C_{31} and C_{33} *n*-alkanes were trapped out. The relative abundance of the alkanes in each sample was determined so that the differing contributions of *n*-alkanes from each sample could be taken into account. This resulted in a weighted mean depth for the origin of each alkane (Table 6.7).

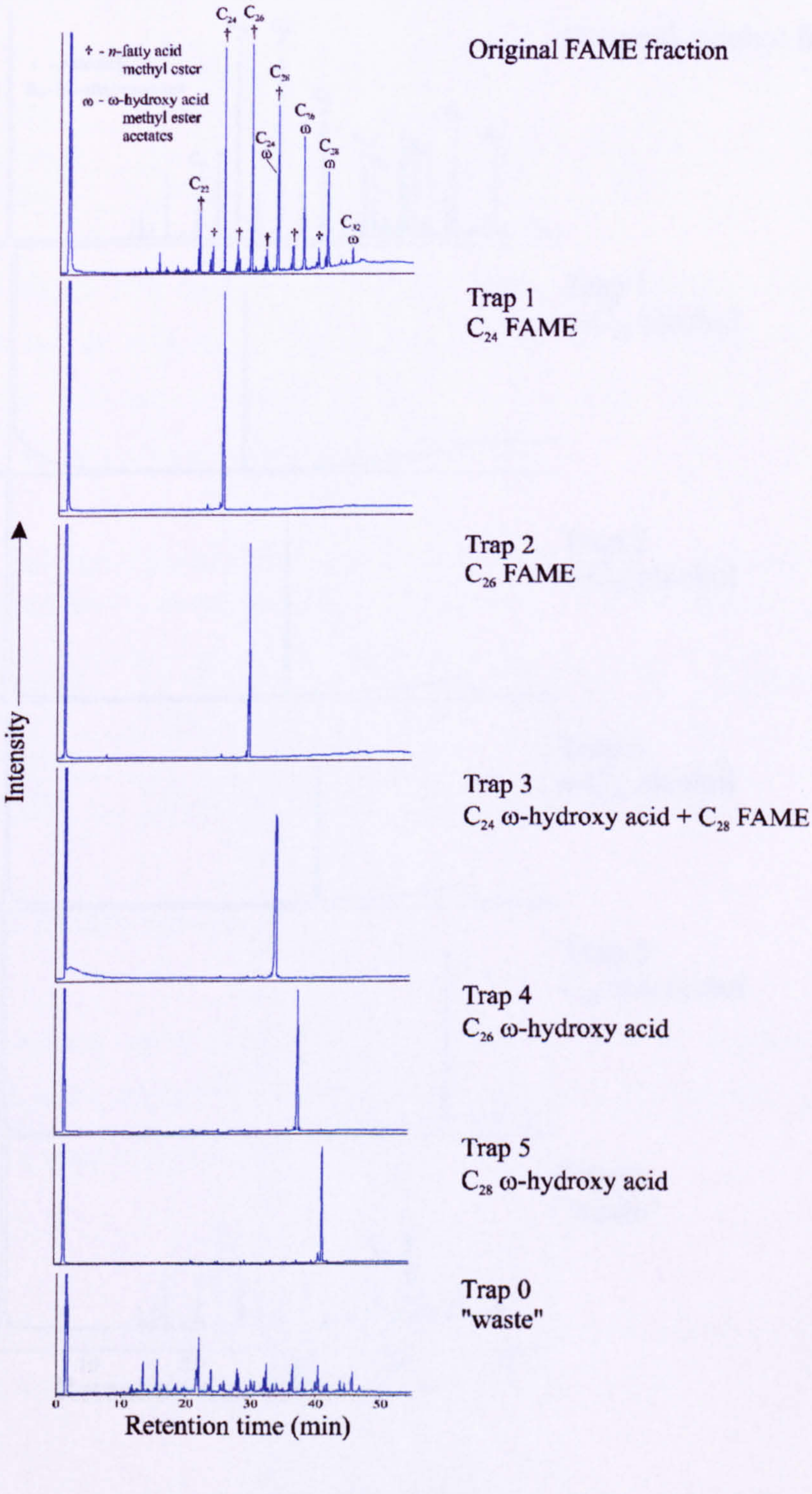

Figure 6.5 Gas chromatograms of carboxylic acid fraction and trapped products (the latter collected from 142 runs). The chromatograms (Trap 1 to 5) represent aliquots of the trapped component reanalysed under the same GC conditions in each trap. Trap 0 represents trapped compounds other than those isolated in traps 1 to 5. All compounds including derivatising agents were submitted for radiocarbon dating (Tables 6.6 and 6.9).

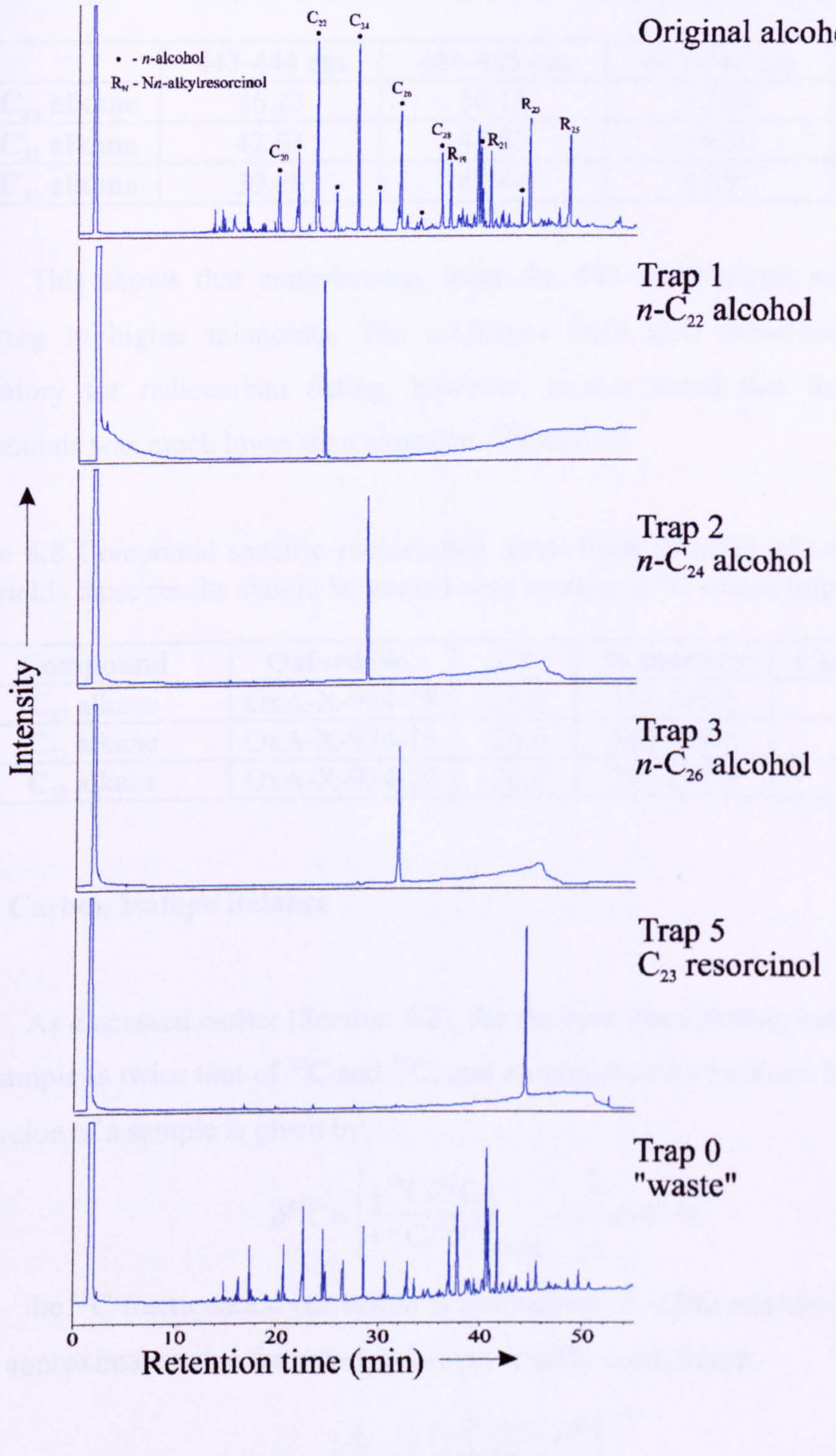

Figure 6.6 Gas chromatograms of alcohol fraction and trapped products (the latter collected from 60 runs). The chromatograms (Trap 1 to 5) represent aliquots of the trapped component reanalysed under the same GC conditions in each trap. Trap 0 represents trapped compounds other than those isolated in traps 1 to 5. All compounds including derivatising agents were submitted for radiocarbon dating (Tables 6.6 and 6.9).

Table 6.7 Percentage contributions of *n*-alkanes (relative to total *n*-alkanes) from different depths to radiocarbon dated samples, including average midpoint of depths.

	443-444 cm	**444-445 cm**	**445-446 cm**	**Midpoint**
% C_{23} alkane	36.23	50.13	13.64	444.3 cm
% C_{31} alkane	42.63	42.87	14.50	444.2 cm
% C_{33} alkane	39.68	42.41	17.91	444.3 cm

This shows that contributions from the 443 cm horizon were predominant, resulting in higher midpoints. The *n*-alkanes were also submitted to the Oxford laboratory for radiocarbon dating, however, it was noted that the yield of these compounds was much lower than expected (Table 6.8).

Table 6.8 Compound specific radiocarbon dates from BFM(1) 443-447 cm. * due to low yields these results should be treated with caution. $\delta^{13}C$ values imposed by Oxford.

Compound	**Oxford No.**	**$\delta^{13}C$**	**% modern**	**Carbon yield μg**
C_{23} alkane	OxA-X-924-18	-26.0	466.2±6.5	21
C_{31} alkane	OxA-X-924-19	-26.0	342.3±9.6	12*
C_{33} alkane	OxA-X-924-20	-26.0	293.1±7.8	14*

6.13 Carbon Isotope Balance

As discussed earlier (Section 6.2), the isotopic fractionation between ^{12}C and ^{14}C in a sample is twice that of ^{12}C and ^{13}C, and a correction factor must be applied. As the $\delta^{13}C$ value of a sample is given by:

$$\delta^{13}C = \left[\frac{(^{13}C/^{12}C)}{(^{13}C/^{12}C)_{vPDB}} - 1 \right] \times 10^3 \text{ ‰}$$

the ^{13}C fractionation correction is normalised to -25‰ relative to vPDB. As this is the approximate value for wood and is universally used, hence:

$$\frac{A_c}{A_m} = \left[\frac{1+(-25/10^3)}{1+(\delta^{13}C/10^3)} \right]^2$$

for the fractionation corrected ^{14}C activity of the sample (A_c) relative to the measured activity (A_m). This can be simplified to give an approximate age difference:

$$t_c - t_m \approx 16(\delta^{13}C + 25) \text{ years}$$

where t_c is corrected age and t_m is the measured age in years.

Therefore for every 1‰ difference from -25‰, an age correction of 16 years must be added or subtracted. However, the AMS at Oxford measures the $^{14}C/^{13}C$ ratio and not $^{14}C/^{12}C$, therefore a 1‰ difference will result in an age correction of only 8.2 years.

Similar to the $\delta^{13}C$ value of a compound, its ^{14}C content can be expressed as a $\Delta^{14}C$ value:

$$\Delta^{14}C = \left[\frac{^{14}C/(^{12}C+^{13}C)_{SAMPLE}}{^{14}C/(^{12}C+^{13}C)_{STANDARD}} - 1 \right] \times 10^3 \text{ ‰}$$

A modern oxalic acid standard is used and its $^{14}C/(^{12}C+^{13}C)$ ratio has been determined as 1.176×10^{-12}. For compounds that have been derivatised, a correction for the $\Delta^{14}C$ of the derivatising agent must be made. This can be done using an isotopic mass balance approach, where the $\Delta^{14}C$ of the derivatised molecule is adjusted by using a previously determined value of the derivatising agent and the equation

$$\Delta_B = \frac{\Delta_{BD} - (f_D \Delta_D)}{f_B}$$

Where Δ_B, Δ_{BD} and Δ_D, are the $\Delta^{14}C$ values for the underivatised (parent) compound, the derivatised molecule, and the derivatising carbon atoms, respectively and f_B and f_D are the fractions of parent carbon and derivative carbon in the derivatised molecule.

However, care must be taken not to neglect the $\delta^{13}C$ values of the separate carbon components, by just considering their $\Delta^{14}C$ values. Although the biggest error in the radiocarbon determination of a derivatised compound comes from the $\Delta^{14}C$ value of derivative carbons, a significant contribution can be from its $\delta^{13}C$ value, if it varies from the parent compound. Therefore a correction factor including all $\delta^{13}C$ values must be included when determining the $\Delta^{14}C$ of a parent molecule:

$$\frac{A_c}{A_m} = \left[\frac{1+(-25/10^3)}{1+\left(\delta^{13}C_{BD} - \left(\frac{f_D \delta^{13}C_D}{f_B \times 10^3} \right) \right)} \right]^2$$

Where $\delta^{13}C_{BD}$ and $\delta^{13}C_D$ are the $\delta^{13}C$ values of the derivatised molecule and derivative carbon atoms, respectively, and this can then be simplified to give an approximate age difference:

$$t_c - t_m \approx 8.2\left[\frac{\delta^{13}C_{BD} - \left(f_D \delta^{13}C_D\right)}{f_B} + 25\right] \text{ years}$$

This is the correction that must be made after the $\Delta^{14}C$ value has been determined using the isotopic mass balance, to account for any $\delta^{13}C$ differences between derivatising agents and parent molecules.

The radiocarbon contents of the lipids were adjusted to account for radiocarbon contributions from derivatising agents and $\delta^{13}C$ values of the lipids and the derivative carbon (Table 6.9) that they contain. The corrected results showing radiocarbon content of the underivatised lipids are contained in Table 6.10.

Table 6.9 Radiocarbon contents and $\delta^{13}C$ values of derivatising agents.

Reagent	Oxford No.	$\delta^{13}C$	% modern C
Acetic Anhydride	OxA-9174	-47.6	0.00±0.02
BF_3/Methanol	OxA-9175	-41.5	0.13±0.05

Table 6.10 Percentage modern carbon content of lipid samples from BFM(1) 444-445 after mass balance approach and age correction for $\delta^{13}C$ of derivatising agent.

Compound	Oxford No.	$\delta^{13}C$ ‰	% modern C
C_{24} fatty acid	OxA-X-887-21	-31.4	64.4±0.6
C_{26} hydroxy acid	OxA-X-887-22	-30.7	64.4±0.5
C_{28} hydroxy acid	OxA-X-887-20	-30.1	65.0±0.6
C_{22} alcohol	OxA-X-887-23	-29.3	79.4±5.4
β-sitosterol/stanol	OxA-X-887-24	-31.6	64.1±0.5
C_{23} alkane	OxA-X-924-18	-33.1	473.1±6.5
C_{31} alkane	OxA-X-924-19	-32.1	346.6±9.6
C_{33} alkane	OxA-X-924-20	-31.6	296.5±7.8

The radiocarbon determinations of β-sitosterol/stanol, C_{24} fatty acid, C_{26} and C_{28} hydroxy acid were calibrated using OxCal v3.3 (Bronk Ramsey, 1995) and the calibrated dates are shown in Table 6.11. The probability distributions of these compounds are also shown on Figure 6.7.

Table 6.11 Calibrated dates of lipid samples from BFM(1) 444-445. Figures in brackets show percentage certainty of true date lying within these dates.

Compound	Calibrated Date 1σ	Calibrated Date 2σ
β-sitosterol/stanol	2030BC-1990BC (9.2%) 1980BC-1870BC (44.7%) 1850BC-1810BC (8.3%) 1800BC-1770BC (6.0%)	2140BC-2080BC (4.8%) 2050BC-1740BC (90.6%)
C_{24} fatty acid	1950BC-1740BC (68.2%)	2130BC-2080BC (2.1%) 2040BC-1680BC (93.3%)
C_{26} hydroxy acid	1950BC-1750BC (68.2%)	2040BC-1730BC (92.0%) 1720BC-1680BC (3.4%)
C_{28} hydroxy acid	1880BC-1680BC (68.2%)	1960BC-1600BC (93.1%) 1570BC-1520BC (2.3%)

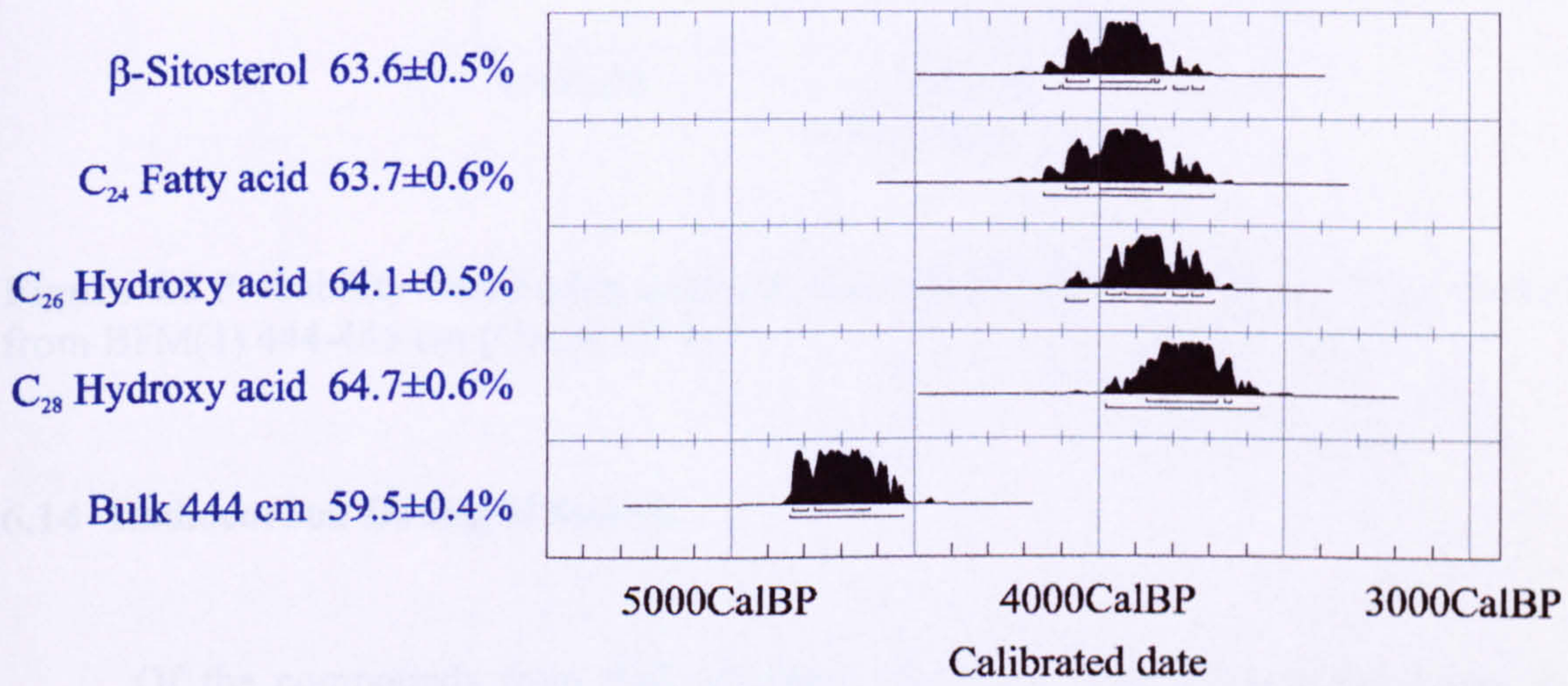

Figure 6.7 Probability distributions of β-sitosterol/stanol, C_{24} FAME, C_{26} hydroxy acid, C_{28} hydroxy acid and bulk peat from BFM(1) 444-445 cm (OxCal v3.3).

The calibrated dates of the lipids (Table 6.11) confirm that all of the compounds have the same radiocarbon contents, consistent with them all originating from the same horizon. The younger age of the lipids than the bulk peat may be due to the bulk peat containing components which have an 'old' carbon source. The C_{22} alcohol, however, has an elevated radiocarbon content even when considering the large error associated with the small sample size (15 μgC). This could be a result of low level modern contamination which is only noticeable when sample size is small, a fractionation effect elevating the ^{14}C content of the sample or the compound having a younger origin. This increase is more likely to be a small sample size effect as this is the only major

difference with the other compounds. The calibrated probability distribution of the alcohol (Fig. 6.8) shows a broad date range for this compound which makes it unusable in radiocarbon dating at this concentration.

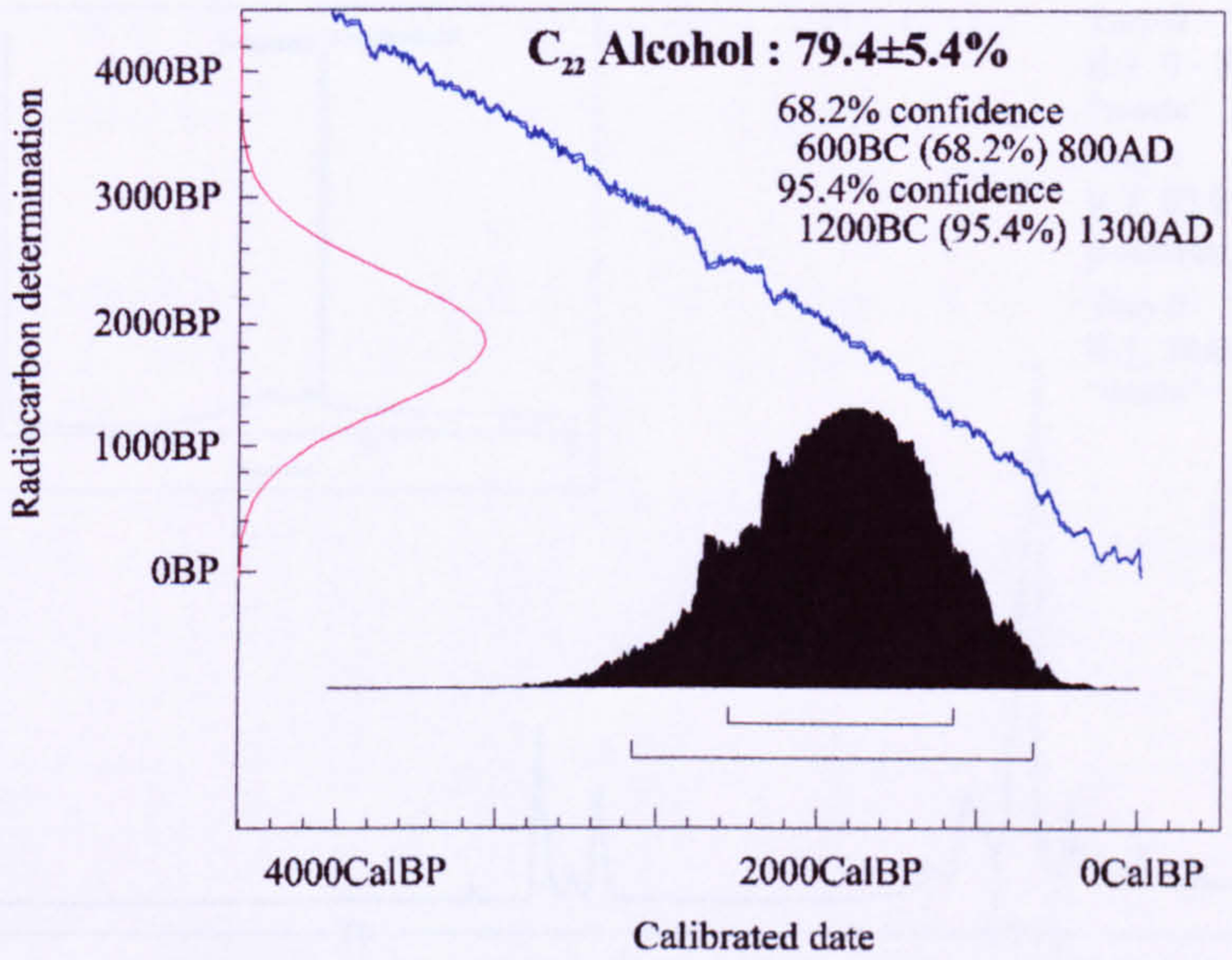

Figure 6.8 Probability distribution with age ranges and calibration curve of C_{22} alcohol from BFM(1) 444-445 cm (OxCal v3.3).

6.14 Radiocarbon Dating of Sterols

Of the compounds from 444 cm depth that have been radiocarbon dated, β-sitosterol and 3-stigmastanol were selected for radiocarbon dating throughout the 30 cm interval between 420 and 448 cm. These compounds were chosen because they are in high abundance in the peat, have been shown to be relatively immobile in water and can be linked to the plants that occur within the horizons, especially *Sphagnum* (Karunen *et al.*, 1983). However, these compounds coelute on the GC column and it would be impossible to collect them separately. It was decided that since the stanol is a diagenetic product of the sterol the radiocarbon determination would be expected to be the same that therefore they could be collected together. The β-sitosterol and 3-stigmastanol were collected at 3 cm intervals (corresponding to the bulk peat radiocarbon dates) in a single trap and radiocarbon dated (Fig. 6.9). Sterol fractions were quantified by GC and passed through the PCGC system so that β-sitosterol and 3-stigmastanol were collected in trap 1 and the waste in trap 0. Six preliminary runs to determine retention times of the

compounds to be trapped were performed for each sample. GC temperature conditions, number of trapping runs and trap window times for each series of runs are shown in Table 6.12.

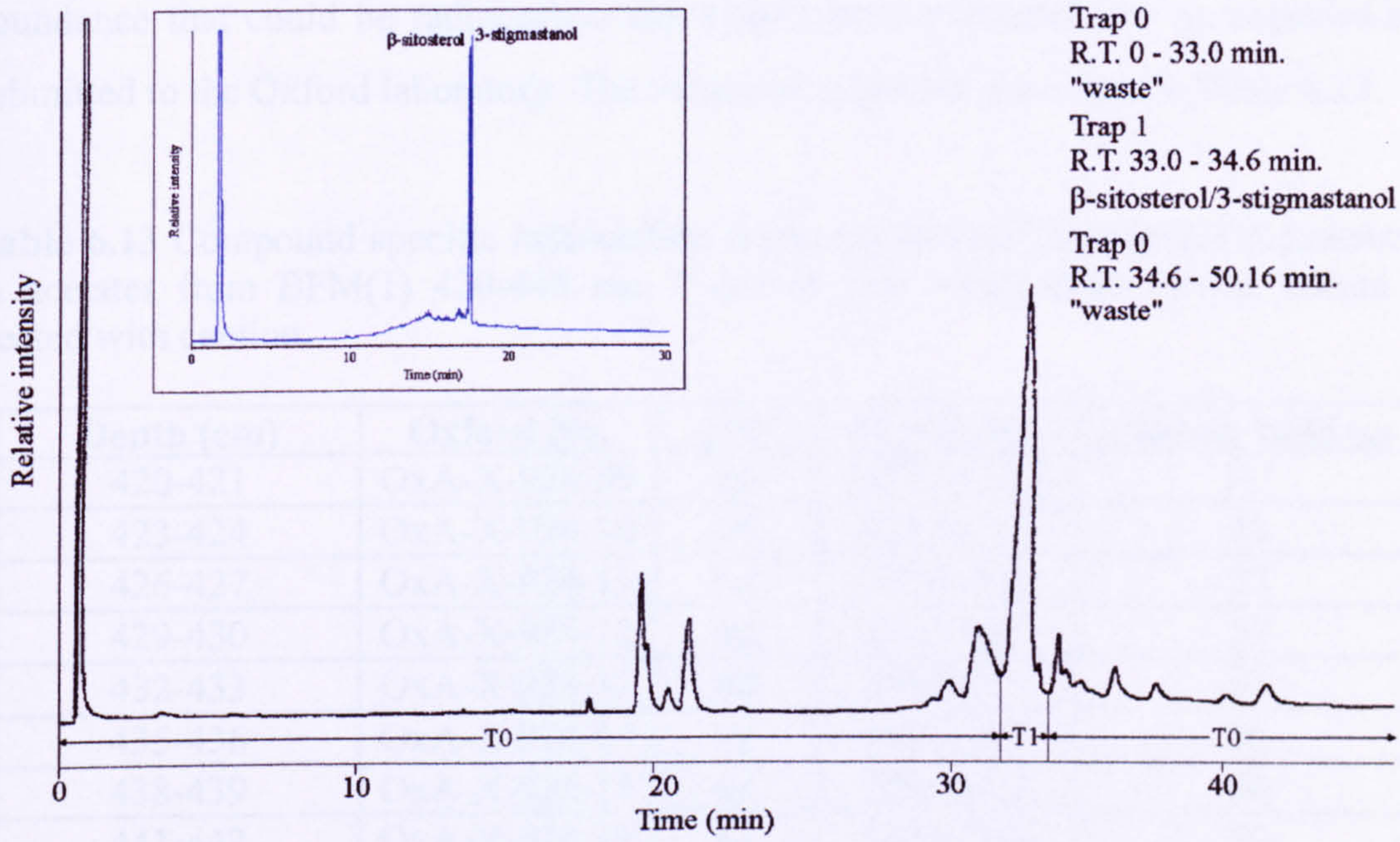

Figure 6.9 PCGC gas chromatogram of sterol fraction as acetates from core BFM1 at 444 cm depth. Insert represents an aliquot of the contents of Trap 1 reanalysed under the same GC conditions.

Table 6.12 GC oven conditions and trap windows used for the accumulation of β-sitosterol and 3-stigmastanol between 420 and 448 cm.

Depth	GC Conditions	No. of Runs	Trap Window
420-421	50(1)-220@12-300@4(10)	20	31.8-32.8 min
423-424	50(1)-220@12-300@4(9)	26	32.2-33.2 min
426-427	50(1)-220@12-300@4(9)	32	32.0-33.0 min
429-430	50(1)-220@12-300@4(9)	20	32.3-33.6 min
432-433	50(1)-220@12-300@4(9)	40	32.0-33.0 min
435-436	50(1)-220@12-300@4(9)	25	32.0-33.0 min
438-439	50(1)-220@12-300@4(5)	42	32.0-33.8 min
441-442	50(1)-220@12-300@4(5)	42	31.6-33.6 min
447-448	50(1)-220@12-300@4(10)	62	31.6-32.6 min

Differences in the position and time intervals of the trapping window (Table 4.11), reflect small differences in the He carrier gas pressure and presence (or absence) of closely eluting peaks. The length of the runs was determined by the time taken to elute all of the GC detectable material from each injection. This is important as if all the

material is not eluted it can appear in subsequent runs and interfere with the target compounds.

After the accumulation of the sterols, they were quantified by GC and found to be between 40 and 95% lower in abundance than expected. However, as they were in an abundance that could be radiocarbon dated they were transferred to tin capsules and submitted to the Oxford laboratory. The values received are presented in Table 6.13.

Table 6.13 Compound specific radiocarbon determinations of β-sitosterol/stigmastanol as acetates from BFM(1) 420-448 cm. * due to low yields these results should be treated with caution.

Depth (cm)	Oxford No.	$\delta^{13}C$	% modern	Carbon yield μg
420-421	OxA-X-924-09	nd	1430.7±36.3	11*
423-424	OxA-X-924-10	nd	426.6±3.8	43
426-427	OxA-X-924-11	nd	522.1±6.5	27
429-430	OxA-X-924-12	nd	201.7±2.5	37
432-433	OxA-X-924-13	nd	246.6±4.1	33
435-436	OxA-X-924-14	nd	165.1±1.8	46
438-439	OxA-X-924-15	nd	102.7±1.4	64
441-442	OxA-X-924-16	nd	128.8±1.6	52
447-448	OxA-X-924-17	nd	613.0±15.3	18*

These results (Table 6.13) along with those obtained for the *n*-alkanes separated from the peat (Table 6.8) all have a supermodern carbon content. All of these samples were run at the same time and it was first thought that these had in some way become contaminated. However, analysis of the products by GC showed that only the desired compounds were present but at a lower abundance than expected. If the contamination had been from an extraneous ^{14}C enriched compound that had coeluted with the trapped compounds, only the sterols or the *n*-alkanes would have been affected and not both. Low level contamination that becomes significant when yields are small could have affected these results, but this is unlikely as previous samples at this abundance showed only a slight elevation in modern carbon (C_{22} alcohol, Table 6.6). The previous radiocarbon date for BFM(1)-444-445 β-sitosterol/3-stigmastanol gave a result comparable with the other compounds and the bulk peat, and this would suggest that the samples submitted have an elevated ^{14}C content as a result of passing through the PCGC system. One possibility could be that isotopic fractionation of the trapped compounds could be occurring and a higher relative proportion of ^{14}C to ^{12}C isotopomers were collected.

6.15 Chromatographic Isotope Effect

The chromatographic isotope effect (CIE) or inverse isotope effect is so-called because in some cases heavier isotopomers elute earlier than lighter ones. This phenomenon is most commonly seen in irm-GC/MS systems where the *m/z* 45 signal is seen first ($^{13}CO_2$) as ^{13}C substituted isotopomers of organic compounds elute before *m/z* signal 44 ($^{12}CO_2$). This gives rise to the S-shaped trace that is common in these systems (Fig. 6.10).

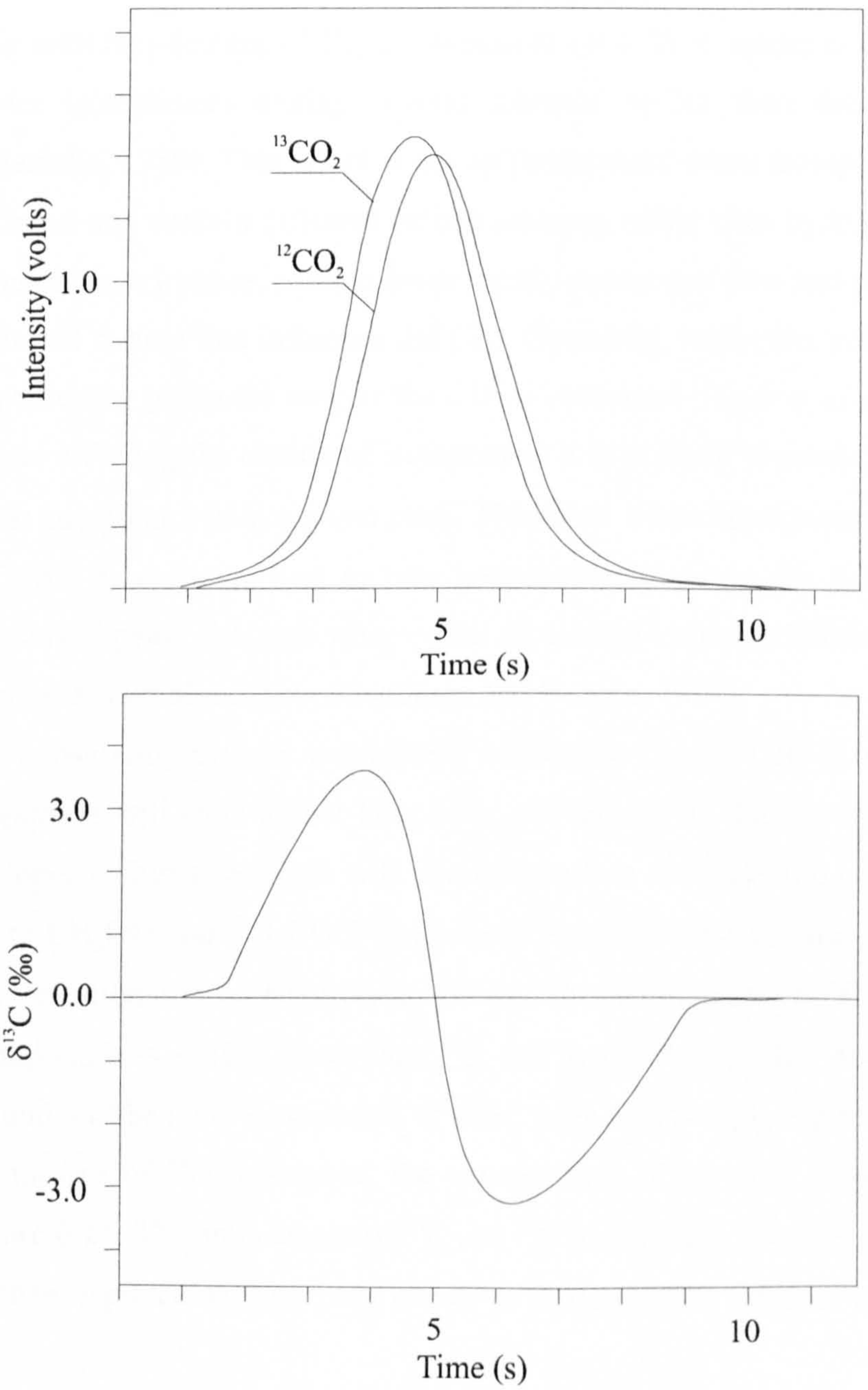

Figure 6.10 Schematic illustration of the time displacement between $^{13}CO_2$ and $^{12}CO_2$ that causes the S-shaped 45/44 ratio signal.

The CIE occurs because where heavier isotopes are present within an organic molecule, the internuclear carbon-hydrogen distances become shorter. This results in slightly lower molar volumes and boiling points. Therefore the shape and size of the solute molecules, not the mass difference, is found to play a significant role in the elution of isotopomers (Matucha *et al.*, 1991). However, when compounds are introduced into a capillary column, van der Waals dispersion forces dominate the different solute/stationary phase interactions, resulting in earlier elution of the heavier isotopomer (Matucha, 1995). The CIE can be quite dramatic when compounds are totally labelled with heavier isotopes. Gas chromatography of C_{15}-C_{17} perdeuterated *n*-alkanes along with non-deuterated C_{14}-C_{17} standards on a 25 m apolar column resulted in the heavier isotopomers eluting several minutes earlier than the un-modified standards (Matucha, 1989). This effect is not so pronounced when isotopomers are not totally substituted and contain different carbon isotopes rather than hydrogen isotopes. Polarity of the stationary phase, column temperature, carrier gas flow and polarity of the compounds are all factors that influence the CIE. Generally, where the polarities of the analyte and stationary phase are similar the CIE is enhanced (Ricci *et al.*, 1994). With so many factors affecting the elution of isotopomers it is difficult to predict the isotopic composition at any point within a given peak. Therefore, when determining $\delta^{13}C$ values from irm-GC/MS it is always best to take measurements across the full width of a completely resolved peak, although when peaks do overlap valuable information can be extracted using software algorithms (Goodman and Brenna, 1994).

When considering organic compounds containing ^{14}C the CIE is increased and heavier isotopomers will elute earlier than those containing ^{13}C. However, the position of the ^{14}C isotopes within a molecule will also affect when the molecule will elute. This is analogous to CH_3OD and CH_2DOH which both have different vapour pressures and different GC retention times (Bigeleisen, 1961). The abundance of ^{14}C in naturally occurring compounds is ~ 10^{-10} lower than ^{13}C and therefore very few molecules of a given compound will be a ^{14}C isotopomer. If a GC peak was completely combusted and the resulting masses of CO_2 measured, the composition of the peak would appear as shown in Figure 6.11. The abundances of ^{14}C and ^{13}C in naturally occurring samples are much lower than depicted and are only drawn to represent the order of elution of the isotopes.

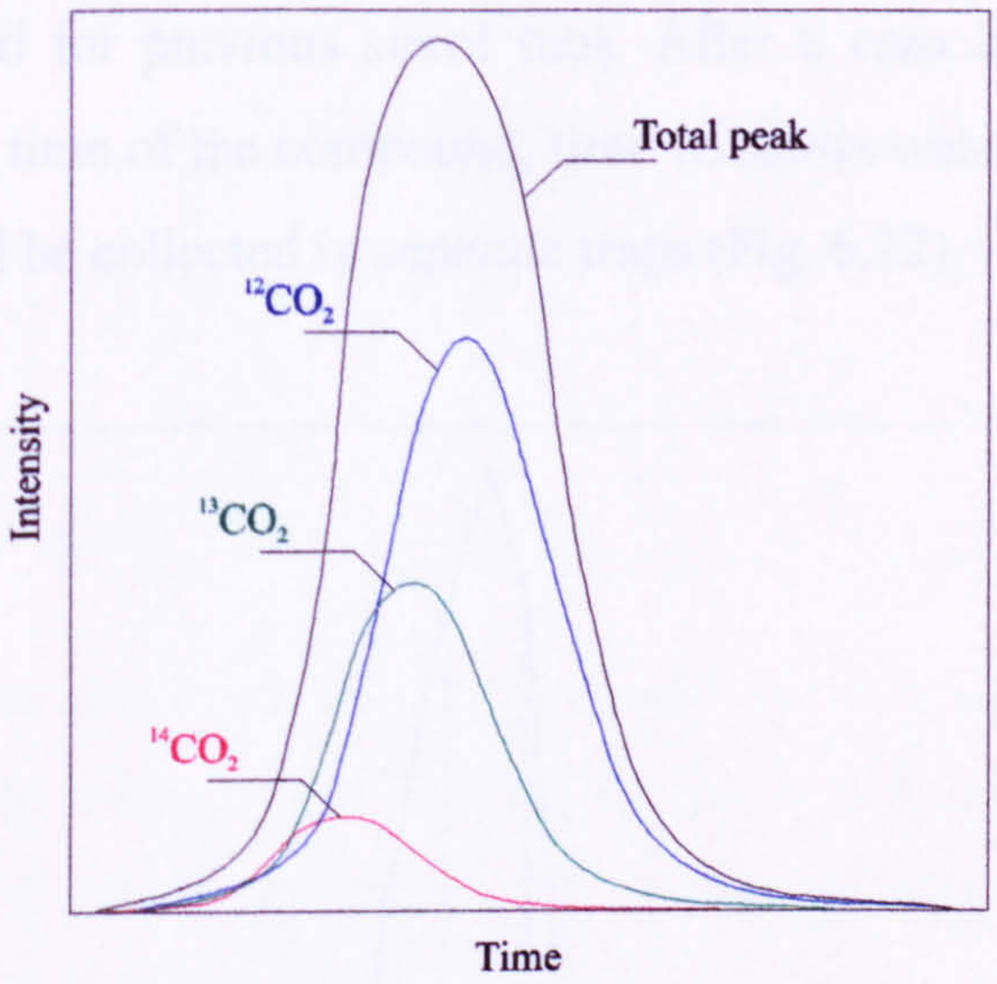

Figure 6.11 Illustration of the $^{14}CO_2$, $^{13}CO_2$ and $^{12}CO_2$ contributions to a CO_2 peak as a result of the combustion of a GC resolved compound. The abundance of $^{14}CO_2$ and $^{13}CO_2$ are exaggerated for graphical purposes.

The observed enrichment of ^{14}C seen in the sterol and alkane samples could therefore be a result of the CIE and a time delay of eluting compounds between the flame ionisation detector (FID) and the traps. Possibilities to cause the incomplete trapping of a peak could be: an obstruction between the FID and traps, activation of the transfer capillary and differential retention of analytes, or a temperature drop between the FID and the traps. It is unlikely that there was an obstruction in the system as flow rates of the carrier gas were normal and it is more likely that the transfer capillary was touching a part of the GC oven causing a cool spot to develop. To correct for the incomplete trapping of a compound and enrichment of ^{14}C, the proportion of the peak trapped must be established.

The CIE is determined by many factors and the only way to accurately establish the elution of the isotopomers is to measure this directly. The direct measurement of ^{12}C and ^{13}C isotopomers can be made (as in irm-GC/MS), but due to the low abundance of ^{14}C in naturally occurring compounds their isotopomers cannot be easily measured using analytical techniques available at Bristol. However, sections of a single peak can be trapped out and subsequently radiocarbon dated, providing ^{14}C, ^{13}C and ^{12}C isotope ratios for each segment. This was performed using a solution of β-sitosterol (Applied Science Laboratories, USA) acetate in hexane (3.1 μg μl^{-1}, 90 × 2 μl injections) and trapping four sections of the whole peak. The GC conditions were 50°C (1 min), 50-

220°C @ 12°C min^{-1}, 220-300°C @ 3°C min^{-1}, 300°C (3 min). All other conditions were identical to those used for previous sterol runs. After 6 runs had been performed to establish the retention time of the compound, time windows were programmed so that 4 parts of the peak could be collected in separate traps (Fig. 6.12).

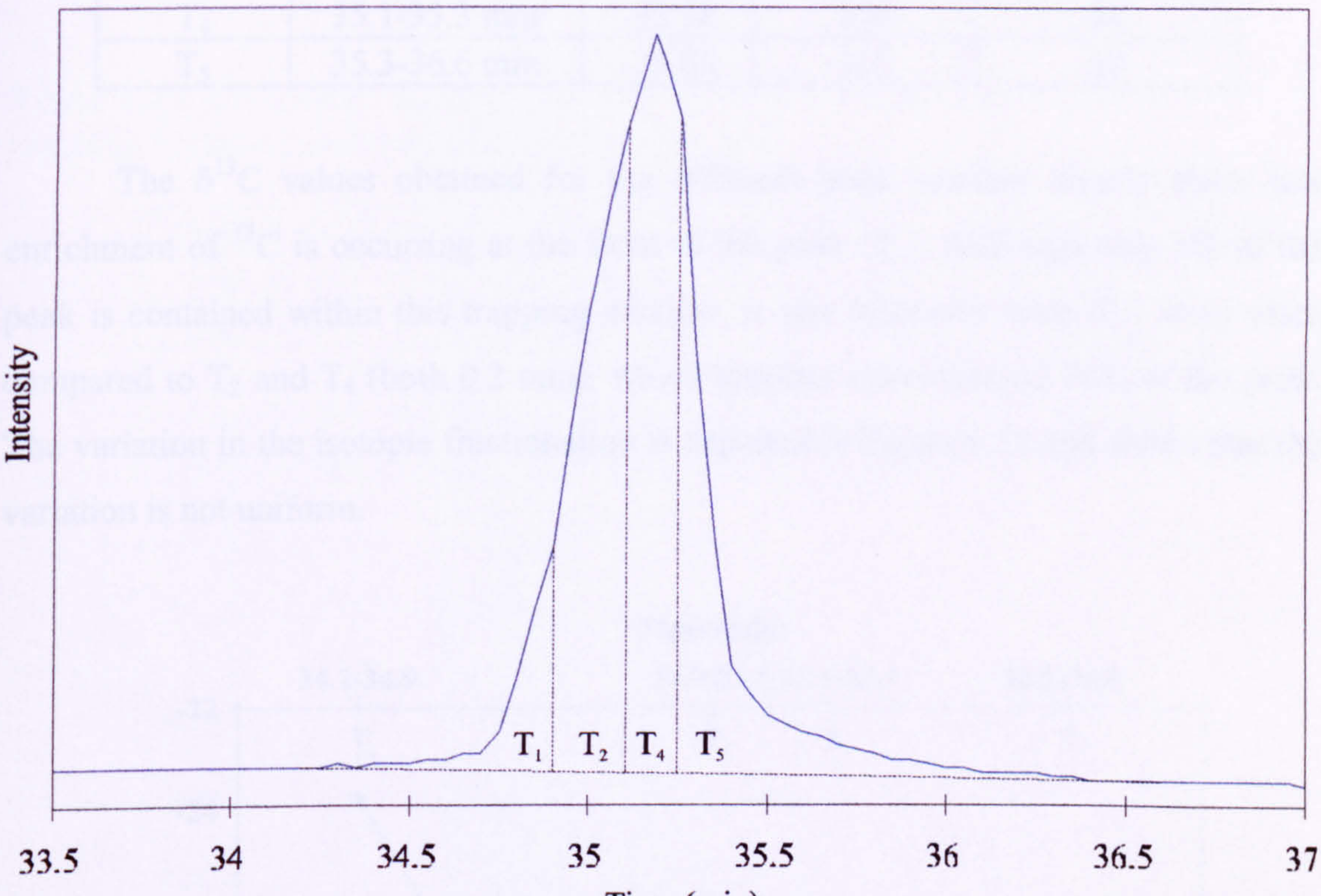

Figure 6.12 Graph showing the GC profile of β-sitosterol acetate and trap windows. T_1, T_2, T_4, and T_5 represent approximately 8, 30, 44, and 18% by area, respectively.

The contents of each trap were collected and quantified by GC. A small aliquot of each was retained for irm-GC/MS analysis and the remainder submitted to the Oxford laboratory for radiocarbon analysis. $\delta^{13}C$ values for contents of each trap are included in Table 6.14.

Table 6.14 $\delta^{13}C$ values of trapped peak sections and total β-sitosterol. Yields based on quantities of component injected and area of peak trapped.

Trap No.	Trap Time	$\delta^{13}C$ ‰	Yield μg	% of Total
Total	-	-34.63	-	-
T_1	34.2-34.9 min	-23.79	47	8
T_2	34.9-35.1 min	-34.89	184	30
T_4	35.1-35.3 min	-35.18	270	44
T_5	35.3-36.6 min	-35.65	112	18

The $\delta^{13}C$ values obtained for the different peak sections clearly show that enrichment of ^{13}C is occurring at the front of the peak (T_1). Although only 8% of the peak is contained within this trapping window, it was relatively wide (0.7 min) when compared to T_2 and T_4 (both 0.2 min), which together encompassed 74% of the peak. The variation in the isotopic fractionation is depicted in Figure 6.13 and shows that the variation is not uniform.

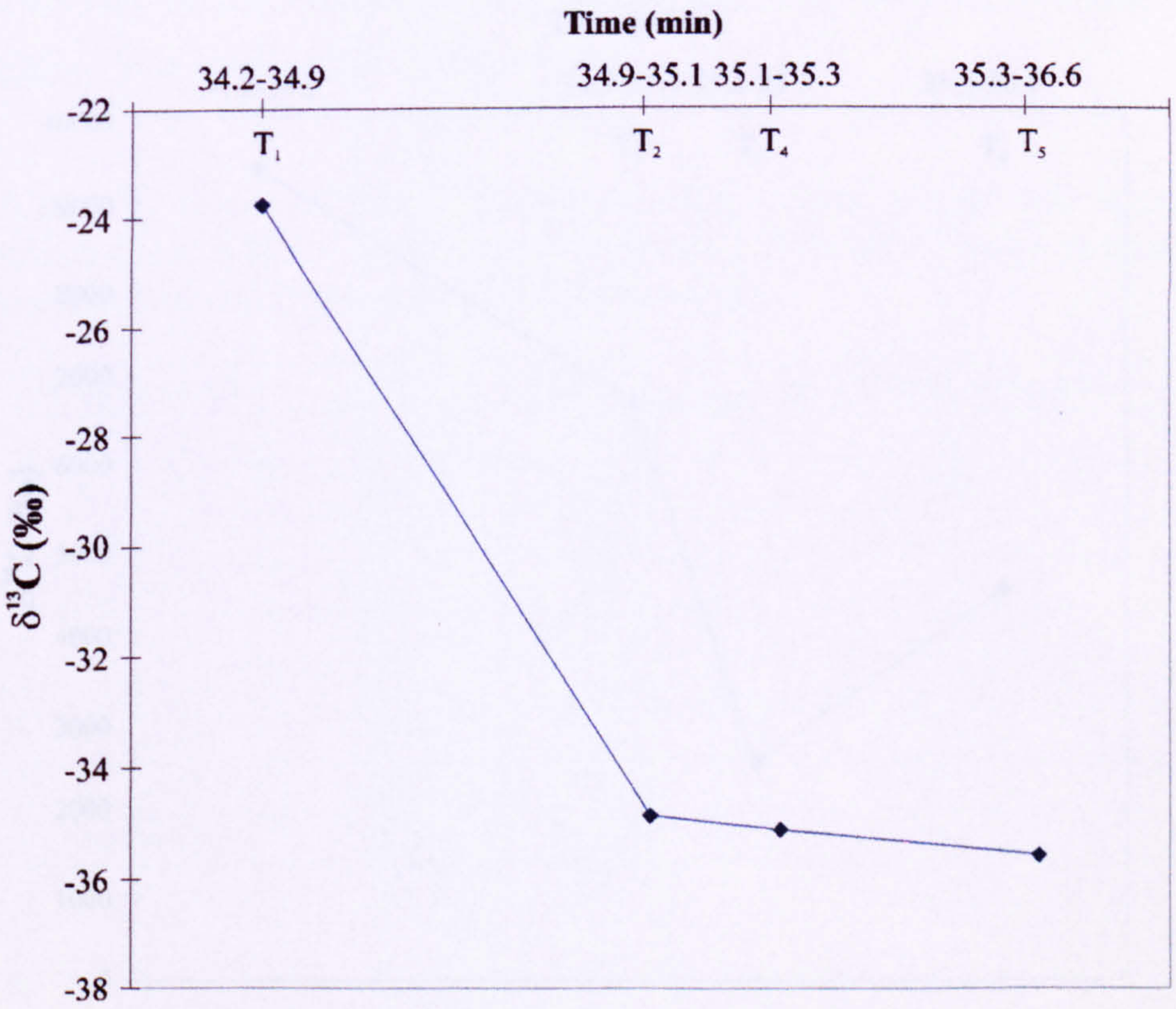

Figure 6.13 Graph showing the $\delta^{13}C$ values of β-sitosterol acetate trap contents.

A similar distribution is seen for ^{14}C (Fig 6.14, Table 6.15), except that the fractionation is more pronounced as the heavier isotopes elute earlier. These results all

have elevated ^{14}C contents relative to modern samples as the β-sitosterol used had been artificially enriched with ^{14}C (radiocarbon determination of unprepped sample, 5792.6±38.4% modern carbon). This shows that if the front of a peak is preferentially collected to the tail, the resulting component can be enriched in the heavier isotopomers.

Table 6.15 Compound specific radiocarbon determinations of β-sitosterol acetate (Applied Science Laboratories, USA) trap contents.

Oxford No./Trap No.	% Modern C	δ^{13}C ‰	Yield μgC
OxA-X-945-07 / T1	972.2±7.3%	-26.0	44
OxA-X-945-08 / T2	716.2±9.8%	-26.0	23
OxA-X-945-09 / T4	323.2±2.9%	-26.0	56
OxA-X-945-10 / T5	510.3±3.1%	-26.0	65
OxA-X-945-11 / Total	5762.6±38.4%	-26.0	114

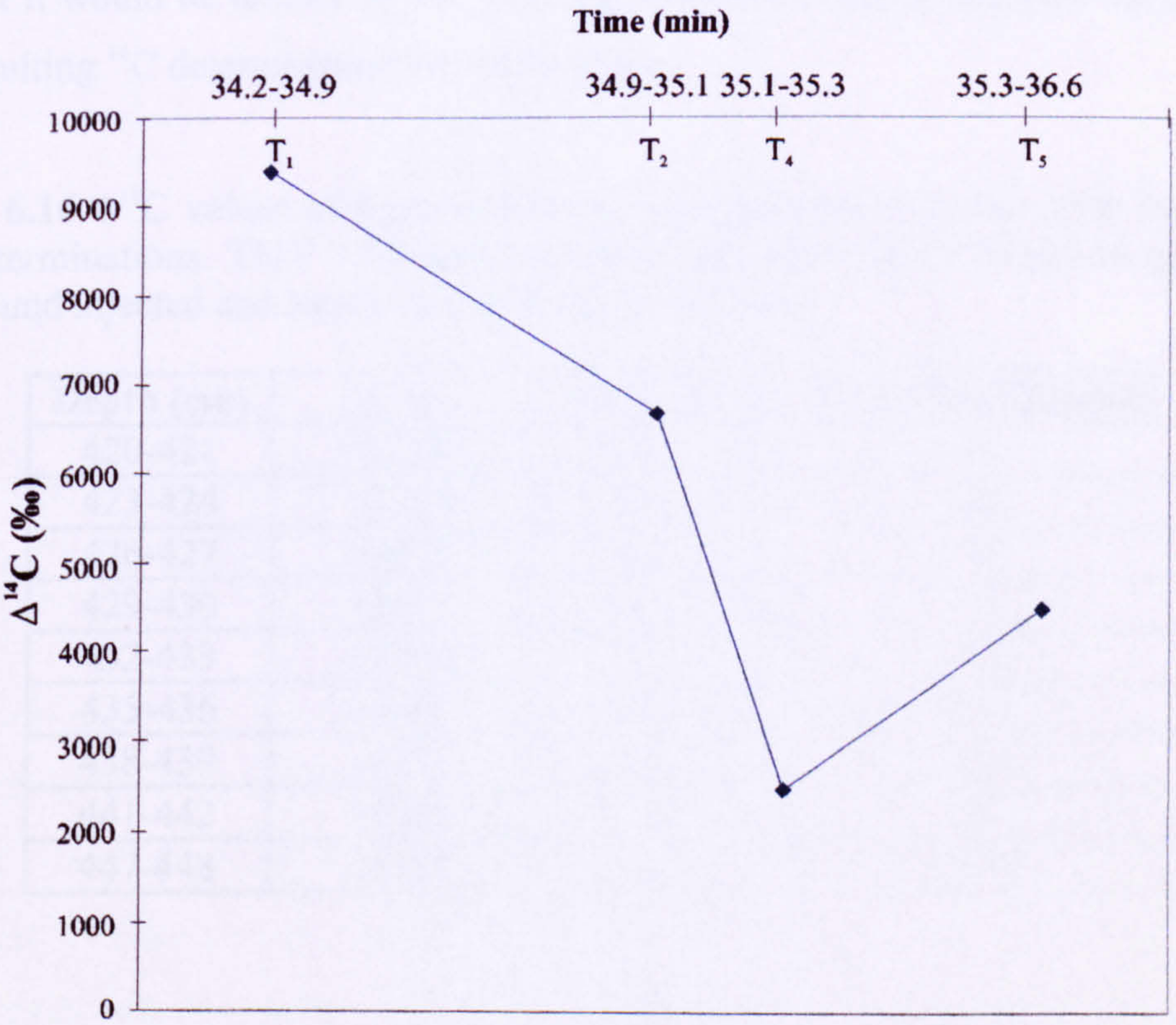

Figure 6.14 Graph showing the Δ^{14}C values of β-sitosterol acetate (Applied Science Laboratories, USA) trap contents.

Assuming that the trapped samples in Table 6.13 were ^{14}C enriched because only the front of the peak was collected, the Δ^{14}C values calculated from the modern carbon

values from the supermodern sterols could be corrected. Also, an estimation of the proportion of each peak that was collected needed to be made. This was achieved by determining the amounts injected into the PCGC system, less the 2% of the sample that was lost to the FID and losses in transferring the trapped compounds from the U-tubes to the tin capsules and calculating the quantities of compound lost based on carbon yield determinations (Table 6.16). Once this was done a clear correlation was noted between the percentage of peak trapped and the $\Delta^{14}C$ values i.e. the greater the proportion of peak trapped, the lower the $\Delta^{14}C$ value (Fig. 6.15). This correlation is not seen when relating yields of carbon (Table 6.13) to the radiocarbon determination and dismisses any underlying ^{14}C contamination as this would increase the $\Delta^{14}C$ value proportionally to the amount of carbon present. This is clearly shown in Table 6.13 where although the carbon yield of the compound from 423-424 cm (43 μg) is higher than that of 429-430 or 432-433 cm (37 and 33 μg) its percentage of modern ^{14}C is increased (increase of 6 and 10%, respectively). If a supermodern contaminant was present it would be diluted by the extra carbon input from the trapped component and the resulting ^{14}C determination would be lower.

Table 6.16 $\Delta^{14}C$ values of trapped β-sitosterol/stigmastanol acetate with supermodern ^{14}C determinations. TMY = Theoretical Maximum Yield and is based on quantities of compound injected and losses due to PCGC procedure.

Depth (cm)	$\Delta^{14}C$	TMY μg	% of TMY trapped
420-421	+13307	231	6
423-424	+3266	293	18
426-427	+4221	251	13
429-430	+1017	143	32
432-433	+1466	153	26
435-436	+651	148	37
438-439	+27	134	58
441-442	+288	132	47
447-448	+5130	222	10

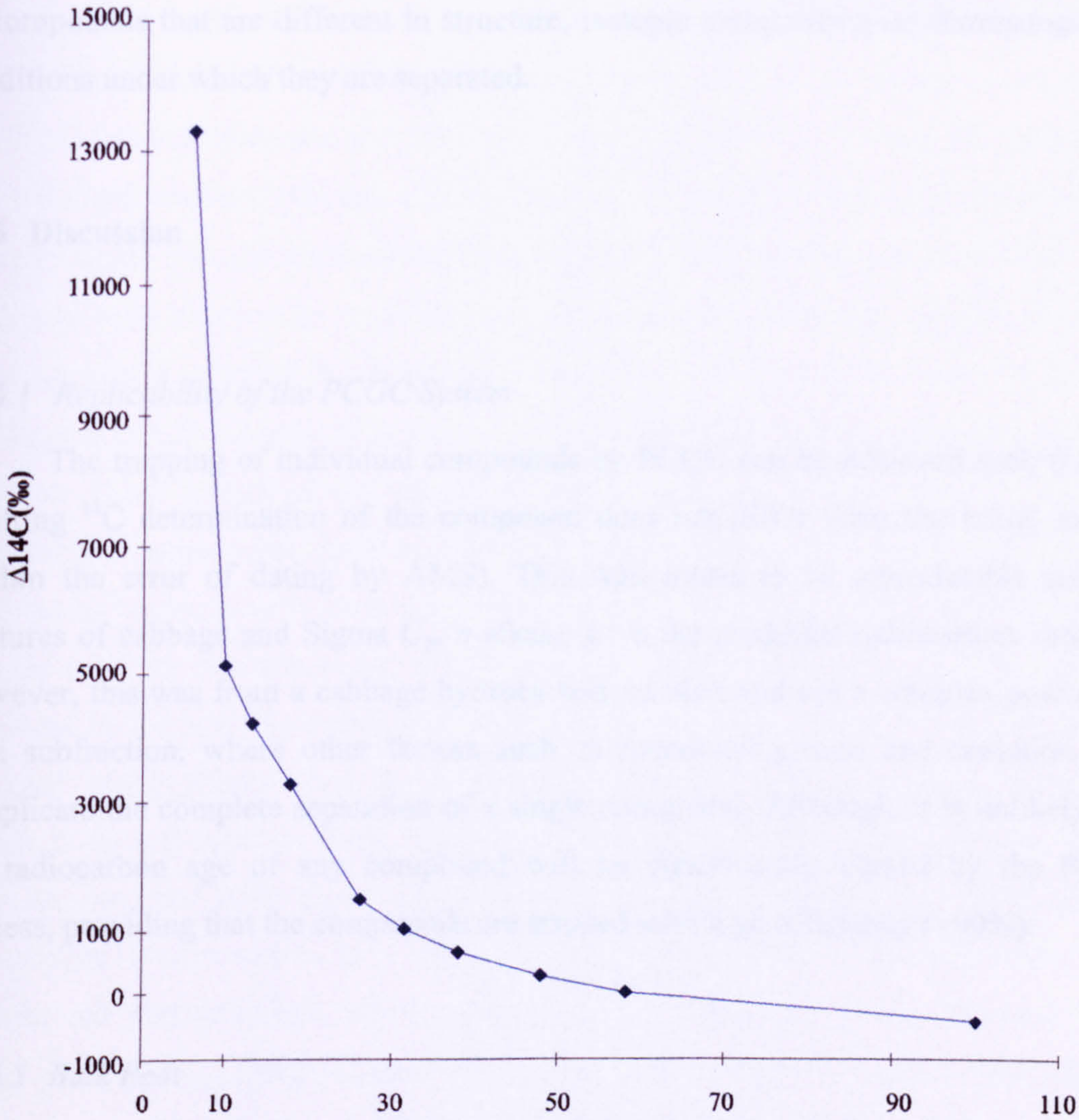

Figure 6.15 Graph showing the $\Delta^{14}C$ values of β-sitosterol/stigmastanol acetate plotted against the percentage of component trapped. This includes all values for samples between 420 and 447 cm.

Although the ^{14}C contents of the compounds from different horizons are likely to differ, based on the bulk dates from each horizon they are all thought to contain ~60% modern carbon (Table 6.2). On such a scale as Figure 6.15, the difference in a few percent of modern carbon to a sample would have little effect on the trend and therefore the samples can be compared with each other. Therefore, this graph can be used to correct for <100% trapping of PCGC compounds. However, this cannot substitute radiocarbon determinations for fully trapped peaks as the associated errors are large. The CIE for different compounds or compounds with different isotopomeric ratios would also change the distribution of ^{14}C within a chromatographic peak. Therefore, there is no single model that could represent ^{14}C fractionation in a peak and be applied

to compounds that are different in structure, isotopic composition or chromatographic conditions under which they are separated.

6.16 Discussion

6.16.1 Replicability of the PCGC System

The trapping of individual compounds by PCGC can be achieved such that the resulting ^{14}C determination of the compound does not differ from the initial sample (within the error of dating by AMS). This was found to be reproducible and the mixtures of cabbage and Sigma C_{29} *n*-alkane gave the predicted radiocarbon contents. However, this was from a cabbage hydrocarbon fraction and not a complex peat sterol lipid subfraction, where other factors such as functional groups and coelution may complicate the complete separation of a single compound. Although, it is unlikely that the radiocarbon age of any compound will be significantly altered by the PCGC process, providing that the compounds are trapped with high efficiency (>90%).

6.16.2 Bulk Peat

The radiocarbon determinations of the bulk peat samples indicate that the observed shift in plant inputs at approximately 435 cm depth occurred at 4698 ± 11 y BP (2759-2738 BC 1σ). However, some of this data set gave dates that were 300-400 y older (BFM1-441, BFM1-429 and BFM1-420). Sample BFM1-444 was dated at 4725 ± 105 y BP (2880-2670BC 1σ) and when "wiggle-matched" produced a date of 4778 ± 13 y BP (2841-2815BC 1σ) which is more likely to reflect the true age of the horizon. Comparisons between lipid and "wiggle-matched" bulk peat dates cannot be made as insufficient accurate lipid dates were obtained throughout the 30 cm depth interval.

6.16.3 BFM1-444 Lipids

Of the lipids trapped from BFM1-444, the radiocarbon determination of β-sitosterol/3-stigmastanol (3800 ± 130 y BP) was found to be the most comparable with the bulk peat date (4725 ± 105 y BP), although the peat was considerably older. Other studies comparing ^{14}C contents of lipid subfractions and soil (Bol *et al.*, 1996) found that the carboxylic acids were considerably younger than the surrounding horizons. This

was attributed to a possible water-soluble component in the carboxylic acid fraction which was leached in from younger horizons. However, this component is not present in PCGC trapped lipids and therefore would not alter their ^{14}C content. The separation of single hydrocarbons (C_{29} and C_{31} *n*-alkanes) from marine sediments has also yielded younger lipids than the surrounding bulk organic matter (Eglinton *et al.*, 1997). These *n*-alkanes were likely to be an allochthonous input from the riverine input of terrestrial plants and their enriched ^{14}C values were ascribed to their production as a result from the fixation of CO_2 directly from the atmosphere. Therefore they were not subject to any reservoir (hard water) effect which would be likely to deplete the ^{14}C in other sedimentary components such as prymnesiophyte alkenes. The peat lipids are also likely to be predominantly from the major plant species, *E. vaginatum* which fixes CO_2 directly from the atmosphere and therefore would be less likely to incorporate any CO_2 dissolved in the peat bog water. The 'old' date for the bulk peat could be attributed to the hard water effect, when the bog was wet, pools containing algae could have collected on the surface. These algae may have sampled dissolved carbonate, which may or may not have been in equilibrium with the atmosphere. Therefore any radiocarbon determination of a peat constituent that includes algal remnants may include 'old' carbon and therefore produce a falsely 'old' date. The C_{24} fatty acid (3795 ± 105 y BP) and C_{26} (3800 ± 100 y BP) and C_{28} ω-hydroxy acids (3730 ± 100 y BP) all exhibit very similar dates and therefore are likely to be from a source of the same age. Although the C_{24} fatty acid has been found almost ubiquitously in the plant species from BFM (Nott, 2000), the hydroxy acids were absent in fresh plant material. However, such compounds have been linked to the senescent parts of *Sphagnum* moss (Ekman and Karunen, 1982) and therefore are most likely to be suberin degradation components of peat-forming plants. The age difference between the acidic lipids and the sterols may be due to the different parts of the plant where these lipids are found i.e. the hydroxy acids being produced predominantly in lower parts of the plant and sterols being components of the whole plant. Therefore CO_2 fixed from the atmosphere is directed to the production of hydroxy acid components in lower parts of the plant/peat, producing younger dates.

6.16.4 Radiocarbon Dating of Sterols

The large errors associated with small amounts and incomplete trapping of these compounds do not allow them to be adjusted so that they could be "wiggle-matched"

and compared to bulk peat dates. However, it is likely that these sterols would produce younger dates than the peat as previously determined for BFM1-444 as these lipids are not likely to incorporate "old" CO_2. The supermodern radiocarbon dates produced from these compounds highlights the possible problems associated with trapping by PCGC and to avoid these in the future, several precautions must be taken. The biggest uncertainty with this process is fractionation of compounds within the PCGC system. To determine if fractionation has occurred before radiocarbon dating, the $\delta^{13}C$ values of the trapped compound can be compared with that of the untrapped component. Any difference in the $^{13}C/^{12}C$ ratio might therefore reflect a similar $^{14}C/^{12}C$ difference, however, this cannot account for losses in ^{14}C where the $^{13}C/^{12}C$ ratio would remain very similar i.e. losses at the front of a chromatographic peak. This can be accounted for in several ways:

I. Any part of a compound that is not trapped will be carried over into the waste trap. This can then be studied by GC to determine if any part of the target peak has not been trapped. However, the preparative trapping device can sometimes allow a small proportion of the target compounds to pass through to the waste trap without causing fractionation.

II. If a compound of known $\delta^{13}C$ value and radiocarbon content is added to the fraction prior to separation by PCGC then any fractionation of this compound when trapped would similarly affect the target compound.

III. The determination of quantities of trapped compounds is also an effective way to determine if inefficient trapping has occurred. This can be done by calculating the quantities injected and those trapped by GC analyses of the fraction and trap contents. Therefore any loss in compound not attributed to losses to the FID in transfer are likely to be associated with fractionation in the preparative device. Also the GC profile will reveal any other compound also trapped with the target lipid.

Contamination of the trapped compound is only likely to occur by lipids that elute in the same trap window as the target compound. Therefore any contaminant can be identified by separation on GC using a different column and rejected before radiocarbon dating. Contamination from other sources was not seen in this study and can be eliminated by following the applied protocols.

6.17 Summary

The main objective of this chapter was to establish methods for the radiocarbon dating of specific compounds isolated from peat. This was achieved by determining the replicability of the PCGC system and possible sources of contamination. Several considerations needed to be addressed so that reliable dates of single compounds could be produced. These include the use of a mass balance approach to provide corrected isotopic data for derivatised compounds, quantification of extraneous carbon introduced after isolation and the use of $\delta^{13}C$ values to assess fractionation occurring within the PCGC system.

The major findings of this research were:

1. As long as the performance of the PCGC system is monitored and fractionation effects are shown not to occur, this method has shown to be highly reproducible for the isolation of single compounds for radiocarbon dating.

2. Isolation of single compounds from peat must be >100μg in order to provide useful dates that can be compared to bulk peat determinations. Therefore compounds must be in sufficient quantity in the original fraction and not in low relative abundance to other compounds. The number of repeated injections must be kept to a minimum to prevent accumulation of contamination that is associated with each injection e.g. column bleed.

3. Radiocarbon determination of bulk peat placed the change from *E. vaginatum* dominated vegetation to *S. imbricatum* dominated vegetation at 4698 ± 11 y BP. However, based on lipid ^{14}C determinations which are less likely to be affected by contributions from reservoir CO_2, it is likely that this occurred later.

4. Fractionation due to time delay between the FID and the traps can significantly alter the radiocarbon content of trapped lipids. This emphasises the need for a target compound to be well resolved on the GC column so that a sufficiently long trap window can be set such that all of the compound is collected. To achieve this flow rates, temperature program, phase and column length can be modified to optimise GC conditions.

7. OVERVIEW AND FUTURE WORK

7.1 Introduction

The main aims of this thesis were to provide a better understanding of the sources of lipid components present in peat, with a view to producing a lipid stratigraphy that both reflects and enhances the macrofossil record. Some of these identified components could then be used to develop methods for the compound specific radiocarbon dating of peats, such that future dating of these systems could be refined and more reliable dates inferred for palaeoclimatic studies.

Although specific biomarkers of each individual species were not elucidated, lipid profiles were found to change with different plant inputs and these were used to provide plant input information where macrofossil data were absent. Diagenetic alteration of peat lipids were investigated and novel peat sterol degradation products were identified. Lipid data produced from relatively fresh peat samples and plants were applied to humified peat horizons and peat inputs inferred. Radiocarbon dating of specific compounds provided an alternative date for the major change in plant species recorded in the macrofossil data for this peat profile as well as emphasising the limitations associated with PCGC AMS dating of peat lipids.

7.2 Lipid Stratigraphy

Previous studies relating past environments to lipid stratigraphy in peat bogs have had limited success and have involved the correlation of pollen, macrofossil and lipid records. However, these approaches provided only limited agreement and did not include specific biomarker compounds for the peat inputs. The present study has investigated the composition of peat on a molecular scale at different depths on both a low and high resolution scale.

Examination of the lipids at major excursions in the macrofossil record revealed:

1. Although the *n*-alkane distributions of the samples remained similar, the relative quantities of the C_{23} and C_{25} homologues were found to vary. Ratios of these

alkanes (especially C_{25}) to the C_{31} homologue reflected high abundances of *Sphagnum* species in the macrofossil record.

2. Low CPI values of *n*-alkanes (<5) may reveal non-higher plant peat components not recorded in macrofossil data.

3. The carbon preference index for the *n*-alkanes also seemed to reflect *Sphagnum* input in the peat and this was found not to influenced by the elevated abundances of the C_{25} and C_{23} homologues which are also found in *Sphagnum* peats.

4. The ββ/(αβ+ββ) hopane and hopanol ratio was found to decrease with depth. This was attributed to progressive isomerisation of the ββ to the αβ epimer. However, at 425 cm depth an increase in the ββ epimer was observed. This increase could be a result of an increased water content of the peat (in turn resulting in an increased *Sphagnum* content) making the peat less acidic around the time of deposition.

5. *n*-Alkanoic acid distributions were found not to be representative of the plants that were revealed in macrofossil records. This was attributed to the rapid degradation of shorter chain homologues ($<C_{18}$).

Examination of the lipids over the major change in peat-forming plants in the macrofossil record revealed:

1. The C_{23} to C_{31} *n*-alkane ratio showed a slight increase in the relative abundance of the C_{23} homologue across the 419-448 cm interval. However, there was a sharp decrease in C_{23} coincident with the macrofossil switch between *Sphagnum* and *Eriophorum*.

2. The C_{25} to C_{31} *n*-alkane ratio was found to directly relate to the *Sphagnum* macrofossil data, and this lipid data revealed that the sharp switch between *Sphagnum* and other peat components, occurred between 432 and 433 cm depth.

3. The degradation of compounds such as sterols and hopanoids was not visible over such a short timescale (300 y).

4. The *n*-alkanol CPI values may be an indicator of the specific Ericaceous plant *V. oxycoccus* which has a high predominance of odd numbered homologues.

7.3 Hydroxy and Ketonic Androstanes

The androstane type compounds identified in BFM peat have not been reported in previous studies of immature peatified remains. Structural similarities and $^{13}C/^{12}C$ isotopic ratios of β-sitosterol/3-stigmastanol and 3β-hydroxy-5α-androstan-17-one suggested that the androstane type compounds were sterol degradation products, of which the desmethyl androstanes are likely to have several sterols (β-sitosterol, stigmasterol and campesterol) as their precursors. Previous studies revealed that aerobic bacteria can produce androstane compounds from sterols, but only under anaerobic conditions. The absence of the compounds above 3 m and proposed microbially derived origin suggests that the bacteria responsible for their presence, either only populate those depths of the peat, were active only at deposition of these peat layers, only degrade these compounds under the conditions present at these depths or that the degradation requires a long period of time to occur. The presence of methyl androstane compounds in the deepest part of the peat core correspond with the presence of 4-methyl sterols and it was proposed that the androstane compounds were degradation products of these sterols.

7.4 Early peat formation

The identification of lipids from horizons where macrofossil records documented plant remains, allowed for the transfer of this data to humified sections of the core. Stages for the development of BFM was then proposed and compared to the model established by Foss (1987). The main findings of this were:

1. The presence of 4-methyl androstanes and dinosterol at 957-959 and 977-979 cm depth suggested that dinoflagellates were present during the deposition of these sediments. This suggests that before the peat bog was established, a lacustrine environment existed.

2. Isotope data obtained from the hydrocarbon fraction suggested that the lowest peat horizon (987-982 cm) was sedge dominated and was likely to be from the infilling of these plant remains from the margins of the lake.

3. The peat layer between 977 and 820 cm, although indistinguishable by inspection, was shown to be composed of two types of peat. $\delta^{13}C$ values of *n*-alkanes showed that the lower section appeared to be dominated by *Sphagnum* peat. The upper section peat was found to contain a high abundance of *n*-alkyl resorcinols indicating a sedge input and bulk isotope ratio analysis suggested that the peat also had a high *Sphagnum* input. Above 820 cm the presence of *n*-alkyl resorcinols and comparison of $\delta^{13}C$ *n*-alkane values from the peat and plant species suggested that sedge was the most abundant plant component.

4. Four stages in the early formation of BFM were proposed: (1) Glacial retreat left hollows which filled with water, creating lakes. Sedge from the lake margins and floating *Sphagnum* mats formed the first peat layer at the bottom of the lake; (2) Return of periglacial conditions in the Younger-Dryas led to ice formation and the cessation of peat deposition; (3) The climate warmed again, the ice retreated and peat development began afresh. *Sphagnum*-dominated peat was formed due to the input of floating *Sphagnum* species on the top of the lake; (4) The peat development continued with sedge species at the lake margins dominating the input as they grew in towards the centre of the lake. This continued until sedge species had filled in the lake.

7.5 Radiocarbon Dating of Specific Compounds

The main aims of this research were to establish methods for the isolation of specific compounds from peat, for radiocarbon dating. As only on a molecular level, can ^{14}C ages be related to individual compounds whose structures indicate an unmistakable link to a known precursor. This was achieved by determining the replicability of a PCGC system and possible sources of contamination. This also included the use of a mass balance approach to provide corrected isotopic data for derivatised compounds, quantification of extraneous carbon introduced after isolation and the use of $\delta^{13}C$ values to assess fractionation occurring within the PCGC system.

The major findings of this research were:

1. The isolation of single compounds for radiocarbon dating was found to be highly reproducible as long as the performance of the PCGC system was monitored and fractionation effects are shown not to occur.

2. Isolation of single compounds from peat must be >100μg in order to provide useful dates that can be compared to bulk peat determinations

3. Radiocarbon dating of single compounds produced younger results than the age determination of the bulk peat. This was attributed to the hard water effect, when the bog was wet, pools containing algae could have collected on the surface. These algae may have sampled dissolved carbonate, which may or may not have been in equilibrium with the atmosphere. Therefore any radiocarbon determination of a peat constituent that includes algal remnants may include 'old' carbon and therefore produce a falsely 'old' date. Apart from algal or bacterial lipids it is unlikely that radiocarbon dating of specific compounds will yield widely varying dates as the accumulation of raised peat depends almost exclusively on the preservation of autochthonous plant remains. Therefore the radiocarbon content of any lipid component found to differ from others present in the same horizon is likely to be due to fixing CO_2 from another source other than directly from the atmosphere. Therefore the radiocarbon dating of compounds isolated from 444 cm are likely to produce dates that represent organic matter that has sampled carbon from the atmosphere.

4. Radiocarbon determination of bulk peat placed the change in *E. vaginatum* to *S. imbricatum* at 4698 ± 11 y BP, however, from lipid ^{14}C determinations which are less likely to affected from reservoir CO_2, it is likely that this switch occurred later.

5. *n*-Alkanoic acids and ω-hydroxy acids are probably formed in lower parts of the plants than sterols, resulting in their younger ages.

6. Fractionation due to time delay between the FID and the traps can significantly alter the radiocarbon content of trapped lipids. This emphasises the need

for a target compound to be well resolved on the GC column so that a sufficiently long trap window can be set such that all of the compound is collected.

7.6 Future Work

The organic geochemistry of peat deposits still has many aspects to be explored. Specific biomarkers for each of the plant species present in BFM peat, have yet to be determined. However, variations in quantities of compounds common to several species have been shown to reflect input change. Specific lipid biomarkers may be present in fractions such as the ketone and wax ester fraction, which was briefly examined in this study but not fully characterised due to high molecular weight compounds that could not be isolated by PCGC using thick film columns. Suggestions to carry out this work follow:

1. Further separation of compounds found within the ketone and wax ester fraction may reveal compounds specific to individual species of peat-forming plants.

2. Compounds thought to be triterpenoid and sterol acetates, found in the ketone and wax ester fraction could be hydrolysed to release the alcohol components. These can then be rederivatised with BSTFA and their TMS ethers characterised by GC/MS.

3. Degradation studies of individual peat-forming plants may help determine specific sources of compounds found within peat.

4. Degradation studies of lichens and algae found on the surface of the bog but not present in the macrofossil record may reveal lipid components specific to these sources. These can then be used to provide proxy environmental records, complementing existing macrofossil profiles.

5. Comparisons of humification records (colorimetric methods) and lipid degradation profiles from peat may determine whether structural deterioration and changes in peat colour are related to molecular processes. This can then be used to enhance existing humification records.

The radiocarbon dating of single compounds has been shown to be invaluable for the age determination of separate components in heterogeneous matrices such as peat and other sedimentary materials. However, AMS limitations requires that >100 μg of carbon be present to produce reliable dates. Therefore isolation of target compounds requires sufficient abundance in the source material for adequate carbon to be yielded. For quantities of peat used in the current study, the lipid compounds that can be reliably radiocarbon dated are limited to major sterols, carboxylic acids, *n*-alkanes and *n*-alkanols. Therefore, for the radiocarbon determination of other compounds the following details must be considered:

1. Compounds such as hopanes and hopanols may sample carbon from a source with a different age to the lipids already isolated and radiocarbon dated. However, hopanoids were not found to be in sufficient abundance in the horizons used for radiocarbon dating. Therefore extraction of lipids from a horizon containing ample hopanoid compounds and comparison of their radiocarbon dates may reveal differences in age and possible source.

2. To determine the ^{14}C content of less abundant lipids, the amount of peat used for extraction could be increased to about 5 g dry peat. In this quantity most of the lipids identified in BFM would be in sufficient abundance for isolation and AMS dating. These compounds, if taken from the same horizon, would provide a better understanding of the age differences pertaining to individual components.

3. An improvement to the replicability experiment, carried out in this study, could be made so that both 'modern' and 'dead' compounds are isolated using PCGC. This would involve obtaining compounds with known radiocarbon content (*n*-alkanes containing approximately 0 and 100% modern carbon) and mixing them in known quantities. These can then be trapped out, radiocarbon dated and a calibration graph of the PCGC system be produced. This graph would show differences between calculated and determined radiocarbon content and therefore extraneous carbon inputs, both dead and modern.

4. Single compounds isolated from blanket peat, which are more likely to contain allochthonous inputs, could be radiocarbon dated. Although blanket peat does not usually contain the detailed past environmental records found in ombrotrophic

mires, the wider range of ages would help determine possible sources of allochthonous lipids.

This study set out to establish methods for the radiocarbon dating of specific compounds isolated from peat so that more reliable data corresponding to climate change timescale could be produced. Therefore if this study was repeated the aims listed in Chapter 1.6 would be altered to include:

1. A preliminary study of the lipids in Bolton Fell Moss peat to ensure that adequate peat could be collected so that lipid components representative of peat forming plants could be separated at high resolution in quantities suitable for radiocarbon dating by AMS.

2. The study of the lipid stratigraphy in two separate cores over a depth where macrofossil data reveals that the peat components are the same in both cores. This would help to identify the extent of lipid variation due to contribution of unidentified organic matter and which lipids are most representative of macrofossils.

3. Calibration of the PCGC system using a single compound with radiocarbon contents of 0-100% modern carbon. This will reveal possible contributions of both modern and ancient carbon contamination.

8. EXPERIMENTAL

8.1 General

Solvents - All solvents used were of Rathburn® HPLC Grade. Water was doubly distilled prior to use.

Glassware - All glassware was cleaned by soaking in a solution of Micro-60® (24 hr) and then rinsed with acetone and distilled water. Prior to use all glassware was rinsed with dichloromethane and allowed to dry.

Sample storage - Peat samples were stored in the dark in the freezer at -20°C. Lipid fractions were stored in the refrigerator at 4°C.

8.2 Peat Coring

The peat cores were taken from Bolton Fell Moss, Cumbria, UK (National Grid Reference NY495695) on the 18th September 1996. Two 5 m profiles (BFM1 and BFM2) were extracted from the centre of the bog using 50 cm monolith tins for the first 50 cm and then a 9 cm (30 cm length) bore Russian Corer (Barber, 1984). A 10 m core (BFMN) was also extracted using a 5 cm (30 cm length) bore corer. Once extracted these cores were placed in labelled plastic tubing (9 cm i.d., 30 cm length) and wrapped in polythene. These cores were then frozen (-20°C) until sectioned. For lipid analyses 0.5-1 cm slices were removed from the core at the chosen depths (discarding the outer layer which may be contaminated) and freeze dried before analysis. 4 cm^3 sub-samples at 1 cm intervals between 250-600 cm were removed from the wet peat and placed in double distilled water for macrofossil analysis.

8.3 Lipid Extraction

The freeze dried peat (0.3-0.5 g) was powdered in a mortar and pestle so that it passed through a 0.5 mm sieve and then total lipids were extracted by sonication/centrifugation (3x100% MeOH, 2x1:1 MeOH/DCM and 5x100% DCM) or Soxhlet extraction with DCM/acetone (9:1 v/v) for 24 hr. The total extracts were each separated into acid and neutral fractions by solid phase extraction (Aminopropyl Bond Elut; for each sample a new column was prewashed with DCM and DCM/isopropanol (2:1 v/v)). The neutral fraction was recovered with DCM/isopropanol (2:1 v/v) and the acid fraction was subsequently recovered with 2% acetic acid in diethyl ether. The neutral fraction was fractionated further into hydrocarbon, aromatic, ketone/wax ester, alcohol/sterol and polar fractions by thin layer (silica gel 60, 0.25 mm thick: solvent: hexane: ethyl acetate (7:2 v/v + 1% acetic acid), or 'flash' column chromatography using a small column (capacity *ca.* 3 ml, bore 5 mm) with silica gel (0.6 g; Fluka 60, 0.035-0.070 mm particle size, 220-240 mesh) as adorbant. For flash chromatography a solvent system was used where elution with increasingly polar solvents yielded five fractions: (i) hexane 3 ml, containing hydrocarbons, (ii) hexane/DCM 9:1 (v/v) 1.5 ml, (iii) DCM 5.5 ml, containing methyl ketones and wax esters, (iv) DCM/methanol 1:1 (v/v) 3 ml, containing alcohols and sterols, (v) methanol 2.5 ml, containing more polar compounds (Fig. 8.1). A known amount (100 μl, 200 ng μl^{-1} per compound in DCM) of a standard solution (5α-cholestane, 10-nonadecanone, hexadecyl octadecanoate, 5β-pregnan-3-one, 2-hexadecanol, 5β-pregnan-3α-ol and heptadecanoic acid) was added to the peat prior to extraction.

8.4 Lipid Extraction with Water

Freeze dried peat (0.68 g) was added to Milli-Q water (40.8 ml) and magnetically stirred for 20 hr at 20°C. The supernatant was decanted off and centrifuged (3500 rpm, 10 min). The resulting supernatant was filtered and extracted with DCM (3 x 20 ml). This was washed with further DCM (30 ml) and dried over anhydrous sodium sulphate (48 h). The DCM phase was evaporated under reduced pressure at 25°C and the total lipid extract was fractionated by 'flash' column chromatography as above.

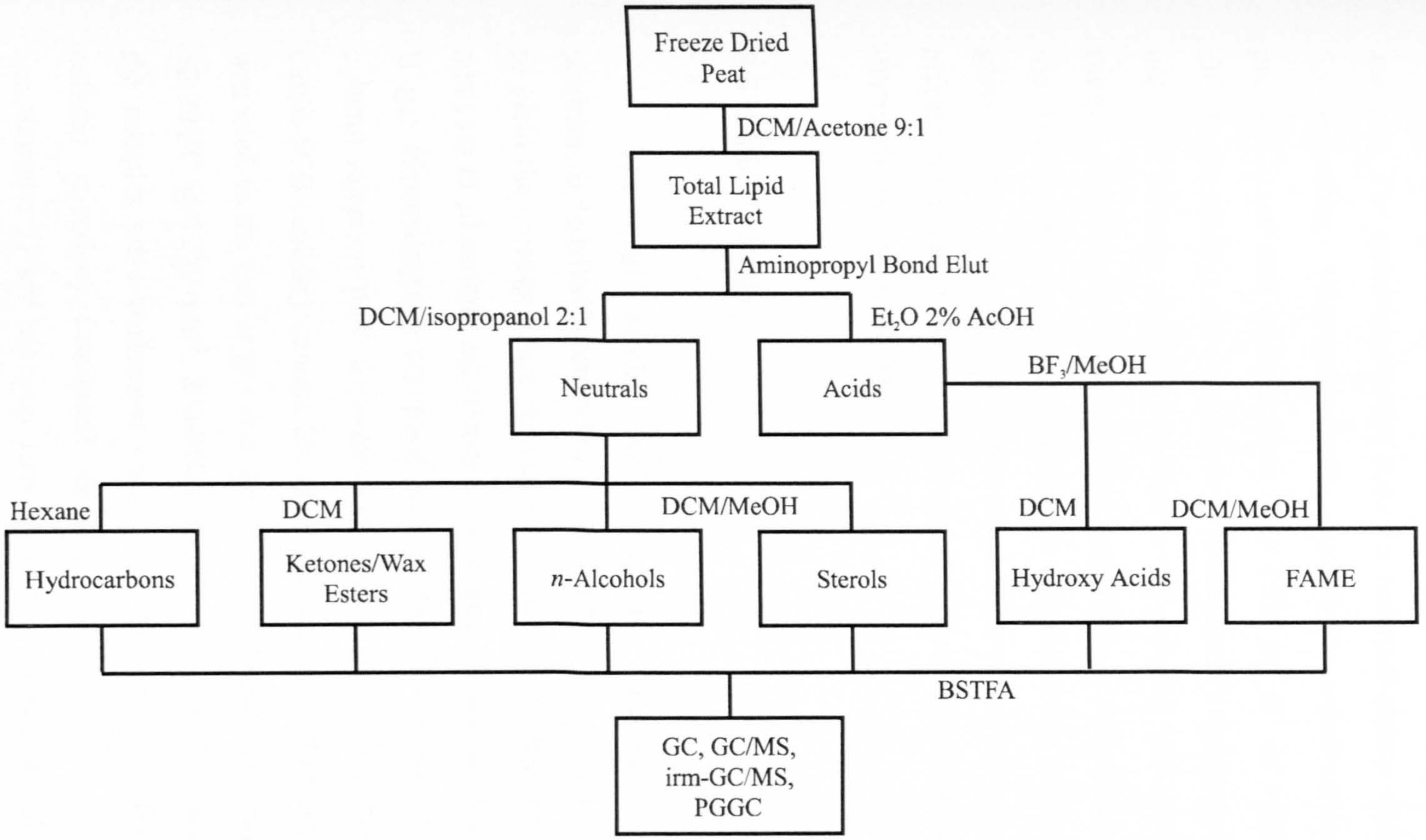

Figure 8.1 Schematic diagram of the analytical protocol.

8.5 Quantification Standards

An internal standard mixture was added to samples prior to extraction. Samples that were going to be used for AMS dating had an external standard added prior to GC analysis. The standard mixture used for non-radiocarbon dating samples comprised of 5α-cholestane, 10-nonadecanone, hexadecyl octadecanoate, 2-hexadecanol, 5β-pregnan-3α-ol and heptadecanoic acid (200 ng μl^{-1} of each compound dissolved in DCM). Standard mixes were allowed to reach room temperature and shaken well before use. The volume of standard added to the samples was dependent on the size of the sample. Typical aliquots added were: peat (100 µl) and plant material (25 µl). After use, the flasks were sealed with PTFE tape and the levels of solvent were marked on the glass in order to establish whether evaporation of solvent occurred during storage in the refridgerator. Hence, it was determined that no significant losses of solvent occured during the period of storage.

8.6 Lipid Analysis

The acid, alcohol and sterol/polar fractions were heated with *N,O*-bis(trimethylsilyl)trifluoroacetamide (BSTFA) + 1% trichloromethylsilane at 70°C (1 h) to yield the corresponding derivative trimethylsilyl ethers prior to analysis by GC. GC analyses (1 µl sample injections) were undertaken using a Hewlett-Packard 5890 series II gas chromatograph equipped with a flame ionisation detector (FID) and an on-column injection port. Separation of compounds was achieved using a fused silica CPSil-5CB capillary column (50 m x 0.32 mm i.d.; film thickness 0.12 µm). Hydrogen was used as the carrier gas and the GC oven temperature was programmed as follows: 50-200°C @ 12°C min^{-1}, 200-300°C @ 3°C min^{-1}, 300°C (20 min). GC/MS analyses of the samples were performed on a Carlo Erba Mega 5160 gas chromatograph (on-column injection) interfaced directly with a Finnigan 4500 quadrupole mass spectrometer (70eV electron ionisation, source temperature 170°C, 1 scan s^{-1}). The column and temperature program were the identical to those used for GC analyses. Helium was used as the carrier gas. Some total lipid and neutral extracts were derivatised with BSTFA and analysed by GC using a capillary column (DB-1; J&W Scientific; 15 m x 0.32 mm i.d., 0.10 µm film thickness). The components were eluted

using hydrogen as carrier gas with a temperature program as follows: 50°C (2 min), 50-350 @ 10°C min^{-1}, 350°C (10 min).

8.7 Hydrolysis of Plant Material

Intact *E. angustifolium* and *E. vaginatum* plants were taken from the surface of Bolton Fell Moss in 1998. These plants were then separated into aerial and subterranean parts and air dried. The resulting material was powdered in a mortar and pestle so that it passed through a 0.5 mm sieve and Soxhlet extracted with DCM/acetone (9:1 v/v, 24 h). The remaining Soxhlet extracted plant material, (~0.02 g + 25 µl of standard mix (5*n*-pentylresorcinol, 5α-cholestane, 10-nonadecanone, heptadecanoic acid, 2-hexadecanol and hexadecyloctadecanoate), 200 ng $µl^{-1}$ per compound), *E. angustifolium* roots, *E. angustifolium* leaves, *E. vaginatum* roots and *E. vaginatum* leaves were saponified with 0.5 M methanolic NaOH solution (3 ml, 100°C, 2 h), acidified to pH 1 (HCl) and 1 ml of double distilled water was added. Free lipids were extracted with DCM (3 x 2 ml) and the organic extracts were combined and passed through an anhydrous $MgSO_4$ column. The solvent was removed under a gentle stream of nitrogen and half of the resulting lipids were eluted (aminopropyl Bond Elut cartridge) with DCM/isopropanol and diethyl ether + 2% AcOH to separate neutrals and acids, respectively. These were then derivatised with BSTFA (70°C, 1 h) and analysed by GC and GC/MS.

8.8 Separation of Cyclic and Acyclic Compounds

The alcohol/sterol fraction was separated into two fractions by urea adduction. The alcohol/sterol fraction was dissolved in 1.5 ml hexane/acetone (2:1 v/v) and a warmed (50°C), saturated solution of urea in MeOH (1 ml) was added to it dropwise with agitation. The mixture was centrifuged (3000 rpm, 2 min) and the supernatant decanted off. The remaining crystals were washed with DCM (0.5 ml), centrifuged (3000 rpm, 2 min) and the solvent added to the supernatant. The resulting solution was adducted twice more as above and the final solution was passed through a defatted cotton wool plug. To this double distilled water (5 ml) was added, extracted with DCM (3 x 2 ml) and the organic layer passed through a Na_2SO_4 (~0.5 cm^3) column to yield the non-adducted fraction (cyclic compounds). The crystals were combined, double

distilled water (5 ml) added and extracted as above to yield the adducted fraction (acyclic compounds)

8.9 Separation of Hydroxy Acids and FAMES

The acid fraction was derivatised with BF_3/MeOH (1 ml, 60°C, 1 hr), the reaction mixture was quenched with water (5 ml) and extracted with DCM (3 x 2 ml). The solvent was removed and the resulting residue redissolved in 1 ml DCM which was put onto a small column (capacity *ca.* 3 ml, bore 5 mm) with silica gel (0.6 g; Fluka 60, 0.035-0.070 mm particle size, 220-240 mesh) as adorbant and eluted with 4.5 ml DCM to yield FAME's and then a further 5 ml of DCM/MeOH (1:1 v/v) to yield hydroxy methyl esters.

8.10 Isotope Ratio Monitoring-Gas Chromatography-Mass Spectrometry (irm-GC/MS)

The sterol fraction was analysed using a Varian 3400 GC coupled, via a combustion interface (copper and platinum wires (0.1 mm o.d.) in an alumina reactor (0.5 mm i.d.) maintained at a constant temperature of 860°C), to a Finnigan MAT Delta-S isotope ratio mass spectrometer. The GC column was a fused silica capillary column (BP-1; Chrompack; 50 m x 0.32 mm i.d., 0.25 μm film thickness). The GC temperature program was identical to that used for GC of the sterol fraction. All samples were analysed in triplicate.

8.11 Derivatisation of Compounds for Preparative Gas Chromatography

Compounds to be separated by PCGC were derivatised with 100 μl acetic anhydride/ 100 μl pyridine (60°C, 15 min) for alcohols, sterols and hydroxy methyl esters to produce the corresponding acetates and 1 ml BF_3/MeOH (70°C, 1 hr) for acids to produce methyl esters.

8.12 Preparative Gas Chromatography

Single compounds were separated by PCGC. The system consists of a Hewlett-Packard 5890 series II GC equipped with a FID, on-column injection port and a HP 7673A autoinjector, a zero-dead-volume effluent splitter (49:1), heated transfer capillary (300°C) and a Gerstel preparative trapping device (Figs. 8.2-4). The preparative trapping device consists of an eight-port zero-dead-volume valve in a heated interface (300°C) and seven 500 µl glass traps (six sample traps and a waste trap) at room temperature. Before each preparative sequence the system was tested for leaks by manually opening each trap to a flow meter. A carrier gas pressure of 10 psi was used and the time taken for 1 cm^3 of He to flow out of the system was measured to determine leaks in the system. Compounds were separated using a "megabore" fused silica capillary column (DB1; J&W Scientific; 30 m x 0.53 mm i.d., 0.5 µm film thickness). Helium was used as the carrier gas and the GC oven temperature was programmed as follows: 50(1)-220°C @ 12°C min^{-1}, 220-300°C @ 4°C min^{-1}, 300°C (10 min) for sterols, FAMEs and hydroxy acids, 50(1)-220°C @ 12°C min^{-1}, 220-300°C @ 4°C min^{-1}, 300°C (7 min) for alcohols and 50(1)-230°C @ 15°C min^{-1}, 230-300°C @ 4°C min^{-1}, 300°C (3 min) for hydrocarbons. Six GC runs were performed before every preparative sequence to assign trapping windows for the target compounds. These windows were based on the average over the six runs and were continuously monitored and adjusted over the preparative sequence to prevent drifting. Preparative sequences consisted of 50-100 repeated injections to collect sufficient quantities of material for AMS. After isolation, the glass tubes containing the trapped components were detached, and the contents were recovered by addition of hexane (1.5 ml) and transferred to 2 ml glass vials (of which an aliquot (10 µL) was removed and transferred to a GC autosampler vial for determination of purity and yield). The solvent was removed under a stream of nitrogen, the residue redissolved in 2 x 50 µL hexane and transferred to tin capsules using the "Russian Doll" technique. A large pressed tin capsule (8 x 5 mm) was opened out and a smaller opened tin capsule (5 x 3.5 mm) placed inside, into which a small amount of tin powder was added so as to cover the bottom of the capsule. The compounds were then transferred to the capsules dropwise from a syringe and each drop was dried under a very gentle stream of nitrogen before the next drop was added. When all the hexane had been removed the capsules were closed, compressed to remove all the air and placed in clean vials ready for submission to the AMS system. Prior to trapping compounds the

glass traps were flushed through with acetone, DCM and hexane and then placed in a furnace (450°C, 2 h) to remove any contamination.

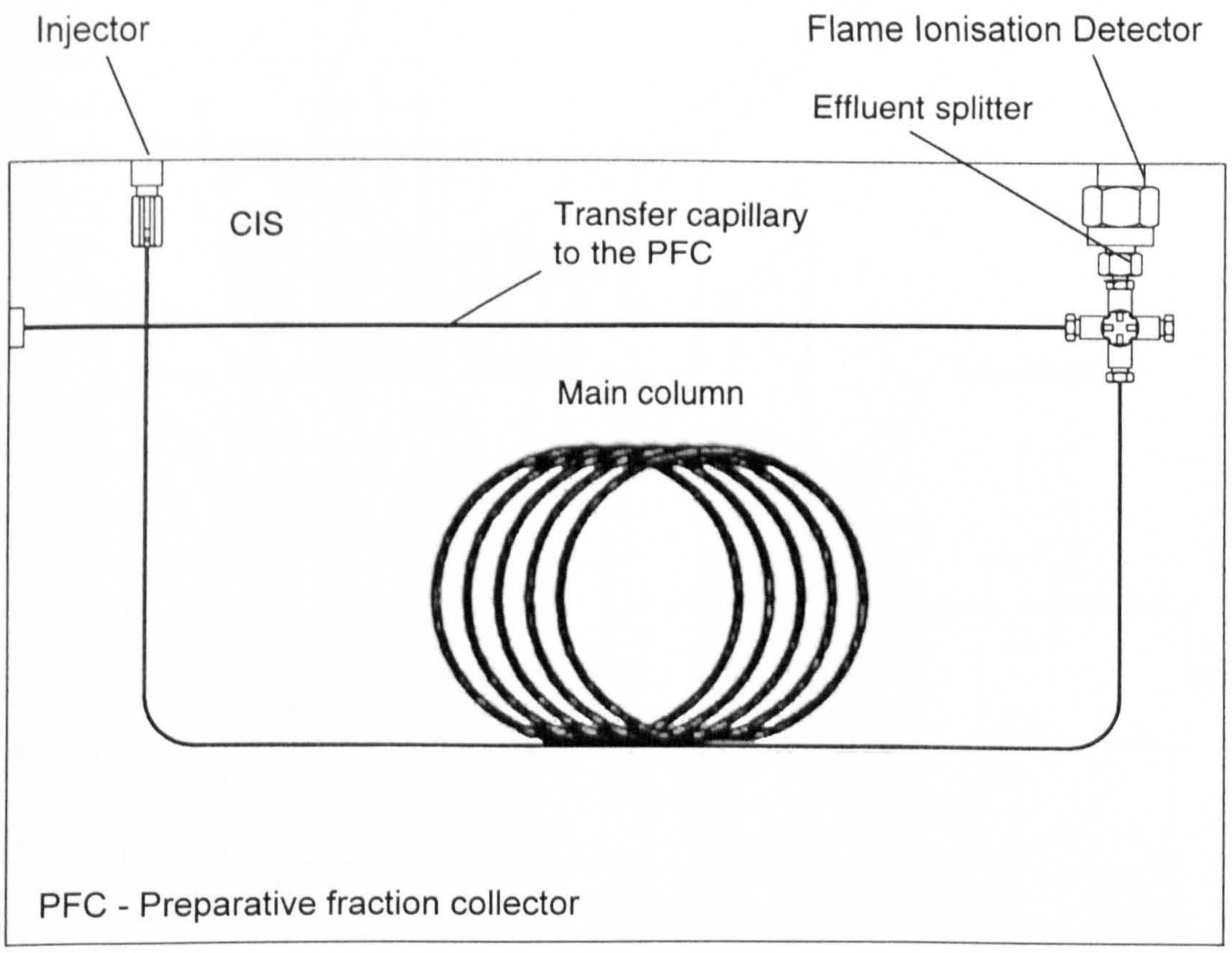

Figure 8.2 PCGC oven showing 49:1 effluent splitter

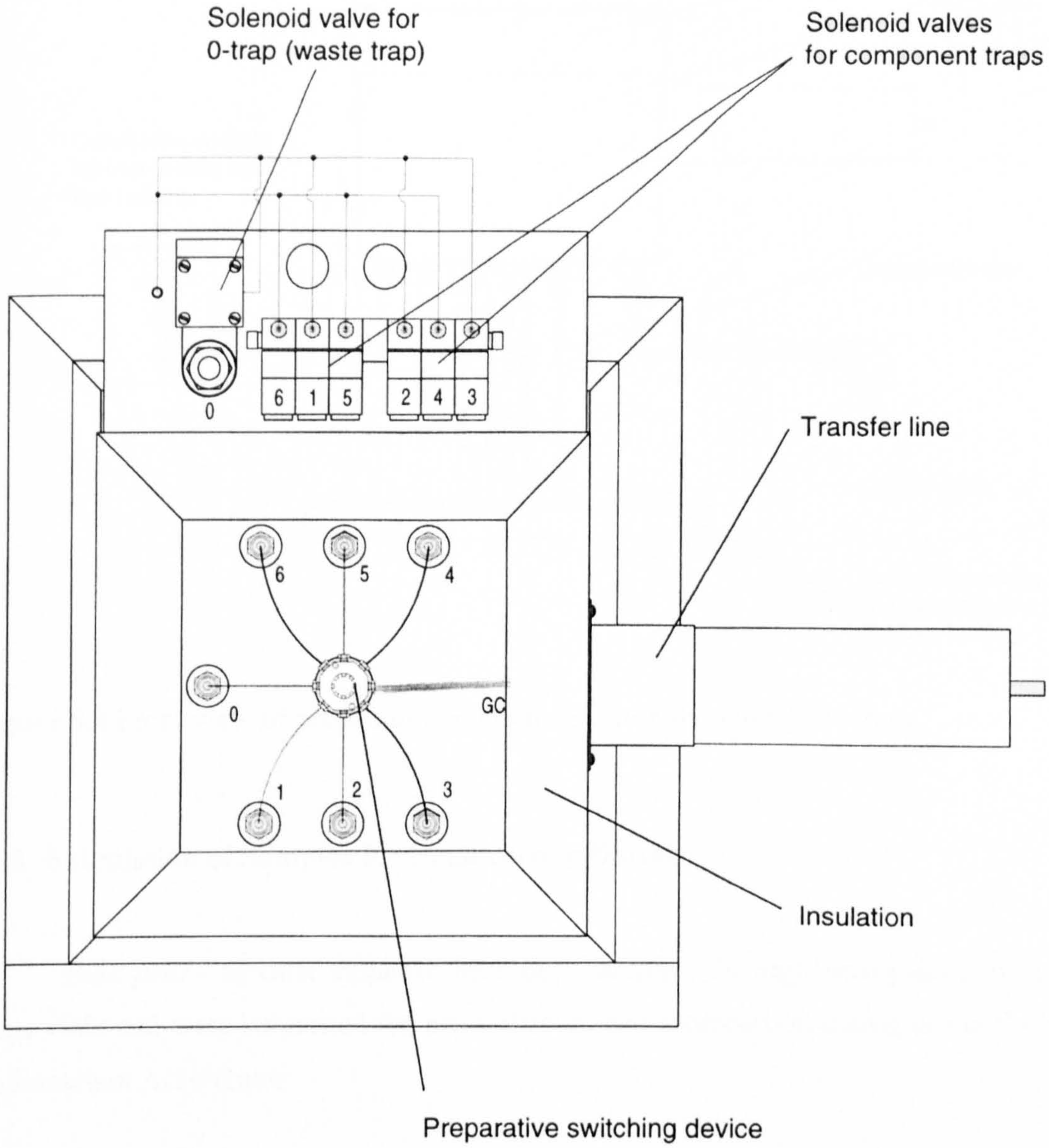

Figure 8.3 Top view of preparative fraction collector.

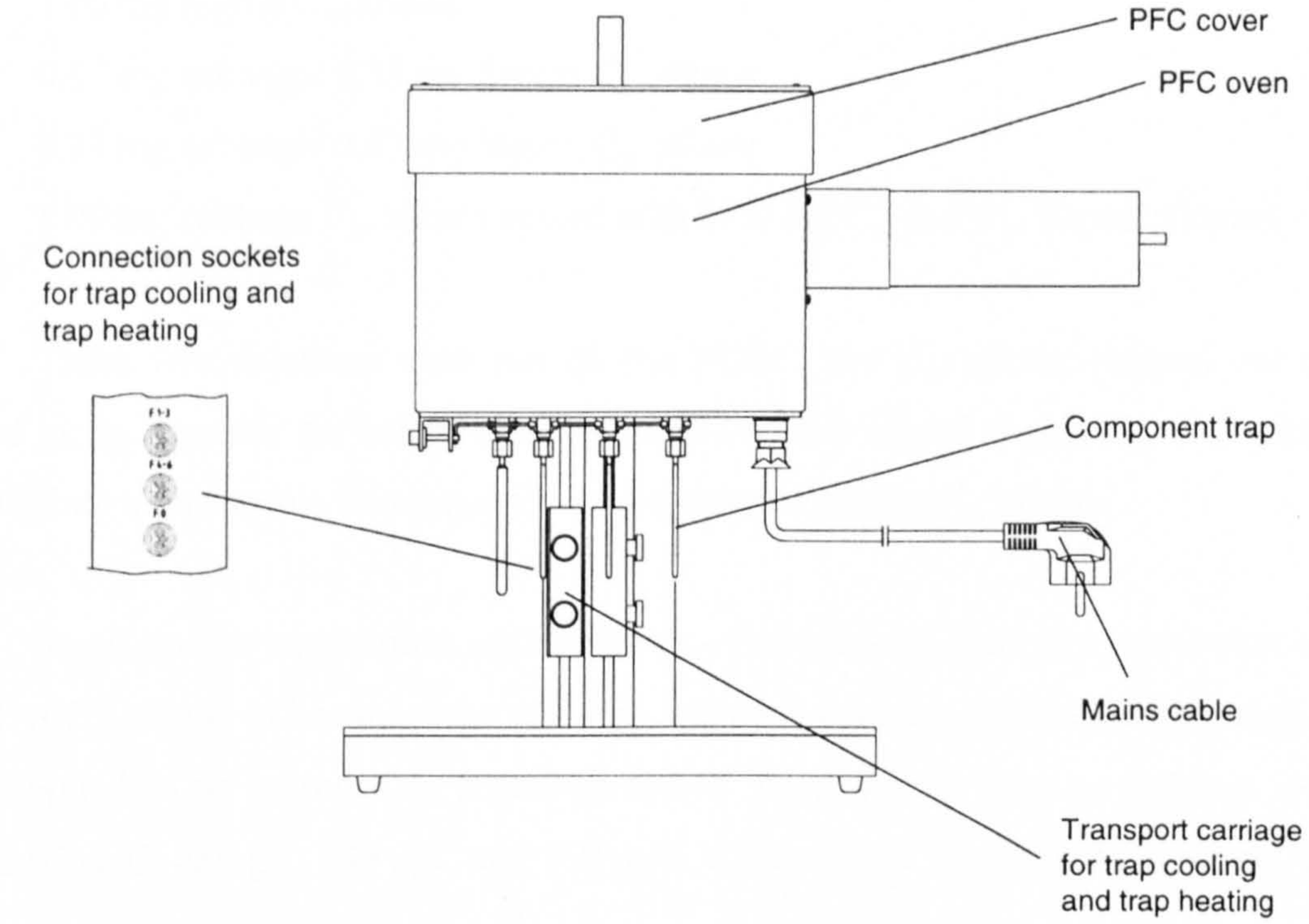

Figure 8.4 Front view of preparative fraction collector showing glass traps.

8.13 Submission of Samples for Radiocarbon Dating

Bulk peat - Soxhlet extracted bulk peat samples (20 mg) were placed in clean glass vials and were submitted for pre-treatment and radiocarbon dating at the Oxford Radiocarbon Accelerator.

Replicability of PCGC samples - Cabbage leaves *Brassica oleracea* (98.84 g) were washed with 400 ml of hexane and the resulting solution was evaporated to dryness on a rotary evaporator. The resulting lipid was then dissolved in 1 ml of hexane and divided into 5 equal portions, of which each were fractionated using a small column (capacity *ca.* 3 ml, bore 5 mm) with silica gel (0.6 g; Fluka 60, 0.035-0.070 mm particle size, 220-240 mesh) as adsorbant and eluted with 3 ml of hexane. The resulting extracts were combined and the quantity of *n*-C_{29} alkane established by coinjection with 5α-cholestane on the GC. Together with *n*-alkanes (Sigma) *n*-nonacosane, *n*-triacontane and *n*-octacosane, five 250 μl solutions of hydrocarbons were prepared:

1.00 mg cabbage C_{29} alkane

1.00 mg Sigma C_{29} alkane

0.67 mg cabbage/ 0.33 mg Sigma C_{29} alkane

0.33 mg cabbage/ 0.67 mg Sigma C_{29} alkane

1.00 mg cabbage C_{29} alkane spiked with 1.00 mg C_{28} and C_{30} Sigma alkanes.

These five solutions were run on the PCGC, the C_{29} alkane trapped out and placed in tin capsules for submission for AMS. Also 1 mg of Sigma C_{29} was placed directly into a tin capsule for comparison with prepped Sigma C_{29} alkane.

Small sample combustion rig standards - Solutions of modern cocoa butter and 'dead' *n*-C_{18} alkane in hexane were made up and approximate quantities (in μg carbon) were applied to tin capsules as described above. The samples were as follows: *n*-C_{18} alkane 50 μgC, 75 μgC, 100 μgC and 150 μgC. Cocoa butter 50 μgC, 100 μgC and 150 μgC.

8.14 Treatment of Contamination

After separation on PCGC all samples were handled in a "clean" room specifically designed for the handling of compounds to be submitted for AMS radiocarbon dating.

REFERENCES

Aaby, B., Jacobsen, J., and Jacobsen, O. S. (1979). ^{210}Pb dating and Pb deposition in the ombrotrophic peat bog, Draved Mose, Denmark. *Danmarks Geologiske Undersøgdse (Arbog 1978)*, 45-68.

Appleby, P. G., Nolan, P. J., Oldfield, F., and Richardson, N. (1988). ^{210}Pb dating of lake sediments and ombrotrophic peats by gamma essay. *Science of the Total Environment* **69**, 157-177.

Baker, E. A. (1982). Chemistry and morphology of plant epicuticular waxes. *In* "The Plant Cuticle" (D. F. Cutler, Ed.), pp. 139-166. Academic Press.

Barber, K. E. (1984). A large capacity Russian-pattern sediment sampler. *Quaternary Newsletter* **44**, 28-31.

Barber, K. E. (1985). Peat stratigraphy and climatic changes: Some speculations. *In* "The Climatic Scene: Essays in Honour of Gordon Manley." (M. J. Tooley, and G. M. Sheail, Eds.), pp. 175-185. Allen and Unwin, London.

Barber, K. E. (1993). Peatlands as scientific archives of past biodiversity. *Biodiversity and Conservation* **2**, 474-489.

Barber, K. E., Chambers, F. M., and Maddy, D. (1994a). Sensitive high-resolution records of Holocene palaeoclimate from ombrotrophic bogs. *In* "Palaeoclimate of the Last Glacial/Interglacial Cycle" (B. M. Funnell, and R. L. F. Kay, Eds.). NERC Earth Science Department, Southampton.

Barber, K. E., Chambers, F. M., Maddy, D., Stoneman, R., and Brew, J. S. (1994b). A sensitive high-resolution record of Late Holocene climatic change from a raised bog in Northern England. *The Holocene* **4**, 198-205.

Barber, K. E., Dumayne-Peaty, L, Hughes, P, Mauquoy, D, Scaife, R. (1998). Replicability and variability of the recent macrofossil and proxy-climate record from raised bogs: field stratigraphy and macrofossil data from Bolton Fell Moss, Cumbria, England. *Journal of Quaternary Science* **13,** 515-528.

Barbetti, M. (1980). Geomagnetic strength over the last 50,000 years and changes in the atmospheric ^{14}C concentration: Emerging trends. *Radiocarbon* **22,** 192-199.

Bard, E., Arnold, M., Hamelin, B., TisneratLaborde, N., and Cabioch, G. (1998). Radiocarbon calibration by means of mass spectrometric $^{230}Th/^{234}U$ and ^{14}C ages of corals: An updated database including samples from Barbados, Mururoa and Tahiti. *Radiocarbon* **40**(3), 1085-1092.

Bhattacharyya, P. K., Rao, M. K., Natarajan, R. D., Ramogopal, M., Madyastha, P., and Madyastha, K. M. (1984). Microbial oxidation of sterol side-chains. *Journal of the Indian Chemical Society* **66,** 1-15.

Bieger, T., Abrajano, T. A., and Hellou, J. (1997). Generation of biogenic hydrocarbons during a spring bloom in New Foundland coastal (NW Atlantic) waters. *Organic Geochemistry* **26,** 207-218.

Bigeleisen, J. (1961). Statistical mechanics of isotope effects on the thermodynamic properties of condensed systems. *Journal of Chemical Physics* **34,** 1485-1493.

Bennett, C. L., Beukens, R. P., Clover, M. R., Gove, H. E., Liebert, R. B., Litherland, A. E., and Purser, K. H. (1977). Radiocarbon dating using accelerators: Negative ions provide the key. *Science* **198,** 508-509.

Blackford, J. J., and Chambers, F. M. (1991). Proxy records of climate from blanket mires: Evidence for a Dark Age (1400BP) climatic deterioration in the British Isles. *The Holocene* **1,** 63-67.

Blackford, J. J., and Chambers, F. M. (1993). Determining the degree of peat decomposition for peat-based palaeoclimatic studies. *International Peat Journal* **5,** 7-24.

Bol, R., Huang, Y., Meridith, J. A., Eglinton, G., Harkness, D. D., and Ineson, P. (1996). The ^{14}C age and residence time of organic-matter and its lipid constituents in a stagnohumic gley soil. *European Journal of Soil Science* **47,** 215-222.

Boon, J. J., Rijpstra, W. I. C., De Lange, F., and De Leeuw, J. W. (1979). Black Sea sterol - a molecular fossil for dinoflagellate blooms. *Nature* **277,** 125-127.

Bowman, S. (1990). "Radiocarbon Dating." British Museum Publications, London.

Bradley, R. S. (1996). Dating Methods I. *In* "Quaternary Palaeoclimatology" (R. S. Bradley, Ed.), pp. 47-119. Chapman and Hall, Padstow.

Broecker, W. S., and Bender, M. L. (1972). Age determinations on marine strandlines. *In* "Calibration of hominoid evolution" (W. W. Bishop, and J. A. Miller, Eds.), pp. 19-38. Scottish Academic Press, Edinburgh.

Bronk Ramsey, C. (1995). Radiocarbon calibration and analysis of stratigraphy. The OxCal Program. *Radiocarbon* **37,** 425-430.

Brooks, P. W., Eglinton, G., Gaskell, S. J., McHugh, D. J., Maxwell, J. R., and Philp, R. P. (1976). Lipids of recent sediments. Part II: Branched and cyclic alkanes and alkanoic acids of some temperate lacustrine and sub-tropical lagoonal/tidal flat sediments. *Chemical Geology* **18,** 21-38.

Burr, G. S., Beck, J. W., Taylor, F. W., Recy, J., Edwards, R. L., Cabioch, G., Correge, T., Donahue, D. J., and O'Malley, J. M. (1998). A high-resolution radiocarbon calibration between 11,700 and 12,400 calendar years BP derived from ^{230}Th ages of corals from Espiritu Santo Island, Vanuatu. *Radiocarbon* **40,** 1093-1105.

Chaffee, A. L., and Johns, R. B. (1983). Polycyclic aromatic-hydrocarbons in Australian coals. 1. Angularly fused pentacyclic triaromatic and tetraaromatic components of Victorian brown coal. *Geochimica et Cosmochimica Acta* **47,** 2141-2155.

Clymo, R. S. (1984). The limits to peat bog growth. *Proceedings of the Royal Society of London Series B-Biological Sciences* **303,** 605-654.

Costagnoli, G., and Lal, D. (1980). Solar modulation effects in terrestrial production of ^{14}C. *Radiocarbon* **22,** 133-158.

Crozaz, G., and Langway, C. C. J. (1966). Dating Greenland firn-ice cores with ^{210}Pb. *Earth and Planetary Science Letters* **1,** 194-196.

Crozaz, G., Picciotto, E., and De Breuck, W. (1964). Antarctic snow chronology with Pb-210. *Journal of Geophysical Research* **69,** 2597-2604.

Dastillung, M., and Albrecht, P. (1977). Δ^2-sterenes as diagenetic intermediates in sediments. *Nature* **269,** 678-679.

Dastillung, M., Albrecht, P., and Ourisson, G. (1980a). Aliphatic and polycyclic alcohols in sediments: Hydroxylated derivatives of hopane and of 3-methylhopane. *Journal of Chemical Research* **S,** 168-169.

Dastillung, M., Albrecht, P., and Ourisson, G. (1980b). Aliphatic and polycyclic ketones in sediments: C_{27}-C_{35} ketones and aldehydes of the hopane series. *Journal of Chemical Research* **S,** 166-167.

Dehmer, J. (1993). Petrology and organic geochemistry of peat samples from a raised bog in Kalimantan (Borneo). *Organic Geochemistry* **20,** 349-362.

Dehmer, J. (1995). Petrological and organic geochemical investigation of recent peats with known environments of deposition. *International Journal of Coal Geology* **28,** 111-138.

Del Rio, J. C., Gonzalez-Vila, F. J., and Martin, F. (1992). Variation in the content and distribution of biomarkers in two closely situated peat and lignite deposits. *Organic Geochemistry* **18,** 67-78.

Van Dorsselaer, A., Albrecht, P., and Ourisson, G. (1977). Identification of novel 17-α(H)-hopanes in shales, coals and petroleum. *Bulletin de Societe Chimique de France* **2,** 165-170.

Dupont, L. M. (1986). Temperature and rainfall variation in the late Holocene based on comparative palaeoecology of a hummock and a hollow. *Review of Palaeobotany and Palynology* **48,** 71-159.

Edwards, R. L., Beck, J. W., Burr, G. S., Donahue, D. J., Chappell, J. M. A., Bloom, A. L., Druffel, E. R. M., and Taylor, F. W. (1993). A large drop in atmospheric $^{14}C/^{12}C$ and reduced melting in the Younger Dryas, documented with ^{230}Th age of corals. *Science* **260,** 962-968.

Eglinton, T. I., Aluwihare, L. I., Bauer, J. E., Druffel, E. R. M., and McNichol, A. P. (1996). Gas-chromatographic isolation of individual compounds from complex matrices for radiocarbon dating. *Analytical Chemistry* **68,** 904-912.

Eglinton, T. I., BenitezNelson, B. C., Pearson, A., McNichol, A. P., Bauer, J. E., and Druffel, E. R. M. (1997). Variability in radiocarbon ages of individual organic compounds from marine sediments. *Science* **277,** 796-799.

Ekman, R., and Karunen, P. (1982). Esterified long-chain hydroxy-acids in green and senescent parts of the peat moss *Sphagnum fuscum*. *Phytochemistry* **21,** 121-123.

El-Daoushy, F., Tolonen, K., and Rosenberg, R. (1982). ^{210}Pb and moss-increment dating of two Finnish *Sphagnum* hummocks. *Nature* **296,** 429-431.

Ensminger, A. (1977). Evolution de composes polycycliques sedimentaires. *PhD Thesis*. Louis Pasteur University, Strasbourg.

Evershed, R. P., and Connolly, R. C. (1994). Post-mortem transformations of sterols in bog body tissues. *Journal of Archaeological Science* **21,** 577-583.

Farrimond, P., and Flanagan, R. L. (1996). Lipid stratigraphy of a Flandrian peat bed (Northumberland, UK): comparison with the pollen record. *The Holocene* **6,** 69-74.

Farrimond, P., Taylor, A., and Telnaes, N. (1998). Biomarker maturity parameters: the role of generation and thermal degradation. *Organic Geochemistry* **29,** 1181-1197.

Ficken, K. J., Barber, K. E., and Eglinton, G. (1998). Lipid biomarker, $\delta^{13}C$ and plant macrofossil stratigraphy of a Scottish montane peat bog over the last two millennia. *Organic Geochemistry* **28,** 217-237.

Fieser, L. F., and Fieser, M. (1959). "Steroids." Reinhold Publishing Corporation, New York.

Foss, P. (1987). The Distribution and Formation of Irish Peatlands. *In* "The IPCC Guide to Irish Peatlands" (C. O'Connel, Ed.). Irish Peatland Conservation Council, Dublin.

Fowler, A. J., Gillespie, R., and Hedges, R. E. M. (1986a). Radiocarbon dating of sediments. *Radiocarbon* **28,** 441-451.

Fowler, A. J., Gillespie, R., and Hedges, R. E. M. (1986b). Radiocarbon dating of sediments by accelerator mass-spectrometry. *Physics of the Earth and Planetary Interiors* **44,** 15-20.

Godwin, H. (1981). "The Archives of the Peat Bogs." Cambridge University Press, Cambridge.

Goodman, K., and Brenna, J. (1994). Curve-fitting for recovery of high accuracy and precision isotope ratios in gas chromatography-combustion isotope ratio mass spectrometry. *Analytical Chemistry* **66,** 1294-1301.

Hammond, A. P., Goh, K. M., Tonkin, P. J., and Manning, M. R. (1991). Chemical pretreatments for improving the radiocarbon-dates of peats and organic silts in a gley podzol environment - Grahams Terrace, North Westland. *New Zealand Journal of Geology and Geophysics* **34,** 191-194.

Hare, P. E., and Mitterer, R. M. (1968). Laboratory simulation of amino acid diagenesis in fossils. *Carnegie Institution of Washington Yearbook* **67,** 205-208.

Hayes, J., Freeman, K., Popp, B., and Hoham, C. (1990). Compound specific isotopic analyses: A novel tool for reconstruction of ancient biogeochemical processes. *Organic Geochemistry* **16,** 1115-1128.

Hedges, R. E. M. (1991). How Old is Pharaoh's Coffin? *Chemistry Review* **1,** 2-6.

Van Hook, W. (1969). Isotope Separation by Gas Chromatography. *In* "Isotope Effects in Chemical Processes" (R. Gould, Ed.), pp. 99-118. ACS Publications.

Huang, Y. S., Bol, R., Harkness, D. D., Ineson, P., and Eglinton, G. (1996). Postglacial variations in distributions, ^{13}C and ^{14}C contents of aliphatic-hydrocarbons and bulk organic-matter in 3 types of British acid upland soils. *Organic Geochemistry* **24,** 273-287.

Hulme, M., and Barrow, E. (1997). "Climate of the British Isles: Present, past and future." Routledge, London.

Ingram, H. A. P. (1978). Soil layers in mires: Function and terminology. *Journal of Soil Science* **29,** 224-227.

Innes, H. E., Bishop, A. N., Head, I. M., and Farrimond, P. (1997). Preservation and diagenesis of hopanoids in Recent lacustrine sediments of Priest Pot, England. *Organic Geochemistry* **26,** 565-569.

Ives, A. J., and O'Neil, A. N. (1958). The chemistry of peat. Part 1. The sterols of peat moss (*Sphagnum*). *Canadian Journal of Chemistry* **36,** 434-439.

Karunen, P., Ekman, R., and Salin, M. (1983). *Sphagnum* mosses as sources of sterols in peat. *In* "International Symposium on Peat Utilisation (Proceedings)" (C. H. Fuchsman, and S. A. Spigarelli, Eds.), pp. 487-493. Bemidji State University Centre of Environmental Studies, Bemidji.

Karunen, P., and Salin, M. (1980). Lipid composition of *Sphagnum fuscum* shoots of various ages. *Kemia-Kemi (Finnish Chemistry)* **7,** 500-502.

Ketola, M., Luomala, E., Pihlaja, K., and Nyronen, T. (1987). Composition of long-chain fatty compounds and sterols of four milled peat samples from Finnish peatlands. *Fuel* **66,** 600-606.

Kivinen, E., and Pakarinen, P. (1981). Geographical distribution of peat resources and major peatland complex types in the world. *Suomalaisen Tiedeakatemian Toimituksia, Series AIII Geologica-Geographica* **132,** 1-28.

Koide, M., Bruland, K. W., and Golgberg, E. D. (1973). $^{238}Th/^{232}Th$ and ^{210}Pb geochronologies in marine and lake sediments. *Geochimica et Cosmochimica Acta*, 1171-1187.

Kolattukudy, P. E., Croteau, R., and Bruckner, J. S. (1976). Biochemistry of Plant Waxes. *In* "Chemistry and Biochemistry of Natural Waxes" (P. E. Kolattukudy, Ed.), Vol. Publishing Company, pp. 289-347. Elsevier Scientific, Amsterdam.

Korff, S., and Mendell, R. B. (1980). Variation in radiocarbon production in the Earth's atmosphere. *Radiocarbon* **22,** 159-165.

Lehtonen, K., and Ketola, M. (1990). Occurrence of long-chain acyclic methyl ketones in *Sphagnum* and *Carex* peats of various degrees of humification. *Organic Geochemistry* **15,** 275-280.

Lehtonen, K., and Ketola, M. (1993). Solvent-extractable lipids of *Sphagnum*, *Carex*, *Bryales* and *Carex-Bryales* peats - content and compositional features vs. peat humification. *Organic Geochemistry* **20,** 363-380.

Lehtonen, K., Ketola, M., and Pihlaja, K. (1991). Water-soluble lipids in *Carex* and *Sphagnum* peats. *International Journal of Environmental Analytical Chemistry* **43**, 235-244.

Ludwig, B., Hussler, G., Wehrung, P., and Albrecht, P. (1981). C_{26}-C_{29} triaromatic steroid derivatives in sediments and petroleum. *Tetrahedron Letters* **22**, 3313-3316.

Mackenzie, A. S., Hoffmann, C. F., and Maxwell, J. R. (1981). Molecular-parameters of maturation in the Toarcian shales, Paris basin, France. 3. Changes in aromatic steroid hydrocarbons. *Geochimica et Cosmochimica Acta* **45**, 1345-1355.

Mackenzie, A. S., Patience, R. L., Maxwell, J. R., Vandenbroucke, M., and Durand, B. (1980). Molecular parameters of maturation in the Toarcian shales, Paris basin, France. 1. Changes in the configurations of acyclic isoprenoid alkanes, steranes and triterpanes. *Geochimica et Cosmochimica Acta* **44**, 1709-1715.

McLean, J., Rettie, G. H., and Spring, F. S. (1958). Triterpenoids from peat. *Chemistry and Industry*, 1515-1516.

Matveyeva, I. A., and Petrov, A. A. (1992). Petroleum C_{19}-C_{23} steranes. *Petroleum Chemistry* **32**, 360-366.

Matucha, M. (1989). Radioactivity detection in capillary gas chromatography of ^{3}H- and ^{14}C-labelled compounds. *Chromatographia* **217**(11/12), 552-558.

Matucha, M. (1995). Isotope effects in gas chromatography of labelled compounds. *In* "Synthesis and Applications of Isotopically Labelled Compounds." (J. Allen, Ed.), pp. 489-494. Wiley, New York.

Matucha, M., Jokisch, W., Verner, P., and Anders, G. (1991). Isotope effect in gas chromatography-combustion isotope ratio mass spectrometry at low signal levels. *Journal of Chromatography* **588**, 251-258.

Meylan, W., and Howard, P. (1995). Atom/fragment contribution method for estimating octanol/water partition coefficients. *Journal of Pharmaceutical Science* **84**, 83-92.

Nagasawa, M., Bae, M., Tamura, G., and Arima, K. (1969). Microbial transformation of sterols. Part II. Cleavage of sterol side chains by microorganisms. *Agricultural and Biological Chemistry* **33**, 1644-1650.

Nagasawa, M., Watanabe, N., Hashiba, H., Tamura, G., and Arima, K. (1970). Microbial transformations of sterols. Part III. Substrate specificity for cleaving steroid side chains by *Arthrobacter simplex*. *Agricultural and Biological Chemistry* **34**, 798-800.

Nichols, P. D., Volkman, J. R., Palmisano, A. C., Smith, G. A., and White, D. C. (1988). Occurrence of an isoprenoid C_{25} diunsaturated alkene and high neutral lipid content in Antarctic sea-ice diatom communities. *Journal of Phycology* **24**, 90-96.

Nott, C. J. (2000). Biomarkers in ombrotrophic mires as palaeoclimate indicators. *PhD Thesis*. University of Bristol, Bristol.

Nott, C. J., Xie, S., Avsejs, L. A., Maddy, D., Chambers, F. M., and Evershed, R. P. (2000). n-Alkane distributions in ombrotrophic mires as indicators of vegetation change related to climatic variation. *Organic Geochemistry* **31**, 231-235.

Oden, S. (1919). Die huminsauren. *Kolloidchemische Beihefte* **11**, 75.

Ourisson, G., Albrecht, P., and Rohmer, M. (1979). The hopanoids - The palaeochemistry and biochemistry of a group of natural products. *Pure and Applied Chemistry* **51**, 709-729.

Peakman, T. M., Lamb, N. A., and Maxwell, J. R. (1984). Naturally occurring spiro steroid hydrocarbons. *Tetrahedron Letters* **25**, 349-352.

Peters, K. E., and Moldowan, J. M. (1993). "The Biomarker Guide." Prentice-Hall, New Jersey.

Pilcher, J. R., Baillie, M. G. L., Schmidt, B., and Becker, B. (1984). A 7,272-year tree-ring chronology for Western-Europe. *Nature* **312,** 150-152.

Quirk, M. M., Wardroper, A. M. K., Wheatley, R. E., and Maxwell, J. R. (1984). Extended hopanoids in peat environments. *Chemical Geology* **42,** 25-43.

Ricci, M., Merritt, D., Freeman, K., and Hayes, J. (1994). Acquisition and processing of data for isotope-ratio-monitoring mass spectrometry. *Organic Geochemistry* **21,** 561-571.

Ries-Kautt, M., and Albrecht, P. (1989). Hopane-derived triterpenoids in soils. *Chemical Geology* **76,** 143-151.

Riolo, J., and Albrecht, P. (1985). Novel rearranged ring C monoaromatic steroid hydrocarbons in sediments and petroleums. *Tetrahedron Letters* **26,** 2701-2704.

Robinson, N., Cranwell, P. A., Eglinton, G., and Jaworski, G. H. M. (1987). Lipids of four species of freshwater dinoflagellates. *Phytochemistry* **26,** 411-421.

Rohmer, M., Dastillung, M., and Ourisson, G. (1980). Hopanoids from C_{30} to C_{35} in Recent muds - Chemical markers for bacterial activity. *Naturwissenschaften* **67,** 456-458.

Rubinstein, I., Sieskind, O., and Albrecht, P. (1975). Rearranged sterenes in a shale. Occurrence and simulated formation. *Journal of the Chemical Society Perkin Transactions* **1,** 1833-1836.

Seifert, W. K., and Moldowan, J. M. (1981). Palaeoreconstruction by biological markers. *Geochimica et Cosmochimica Acta* **45,** 783-794.

Siegethaler, Y., Heimann, M., and Oeschger, H. (1980). ^{14}C variations caused by changes in the global carbon cycle. *Radiocarbon* **22,** 177-191.

Spurk, M., Friedrich, M., Hofmann, J., Remmele, S., Frenzel, B., Leuschner, H. H., and Kromer, B. (1998). Revisions and extension of the Hohenheim oak and pine chronologies: New evidence about the timing of the Younger Dryas/Preboreal transition. *Radiocarbon* **40,** 1107-1116.

Stuiver, M., and Quay, P. D. (1980). Patterns of atmospheric ^{14}C changes. *Radiocarbon* **22,** 166-176.

Stuiver, M., Reimer, P. J., Bard, E., Beck, J. W., Burr, G. S., Hughen, K. A., Kromer, B., McCormac, G., VanderPlicht, J., and Spurk, M. (1998). INTCAL98 radiocarbon age calibration, 24,000-0 cal BP. *Radiocarbon* **40,** 1041-1083.

Thorarinsson, S. (1981). The application of tephrochronology in Iceland. *In* "Tephra Studies" (S. Self, and R. J. S. Sparks, Eds.), pp. 109-134. D. Reidel, Dordrecht.

Volkman, J. K., Barrett, S. M., Blackburn, S. I., Mansour, M. P., Sikes, E. L., and Gelin, F. (1998). Microalgal biomarkers: A review of recent research developments. *Organic Geochemistry* **29,** 1163-1179.

Volkman, J. K., Kearney, P., and Jeffrey, S. W. (1990). A new source of 4-methyl and 5α(H)-stanols in sediments: prymnesiophyte microalgae of the genus *Pavlova*. *Organic Geochemistry* **15,** 489-497.

de Vries, H. L. (1958). Variation in the concentration of radiocarbon with time and location on Earth. *Koninklijke Nederlandse Akademie van Wetenschappen-Proceedings Series B-Physical Sciences* **61,** 94-102.

Wakeham, S. G., Farrington, J. W., Gagosian, R. B., Lee, C., DeBaar, H., Nigrelli, G. E., Tripp, B. W., Smith, S. O., and Trew, N. M. (1980). Organic matter fluxes from sediment traps in the equatorial Atlantic Ocean. *Nature* **286,** 798-800.

Walton, T. J. (1990). Waxes, Cutin and Suberin. *In* "Methods in Plant Biochemistry" (J. L. Harwood, and J. R. Bowyer, Eds.), Vol. 4, pp. 105-158. Academic Press, London.

White, J. W. C., Ciais, P., Figge, R. A., Kenny, R., and Markgraf, V. (1994). A high-resolution record of atmospheric CO_2 content from carbon isotopes in peat. *Nature* **367,** 153-156.

Zlatkis, A., and Pretorius, V. (1971). "Preparative Gas Chromatography." Wiley-Interscience, New York.

APPENDIX I

Molecular Structures

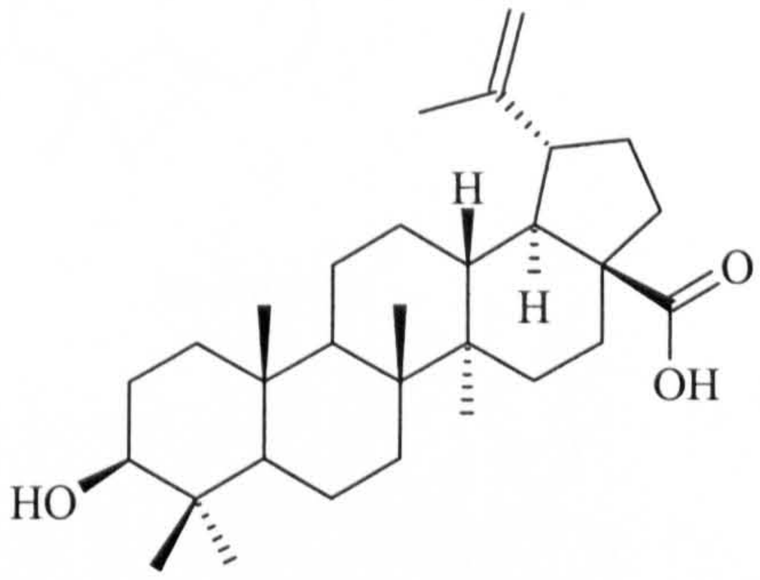

Betulinic acid (3β-hydroxylup-20(29)-en-28-oic acid)

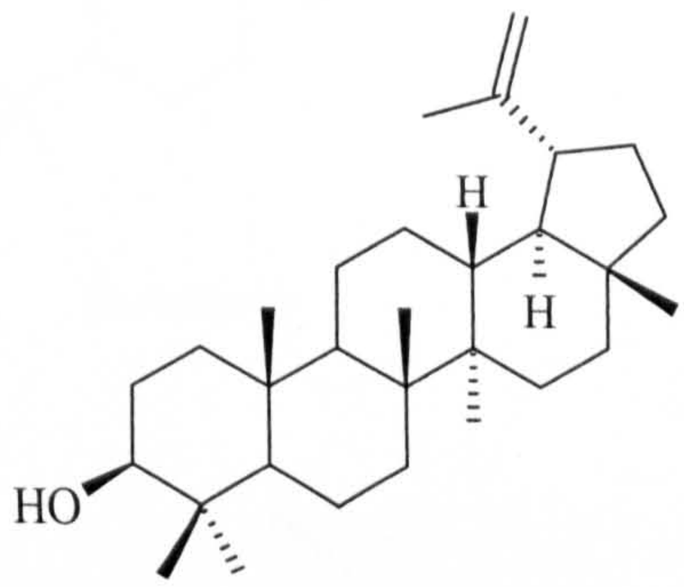

Lupeol (lup-20(29)-en-3β-ol)

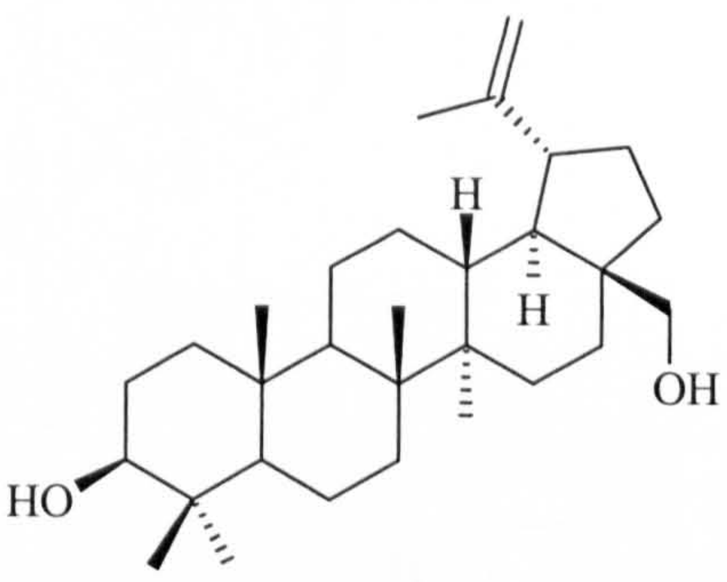

Betulin (lup-20(29)-ene-3β,28-diol)

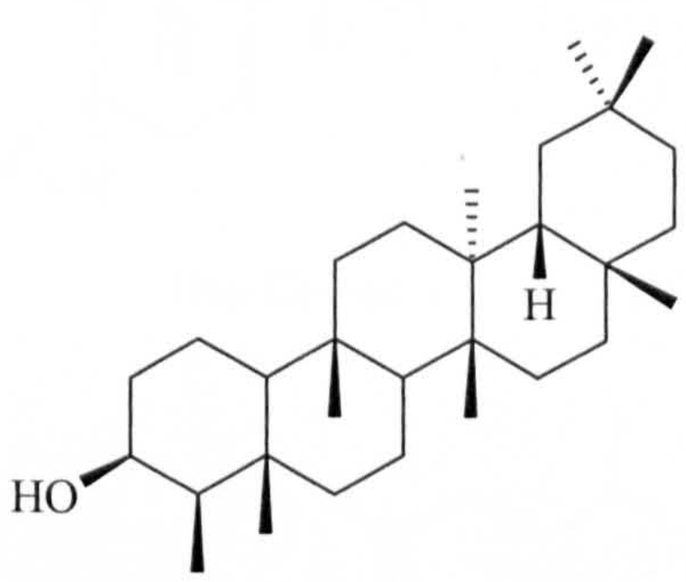

Friedelan-3β-ol

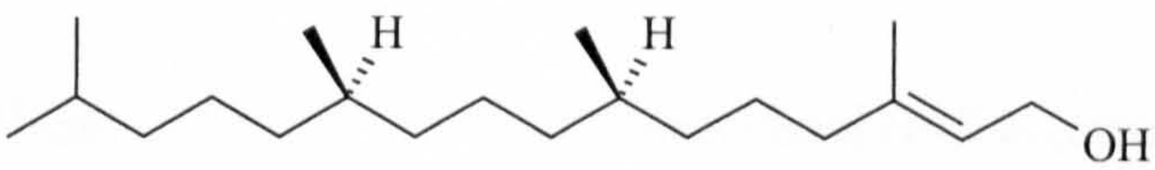

Phytol (3,7,11,15-tetramethylhexadec-2-en-1-ol)

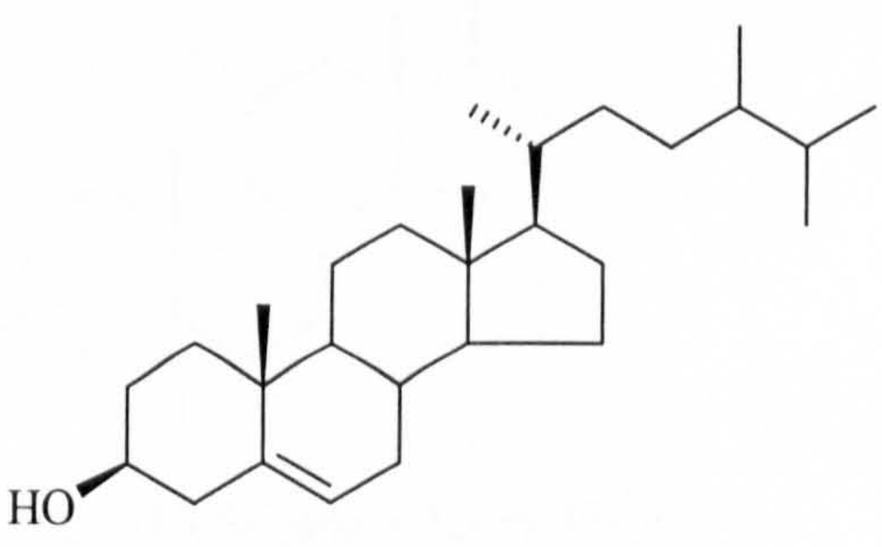

Campesterol (24*R*-ergost-5en-3β-ol)

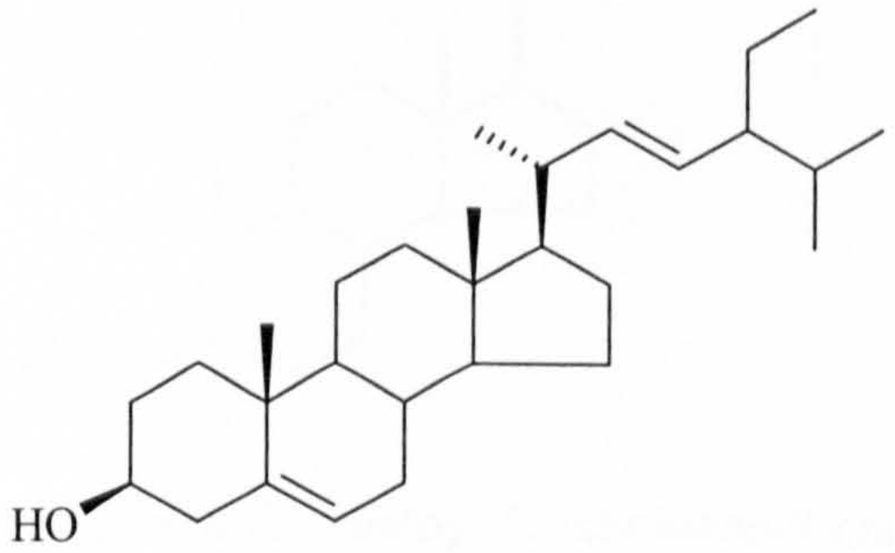

Stigmasterol (22*E*,24*R*-stigmasta-5,22-dien-3β-ol)

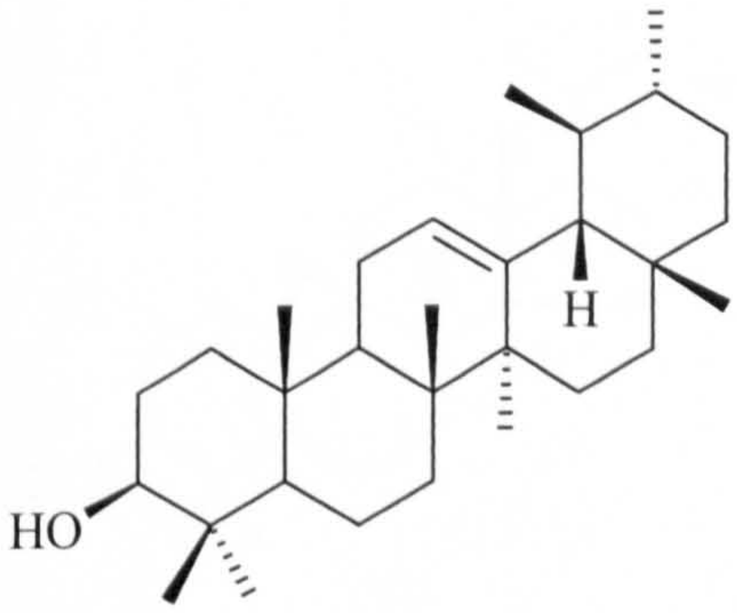

α-Amyrin

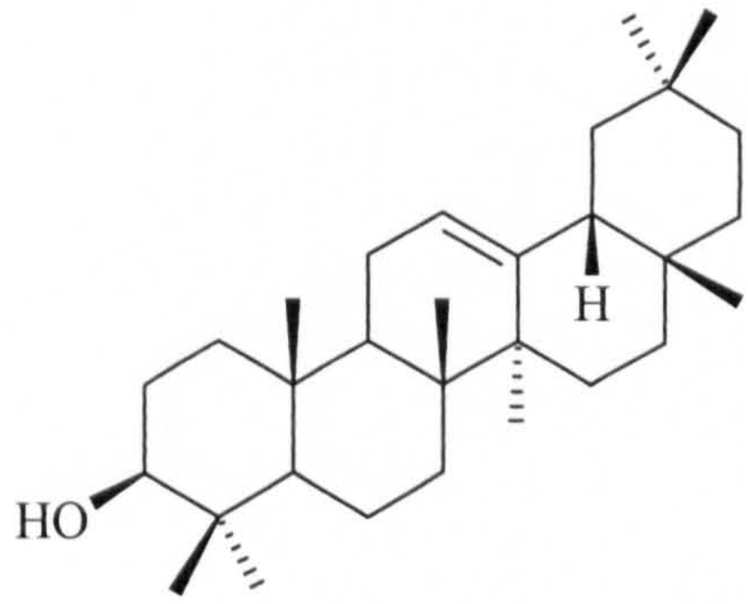

β-Amyrin

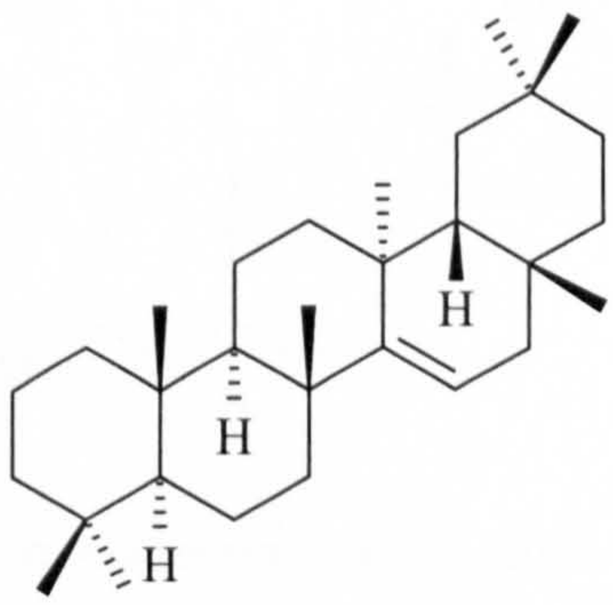

Taraxer-14-ene

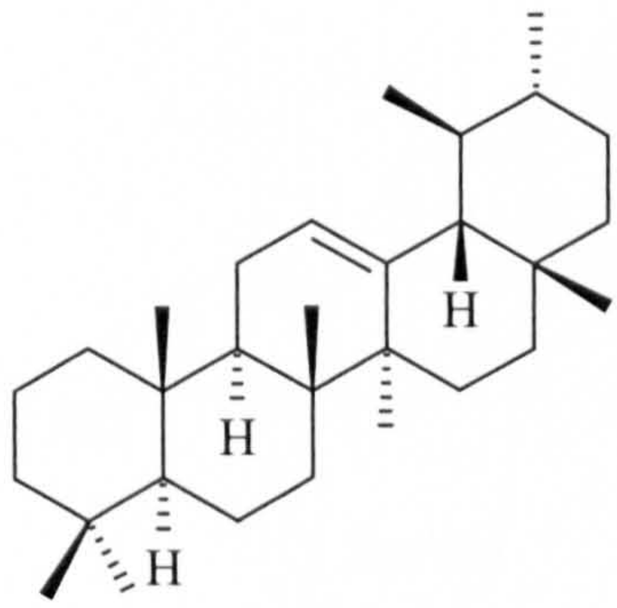

Urs-12-ene

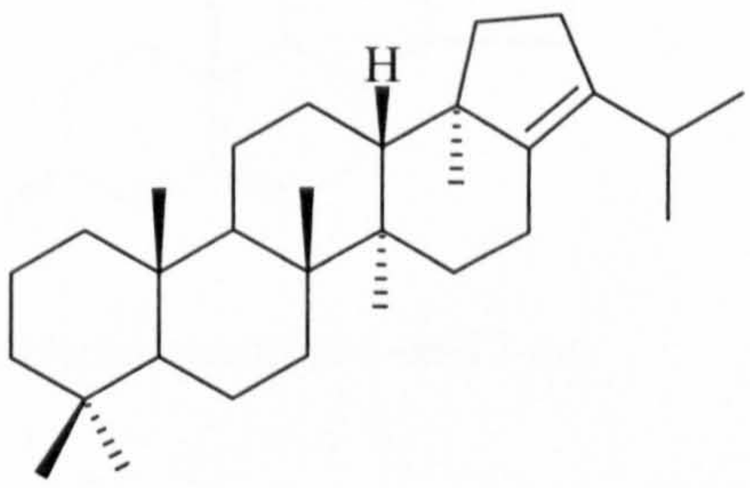

Hop-17(21)-ene

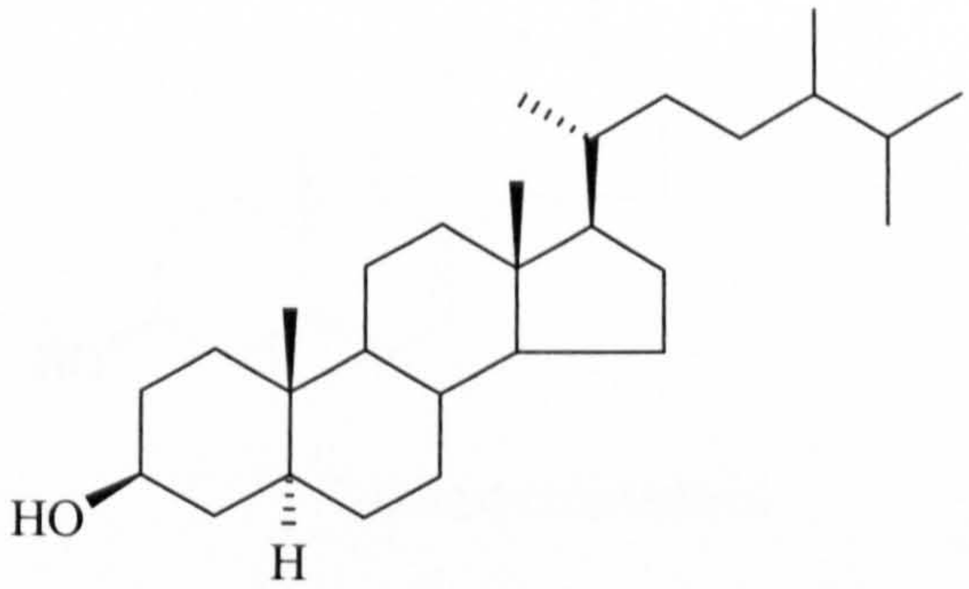

Campestanol (24*R*-ergostan-3β-ol)

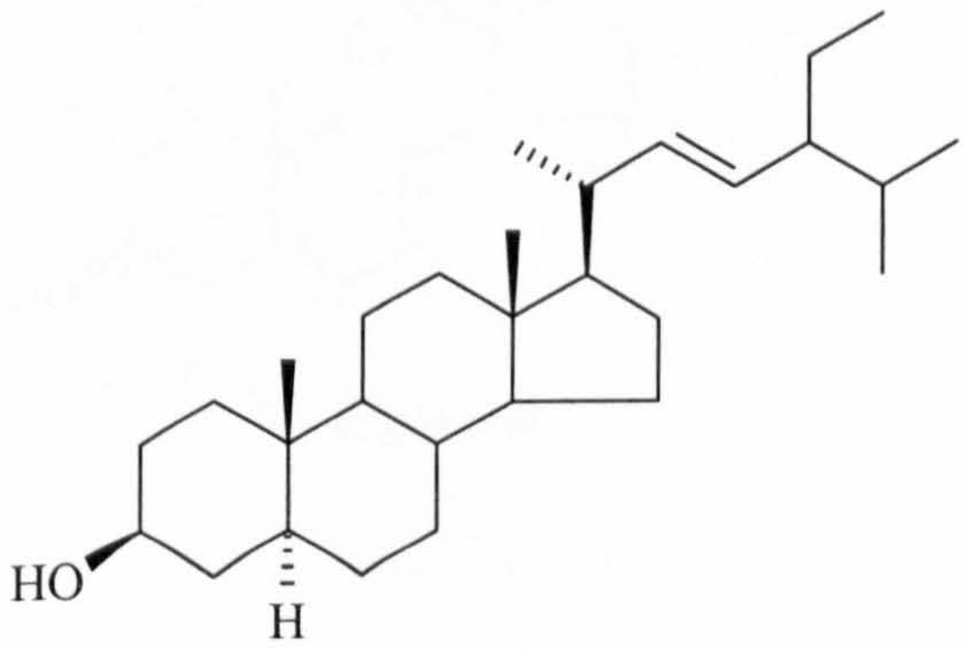

22*E*,24*R*-Stigmast-22-en-3β-ol

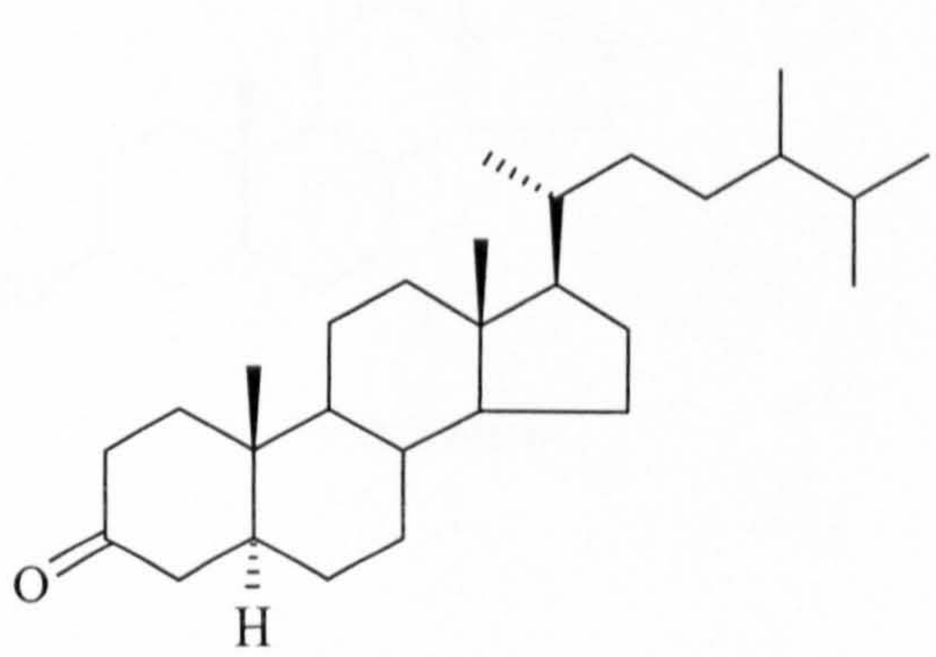

Campesterone (24-methyl-5α-cholestan-3-one)

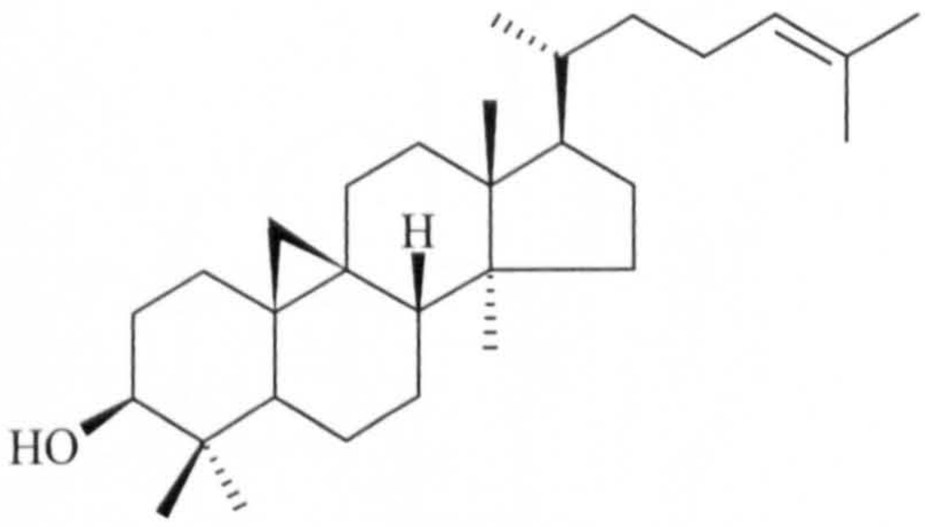

Cycloartenol

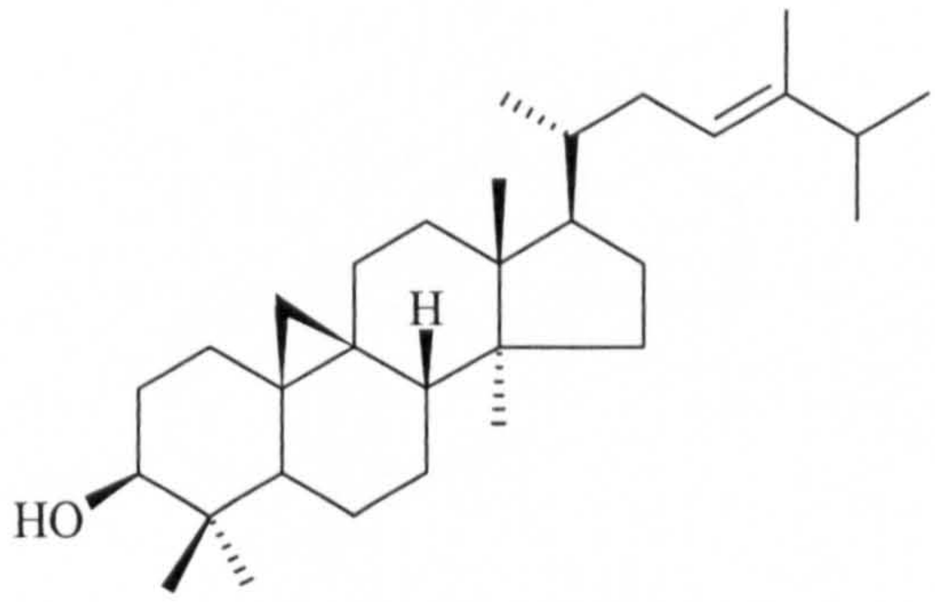

Methyl cycloartenol

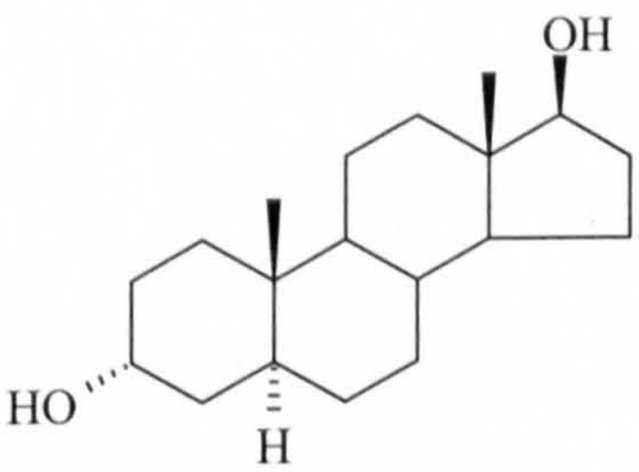

5α-Androstane-3α,17β-diol

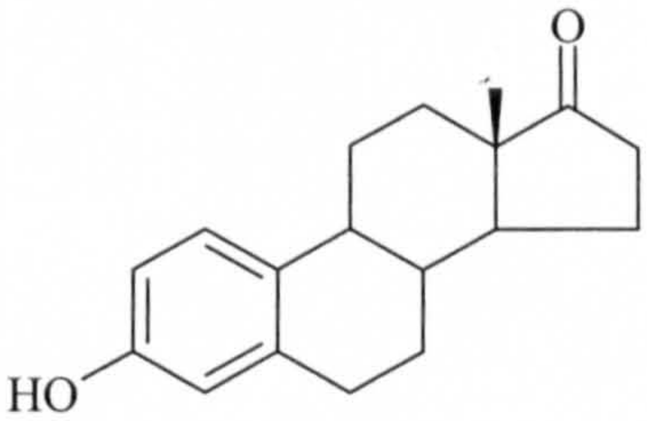

Estrone

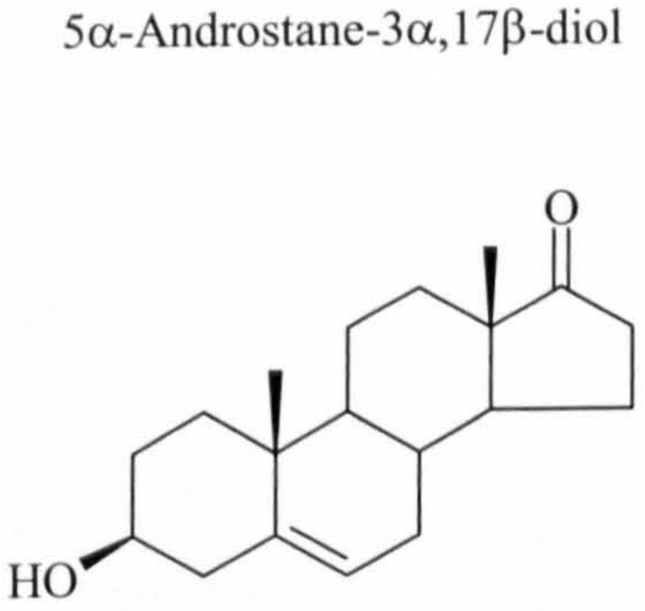

3β-Hydroxyandrost-5-en-17-one

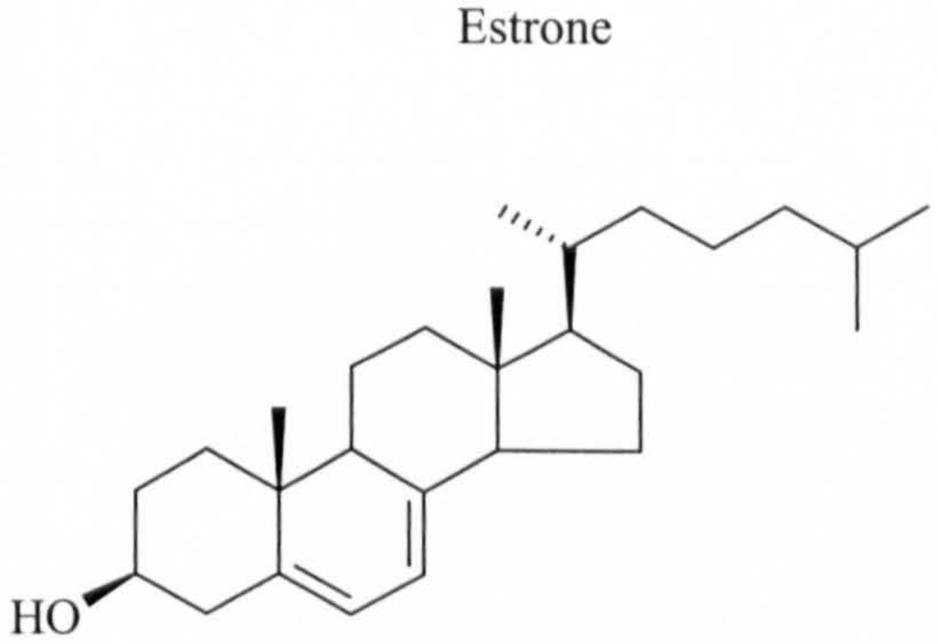

7-Dehydrocholesterol

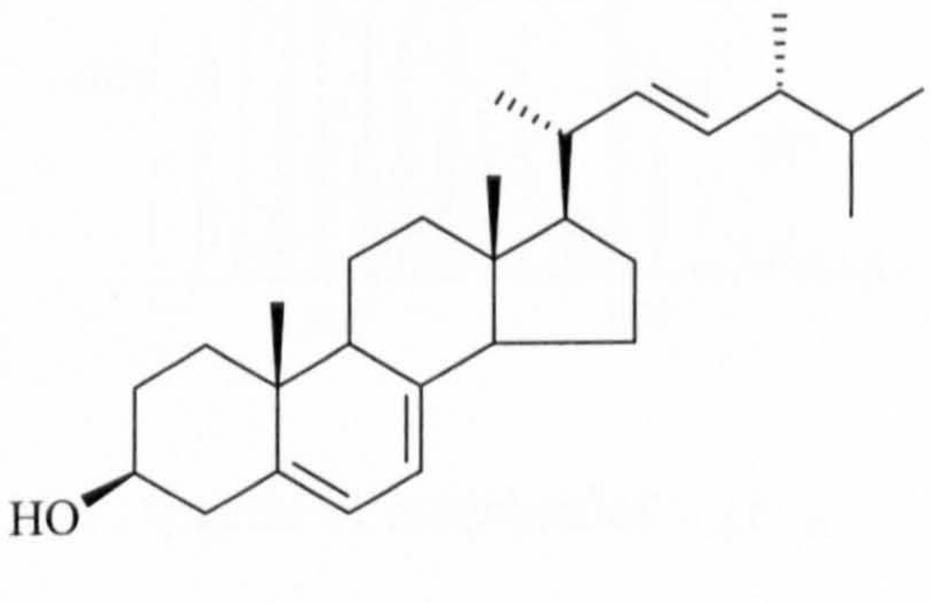

Ergosterol

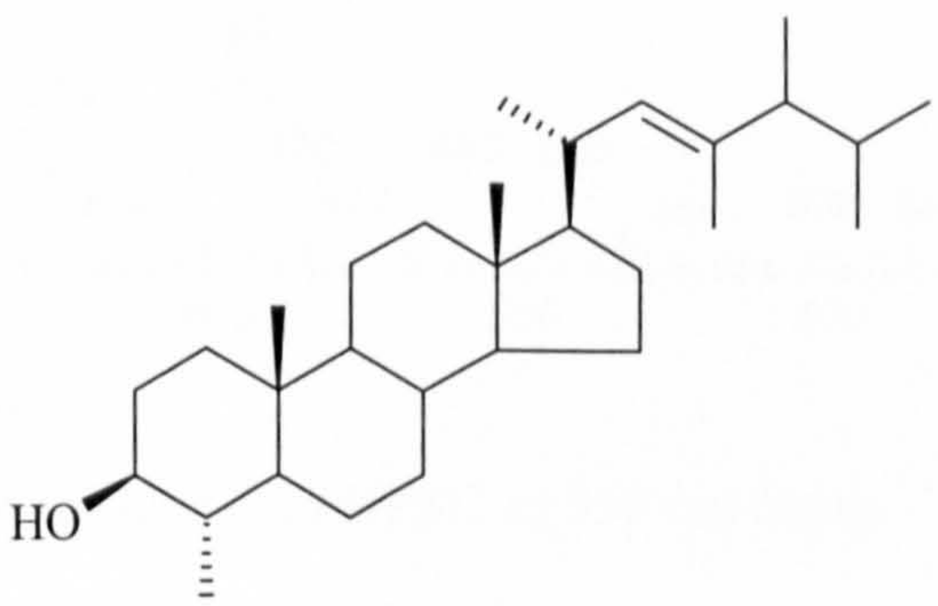

Dinosterol

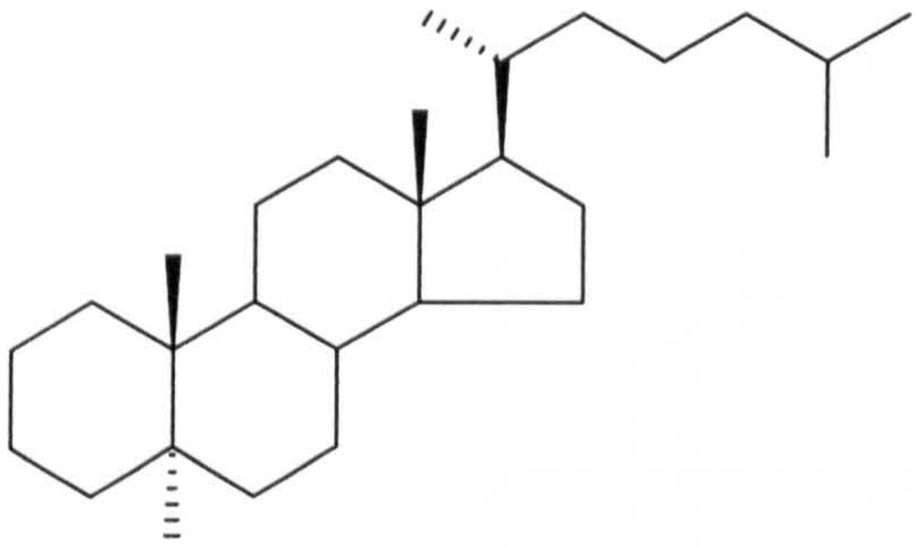

5α-Cholestane

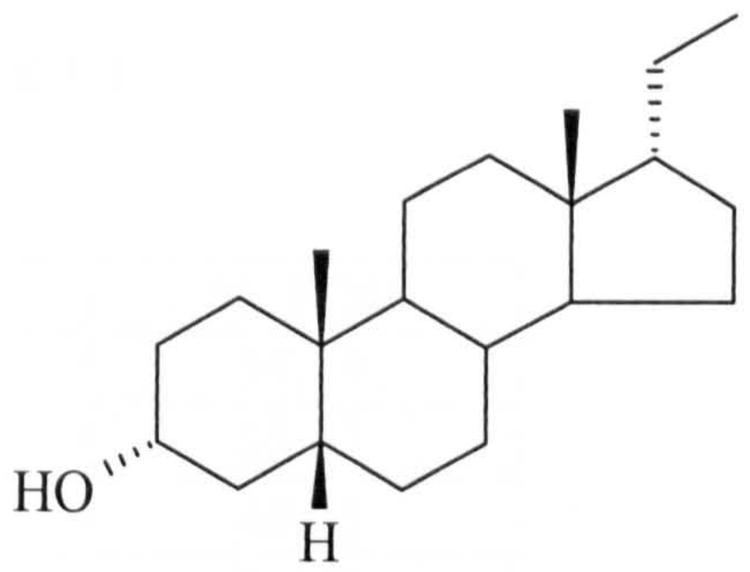

5β-Pregnan-3α-ol

APPENDIX II

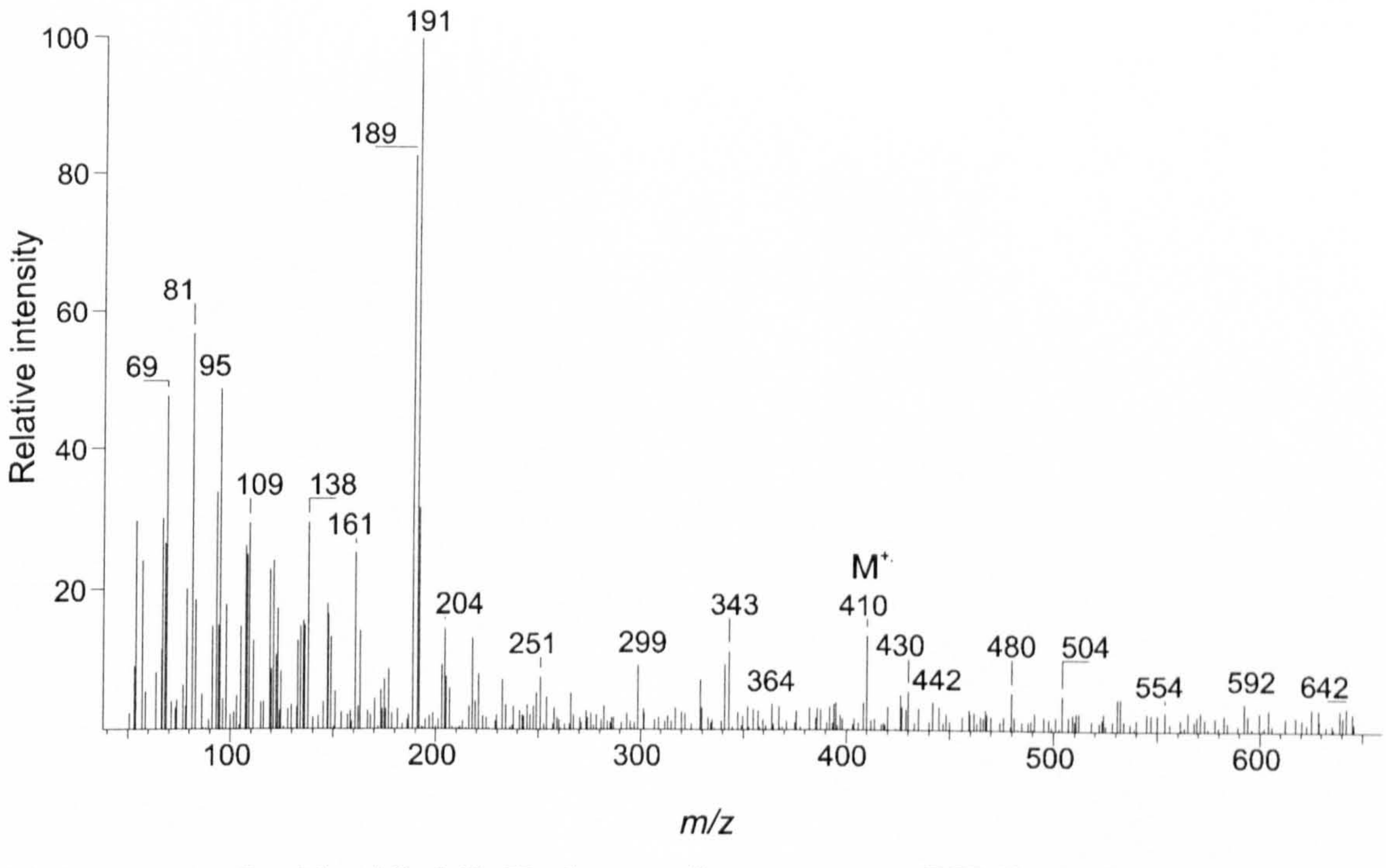

Mass spectra of unidentified $C_{30}H_{50}$ hopane from peat core BFM2 at 359 cm depth.

APPENDIX III

Sample	% TOC
BFM(N) 805-807	54.79
BFM(N) 870-872	55.37
BFM(N) 957-959	48.73
BFM(N) 977-979	2.448
BFM(N) 984-986	41.26
BFM(N) 994-996	0.3475

Total organic carbon as % dry weight of sediment (% TOC) for core BFM(N).

THESIS CONTAINS CD ROM